

# **Integrated Ground-Water Monitoring Strategy for NRC-Licensed Facilities and Sites: Case Study Applications**

**Advanced Environmental  
Solutions, LLC**

**U.S. Nuclear Regulatory Commission  
Office of Nuclear Regulatory Research  
Washington, DC 20555-0001**

## AVAILABILITY OF REFERENCE MATERIALS IN NRC PUBLICATIONS

### NRC Reference Material

As of November 1999, you may electronically access NUREG-series publications and other NRC records at NRC's Public Electronic Reading Room at <http://www.nrc.gov/reading-rm.html>. Publicly released records include, to name a few, NUREG-series publications; *Federal Register* notices; applicant, licensee, and vendor documents and correspondence; NRC correspondence and internal memoranda; bulletins and information notices; inspection and investigative reports; licensee event reports; and Commission papers and their attachments.

NRC publications in the NUREG series, NRC regulations, and *Title 10, Energy*, in the Code of *Federal Regulations* may also be purchased from one of these two sources.

1. The Superintendent of Documents  
U.S. Government Printing Office  
Mail Stop SSOP  
Washington, DC 20402-0001  
Internet: [bookstore.gpo.gov](http://bookstore.gpo.gov)  
Telephone: 202-512-1800  
Fax: 202-512-2250
2. The National Technical Information Service  
Springfield, VA 22161-0002  
[www.ntis.gov](http://www.ntis.gov)  
1-800-553-6847 or, locally, 703-605-6000

A single copy of each NRC draft report for comment is available free, to the extent of supply, upon written request as follows:

Address: U.S. Nuclear Regulatory Commission  
Office of Administration  
Mail, Distribution and Messenger Team  
Washington, DC 20555-0001

E-mail: [DISTRIBUTION@nrc.gov](mailto:DISTRIBUTION@nrc.gov)  
Facsimile: 301-415-2289

Some publications in the NUREG series that are posted at NRC's Web site address <http://www.nrc.gov/reading-rm/doc-collections/nuregs> are updated periodically and may differ from the last printed version. Although references to material found on a Web site bear the date the material was accessed, the material available on the date cited may subsequently be removed from the site.

### Non-NRC Reference Material

Documents available from public and special technical libraries include all open literature items, such as books, journal articles, and transactions, *Federal Register* notices, Federal and State legislation, and congressional reports. Such documents as theses, dissertations, foreign reports and translations, and non-NRC conference proceedings may be purchased from their sponsoring organization.

Copies of industry codes and standards used in a substantive manner in the NRC regulatory process are maintained at—

The NRC Technical Library  
Two White Flint North  
11545 Rockville Pike  
Rockville, MD 20852-2738

These standards are available in the library for reference use by the public. Codes and standards are usually copyrighted and may be purchased from the originating organization or, if they are American National Standards, from—

American National Standards Institute  
11 West 42<sup>nd</sup> Street  
New York, NY 10036-8002  
[www.ansi.org](http://www.ansi.org)  
212-642-4900

Legally binding regulatory requirements are stated only in laws; NRC regulations; licenses, including technical specifications; or orders, not in NUREG-series publications. The views expressed in contractor-prepared publications in this series are not necessarily those of the NRC.

The NUREG series comprises (1) technical and administrative reports and books prepared by the staff (NUREG-XXXX) or agency contractors (NUREG/CR-XXXX), (2) proceedings of conferences (NUREG/CP-XXXX), (3) reports resulting from international agreements (NUREG/IA-XXXX), (4) brochures (NUREG/BR-XXXX), and (5) compilations of legal decisions and orders of the Commission and Atomic and Safety Licensing Boards and of Directors' decisions under Section 2.206 of NRC's regulations (NUREG-0750).

**DISCLAIMER:** This report was prepared as an account of work sponsored by an agency of the U.S. Government. Neither the U.S. Government nor any agency thereof, nor any employee, makes any warranty, expressed or implied, or assumes any legal liability or responsibility for any third party's use, or the results of such use, of any information, apparatus, product, or process disclosed in this publication, or represents that its use by such third party would not infringe privately owned rights.

# Integrated Ground-Water Monitoring Strategy for NRC-Licensed Facilities and Sites: Case Study Applications

Manuscript Completed: August 2007

Date Published: November 2007

Prepared by

V. Price, T. Temples, R. Hodges, Z. Dai, D. Watkins, J. Imrich

Advanced Environmental Solutions, LLC

407 West Main Street

Lexington, SC 29072

T.J. Nicholson, NRC Project Manager

Prepared for

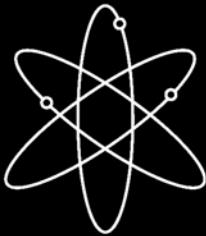
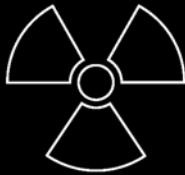
**Division of Fuel, Engineering and Radiological Research**

**Office of Nuclear Regulatory Research**

**U.S. Nuclear Regulatory Commission**

**Washington, DC 20555-0001**

**NRC Job Code Y6020**



## **ABSTRACT**

This document discusses results of applying the Integrated Ground-Water Monitoring Strategy (the Strategy) to actual waste sites using existing field characterization and monitoring data. The Strategy is a systematic approach to dealing with complex sites. Application of such a systematic approach will reduce uncertainty associated with site analysis, and therefore uncertainty associated with management decisions about a site. The Strategy can be used to guide the development of a ground-water monitoring program or to review an existing one. The sites selected for study fall within a wide range of geologic and climatic settings, waste compositions, and site design characteristics and represent realistic cases that might be encountered by the NRC. No one case study illustrates a comprehensive application of the Strategy using all available site data. Rather, within each case study we focus on certain aspects of the Strategy, to illustrate concepts that can be applied generically to all sites. The test sites selected include:

- Charleston, South Carolina, Naval Weapons Station,
- Brookhaven National Laboratory on Long Island, New York,
- The USGS Amargosa Desert Research Site in Nevada,
- Rocky Flats in Colorado,
- C-Area at the Savannah River Site in South Carolina, and
- The Hanford 300 Area.

A Data Analysis section provides examples of detailed data analysis of monitoring data.

### **Paperwork Reduction Act Statement**

This NUREG does not contain information collection requirements and, therefore, is not subject to the requirements of the Paperwork Reduction Act of 1995 (44 U.S.C. 3501 et seq.).

### **Public Protection Notification**

The NRC may not conduct or sponsor, and a person is not required to respond to, a request for information or an information collection requirement unless the requesting document displays a currently valid OMB control number.



## FOREWORD

This research report was prepared by Advanced Environmental Solutions, LLC (AES), under a commercial research contract (NRC-04-03-061) with the U.S. Nuclear Regulatory Commission (NRC). As such, this two-volume report presents a logical framework for assessing what, when, where, and how to monitor with regard to subsurface ground-water flow and transport, in order to ensure that the environs of a licensed nuclear site or facility behave within the expected limits, as prescribed by the performance assessment (PA).

Volume 1 provides the logic, strategic approach, and examples of how to integrate ground-water monitoring with modeling. Specifically, the integrated ground-water monitoring strategy is implemented in an iterative manner, beginning with analysis of any existing site and facility characterization and monitoring data and the relevant conceptual site model (CSM), hydrogeologic model, and/or risk assessment or PA model. The iterative nature of this strategy provides a graded approach for use in developing or evaluating a ground-water monitoring program. In so doing, the analyst derives an initial assessment of what, when, where, and how to monitor to evaluate system performance. The monitoring is then integrated with modeling through the identification, measurement, and analysis of performance indicators (PIs). These PIs include hydrogeologic conditions and process attributes; chemical conditions and constituents; and other features, events, or processes (FEPs) that may significantly influence contaminant flow and transport. As such, PIs may be directly measurable using a monitoring program, or may be derived from compilations and interpretations of geophysical or other indirect data. This integrated ground-water monitoring and modeling strategy offers the following benefits:

- Characterization allows the development of a CSM.
- The CSM allows modeling and/or numerical simulation.
- Modeling allows prediction of system behavior, while monitoring allows refinement of models.
- Refinement supports confidence in the performance assessment, as well as the need for (and selection of) remediation approaches in the event of a contaminant release.

Volume 2 presents practical examples of the applications of this strategy, which provide practical means of testing, evaluating, and improving both the ground-water monitoring program and its related model. Although the strategy and its applications were originally planned for decommissioning sites, they are also very useful for assessing ground-water monitoring programs, remediating ground water, and identifying and selecting approaches to preclude offsite migration of abnormal radionuclide releases at nuclear facilities.

This approach is consistent with the NRC's strategic performance goal of making the agency's activities and decisions more effective, efficient, realistic, and timely by characterizing and monitoring radionuclide transport in ground water. Toward that end, this report demonstrates, using examples relevant to nuclear facility performance, that ground-water monitoring and modeling can be integrated within a systems approach. This information will assist NRC licensing staff and regional inspectors, Agreement State regulators, and licensees in their decision-making by promoting a greater understanding of ground-water monitoring concepts that relate to PA models. Nonetheless, this report is not a substitute for NRC regulations, and compliance is not required. Consequently, the approaches and methods described in this report are provided for information only, and publication of this report does not necessarily constitute NRC approval or agreement with the information contained herein. Similarly, use of product or trade names in this report is intended for identification purposes only, and does not constitute endorsement by either the NRC or AES.

Christiana Lui, Director  
Division of Risk Analysis  
Office of Nuclear Regulatory Research

## EXECUTIVE SUMMARY

This document discusses results of applying the Integrated Ground-Water Monitoring Strategy (the Strategy) to actual sites using existing field characterization and monitoring data. The sites selected for study fall within a wide range of geologic and climatic settings, inventory compositions, and site design characteristics and represent realistic cases that might be encountered by the NRC.

Within each case study we focus on certain aspects of the Strategy, to illustrate concepts that can be applied generically to all sites.

The six test sites selected include:

Chapter 2. Charleston, SC Naval Weapons Station. This study illustrates the value of detailed geological study aided by shallow seismic reflection data to develop a conceptual site model (CSM). The resulting model explained monitoring observations and allowed simulation of plume movement that matched observed concentrations. Wells could be recommended for deletion, and an additional sentinel well for model confirmation was recommended.

Chapter 3. Brookhaven National Laboratory on Long Island, New York. At this site 3-D visualization (e.g., Figures 3-11 and 3-12 on page 3-20) allowed better communication of plume movement.

Chapter 4. The USGS Amargosa Desert Research Site in Nevada. A revised CSM integrating all available site data, including resistivity soundings, allowed re-interpretation of observed tritium vapor movements. With the revised CSM, a simple spreadsheet model was used and provided a good match to observed tritium distribution.

Chapter 5. Rocky Flats in Colorado. This site provides an opportunity to observe episodic pulses of contaminant apparently being released from a vadose zone source in response to water table changes. Data from one well are used to address the issue of defining long-term trends (the Mann-Kendall test) and when it is appropriate to stop sampling a well. The data are also discussed in Chapter 8.

Chapter 6. C-Area at the Savannah River Site in South Carolina. This site has both tritium and chlorinated solvent plumes. An adjacent location that was characterized as a potential landfill site provides data that may not be consistent with the CSM used to model the C-Area ground water. Because of the site's isolation, there are no risk consequences of the possible CSM error.

Chapter 7. The Hanford 300 Area. A revision to the CSM is suggested that includes river water dynamics as part of the hydrogeologic model.

In addition a section on Data Analysis appears as Chapter 8 of this document. This chapter is not intended to be a review of statistics, but to give some examples of data analysis. A FORTRAN program to calculate well to well correlations and Mann-Kendall parameters is included.

# CONTENTS

ABSTRACT.....	iii
FOREWORD.....	v
EXECUTIVE SUMMARY.....	vi
CONTENTS.....	vii
FIGURES.....	xi
TABLES.....	xvi
ACRONYMS AND ABBREVIATIONS.....	xvii
1 Introduction.....	1-1
1.1 Charleston Naval Weapons Station.....	1-4
1.2 Brookhaven National Laboratory.....	1-4
1.3 USGS Amargosa Desert Research Site.....	1-5
1.4 Rocky Flats.....	1-5
1.5 Savannah River C-Area.....	1-5
1.6 Hanford Site 300 Area.....	1-6
1.7 Data Analysis.....	1-6
2 Charleston Naval Weapons Station.....	2-1
2.1 Introduction.....	2-1
2.2 Compilation and Analysis of Available Data.....	2-2
2.2.1 Regional Geology.....	2-2
2.2.2 Site Hydrogeology.....	2-3
2.3 Conceptual Site Modeling.....	2-6
2.3.1 First Approach: Analytical Model:.....	2-6
2.3.2 Second Approach: Numerical Model / Simple Geology:.....	2-7
2.3.3 Third Approach: Numerical Model / Complex Geology.....	2-8
2.4 Designing a Performance Confirmation Monitoring Network.....	2-10
2.5 Strategy Application Conclusions.....	2-14
2.6 Charleston References.....	2-16
Appendix 2-A.....	2-17
3 Brookhaven National Laboratory.....	3-1
3.1 Introduction.....	3-1
3.2 Compilation of Available Data.....	3-2
3.2.1 Site Background.....	3-2
3.2.2 Geologic Information.....	3-4
3.2.3 Hydrogeologic Information.....	3-4
3.2.4 Hydrologic Data.....	3-5
3.2.5 Tritium Plume Ground-Water Monitoring Data.....	3-12
3.3 Ground-Water Modeling and Visualization.....	3-19
3.3.1 Plume visualization.....	3-19
3.3.2 Flow and transport modeling.....	3-21
3.3.3 Active Monitoring.....	3-21
3.3.4 Performance Indicators.....	3-23
3.4 Monitoring Strategy Application Conclusions.....	3-24

3.5	Brookhaven References .....	3-24
4	Amargosa Desert Research Site .....	4-1
4.1	Introduction .....	4-1
4.2	Compilation of Available Data .....	4-1
4.2.1	Geologic Setting .....	4-2
4.2.2	Regional Geologic Information .....	4-4
4.2.3	Site-specific Geologic and Analytical Data .....	4-4
4.3	Application of the Strategy .....	4-13
4.3.1	Chemical Constituents in Ground Water or Soil Gas .....	4-13
4.3.2	Chemical Constituents in Other Fluids .....	4-13
4.3.3	Chemical Constituents in Plants and Animals .....	4-14
4.3.4	Geophysical Modeling and Evaluation .....	4-15
4.3.5	Hydrologic Data .....	4-18
4.3.6	Vadose Zone Data .....	4-21
4.3.7	Meteorological Data .....	4-25
4.3.8	Transport Modeling .....	4-26
4.4	Monitoring Strategy Application Conclusions .....	4-30
4.5	Amargosa References .....	4-31
	Appendix 4-A .....	4-33
	Appendix 4-B .....	4-47
5	Rocky Flats Facility .....	5-1
5.1	Introduction .....	5-1
5.2	Compilation of Available Data .....	5-3
5.3	Geologic Setting .....	5-3
5.3.1	Hydrologic Data .....	5-4
5.4	Application of the Strategy .....	5-6
5.4.1	Case Study 1: Conceptual Site Model Assessment .....	5-6
5.4.2	Case 1: Existing Site Monitoring Data .....	5-7
5.4.3	Case 1: Application of the Strategy .....	5-7
5.4.4	Case 2: VOC Plume Analysis .....	5-12
5.4.5	Case 2: Application of the Strategy .....	5-12
5.4.6	Performance Indicators and FEPs .....	5-14
5.5	Monitoring Strategy Application Conclusions .....	5-15
5.6	Rocky Flats References .....	5-16
6	Savannah River Site, C Area .....	6-1
6.1	Introduction .....	6-1
6.2	Compilation of Available Data .....	6-3
6.3	C-Area Background .....	6-3
6.3.1	Geology and Hydrogeology .....	6-4
6.3.2	Site Characterization and Monitoring .....	6-5
6.3.3	Contaminant Distribution .....	6-6
6.4	Synthesis of a Conceptual Site Model and Flow and Transport Simulations .....	6-8
6.5	Data Visualization .....	6-11
6.6	Alternative Conceptual Models .....	6-12
6.7	Performance Indicators and FEPs .....	6-14
6.8	Monitoring Strategy Application Conclusions .....	6-15

6.8.1	Possible Future Actions .....	6-16
6.9	References .....	6-17
7	Hanford 300 Area .....	7-1
7.1	Introduction .....	7-1
7.2	Compilation of Available Data .....	7-2
7.2.1	Geologic Setting .....	7-2
7.2.2	Regional Geologic Information .....	7-2
7.2.3	Site-specific Geologic Information .....	7-4
7.2.4	Site-specific Hydrogeologic Information .....	7-5
7.2.5	Vadose Zone Data .....	7-8
7.2.6	Hydrologic Data .....	7-9
7.2.7	Seasonal Variability in Water-Table Conditions .....	7-10
7.2.8	300 Area Uranium Plume .....	7-12
7.2.9	Monitoring Considerations .....	7-14
7.3	Application of Ground Water Monitoring Performance Strategy .....	7-15
7.3.1	Performance Indicators and FEPs .....	7-19
7.4	Monitoring Strategy Application Conclusions .....	7-20
7.5	Hanford References .....	7-21
8	Analysis of Characterization and Monitoring Data .....	8-1
8.1	Introduction .....	8-1
8.1.1	Data Types – Characterization versus Monitoring .....	8-1
8.1.2	Data Evaluation versus Statistical Analysis .....	8-2
8.2	Univariate data .....	8-3
8.2.1	Basic Statistical Analysis .....	8-4
8.2.2	Identification of Outlier Points .....	8-4
8.2.3	Quality Control Charts: the T-Test .....	8-5
8.2.4	Applying the Mann-Kendall Test .....	8-7
8.3	Rainfall Data – Sources of Uncertainty for Infiltration .....	8-11
8.3.1	Consider All Water Infiltration Sources .....	8-12
8.3.2	Ensure Rain Station Data Match Facility-Specific Gauging .....	8-12
8.4	Correlations between different wells .....	8-15
8.5	Water Level Measurements .....	8-18
8.6	Unmixing of Multimodal Data .....	8-19
8.7	Multivariate Analysis Methods: Cluster and Factor Analysis .....	8-23
8.7.1	Case Study: Multivariate Data Analysis at Mill Tailing Site .....	8-23
8.8	Analysis of Mapped (Spatial) Data .....	8-28
8.8.1	Outliers in Mapped Data .....	8-29
8.8.2	Uncertainty in Mapped Data .....	8-29
8.8.3	Incongruity between Mapped Variables .....	8-31
8.9	Quality Assurance .....	8-34
8.9.1	Quality Assurance Case Studies .....	8-35
8.10	References .....	8-39
	Appendix 8-A .....	8-42
	Appendix 8-B Fortran 90 code for well-well correlations and for the Mann-Kendall test .....	8-45
	GLOSSARY .....	G-1



## FIGURES

Figure 1-1. Integrated Ground Water Monitoring Strategy framework .	1-2
Figure 2-1. Map showing the location of SWMU 12 at the Charleston Naval Weapons Station (Danielsen, 2003).	2-1
Figure 2-2. This cross section is an example of the complex geology that can result from a changing coastal environment. (Figure from Fern in Saxena, 1976, Fig. 2)	2-2
Figure 2-3. Map of SWMU 12 showing locations of wells and nearby marshes (Danielsen, 2003).	2-3
Figure 2-4. Seismic reflection profiles. The green line is interpreted as the base of the major channel or the older channel, the red line indicates the base of younger channel that has incised into the older channel.	2-4
Figure 2-5. Elevation of the base of the channel contoured from seismic data and well picks. The orange shows the lower elevations, the green shows the higher elevations, and the grey lines represent the seismic profile locations.	2-5
Figure 2-6. Graph of data from the slug test, with hydraulic conductivity (ft/d) on the vertical axis and the cumulative percentage of samples having that value or less plotted on the horizontal axis.	2-6
Figure 2-7. Cross Section of the assumed geology for the analytical solution CSM.	2-7
Figure 2-8. Cross Section of the “Layer Cake Geology” used for our second approach.	2-8
Figure 2-9. The PCE plume from Model II is presented at left, and the computed PCE concentrations at monitoring well MW-03 are much lower than the observed values (right).	2-8
Figure 2-10. The cross-section shows the Major channel and Younger channel, as well as the other hydrofacies in the site.	2-9
Figure 2-11. The simulated PCE plume from Model III is presented at left; computed PCE concentrations at monitoring well MW-03 more closely match observed values (right).	2-9
Figure 2-12. The predicted PCE plume in five years. Circled wells are suggested to be removed from the monitoring program to save money, while a new point is suggested to be added at the yellow dot to test the CSM and simulation results.	2-11
Figure 2-13. Change in water table over time. Note how MW-08 is the only well that doesn’t match the others.	2-12
Figure 2-14. Contour Map of water table using data from July 2004 (feet above MSL).	2-13
Figure 2-15. Contour map of water table using data from July 2004, without well MW-08 (feet above MSL).	2-13
Figure 2-16. Activities and results of the Strategy application at Charleston Naval Weapons Station	2-15
Figure 3-1. Schematic of tritium/VOC plume pump and treat system (DOE, 2000)	3-2
Figure 3-2. Location of the Brookhaven National Laboratory (Scorca et al., 1999)	3-3
Figure 3-3. Hydrostratigraphy of the Brookhaven National Laboratory (BNL, 2004)	3-4
Figure 3-4. Precipitation and water-table altitude at Brookhaven National Laboratory, Suffolk County, N.Y., 1970-97. A. Annual precipitation at Upton. B. Typical water levels in wells (Scorca et al., 1999)	3-9

Figure 3-5. Water-table altitude in 300-mi <sup>2</sup> study area surrounding Brookhaven National Laboratory, Suffolk County, N.Y., August 1995 (Scorca et al., 1999) .....	3-10
Figure 3-6. Schematic of plume configuration below the HFBR (Looney and Paquette, 2000). Used by permission of Battelle Press .....	3-13
Figure 3-7. Simplified calculation of plume thickness immediately downgradient of a vadose zone source (Looney and Paquette, 2000). Used by permission of Battelle Press.....	3-14
Figure 3-8. Cross section of tritium plume emanating from the HFBR (Looney and Paquette, 2000). Used by permission of Battelle Press. ....	3-16
Figure 3-9. December 2005 water table map of BNL with extraction wells (BNL, 2005) .....	3-17
Figure 3-10. Location of tritium plume emanating from the High Flux Beam Reactor (DOE, 2000).....	3-18
Figure 3-11. Oblique view looking northeast of tritium plume with concentrations emanating from the HFBR.....	3-20
Figure 3-12. Oblique view looking northwest of tritium plume with concentrations emanating from the HFBR.....	3-20
Figure 3-13. Computer simulation of tritium plume emanating from the HFBR after twenty years, no pumping .....	3-21
Figure 3-14. Computer simulation of tritium plume emanating from the HFBR after twenty years, pumping monitoring well. ....	3-22
Figure 4-1. Location of ADRS (Stonestrom et al., 2003).....	4-2
Figure 4-2. Cross section of a typical horst and graben sequence (CG, 1992).....	4-3
Figure 4-3. Oblique view of a typical alluvial fan in Death Valley.....	4-3
Figure 4-4. Location of ADRS and soil gas sampling boreholes UZB-2 and UZB-3 (Stonestrom et al., no date) .....	4-4
Figure 4-5. Geologic distribution of clay lenses and marsh deposits in ADRS Wells 301, 302, and 303 (Fischer, 1992) .....	4-5
Figure 4-6. ADRS water table contours (measured in meters MSL) and well locations (Walvoord et al., 2005).....	4-6
Figure 4-7. Map of tritium concentrations in ground water below ADRS (Data from Prudic, 1997).....	4-7
Figure 4-8. Map showing numbered survey locations of Schlumberger soundings (modified from Bisdorf, 2002).....	4-8
Figure 4-9. Cross section of interpreted resistivity and basin fault (Bisdorf, 2002). (Triangles along the top axis correspond to sounding locations as mapped in Figure 4-8. Subvertical solid black line represents basin fault as defined by Bisdorf 2002.) .....	4-9
Figure 4-10. Map showing contours of interpreted resistivity at a depth of 97 m overlying topographic contours (Bisdorf, 2002).....	4-10
Figure 4-11. A vertical cross section made by direct current electrical resistivity (DC-resistivity) imaging near the ADRS (Stonestrom et al., no date).....	4-11
Figure 4-12. Monitoring shaft and instrument borehole showing locations of TCPs and respective geologic information (Fischer, 1992). Thermocouple psychrometers installed in the monitoring shaft are designated with L (left), M (middle), and R (right), followed by a number from 1 to 11 that indicates level in shaft.	

Thermocouple psychrometers installed in the instrument borehole are designated OD1 through OD13. Depth of each thermocouple psychrometer, in meters below land surface, is given in parentheses. (Fischer, 1992).	4-11
Figure 4-13. Monitoring shaft geologic and geophysical information (Fisher, 1992).	4-13
Figure 4-14. Plant sample locations and contours of plant-water tritium concentrations (Andraski et al., 2005)	4-14
Figure 4-15. A comparison of plant water tritium with soil water tritium (Stonestrom et al., no date)	4-15
Figure 4-16. Simplified geologic cross section of the ADRS looking northwest	4-15
Figure 4-17. Three-dimensional resistivity block model of the ADRS looking northwest (Well UZB-2 can be seen in the southwestern portion of the figure) (created with data from Bisdorf, 2002)	4-17
Figure 4-18. Location of the Southern Structural offset as defined by resistivity data in relation to the burial trenches (adapted from Stonestrom et al., no date)	4-18
Figure 4-19. Map of tritium concentrations in ground water below ADRS in relation to the Southern Structural Offset (data from Prudic, 1997)	4-20
Figure 4-20. Plan view of tritium soil gas concentrations in the 1.5m below ground surface interval (data from Striegl et al., 1997)	4-22
Figure 4-21. Soil vapor concentrations of tritium in UZB-2	4-23
Figure 4-22. Tritium soil gas concentrations from UZB-3 (modified from Stonestrom et al., no date)	4-24
Figure 4-23. Carbon dioxide and carbon-14 soil gas concentrations from UZB-2 and UZB-3 (Stonestrom et al., no date)	4-24
Figure 4-24. Data from southeast corner of ADRS (Prudic, 1996)	4-25
Figure 4-25. Conceptual Model for the movement of tritium proposed by Striegl et al., 1996	4-26
Figure 4-26. Comparison of actual data to modeled tritium concentrations in UZB-2 in pCi/L (UZB-2 tritium data from Striegl et al., 1997)	4-28
Figure 4-27. Alternative conceptual model for the distribution of tritium in vadose zone based on Southern Structural offset and UZB-2 tritium concentrations (tritium data from Striegl et al., 1997)	4-29
Figure 5-1. Location of the Rocky Flats Facility in Colorado (DOE, 2005)	5-2
Figure 5-2 Photograph of the Rocky Flats Facility (looking east) Photo is in “Linking Legacies”, DOE publication EM-0319 (DOE 1997) Appendix B, page 190.	5-3
Figure 5-3. Map of Rocky Flats Facility drainage basins (from: <a href="http://lanl.gov/source/orgs/nmt/nmtdo/AQarchive/06springsummer/page5.shtml">http://lanl.gov/source/orgs/nmt/nmtdo/AQarchive/06springsummer/page5.shtml</a> )	5-5
Figure 5-4. Ground-water monitoring well locations and depiction of VOC and nitrate plumes for the Rocky Flats Facility (CDPHE, (No Date))	5-6
Figure 5-5. Conceptual cross-section for the Rocky Flats Facility (Modified from K-H, 2004)	5-7
Figure 5-6. Diagram of multiyear variability in ground-water contaminant concentrations due to water table changes (K-H, 2004)	5-8
Figure 5-7. Conceptual cross section showing affects of water table changes on contaminant movement (modified from K-H, 2004)	5-8
Figure 5-8. Potential changes in ground-water movement due to closure	5-10
Figure 5-9. Predicted water level changes after closure (K-H, 2004)	5-11

Figure 5-10. Generalized depiction of the Rocky Flats Facility TCE plume .....	5-12
Figure 5-11. Conceptual model of complex flow of contaminants .....	5-14
Figure 6-1. Savannah River Site location map. Courtesy of Bill Jones, SRNL. ....	6-1
Figure 6-2. Photograph of the A Area Burning/Rubble Pit during operation.....	6-2
Figure 6-3. Map of C Area with facilities and wells (WSRC, 1998).....	6-3
Figure 6-4. Simplified hydrogeologic cross section near C Area (Kegley et al., 1994). Courtesy of W.P. Kegley. ....	6-5
Figure 6-5. Topographic map of C-Area facility boundary with TCE plume and detected TCE concentrations.....	6-6
Figure 6-6. C Area tritium CPT data .....	6-7
Figure 6-7. C Area TCE CPT data.....	6-8
Figure 6-8. C Area hydrologic Conceptual Site Model .....	6-9
Figure 6-9. C Area simulated transport model for Layer 3 from the CBRP.....	6-10
Figure 6-10. C Area simulated transport model for Layer 7 from the CBRP.....	6-10
Figure 6-11. Cross section of C Area hydrogeologic conceptual model. The Gordon confining unit (green clay) is shown as a green band above the Gordon aquifer. Fourmile Branch is correctly called Four Mile Creek elsewhere in this document... 6- 11	
Figure 6-12. Looking from beneath the Gordon confining unit to the NE towards the plume (All dim points are above the Gordon confining unit).....	6-12
Figure 6-13. Structural contour map of the top of the Gordon confining unit (WSRC, 1992) .....	6-13
Figure 6-14. Maps of ground water flow directions within the Gordon aquifer.....	6-14
Figure 7-1. Hanford Site map including the 300 Area (DOE, 1999).....	7-2
Figure 7-2. Hanford Site regional geologic setting (Vermeul et al., 2003) .....	7-3
Figure 7-3. Structural geologic features of the Hanford Site within the Pasco Basin (Vermeul et al., 2003) .....	7-4
Figure 7-4. Major geological units at the Hanford Site (DOE, 1999) .....	7-5
Figure 7-5. Index map to cross sections shown in Figures 6, 7, and 8 (Peterson, 2005)	7-6
Figure 7-6. West to east cross section along flow path from 300 Area process trenches to the Columbia River (Peterson, 2005).....	7-7
Figure 7-7. North to south cross section along shoreline wells (Peterson, 2005).....	7-7
Figure 7-8. West to east cross section through central portion of 300 Area (Peterson, 2005) .....	7-7
Figure 7-9. Conceptual model of fluid flow beneath single shell tanks at Hanford Site showing fingering, funnel flow, and flow associated with clastic dikes or poorly sealed borehole annular space (Faybishenko, 2000).....	7-9
Figure 7-10. 300 Area water-table elevation, March 1992 (averaged hourly) (Peterson, 2005) .....	7-10
Figure 7-11. 300 Area water-table elevation, May 1992 (averaged hourly) (Peterson, 2005) .....	7-10
Figure 7-12. 300 Area water-table elevation, June 1992 (averaged hourly) (Peterson, 2005) .....	7-11
Figure 7-13. 300 Area water-table elevation, September 1992 (averaged hourly) (Peterson, 2005) .....	7-11

Figure 7-14. 300 Area water-table elevation, December 1992 (averaged hourly) (Peterson, 2005) .....	7-11
Figure 7-15. 300 Area ground water monitoring locations (Peterson, 2005) .....	7-14
Figure 7-16. Hydrogeologic conceptual model of contaminant movement below the Hanford 300 Area (DOE, 2002).....	7-15
Figure 7-17. Transient storage mechanisms (Runkel, 1998).....	7-16
Figure 7-18. Alternative conceptual model of Hanford 300 Area showing potential infiltration and downstream flushing of formation.....	7-17
Figure 7-19. Extent of river water intrusion as estimated from nitrate concentrations in 2002(Yabusaki et al, 2004).....	7-18
Figure 7-20. 300 Area Ground-Water Uranium Concentrations, August 1997.....	7-19
Figure 8-1. Example control chart .....	8-6
Figure 8-2. Mann-Kendall Example .....	8-8
Figure 8-3. Published figure indicating declining PCE concentrations in ug/L (DOE, 2006) .....	8-9
Figure 8-4. Linear regression fit to PCE data from MS-EXCEL .....	8-10
Figure 8-5. Parsing time series data into three groups.....	8-11
Figure 8-6. SRS rain gauging station and well locations. Rain stations are located under respective station identifier A, C, F, H, and S. Well locations are denoted by black dots. Adapted from Jones, 1990.....	8-13
Figure 8-7. Rain data for Stations F and H, which are only two miles apart, show that particularly in summer, rainfall patterns are highly variable, even over short distances.....	8-13
Figure 8-8. Rain Gauges C and S are about 7 miles apart and show significant variation in observed rainfall. ....	8-14
Figure 8-9. Correlation of rainfall as a function of distance in July and January.....	8-15
Figure 8-10. Rejection of outliers .....	8-16
Figure 8-11 Periodic and continuous water level measurements compared for SRS well P- 13D. Courtesy Bill Jones, SRNL.....	8-18
Figure 8-12. Unmixing bimodal data.....	8-20
Figure 8-13. Probability plot.....	8-22
Figure 8-14. Tri-modal distribution .....	8-22
Figure 8-15. Cross section showing concept of merged water bodies. Our study examines whether this water is separated into two isolated chambers. ....	8-24
Figure 8-16. Dendrogram (partial) of the clusters for the water analyses presented in Appendix 8-A. The left-most column is the well name and the right column indicates the observation number.....	8-26
Figure 8-17. Map of chloride plume (blue) superimposed on a vector potentiometric data (arrows), and contoured hydraulic conductivity data (red).....	8-31
Figure 8-18. Typical alluvial fan .....	8-32
Figure 8-19. Diagram of alluvial fans in Wyoming.....	8-33
Figure 8-20. Schematic of monitoring well with steps in installation. ....	8-36
Figure 8-21. pH with time for well ASB8B.....	8-37
Figure 8-22. pH with time for well ABP3 .....	8-38
Figure 8-23 Field and laboratory measurements compared.....	8-39

## TABLES

Table 1-1 Classification of Performance Indicators .....	1-3
Table 2-1. Slug test data compared to the number of hammer blows needed to penetrate 1 ft, averaged over the length of the screen zone.....	2-5
Table 2-2. Estimated flow and transport parameters for Model III. ....	2-10
Table 2-3. Water elevations (ft above MSL) in wells.....	2-12
Table 3-1. Generalized description of geologic and hydrogeologic units underlying Brookhaven National Laboratory and vicinity, Suffolk County, N.Y. (Scorca et al., 1999) .....	3-6
Table 3-2. Hydraulic conductivity of Upper Glacial aquifer at Brookhaven National Laboratory, Suffolk County, N.Y., as indicated by aquifer tests (Scorca et al., 1999) .....	3-7
Table 4-1. Summary of model for estimation of tritium movement in the vadose zone between the Southern Structural Offset and UZB-2 .....	4-27
Table 4-2. Tritium model dispersivity values assigned to various materials.....	4-29
Table 4-3. Comparison of results from the tritium model to actual concentrations in UZB-2 (UZB-2 data from Striegl et al., 1997) .....	4-30
Table 6-1. Hydrologic layer parameters (adapted from Flach et al. (1999) and Geotrans (2001)).....	6-9
Table 8-1 . Statistical analysis of water head observations from Savannah River Site .	8-17
Table 8-2. The identified distributions of three sources and the estimated parameters	8-21
Table 8-3. Correlations between monitoring data variables .....	8-28
Table 8-4. Hydraulic conductivity data .....	8-34

## ACRONYMS AND ABBREVIATIONS

°C	degrees celcius
µg/L	micrograms per liter
ADRS	Amargosa Desert Research Site
AEA	Atomic Energy Act
AES	Advanced Environmental Solutions, LLC
AEC	Atomic Energy Commission
AOCs	Areas of Concern
ASTM	American Society for Testing and Materials
bgs	below ground surface
BNL	Brookhaven National Laboratory
BRP	burning and rubble pit
CERCLA	Comprehensive Environmental Response Compensation and Liability Act
CFC	chlorofluorocarbon
cfs	cubic feet per second
Ci	Curie
cm	centimeters
cm/day	centimeters per day
CO <sub>2</sub>	carbon dioxide
COC	contaminant of concern
cpt	cone penetrometer test
CRBG	Columbia River Basalt Group
CSM	conceptual site model
CV	coefficient of variation
DC-resistivity	direct current resistivity
DCE	dichloroethylene
DNAPL	dense nonaqueous phase liquid
DoD	Department of Defense
DOE	United States Department of Energy
DQO	data quality objective
EDB	ethylene dibromide
EM	electromagnetic
EM	expectation-maximization
EPA	Environmental Protection Agency
ft	feet
ft/d	feet per day
ft/ft	feet per foot
FEPs	features, events, or processes
GC	green clay
GIS	geographic information system
gpm	gallons per minute
GPR	ground-penetrating radar
HFBR	High Flux Beam Reactor
INEEL	Idaho National Engineering and Environmental Laboratory
Kd	distribution coefficient
LANL	Los Alamos National Laboratory
LBNL	Lawrence Berkeley National Laboratory
LLNL	Lawrence Livermore National Laboratory
LLW	low-level waste
LNAPL	light non-aqueous phase liquid
m	meter
MCL	maximum contaminant level
m/d	meters per day

m/m	meters per meter
mg/g	milligrams per gram
MDL	method detection limit
mi	miles
mi <sup>2</sup>	square miles
MLE	maximum likelihood estimation
MNA	monitored natural attenuation
ND	no date
NE	northeast
NRC	Nuclear Regulatory Commission
NURE	National Uranium Resource Evaluation
ORNL	Oak Ridge National Laboratory
OU	Operable Unit
PA	Performance Assessment
PAH	polycyclic aromatic hydrocarbon
pCi/L	picocuries per liter
PCB	polychlorinated biphenyl
PCE	tetrachloroethylene
PCP	pentachlorophenol
PNNL	Pacific Northwest National Laboratory
ppb	parts per billion
PVC	polyvinyl chloride
QA	quality assurance
RCRA	Resource Conservation & Recovery Act
RSB	reactor seepage basin
SCDHS	Suffolk County Department of Health Services
SNL	Sandia National Laboratories
SP	spontaneous potential
SPSS	Statistical Package for the Social Sciences
SRS	Savannah River Site
SRTC	Savannah River Technology Center
SSE	south/southeast
SVE	soil vapor extraction
SWMU	Solid Waste Management Unit
TCA	1,1,1-trichloroethane
TCE	trichloroethylene
TCLP	toxicity characteristics leaching procedure
TCPs	thermocouple psychrometers
TOC	total organic carbon
U(VI)	hexavalent uranium
UMTRA	uranium mill tailings remedial action
USGS	United States Geological Survey
VOC	volatile organic compound

# 1 Introduction

This document discusses results of applying the Integrated Ground-Water Monitoring Strategy (the Strategy) to actual waste sites using existing field characterization and monitoring data. The sites selected for study fall within a wide range of geologic and climatic settings, waste compositions, and site design characteristics and represent realistic cases that might be encountered by the NRC.

We gratefully acknowledge the U.S. Navy, the U.S. Geological Survey, and the U.S. Department of Energy for data used in this report.

A Test Plan submitted to NRC in July, 2005, set forth a plan that was applied to produce this report. No one case study illustrates a comprehensive application of the Strategy using all available site data. Rather, within each case study we focus on certain aspects of the Strategy, to illustrate concepts that can be applied generically to all sites.

The six test sites selected include:

Chapter 2. Charleston, SC Naval Weapons Station,

Chapter 3. Brookhaven National Laboratory on Long Island, New York,

Chapter 4. The USGS Amargosa Desert Research Site in Nevada,

Chapter 5. Rocky Flats in Colorado,

Chapter 6. C-Area at the Savannah River Site in South Carolina, and

Chapter 7. The Hanford 300 Area.

In addition a section on Data Analysis appears as Chapter 8 of this document. This chapter is not intended to be a review of statistics, but to give some examples of data analysis. The Strategy is a systematic approach to dealing with complex sites. Application of such a systematic approach will reduce uncertainty associated with site analysis, and therefore uncertainty associated with management decisions about a site. The Strategy can be used to guide the development of a ground-water monitoring program or to review an existing one. The high level logic, as expressed in Figure 1-1, is simple.

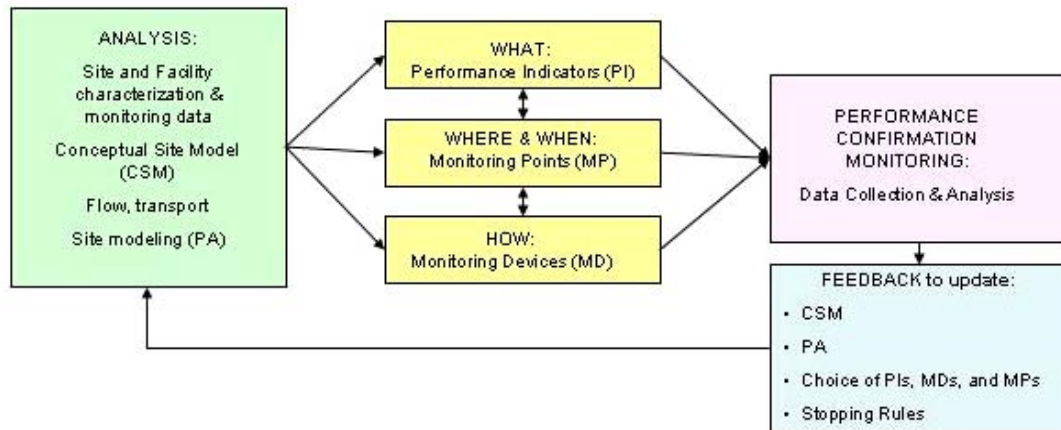


**Figure 1-1. Integrated Ground Water Monitoring Strategy framework .**

One begins by gathering, compiling, and analyzing all available data about the site and its geological and hydrological context. A Conceptual Site Model (CSM) based on geology and hydrogeology is constructed from the data. Engineered features such as trenches and back-filled areas may be important in the CSM. Numerical simulations based on this model may be made to estimate ground water flow directions and rates of contaminant transport.

For any site, there will be performance criteria to be met. Using the CSM, which incorporates hydrogeologic and geochemical information and knowledge of inventory, measurable or observable indicators of site performance can be selected. In this Strategy, these are called Performance Indicators (PIs). Locations and frequency for measuring indicators can also be selected. The indicators may be risk-related potential contaminants, or they may be physical measurements like water levels. The objective is to measure something that helps to indicate whether the overall site/facility/ground-water system is actually functioning as modeled.

The purpose of monitoring in the context of this guide is confirmation of a performance assessment model. Once we have confidence that the site is understood, we can place monitoring points as sentinels to give early detection of off-normal behavior, and to assure compliance with ground-water protection standards. But it is worth repeating that understanding system behavior, not regulatory compliance is the goal of this work.

Site and system Performance Indicators are measurable or observable features that provide insight into reliability of the Conceptual Site Model (CSM). During analysis of data from each site, performance indicators are identified and examined. A table of potential Performance Indicators (PIs) is shown below. Actual PIs will be site-specific.

**Table 1-1 Classification of Performance Indicators**

<p><b>Class 1 - Chemical</b></p> <ul style="list-style-type: none"><li>A. Regulated and Direct Drivers of Risk - U, Cs-134, Pu, Sr-90 these are Primary Performance Indicators (PIs)</li><li>B. Surrogates and Indicators that a process is occurring –<ul style="list-style-type: none"><li>1. gross Alpha for Uranium</li><li>2. Cl or NO3 from same source as risk drivers</li><li>3. degradation products - Am241 for Pu, organic breakdown products for MNA</li></ul></li><li>C. Process control chemical indicators needed to model transport<ul style="list-style-type: none"><li>• pH, alkalinity, conductivity, major cations, major anions, redox indicators...</li></ul></li></ul>
<p><b>Class 2 - Physical</b></p> <ul style="list-style-type: none"><li>• examples include water content, pressure distributions</li><li>• physical properties of rocks</li><li>• physical properties of subsurface fluids</li></ul>
<p><b>Class 3 - Modeled or Derived from Data Analysis</b></p> <ul style="list-style-type: none"><li>A. Distribution of uncertainty This would be determined by examining the distribution of characterization data available to develop a site conceptual model and flow model. Areas of sparse or questionable data would have high uncertainty.</li><li>B. Lack of Congruity - Tests of site conceptual and flow / transport models -<ul style="list-style-type: none"><li>• Do actual plume maps match predicted plumes?</li><li>• Does site geology match regional geology?</li><li>• Does site geology match geology reported from adjacent areas?</li></ul></li><li>C. Outliers Spatial - for example:<ul style="list-style-type: none"><li>• bulls eyes around data points on contoured maps</li><li>• areas of high characterization uncertainty</li></ul>Statistical (no spatial component) -<ul style="list-style-type: none"><li>• univariate includes control chart anomaly,</li><li>• multivariate would include single-sample cluster</li></ul></li></ul>

Short discussions of each site follow and highlight the unique site features, Performance Indicators or lessons learned. More detailed discussions are in subsequent chapters and include data that were available for the analysis.

## **1.1 Charleston Naval Weapons Station**

At this site, a leaking solvent storage tank produced a plume of contaminated ground water. Initial site investigations were conditioned by proximity to a tidal creek, assumed to be the likely surface discharge place for ground water, and by a well with a low water level. Monitoring wells placed between the tank and the creek were free of contamination. Examination of water levels with time revealed that a well initially thought to be down-gradient should have been considered up-gradient. A seismic reflection survey and other geologic data were combined to produce a better Conceptual Site Model (CSM). This model included sandy channels interpreted from the seismic survey. The improved model led to practical suggestions regarding placement of monitoring wells for the purpose of Performance Confirmation Monitoring. Specifically, these results suggest that several wells can be abandoned, and that one additional well should be placed to test whether the plume is advancing.

This case highlighted the importance of continued validation of the conceptual model using site data. In this case three iterations of conceptual and transport modeling were necessary to produce a model with sufficient geologic complexity to reproduce observed results. This iterative process was key to identifying Performance Indicators for the site and for guiding recommended monitoring strategies.

A lesson learned is that periodic water level measurements might not give a true picture of the water table if wells respond differently to rainfall events or surface runoff.

## **1.2 Brookhaven National Laboratory**

At Brookhaven National Laboratory (BNL), tritium leaked from a fuel storage pool into the ground water. Early attempts to understand the leak with horizontal wells beneath the reactor were confounded by the fact that tritium from this slow leak rode the top of the water table laterally until leaving the building footprint. Outside the area covered by the building, infiltrating precipitation moved the plume downward.

The shape of the plume has been delineated with wells and direct-push sampling. The plume shape is very narrow, prompting us to suspect geologic control, such as a sub-glacial channel, now buried, and to explore various modeling scenarios. Modeling suggests the plume shape may simply be a function of high hydraulic conductivity (without the need for a more complex geologic model), and that the plume migration is likely influenced by remediation pumping of extraction wells in the vicinity of the plume.

Because of a high density of sampling points, visualization of the plume is especially effective for communication of its extent. The cover illustration is of the BNL tritium plume.

Risk from the tritium is considered very low, and the main issue, rather than health, is public perception. Data visualization is a direct and readily understood way to share information with the all shareholders.

### **1.3 USGS Amargosa Desert Research Site**

The U.S. Geological Survey (USGS) Amargosa Desert Research Site (ADRS) is at the location of the Nation's first licensed radioactive waste disposal site near Beatty, Nevada. USGS has maintained a research program here since 1975 with the objective of understanding dry climate hydrology. USGS has installed wells and collected data on migration of tritium and other contaminants including carbon-14 and mercury in the vadose zone. USGS has also conducted geophysical (e.g., resistivity) surveys and has modeled migration of tritium and mercury.

USGS reports that modeling results do not match the observed distribution of tritium. We evaluated all available site data to produce an alternative CSM which includes a fault as a preferential pathway for migration of tritium below the waste site. Rough spreadsheet modeling suggests the addition of the fault allows an improved match to the observed tritium concentrations.

The discussion points out the value of using all available data in constructing conceptual models, and the critical monitoring needed to test a proposed conceptual model.

Performance indicators that suggested issues with the conceptual site model included strong bending of water-table contours and the distribution of tritium at the water table.

### **1.4 Rocky Flats**

Established in 1951, the primary mission of the Rocky Flats facility (RF) was to produce weapons components. Decades of these manufacturing operations led to several areas of contamination at this site. This report focuses on application of the Strategy at two areas of chlorinated organic solvent contamination.

In the first area of contamination, analysis of characterization data helped us identify a correlation in water table levels with observed episodic spikes in contaminant concentrations. This finding in turn led to an alternative conceptual model which can aid in determining how long some of the monitoring wells should remain in service.

In the second area of contamination, application of the Strategy revealed that careful plume mapping, including recognition of degradation products as key Performance Indicators, improves source definition. Some RF data are also used in the Data Analysis Chapter.

### **1.5 Savannah River C-Area**

At the Savannah River Site (SRS), we find both tritium and chlorinated solvents issuing from a few sources near the reactor building. Because the facility is on a ground-water divide, contaminants from sources that are close together move in different directions. This site is very well characterized through monitoring wells and direct-push sampling.

Visualization of the ground-water sampling data is useful. Modeling suggests that solvents from this facility could have penetrated a regional confining unit and moved to the north beneath a local surface-water divide. Some sampling was done in the direction of plume movement, but modeling suggests the plume may not have reached the down-

gradient area at the time of sampling. This illustrates the importance of flow simulation to timing of sampling.

Additional data discovered during application of the Strategy suggest that the CSM used by all modelers, including ourselves, maybe too simplistic and that a confining unit could be breached by faulting. It appears that the current data distribution does not permit an adequate test of this hypothesis. The level of risk does not justify further characterization, but it is likely that the CSM is flawed.

Application of the Strategy helped guide recommendations made with regard to further monitoring activities.

### **1.6 Hanford Site 300 Area**

DOE's Hanford Site 300 Area is located immediately adjacent to the Columbia River. River discharge is roughly 50,000 cfs adjacent to the Site, and river elevation (stage) is controlled by dams. Recent work reported by researchers at the Pacific Northwest National Laboratory is used as a backdrop to a discussion of some modeling and monitoring issues including the impact of river stage changes on movement of a uranium plume.

One possible addition to the current CSM is the inertia of river water impinging on the cutbank adjacent to the 300 Area. Indicators (PIs) of this model modification include the distribution of nitrate and uranium plumes adjacent to the river as well as average water table elevations.

### **1.7 Data Analysis**

Chapter 8 briefly discusses approaches to data analysis techniques, and highlights some common pitfalls and issues which can confuse interpretation of monitoring data. Data analysis may lead to results that challenge an existing conceptual site model and the understanding of how site facilities, geology, and ground water interact and behave. Data analysis and data mining are essentially synonymous. This is not a chapter on statistical testing.

Data examples are drawn largely from the DOE Savannah River Site (SRS), the Rocky Flats Site, and from a uranium mining and milling site in the northwestern United States.

Quarterly water levels in wells cannot be simply and reliably related to rainfall data. There is some suggestion that data loggers may provide water level data that can be related to rainfall.

Rainfall data from weather stations across the SRS are compared. Results suggest that ground-water studies including infiltration estimated from rainfall must use very local rainfall data.

Analysis of 20 years of water level data highlights some QA issues with field measurements and with well construction. Data are used to illustrate some statistical methods to identify trends or to group data based on general chemistry as well as contaminants. Anomalous water levels occur at widely separated wells on the same

sampling date, suggesting opportunities for data QA. A FORTRAN program for well-to-well correlation and the Mann-Kendall test is listed.

Also discussed are simple tests of trends in data that may obscure data structure and require examination of the hydrogeologic conceptual model.

A proposed alternative conceptual model at the northwestern U.S. site is that the water table and a lower water bearing zone presented by the site custodian were actually one underground water body because of breach of a proposed confining unit by faulting. Data analysis indicates that a few contaminated wells stand out, but that most wells yield water that can be grouped into two chemically distinct groups or clusters. This supports the site custodian's original conceptual site model that a confining layer has some integrity across the site.

## 2 Charleston Naval Weapons Station

### 2.1 Introduction

The Charleston Naval Weapons Station is located just north of Charleston, South Carolina on about 17,000 acres of land. Solid Waste Management Unit 12 (SWMU 12) is located in the southeastern portion of the base, near the Cooper River (Figure 2-1). This site housed a wood treatment facility that operated from the early 1970s to 1981 (Danielsen, 2003).

The site is relatively flat with a total relief ranging from 3.0 to 8.5 feet above mean sea level. Four structures were located at the site. The area outside of the fence line consists of forest, wetlands, and marshes.

Past operations at the site included use of the hazardous wood preservative pentachlorophenol (PCP). In 1998, a breached 500-gallon underground storage tank was found during a RCRA Facility Investigation, and elevated levels of chlorinated organic solvents were confirmed in site ground water (Danielsen, 2003).



**Figure 2-1. Map showing the location of SWMU 12 at the Charleston Naval Weapons Station (Danielsen, 2003).**

In 2001, a seismic survey performed at the site revealed the presence of shallow high permeability channels in the subsurface. Conceptual site models which included these channels were developed for computer simulations of flow and transport as part of this strategy application. Visualization of contaminant transport over time using these simulations enabled AES to design a Performance Confirmation Monitoring plan that included abandonment of several existing monitoring wells, as well as the placement of one additional sentinel well.

## **2.2 Compilation and Analysis of Available Data**

### **2.2.1 Regional Geology**

The geology of the Charleston Naval Weapons Station is made up of sediments deposited through near-shore coastal processes. Sands grade into clays and back into sands, presenting a complex pattern of layers, as ancient tidal channels meandered through the ancient salt marsh, with intervening beach ridges and sand dunes (Weems and Lemon, 1993). Figure 2-2 is an example of a cross section through a complex coastal environment.

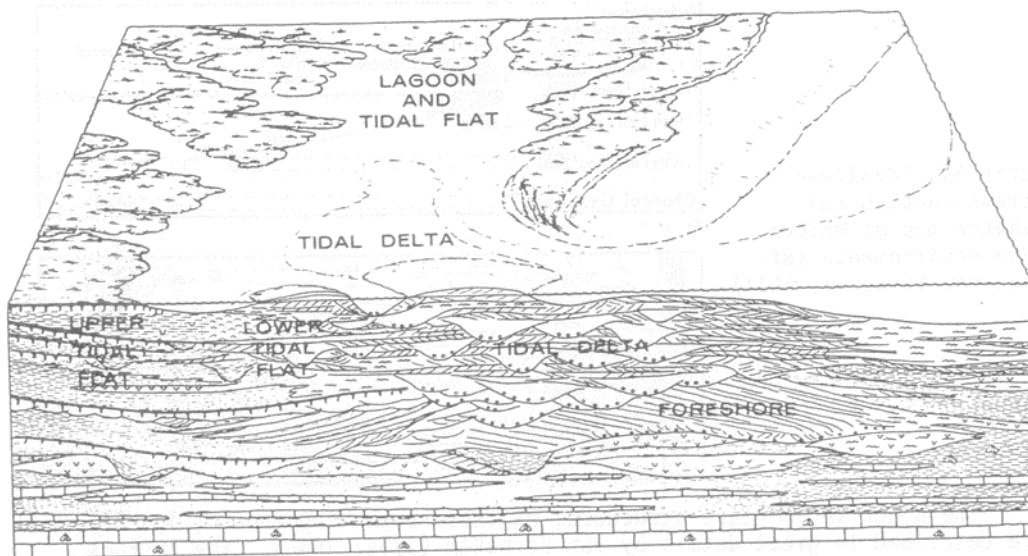


**Figure 2-2. This cross section is an example of the complex geology that can result from a changing coastal environment. (Figure from Fenn in Saxena, 1976, Fig. 2)**

The surface unit in the area is the Wando Formation. The Wando Formation lithology is variable and includes both fluvial and estuarine facies. Typically these include coarse-grained, poorly sorted, cross-bedded sands and clayey, fine- to medium-grained quartz sands, sandy to clayey silts, and sandy to silty clays (Gohn et al., 2000).

At a depth of about 40 ft the Ashley Formation is present. This unit is referred to in characterization reports as the Cooper Marl. The Ashley Formation consists of a relatively homogeneous section of calcareous, phosphatic, microfossiliferous, silty and sandy clays deposited in a fluvial and estuarine environment.

### 2.2.2 Site Hydrogeology

The total area of the contaminant release site, referred to as Solid Waste Management Unit 12 (SWMU 12), is approximately 3 acres. SWMU 12 is relatively flat with a total relief ranging from 3.0 to 8.5 feet above mean sea level. The water table is very shallow, ranging from 2 to 3 feet below ground surface. Danielsen (2003) interprets the ground-water flow to be primarily toward the east with a minor northerly component, except in wet periods, where it flows toward the northern marsh with a slight easterly component (Figure 2-3).

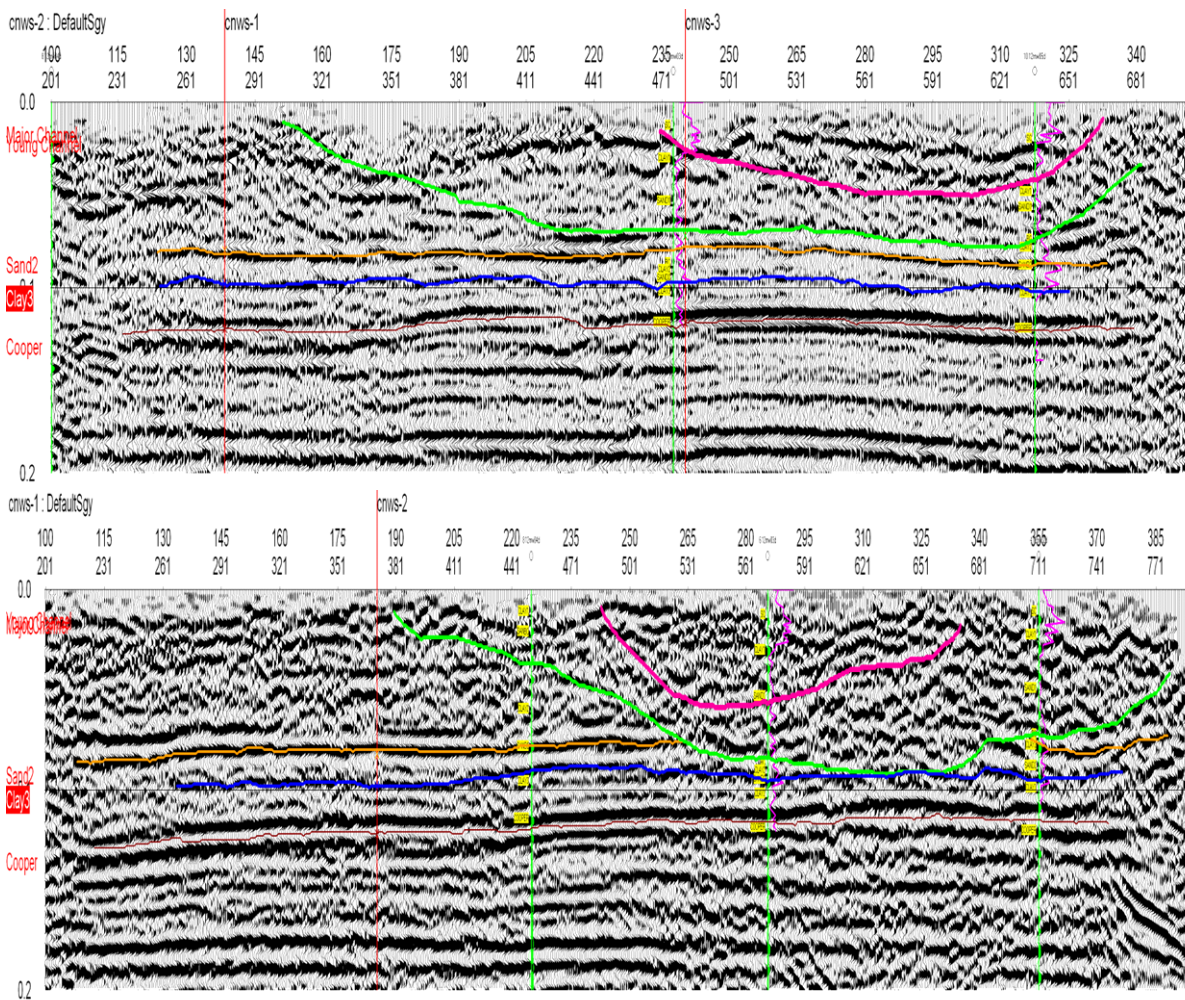


Figure 2-3. Map of SWMU 12 showing locations of wells and nearby marshes (Danielsen, 2003).

In down-gradient parts of the plume, a shallow clay layer does not allow the contaminants to encounter water until a depth of about 8 to 10 ft below ground surface. The contaminated aquifer consists of fine sand beneath clay. The average horizontal

hydraulic conductivity of the aquifer is approximately 1.2 ft/day (DOD, 2005). The potentiometric surface is relatively flat lying, with an average hydraulic gradient of 0.0015 to 0.0017 ft/ft. Recharge most likely occurs primarily through infiltration in areas where the surficial clay is breached or absent (DOD, 2005).

Seismic evidence suggests that parts of the sand aquifer may be ancient buried channels (Figure 2-4 and Figure 2-5). This hypothesis is supported by hydraulic conductivity estimates from slug test data (Table 2-1). When the hydraulic conductivity is graphed verses the cumulative percentage of samples having that value or less (Figure 2-6), we can see two distinct sample populations, these populations correspond to where the slope of the line changes. We interpret the higher conductivity values to belong to wells screened in the channels.



**Figure 2-4. Seismic reflection profiles. The green line is interpreted as the base of the major channel or the older channel, the red line indicates the base of younger channel that has incised into the older channel.**

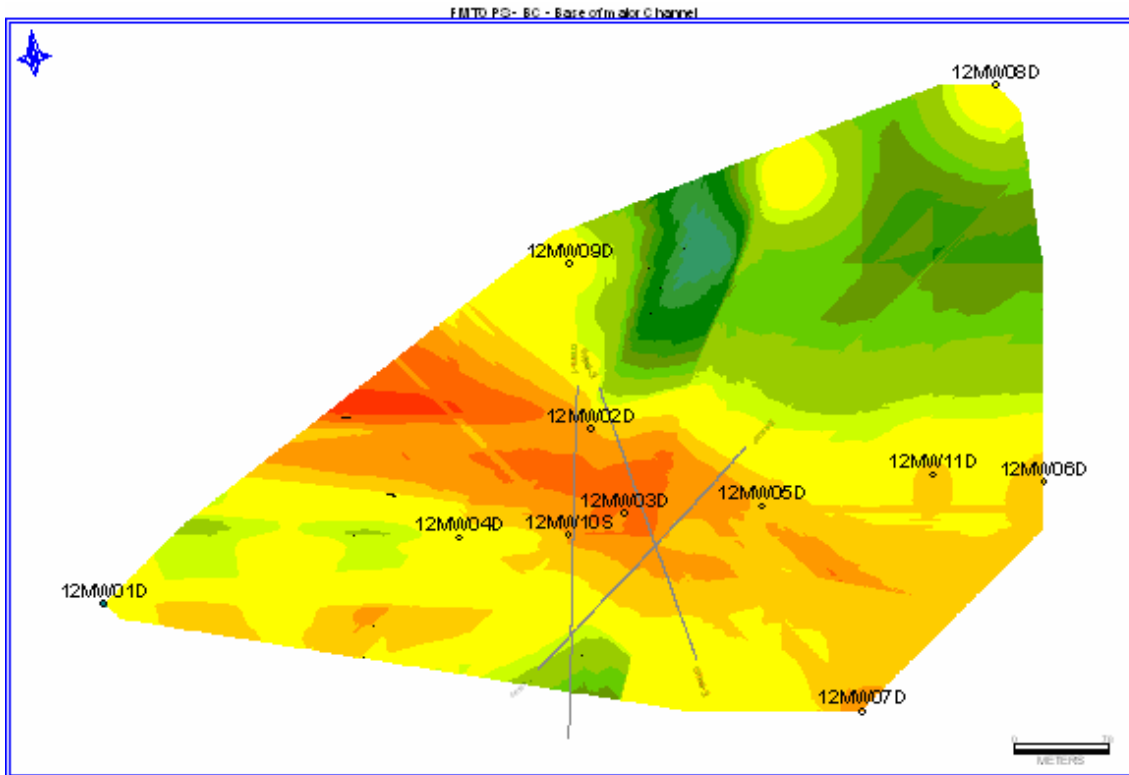


Figure 2-5. Elevation of the base of the channel contoured from seismic data and well picks. The orange shows the lower elevations, the green shows the higher elevations, and the grey lines represent the seismic profile locations.

Table 2-1. Slug test data compared to the number of hammer blows needed to penetrate 1 ft, averaged over the length of the screen zone.

Well	Screen Zone Depth (ft)	Average Blow Counts	Slug test results (ft/d)
12mw01D	29-39	3.43	2.86
12mw01S	4-14	3.95	3.69
12mw02D	21-31	2.38	2.98
12mw02S	4-14	5.14	1.06
12mw03D	20-30	2.29	3.19
12mw03S	4-14	6.10	4.19
12mw04D	22-32	3.19	1.47
12mw04S	4-14	4.00	7.22
12mw05D	38.5-48.5	0.69	0.432
12mw05S	4-14	4.46	3.7
12mw06D	32-42	1.48	0.36
12mw06S	4-14	5.46	0.0873
12mw07D	35-45	1.52	0.19
12mw07S	4-14	2.29	0.93
12mw08D	29-39	0.29	0.073
12mw08S	4-14	5.96	0.17
12mw09D	26-36	1.48	5.3
12mw09S	4-14	4.96	3.2

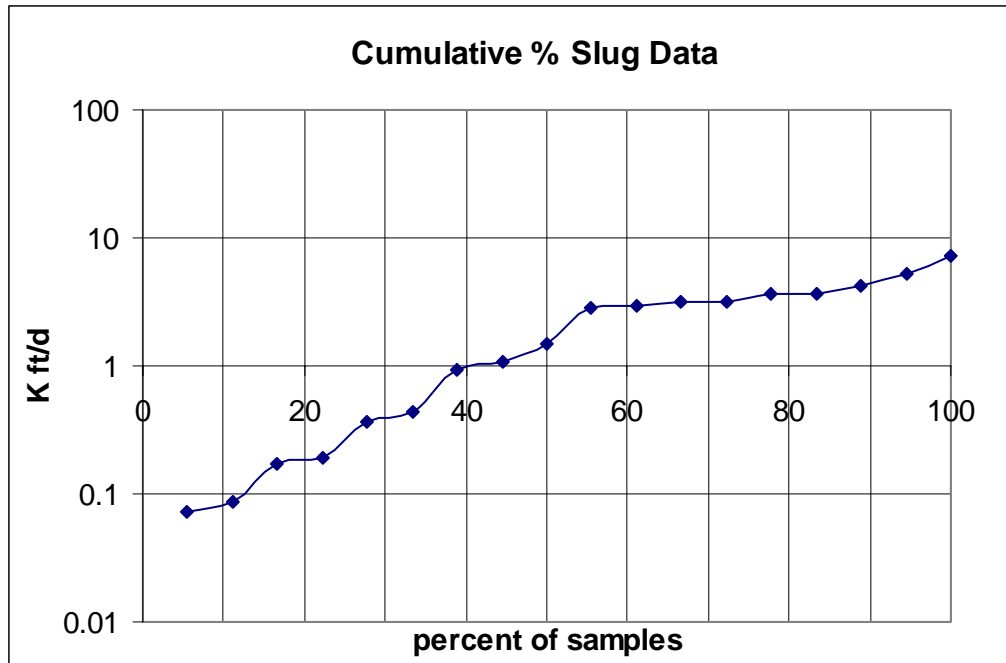


Figure 2-6. Graph of data from the slug test, with hydraulic conductivity (ft/d) on the vertical axis and the cumulative percentage of samples having that value or less plotted on the horizontal axis.

## 2.3 Conceptual Site Modeling

Prior to modeling, the data must be collected and formatted to allow for sequential modeling using a graded approach. Our approach began with a simple Conceptual Site Model that honored existing data. The CSMs were gradually increased in complexity until the model output adequately represented the flow regime for the site as judged by comparison of predicted contaminant levels with monitoring results. In total, three conceptual models were developed. Each of these models is discussed in detail below.

### 2.3.1 First Approach: Analytical Model:

The first approach assumed a one-layer homogeneous aquifer structure with semi-infinite boundary conditions (Figure 2-7). An analytical solution of the reactive solute transport can be obtained with BIOCHLOR (Aziz et al., 2000). The results completely failed to match the plume data. Multiple iterations using different parameters failed to achieve results that matched the field conditions at the site.

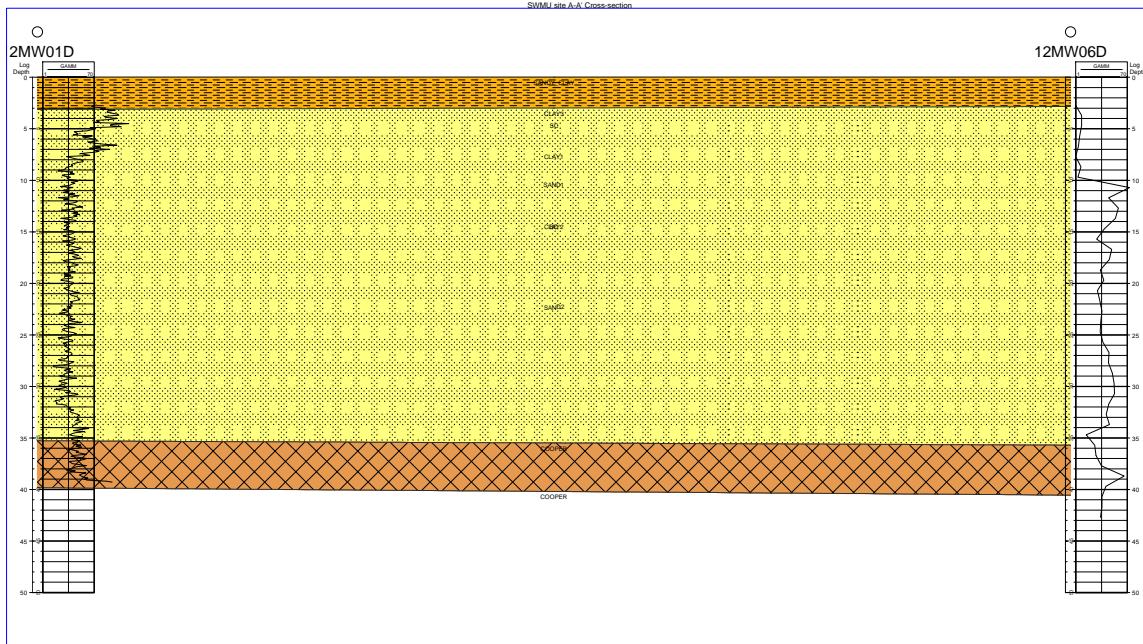


**Figure 2-7. Cross Section of the assumed geology for the analytical solution CSM.**

### **2.3.2 Second Approach: Numerical Model / Simple Geology:**

The second approach used only borehole descriptions and geophysical log data to develop the CSM. This model incorporated a layer-cake multi-aquifer system (Figure 2-8). Petra was used to perform the correlations that were exported into GMS for modeling. In GMS MODFLOW and RT3D were used to simulate the migration of the chlorinated solvents.

The results from Model II yielded a better fit than the first approach but did not adequately define the plume (Figure 2-9).

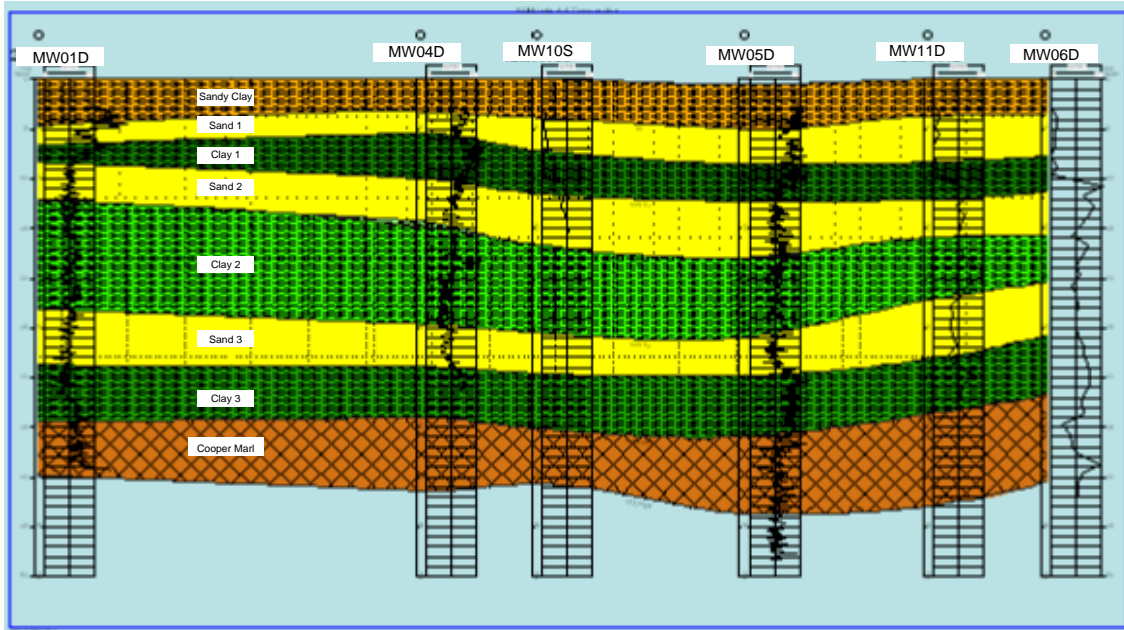


Figure 2-8. Cross Section of the “Layer Cake Geology” used for our second approach.

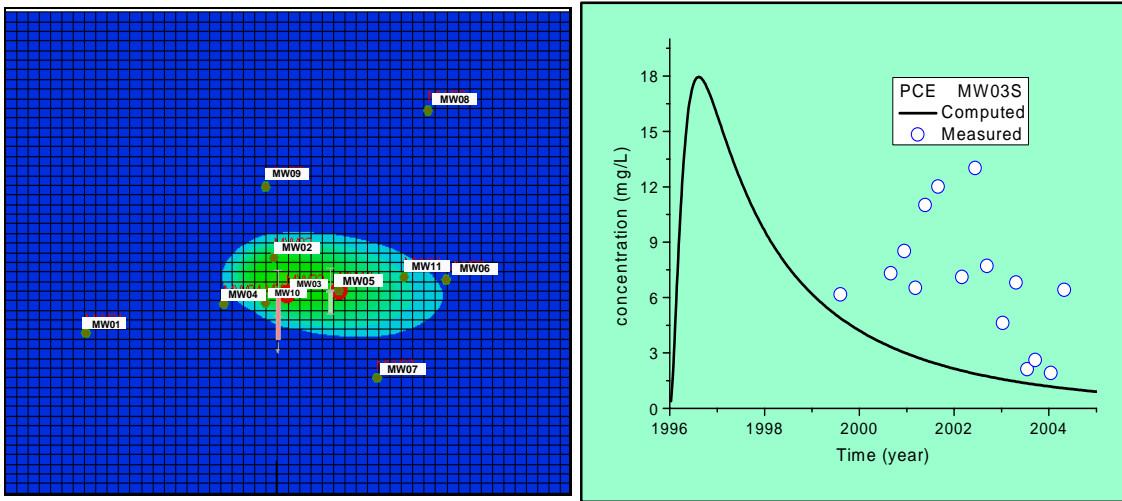
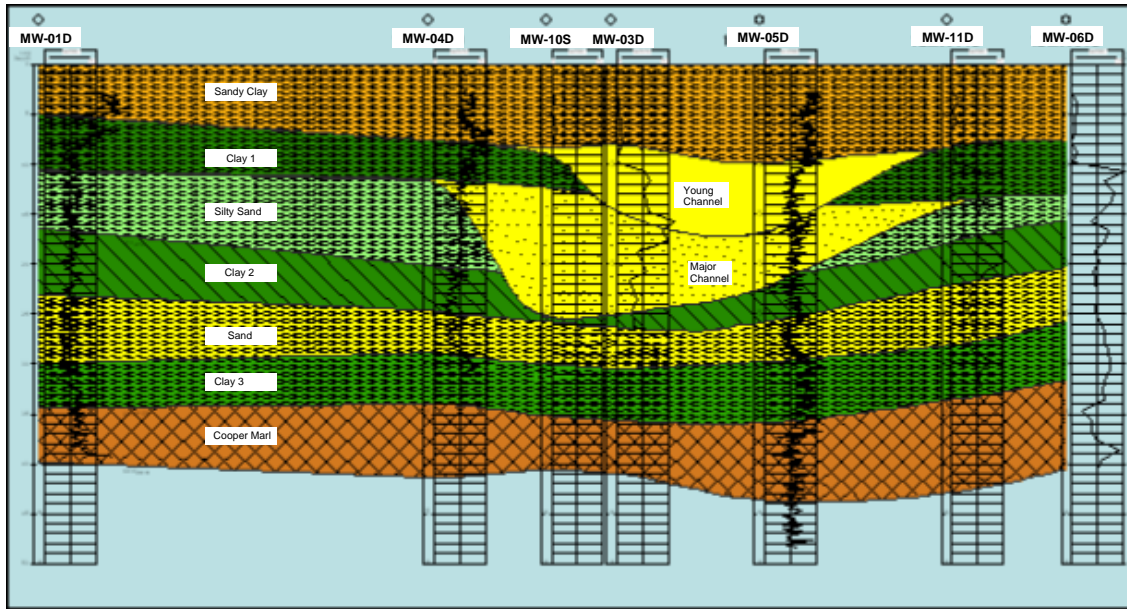


Figure 2-9. The PCE plume from Model II is presented at left, and the computed PCE concentrations at monitoring well MW-03 are much lower than the observed values (right).

### 2.3.3 Third Approach: Numerical Model / Complex Geology

The third approach entailed development of a site model that incorporated both the geologic and seismic data in an attempt to more accurately represent the subsurface geology. These data were input into Petra and PetraSeis (Figure 2-10). Table 2-2 contains the input parameters for Model III. Based on the seismic data two ancient stream channels were mapped through the middle of the PCE source. The channels control the local ground-water flow direction and provide a preferential chemical transport pathway. This new interpretation of the conceptual site model was used to run simulations again in GMS.



**Figure 2-10.** The cross-section shows the Major channel and Younger channel, as well as the other hydrofacies in the site.

By using a relatively high Horizontal K, and a low Kd for both of the channels (Table 2-2), model output from the third simulation closely matched observed PCE concentrations and accurately predicted the direction and extent of the plume (Figure 2-11).

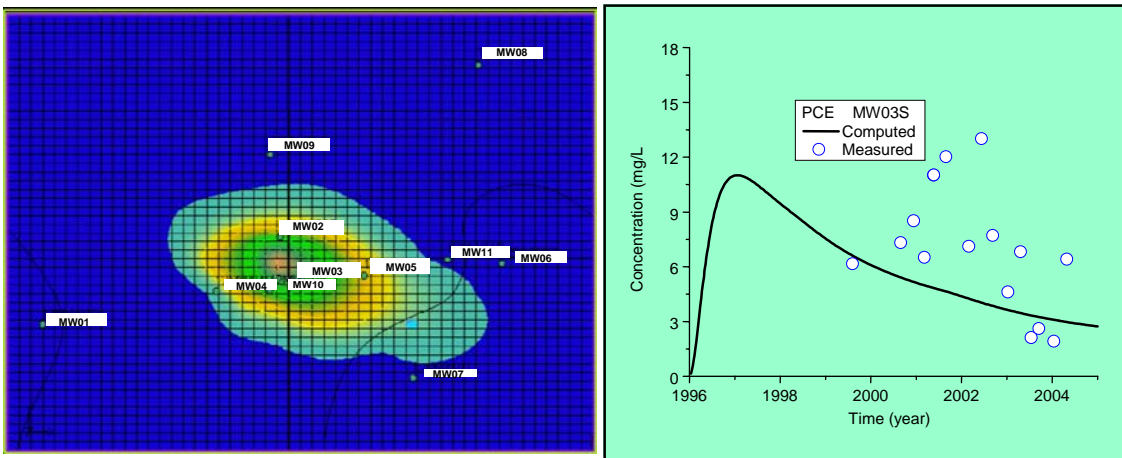


**Figure 2-11.** The simulated PCE plume from Model III is presented at left; computed PCE concentrations at monitoring well MW-03 more closely match observed values (right).

**Table 2-2. Estimated flow and transport parameters for Model III.**

Stratigraphic units	Horizontal K (ft/d)	Vertical K (ft/d)	Long dispersivity	PCE K <sub>d</sub> (mL/g)	TCE K <sub>d</sub> (mL/g)
Sandy clay	0.085	0.05	65	1.15	0.96
Young channel	48	1.2	112	0.43	0.28
Clay 1	0.06	0.01	83	1.36	0.84
Major channel	41	1	98	0.48	0.35
Silty sand	0.2	0.1	75	1.18	0.91
Clay 2	0.05	0.009	50	1.28	0.82
Sand	8	2	50	0.99	0.60
Clay 3	0.005	0.001	50	1.28	0.60
Cooper marl	0.2	0.05	50	1.15	0.96

## ***2.4 Designing a Performance Confirmation Monitoring Network***

After validation of the CSM with actual site data, AES used this model to determine an appropriate monitoring scheme for the contaminant plume. Specifically, the current monitoring program included four wells located outside the predicted 5-year footprint of the PCE plume (see circled wells in Figure 2-12). Removal of these 4 wells from future monitoring is recommended. The monitoring scheme also lacked any monitoring in the vicinity of the predicted plume head. A new monitoring point was recommended to be added at the yellow dot in Figure 2-12.

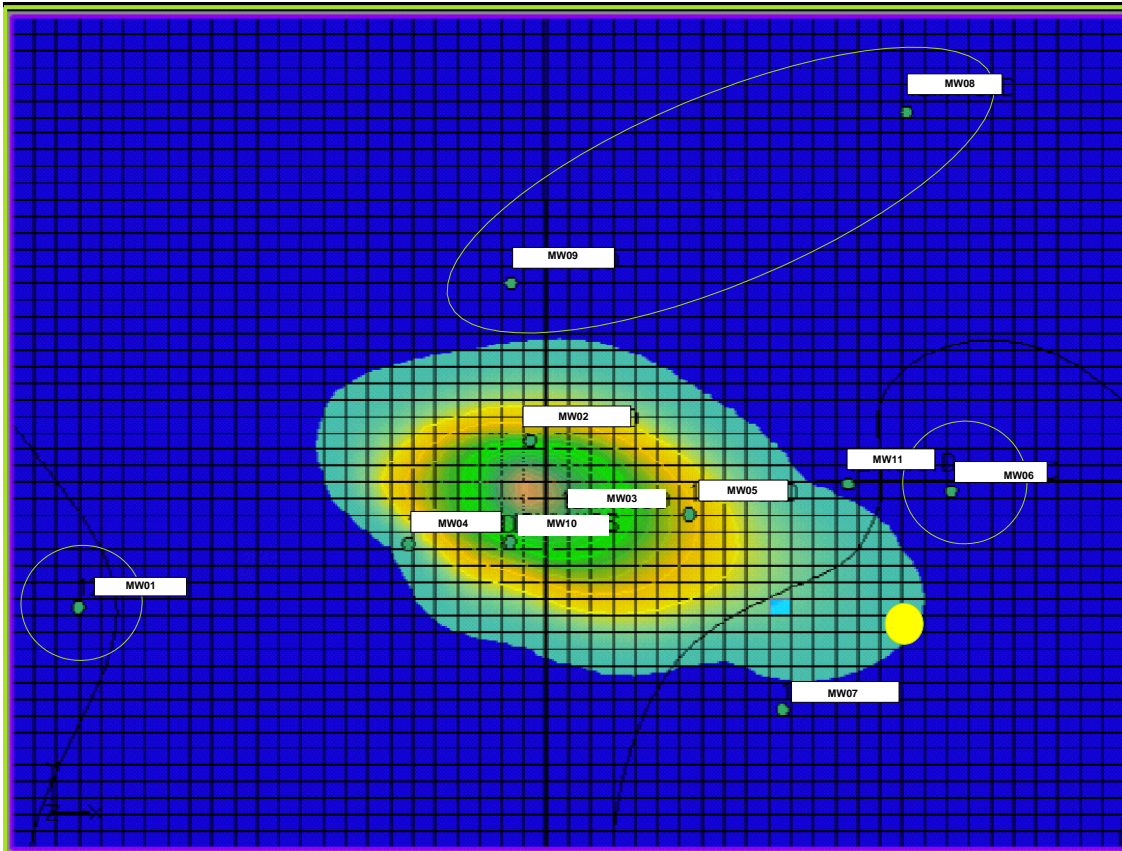


Figure 2-12. The predicted PCE plume in five years. Circled wells are suggested to be removed from the monitoring program to save money, while a new point is suggested to be added at the yellow dot to test the CSM and simulation results.

### 2.4.1.1 Alternate Conceptual Site Model

Further review of water level data (Table 2-3), revealed that MW-08 was an outlier because the water levels did not follow the same patterns as the other wells (Figure 2-13). Because of the nearly flat water table, the water level differences in MW-08 can seriously alter contour maps of the water table (Figure 2-14 and Figure 2-15).

This well should be investigated to determine the cause of the observed water level discrepancies. If the discrepancies are caused by poor well construction or poor data quality, then the water levels in this well should be ignored. If, however, the data proves reliable, this well could indicate the need to further revise the CSM. In particular, close attention should be paid to how the ground-water flow changes with respect to climatic conditions.

**Table 2-3. Water elevations (ft above MSL) in wells.**

Well Name	Apr-98	Jun-98	Aug-99	Jul-04	May-05
12MW01S	5.34	3.32	3.39		
12MW02S	5.26	3.16	3.29		2
12MW03S	5.27	3.16	3.3	2.74	2.07
12MW04S	5.35	3.23	3.4	2.72	2.14
12MW05S			3.19	2.52	1.79
12MW06S			2.65	2.47	1.71
12MW07S			3.14	2.53	1.82
12MW08S			3.61	3.81	1.25
12MW09S			3.28	2.67	1.88

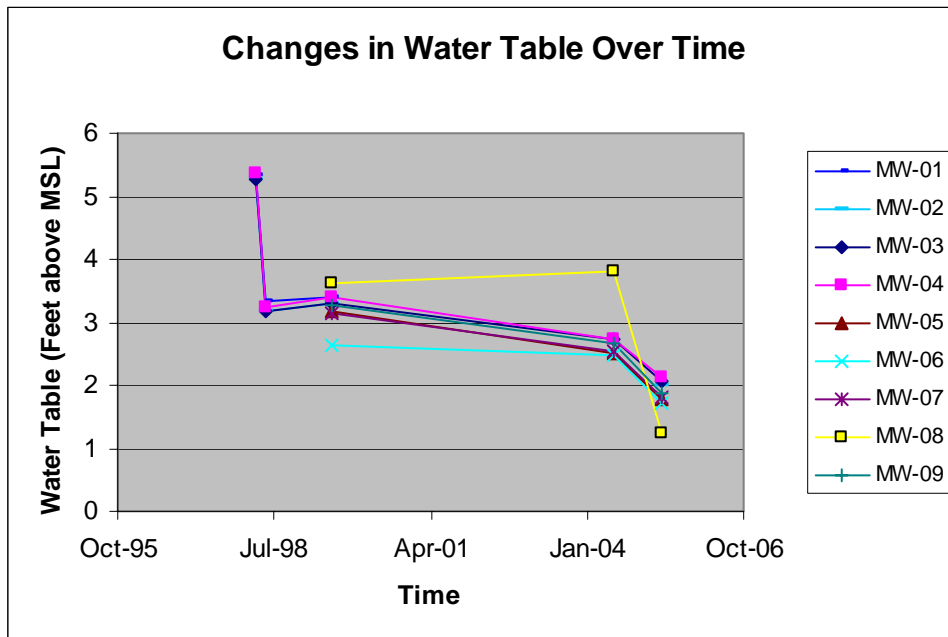


**Figure 2-13. Change in water table over time. Note how MW-08 is the only well that doesn't match the others.**

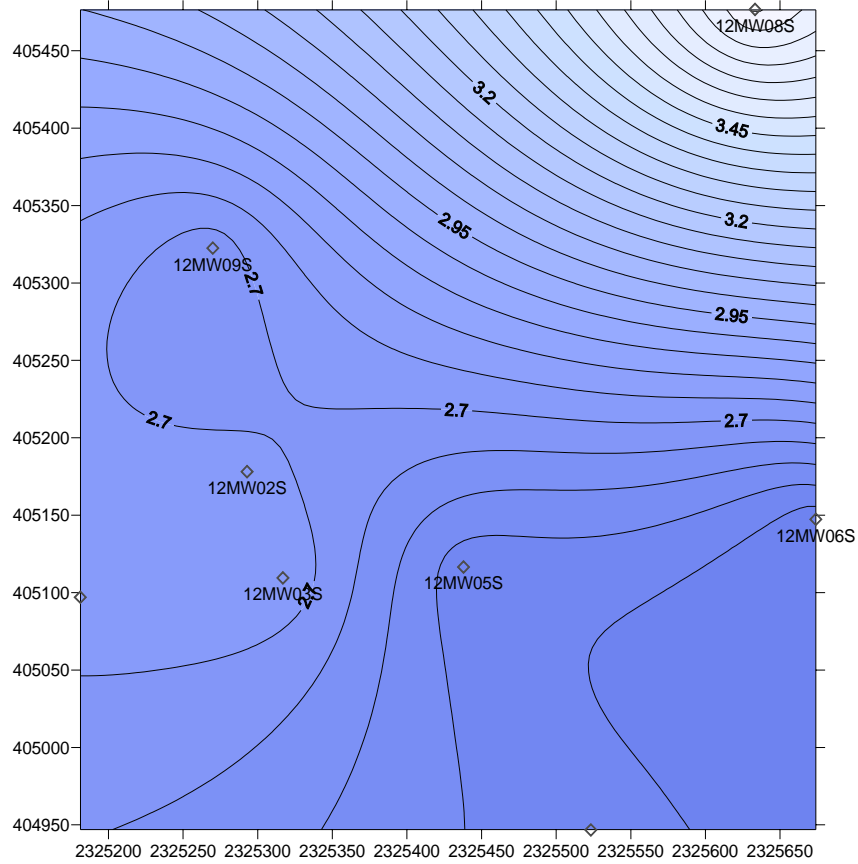


**Figure 2-14. Contour Map of water table using data from July 2004 (feet above MSL)**

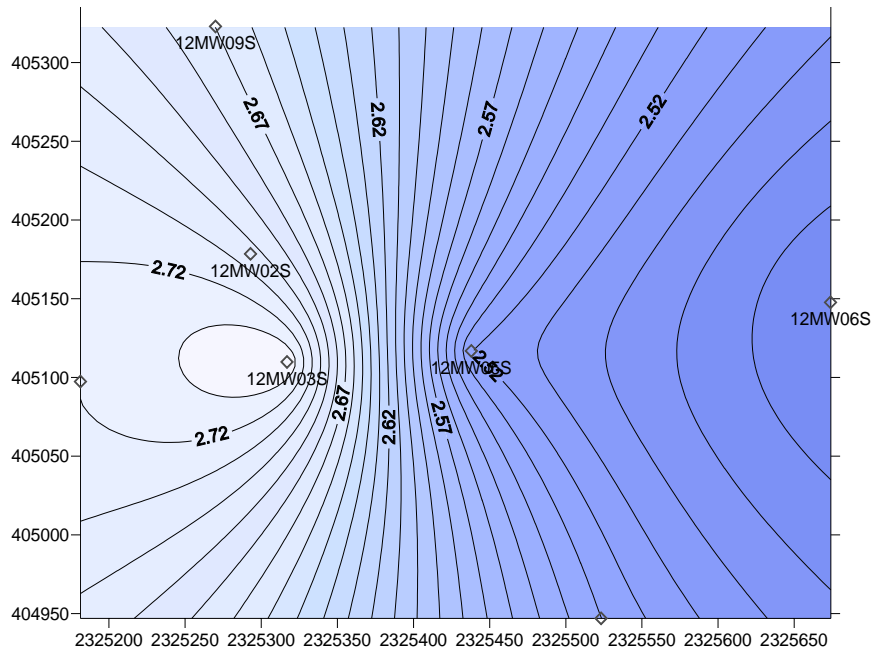


**Figure 2-15. Contour map of water table using data from July 2004, without well MW-08 (feet above MSL)**

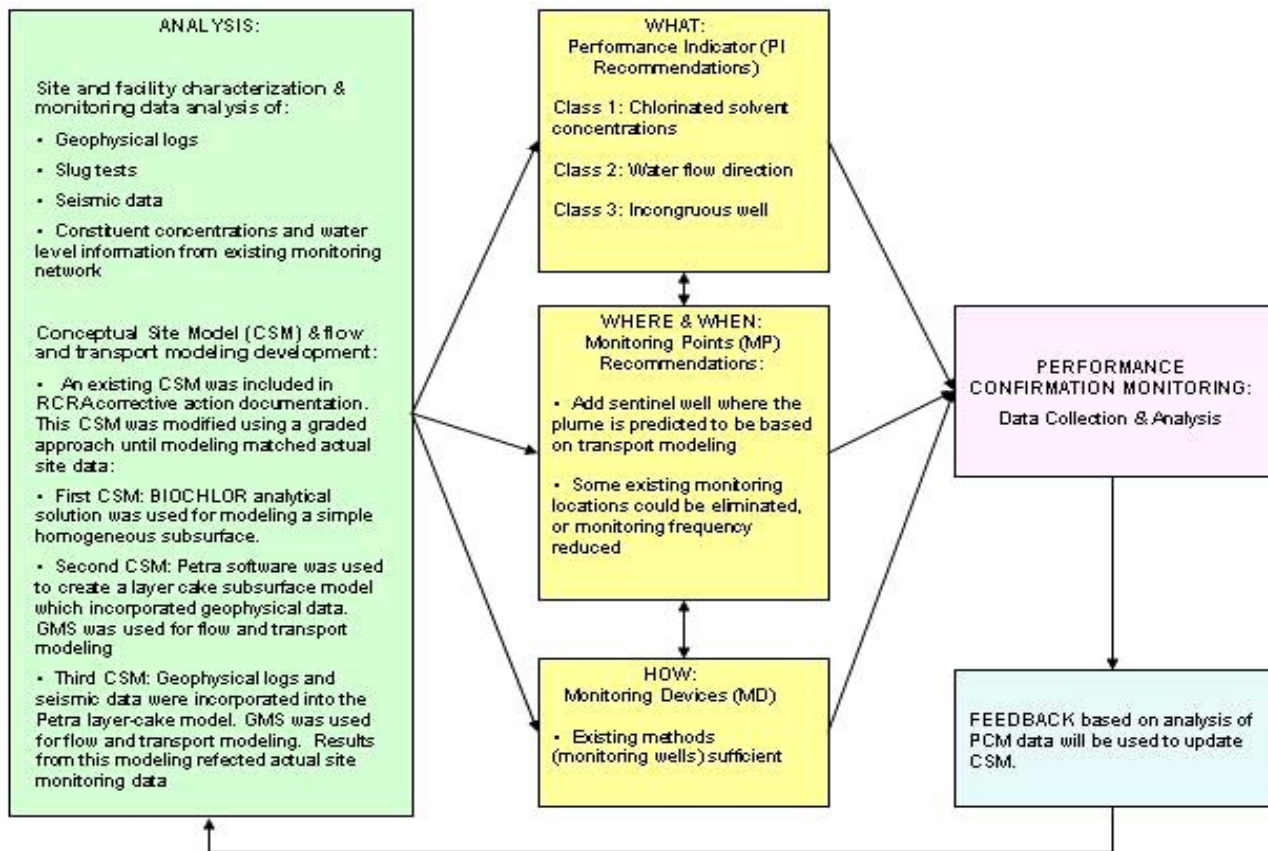
## **2.5 Strategy Application Conclusions**

This study demonstrates the importance of adequate conceptual site modeling as a tool to assess monitoring network performance. In this case, the conceptual site model simulation helped improve understanding of the extent of contamination and guided suggestions which may increase efficiency of the existing monitoring scheme and, significantly reduce monitoring costs. Specifically in this case, four monitoring wells were removed from the network, and one was added in order to better observe the plume frontier.

Outcome from this case suggests that the bias and uncertainty introduced from inadequate conceptual models can exceed those introduced from an inadequate choice of model parameter values. In particular, adequate mapping of the subsurface geology through incorporation of log and seismic survey data with geophysical software was important in developing an accurate conceptual site model.

Time trend analysis of water levels from monitoring wells results in very good correlation, with the exception of MW-08. The discrepancies between MW-08 and the other monitoring wells result in significant variations in the modeled water table surface. Because MW-08 has been identified as an outlier, these discrepancies should be evaluated.

Figure 2-16 presents a visual illustration of the activities and outcomes resulting from application of the Strategy at the Charleston Naval Weapons Station below.



### Charleston – Strategy Application Results

Figure 2-16. Activities and results of the Strategy application at Charleston Naval Weapons Station

## **2.6 Charleston References**

- Aziz, C.E., et al. EPA /600/R-00/008. "BIOCHLOR Version 1.0, User's Manual." 2000.
- Department of Defense. *Site Information for RDT&E Opportunities, Strategic Environmental Research and Development Program*. November 2005.
- Ferm, J.C.. *Depositional Model in Coal Exploration and Development, Sedimentary Environments and Hydrocarbons*, R.S. Saxena, ed. AAPG/NOGS Short Course, New Orleans Geological Society. pp. 60–78. 1976.
- Gohn, G.S., et al. "Preliminary Stratigraphic Database for the Subsurface Tertiary and Uppermost Cretaceous Sediments of Dorchester County, South Carolina." U.S. Geological Survey Open-File Report 00-049-A. 2000.
- Danielsen, M.W. *The Use and Implementation of Innovative Technologies for Investigating Selected Sites at the Naval Weapons Station, Charleston, South Carolina*. Master Thesis for University of South Carolina. 2003.
- Weems, R.E., and E.M., Jr. Lemon. *Geologic Map of the Cainhoy, Charleston, Fort Moultrie, and North Charleston quadrangles, S.C., with text (1:24,000)*. U.S. Geological Survey Map I-1935. 1993.

***Appendix 2-A.***

Summary of Selected Volatile Organic Compounds in Ground Water

**SWMU 12 Naval Weapons Station, Charleston**

Location ID	Sample Date	PCE ug/L	TCE ug/L	cis-1,2-DCE ug/L	Vinyl Chloride ug/L	1,1,1-TCA ug/L	1,1-DCE ug/L	1,1-DCA ug/L	1,2-DCA ug/L
12MW02D	8/30/00	< 5	< 5	< 5	< 2	< 5	< 5	< 5	< 5
12MW02D	11/29/00	< 0.21	< 0.17	< 0.17	< 0.15	< 0.18	0.22	< 0.18	< 0.21
12MW02D	2/27/01	< 0.13	< 0.14	< 0.24	< 0.17	< 0.22	< 0.16	< 0.23	< 0.2
12MW02D	5/15/01	< 0.38	1.5	< 0.31	< 0.19	< 0.27	< 0.26	< 0.29	< 0.35
12MW02D	8/29/01	< 0.13	< 0.14	< 0.24	< 0.17	< 0.22	0.32	< 0.23	< 0.2
12MW02D	12/3/01	< 0.13	< 0.14	< 0.24	< 0.17	< 0.22	< 0.16	< 0.23	< 0.2
12MW02D	2/28/02	< 0.13	< 0.14	< 0.24	< 0.17	< 0.22	< 0.16	< 0.23	< 0.2
12MW02D	6/10/02	< 0.1	< 0.13	< 0.28	< 0.18	< 0.17	< 0.13	< 0.64	< 0.15
12MW02D	9/9/02	2.1	1.2	0.25	< 0.2	0.52	1.2	0.39	< 0.18
12MW02D	1/8/03	0.2	0.36	< 0.28	< 0.18	< 0.17	0.35	< 0.64	< 0.15
12MW02D	4/15/03	< 0.17	< 0.12	< 0.22	< 0.1	< 0.16	< 0.17	< 0.11	< 0.14
12MW02D	7/16/03	< 0.31	< 0.25	< 0.4	< 0.11	< 0.27	< 0.41	< 0.3	< 0.34
12MW02D	8/16/04	< 0.31	< 0.25	< 0.4	< 0.11	< 0.27	< 0.41	< 0.3	< 0.34
12MW02S	8/30/00	0	0	0	0	0	200	12	0
12MW02S	11/29/00	< 0.21	0.24	0.75	< 0.15	< 0.18	110	5.7	< 0.21
12MW02S	2/27/01	< 1.3	< 1.4	< 2.4	< 1.7	< 2.2	160	8.6	< 2
12MW02S	5/15/01	< 3.8	6.4	< 3.1	< 1.9	< 2.7	81	5.4	< 3.5
12MW02S	8/29/01	< 0.21	4.8	< 0.56	< 0.35	< 0.33	23	2.1	< 0.3
12MW02S	12/3/01	< 0.25	0.47	0.66	< 0.35	< 0.44	69	5.5	< 0.39
12MW02S	2/28/02	< 0.63	< 0.68	< 1.2	< 0.87	< 1.1	46	2.8	< 0.98
12MW02S	6/10/02	< 0.52	< 0.64	< 1.4	< 0.88	< 0.84	84	6.7	< 0.76
12MW02S	9/9/02	< 0.82	< 0.83	< 1	< 0.99	< 1.3	58	5.4	< 0.88
12MW02S	1/8/03	< 0.52	2.3	1.6	< 0.88	< 0.84	130	15	< 0.76
12MW02S	4/15/03	< 2.2	< 1.5	2.9	< 1.3	< 2.1	250	27	< 1.8
12MW02S	7/15/03	< 3.1	< 2.5	< 4	< 1.1	< 2.7	100	14	< 3.4
12MW02S	9/17/03	< 1.7	2.1	< 2.2	2.8	< 1.6	150	26	< 1.4
12MW02S	1/14/04	< 2.2	< 1.5	< 2.7	< 1.3	< 2.1	140	29	< 1.8
12MW02S	4/28/04	< 2.6	11	11	3.4	< 2.4	530	200	< 2.7
12MW02S	8/16/04	< 0.31	< 0.25	< 0.4	< 0.11	< 0.27	1.9	< 0.3	< 0.34
12MW03D	8/30/00	0	6	18	0	0	0	0	0
12MW03D	11/30/00	< 0.41	5.8	24	< 0.31	< 0.36	0.99	< 0.35	< 0.42
12MW03D	2/27/01	< 0.13	1.4	6.8	< 0.17	< 0.22	0.54	< 0.23	< 0.2
12MW03D	5/15/01	6	15	15	0.88	9.8	7.5	1.6	< 0.35
12MW03D	8/29/01	< 0.1	12	19	0.73	< 0.17	2.7	< 0.64	< 0.15
12MW03D	12/4/01	< 0.1	33	44	1.3	< 0.17	6.3	< 0.64	< 0.15
12MW03D	3/1/02	< 0.13	3.3	13	0.2	< 0.22	1.2	< 0.23	< 0.2
12MW03D	6/11/02	< 0.1	19	21	< 0.18	< 0.17	3.2	< 0.64	< 0.15
12MW03D	9/10/02	0.7	4.6	14	0.3	0.57	2.1	0.45	< 0.18
12MW03D	1/9/03	< 0.1	2	11	0.73	< 0.17	1.2	< 0.64	< 0.15
12MW03D	4/15/03	< 0.31	3.2	11	0.65	< 0.27	1.9	1.8	< 0.34
12MW03D	7/15/03	< 0.17	3.3	13	0.82	< 0.16	1.9	1.5	< 0.14
12MW03D	8/16/04	< 0.31	4	16	1.8	< 0.27	4.3	4.7	< 0.34
12MW03S	8/30/00	7300	9,500	7,600	1,600	16,000	4,500	4,000	2,300
12MW03S	11/30/00	8500	9000	7000	160	31000	11000	5100	< 170
12MW03S	2/27/01	6500	5200	12000	230	3700	3100	2100	< 200
12MW03S	5/15/01	11000	7900	8900	< 940	76000	29000	20000	< 1700

12MW03S	8/29/01	12000	16000	12000	< 880	73000	34000	23000	< 760
12MW03S	12/5/01	16000	12000	14000	< 880	92000	46000	35000	< 760
12MW03S	3/1/02	7100	5600	13000	600	5300	5400	4500	< 200
12MW03S	6/11/02	13000	5900	13000	1100	32000	20000	16000	260
12MW03S	9/10/02	7700	4700	13000	430	5200	6100	5300	< 190
12MW03S	1/9/03	4600	4300	7300	370	4000	5100	3300	45
12MW03S	4/21/03	6800	3600	9900	640	15000	12000	8800	150
12MW03S	7/17/03	2100	1900	3100	140	580	1200	960	< 85
12MW03S	9/16/03	2600	1400	2800	120	1700	2300	1200	< 50
12MW03S	1/14/04	1900	3000	3300	150	940	1700	1000	< 17
12MW03S	4/27/04	6400	5300	5700	380	8100	10000	5100	65
12MW03S	8/18/04	1200	1400	1700	96	370	1000	590	< 27
12MW04D	8/28/00	< 5	< 5	< 5	< 2	< 5	< 5	< 5	< 5
12MW04D	11/28/00	< 0.21	< 0.17	< 0.17	< 0.15	< 0.18	< 0.17	< 0.18	< 0.21
12MW04D	2/26/01	< 0.13	< 0.14	< 0.24	< 0.17	< 0.22	< 0.16	< 0.23	< 0.2
12MW04D	5/14/01	< 0.38	< 0.34	< 0.31	< 0.19	< 0.27	< 0.26	< 0.29	< 0.35
12MW04D	8/27/01	< 0.38	< 0.34	< 0.31	< 0.19	< 0.27	< 0.26	< 0.29	< 0.35
12MW04D	12/3/01	< 0.1	< 0.13	< 0.28	< 0.18	< 0.17	< 0.13	< 0.64	< 0.15
12MW04D	2/28/02	< 0.13	< 0.14	< 0.24	< 0.17	< 0.22	< 0.16	< 0.23	< 0.2
12MW04D	6/11/02	< 0.1	< 0.13	< 0.28	< 0.18	< 0.17	< 0.13	< 0.64	< 0.15
12MW04D	9/9/02	< 0.16	< 0.17	< 0.2	< 0.2	< 0.26	< 0.33	< 0.24	< 0.18
12MW04D	1/7/03	< 0.1	< 0.13	< 0.28	< 0.18	< 0.17	< 0.13	< 0.64	< 0.15
12MW04D	4/15/03	< 0.31	0.28	< 0.4	< 0.11	< 0.27	< 0.41	< 0.3	< 0.34
12MW04D	7/14/03	< 0.17	< 0.12	< 0.22	< 0.1	< 0.16	< 0.17	< 0.11	< 0.14
12MW04D	8/18/04	< 0.2	< 0.2	< 0.15	< 0.15	< 0.19	< 0.18	< 0.2	< 0.22
12MW04S	8/28/00	< 5	< 5	< 5	< 2	< 5	< 5	< 5	< 5
12MW04S	11/28/00	< 0.21	< 0.17	< 0.17	< 0.15	< 0.18	< 0.17	< 0.18	< 0.21
12MW04S	2/26/01	< 0.13	< 0.14	< 0.24	< 0.17	< 0.22	< 0.16	< 0.23	< 0.2
12MW04S	5/14/01	< 0.38	< 0.34	< 0.31	< 0.19	< 0.27	< 0.26	< 0.29	< 0.35
12MW04S	8/27/01	< 0.38	< 0.34	< 0.31	< 0.19	< 0.27	< 0.26	< 0.29	< 0.35
12MW04S	12/3/01	< 0.1	< 0.13	< 0.28	< 0.18	< 0.17	< 0.13	< 0.64	< 0.15
12MW04S	2/28/02	< 0.13	< 0.14	< 0.24	< 0.17	< 0.22	< 0.16	< 0.23	< 0.2
12MW04S	6/11/02	< 0.1	< 0.13	< 0.28	< 0.18	< 0.17	< 0.13	< 0.64	< 0.15
12MW04S	9/9/02	< 0.16	< 0.17	< 0.2	< 0.2	< 0.26	< 0.33	< 0.24	< 0.18
12MW04S	1/7/03	< 0.1	< 0.13	< 0.28	< 0.18	< 0.17	< 0.13	< 0.64	< 0.15
12MW04S	4/15/03	< 0.31	< 0.25	< 0.4	< 0.11	< 0.27	< 0.41	< 0.3	< 0.34
12MW04S	7/14/03	< 0.17	< 0.12	< 0.22	< 0.1	< 0.16	< 0.17	< 0.11	< 0.14
12MW04S	9/16/03	< 0.17	< 0.12	< 0.22	< 0.1	< 0.16	< 0.17	< 0.11	< 0.14
12MW04S	1/12/04	< 0.31	< 0.25	< 0.4	< 0.11	< 0.27	< 0.41	< 0.3	< 0.34
12MW04S	4/26/04	< 0.31	< 0.25	< 0.4	< 0.11	< 0.27	< 0.41	< 0.3	< 0.34
12MW04S	8/18/04	< 0.31	< 0.25	< 0.4	< 0.11	< 0.27	< 0.41	< 0.3	< 0.34
12MW05D	8/30/00	< 5	9.6	6.2	< 2	< 5	< 5	< 5	< 5
12MW05D	11/30/00	3.1	5.3	2.5	< 0.15	1.4	2.6	< 0.18	< 0.21
12MW05D	2/28/01	< 0.13	1.8	1.4	< 0.17	< 0.22	0.68	< 0.23	< 0.2
12MW05D	5/15/01	< 0.38	1.8	2.1	< 0.19	< 0.27	0.83	< 0.29	< 0.35
12MW05D	8/28/01	< 0.1	0.55	3.5	< 0.18	< 0.17	0.97	< 0.64	< 0.15
12MW05D	12/4/01	< 0.13	1	0.75	< 0.17	< 0.22	0.3	< 0.23	< 0.2
12MW05D	3/1/02	< 0.13	0.74	0.76	< 0.17	< 0.22	0.37	< 0.23	< 0.2
12MW05D	6/11/02	< 0.1	0.89	0.97	< 0.18	< 0.17	0.39	< 0.64	< 0.15
12MW05D	9/10/02	< 0.16	0.56	0.54	< 0.2	< 0.26	< 0.33	< 0.24	< 0.18

12MW05D	1/8/03	< 0.1	0.64	0.39	< 0.18	< 0.17	0.34	< 0.64	< 0.15
12MW05D	4/15/03	< 0.31	0.47	< 0.4	< 0.11	< 0.27	< 0.41	< 0.3	< 0.34
12MW05I	8/30/00	< 5	< 5	< 5	< 2	< 5	< 5	< 5	< 5
12MW05I	11/30/00	12	20	23	0.43	23	12	3.3	< 0.42
12MW05I	2/28/01	0.46	0.73	1.1	< 0.17	0.33	0.46	< 0.23	< 0.2
12MW05I	5/16/01	0.86	0.71	0.31	< 0.19	1.4	0.6	< 0.29	< 0.35
12MW05I	8/29/01	0.7	0.73	< 0.31	< 0.19	0.48	0.59	< 0.29	< 0.35
12MW05I	12/4/01	< 0.13	1	< 0.24	< 0.17	< 0.22	0.25	< 0.23	< 0.2
12MW05I	3/1/02	< 0.13	1.5	< 0.24	< 0.17	< 0.22	0.4	< 0.23	< 0.2
12MW05I	6/11/02	< 0.1	1	< 0.28	< 0.18	< 0.17	0.35	< 0.64	< 0.15
12MW05I	9/10/02	0.17	0.63	< 0.2	< 0.2	< 0.26	< 0.33	< 0.24	< 0.18
12MW05I	1/8/03	< 0.1	0.61	< 0.28	< 0.18	< 0.17	< 0.13	< 0.64	< 0.15
12MW05I	4/15/03	< 0.31	0.3	< 0.4	< 0.11	< 0.27	< 0.41	< 0.3	< 0.34
12MW05I	7/14/03	< 0.17	0.37	< 0.22	< 0.1	< 0.16	< 0.17	< 0.11	< 0.14
12MW05I	8/18/04	< 0.31	< 0.25	< 0.4	< 0.11	< 0.27	< 0.41	< 0.3	< 0.34
12MW05S	8/30/00	580	27,000	1,500	33	640	10,000	66	13
12MW05S	11/30/00	400	22000	890	< 31	440	8500	< 35	< 42
12MW05S	2/28/01	270	12000	580	< 170	360	7100	< 230	< 200
12MW05S	5/16/01	500	16000	690	< 190	590	8900	< 290	< 350
12MW05S	8/29/01	3100	23000	1400	< 190	2600	16000	310	< 350
12MW05S	12/4/01	740	25000	1100	< 350	< 330	13000	< 1300	< 300
12MW05S	3/1/02	360	18000	800	< 350	< 440	9300	< 460	< 390
12MW05S	6/11/02	< 210	23000	1600	< 350	790	13000	< 1300	< 300
12MW05S	9/10/02	600	20000	1600	< 350	< 330	12000	< 1300	< 300
12MW05S	1/8/03	460	20000	1200	< 350	< 330	11000	< 1300	< 300
12MW05S	4/22/03	< 61	21000	1200	< 21	< 53	9400	< 60	< 68
12MW05S	7/17/03	740	20000	1200	< 210	< 330	10000	< 210	< 280
12MW05S	9/16/03	660	16000	1200	< 350	< 460	8900	< 430	< 400
12MW05S	1/14/04	620	18000	1200	< 21	230	8600	< 60	< 68
12MW05S	4/27/04	880	21000	1300	58	210	7800	36	< 34
12MW05S	8/18/04	910	22000	1400	120	290	9600	68	< 43
12MW06D	8/29/00	< 5	< 5	< 5	< 2	< 5	< 5	< 5	< 5
12MW06D	11/29/00	< 0.21	< 0.17	< 0.17	< 0.15	< 0.18	< 0.17	< 0.18	< 0.21
12MW06D	2/27/01	< 0.13	< 0.14	< 0.24	< 0.17	< 0.22	< 0.16	< 0.23	< 0.2
12MW06D	5/14/01	< 0.13	< 0.14	< 0.24	< 0.17	< 0.22	< 0.16	< 0.23	< 0.2
12MW06D	8/28/01	< 0.1	< 0.13	< 0.28	< 0.18	< 0.17	< 0.13	< 0.64	< 0.15
12MW06S	8/29/00	< 5	< 5	< 5	< 2	< 5	< 5	< 5	< 5
12MW06S	11/29/00	< 0.21	< 0.17	< 0.17	< 0.15	0.42	< 0.17	< 0.18	< 0.21
12MW06S	2/27/01	< 0.13	< 0.14	< 0.24	< 0.17	0.29	< 0.16	< 0.23	< 0.2
12MW06S	5/14/01	< 0.13	< 0.14	< 0.24	< 0.17	< 0.22	< 0.16	< 0.23	< 0.2
12MW06S	8/28/01	< 0.38	< 0.34	< 0.31	< 0.19	< 0.27	< 0.26	< 0.29	< 0.35
12MW06S	12/4/01	< 0.13	0.15	< 0.24	< 0.17	< 0.22	< 0.16	< 0.23	< 0.2
12MW06S	3/1/02	< 0.13	< 0.14	< 0.24	< 0.17	< 0.22	< 0.16	< 0.23	< 0.2
12MW06S	6/11/02	< 0.1	< 0.13	< 0.28	< 0.18	< 0.17	< 0.13	< 0.64	< 0.15
12MW06S	9/9/02	< 0.16	< 0.17	< 0.2	< 0.2	< 0.26	< 0.33	< 0.24	< 0.18
12MW06S	1/7/03	< 0.16	< 0.17	< 0.2	< 0.2	< 0.26	< 0.33	< 0.24	< 0.18
12MW06S	4/15/03	< 0.31	< 0.25	< 0.4	< 0.11	< 0.27	< 0.41	< 0.3	< 0.34
12MW07D	8/28/00	< 5	< 5	< 5	< 2	< 5	< 5	< 5	< 5
12MW07D	11/29/00	< 0.21	< 0.17	< 0.17	< 0.15	< 0.18	< 0.17	< 0.18	< 0.21
12MW07D	2/26/01	< 0.13	< 0.14	< 0.24	< 0.17	< 0.22	< 0.16	< 0.23	< 0.2

12MW07D	5/14/01	< 0.13	< 0.14	< 0.24	< 0.17	< 0.22	< 0.16	< 0.23	< 0.2
12MW07D	8/29/01	1	0.44	< 0.31	< 0.19	0.7	0.78	< 0.29	< 0.35
12MW07S	8/28/00	< 5	< 5	< 5	< 2	< 5	< 5	< 5	< 5
12MW07S	11/28/00	< 0.21	< 0.17	< 0.17	< 0.15	< 0.18	< 0.17	< 0.18	< 0.21
12MW07S	2/26/01	< 0.13	< 0.14	< 0.24	< 0.17	< 0.22	< 0.16	< 0.23	< 0.2
12MW07S	5/14/01	< 0.13	< 0.14	< 0.24	< 0.17	< 0.22	< 0.16	< 0.23	< 0.2
12MW07S	8/29/01	0.77	0.38	< 0.31	< 0.19	0.55	0.67	< 0.29	< 0.35
12MW08D	8/29/00	< 5	< 5	< 5	< 2	< 5	< 5	< 5	< 5
12MW08D	11/28/00	< 0.21	< 0.17	< 0.17	< 0.15	< 0.18	< 0.17	< 0.18	< 0.21
12MW08D	2/26/01	< 0.13	< 0.14	< 0.24	< 0.17	< 0.22	< 0.16	< 0.23	< 0.2
12MW08D	5/14/01	< 0.38	< 0.34	< 0.31	< 0.19	< 0.27	< 0.26	< 0.29	< 0.35
12MW08D	8/27/01	< 0.38	< 0.34	< 0.31	< 0.19	< 0.27	< 0.26	< 0.29	< 0.35
12MW08S	8/28/00	< 5	< 5	< 5	< 2	< 5	< 5	< 5	< 5
12MW08S	11/28/00	< 0.21	< 0.17	< 0.17	< 0.15	< 0.18	< 0.17	< 0.18	< 0.21
12MW08S	2/26/01	< 0.13	< 0.14	< 0.24	< 0.17	< 0.22	< 0.16	< 0.23	< 0.2
12MW08S	5/14/01	< 0.38	< 0.34	< 0.31	< 0.19	< 0.27	< 0.26	< 0.29	< 0.35
12MW08S	8/27/01	< 0.38	< 0.34	< 0.31	< 0.19	< 0.27	< 0.26	< 0.29	< 0.35
12MW09D	8/29/00	< 5	< 5	< 5	< 2	< 5	0	0	< 5
12MW09D	11/29/00	< 0.21	< 0.17	< 0.17	< 0.15	< 0.18	0.18	0.24	< 0.21
12MW09D	2/27/01	< 0.13	< 0.14	< 0.24	< 0.17	< 0.22	0.34	0.34	< 0.2
12MW09D	5/15/01	< 0.38	< 0.34	< 0.31	< 0.19	< 0.27	0.3	0.31	< 0.35
12MW09D	8/29/01	< 0.13	< 0.14	< 0.24	< 0.17	< 0.22	0.52	0.33	< 0.2
12MW09D	12/3/01	< 0.1	< 0.13	< 0.28	< 0.18	< 0.17	< 0.13	< 0.64	< 0.15
12MW09D	2/28/02	< 0.13	< 0.14	< 0.24	< 0.17	< 0.22	0.19	< 0.23	< 0.2
12MW09D	6/10/02	< 0.1	< 0.13	< 0.28	< 0.18	< 0.17	< 0.13	< 0.64	< 0.15
12MW09D	9/10/02	< 0.16	< 0.17	< 0.2	< 0.2	< 0.26	< 0.33	< 0.24	< 0.18
12MW09D	1/7/03	< 0.1	< 0.13	< 0.28	< 0.18	< 0.17	< 0.13	< 0.64	< 0.15
12MW09D	4/15/03	< 0.17	< 0.12	< 0.22	< 0.1	< 0.16	< 0.17	0.14	< 0.14
12MW09D	7/16/03	< 0.31	< 0.25	< 0.4	< 0.11	< 0.27	< 0.41	< 0.3	< 0.34
12MW09D	8/16/04	< 0.2	< 0.2	< 0.15	< 0.15	< 0.19	< 0.18	< 0.2	< 0.22
12MW09S	8/29/00	< 5	< 5	< 5	< 2	< 5	120	120	< 5
12MW09S	11/29/00	< 0.21	0.94	0.3	0.49	1	98	97	< 0.21
12MW09S	2/27/01	< 0.13	0.89	0.32	0.24	0.79	86	86	< 0.2
12MW09S	5/15/01	< 3	< 2.7	< 2.4	< 1.5	< 2.2	60	73	< 2.8
12MW09S	8/29/01	< 1	1.3	< 1.9	< 1.4	< 1.7	83	76	< 1.6
12MW09S	12/3/01	< 0.82	< 1	< 2.2	< 1.4	< 1.3	69	73	< 1.2
12MW09S	2/28/02	< 1	< 1.1	< 1.9	< 1.4	< 1.7	52	51	< 1.6
12MW09S	6/10/02	< 0.82	< 1	< 2.2	< 1.4	< 1.3	110	100	< 1.2
12MW09S	9/10/02	< 0.66	1.3	< 0.81	< 0.79	< 1	31	35	< 0.7
12MW09S	1/7/03	< 0.41	< 0.51	< 1.1	< 0.7	< 0.67	18	20	< 0.6
12MW09S	4/16/03	< 0.34	0.47	< 0.44	< 0.21	< 0.33	23	22	< 0.28
12MW09S	7/15/03	< 0.61	0.71	< 0.8	0.39	< 0.53	32	30	< 0.68
12MW09S	9/17/03	< 0.34	0.61	< 0.44	< 0.21	< 0.33	28	28	< 0.28
12MW09S	1/13/04	< 0.43	< 0.31	< 0.55	< 0.26	< 0.41	24	23	< 0.35
12MW09S	4/28/04	< 0.51	< 0.5	< 0.36	< 0.39	< 0.47	26	23	< 0.54
12MW09S	8/16/04	< 0.61	< 0.49	< 0.8	< 0.21	< 0.53	25	20	< 0.68
12MW10S	11/30/00	3300	1900	9300	660	19000	2400	7000	< 420
12MW10S	2/28/01	3100	1100	5500	480	38000	5100	15000	< 390
12MW10S	5/16/01	3500	1800	6400	1600	17000	5600	5000	< 440
12MW10S	8/29/01	4200	3500	9200	1800	19000	7000	6600	< 190

12MW10S	12/5/01	4400	2600	12000	2200	16000	12000	6100	< 300
12MW10S	3/1/02	3400	1600	7300	1400	16000	9300	5400	< 390
12MW10S	6/11/02	2400	1200	6800	1600	6800	4900	2800	< 140
12MW10S	9/10/02	3400	1300	7000	1400	11000	4800	4400	< 120
12MW10S	1/8/03	2400	950	3900	900	17000	5700	7700	79
12MW10S	4/23/03	1800	710	2300	470	5600	4800	2400	< 170
12MW10S	7/16/03	3400	1100	3000	610	9300	9700	4200	< 270
12MW10S	9/16/03	1600	550	2100	480	3600	4400	1800	< 140
12MW10S	1/14/04	1600	580	1900	460	2700	4300	1600	< 27
12MW10S	4/27/04	2200	840	2100	460	4200	5400	2400	37
12MW10S	8/18/04	2100	730		630	3100	3900	2100	27
12MW11D	8/29/00	< 5	< 5	< 5	< 2	< 5	< 5	< 5	< 5
12MW11D	11/29/00	< 0.21	< 0.17	< 0.17	< 0.15	< 0.18	< 0.17	< 0.18	< 0.21
12MW11D	2/27/01	2.3	0.98	0.75	< 0.17	< 0.22	0.41	< 0.23	< 0.2
12MW11D	5/15/01	< 0.38	< 0.34	< 0.31	< 0.19	< 0.27	< 0.26	< 0.29	< 0.35
12MW11D	8/28/01	< 0.13	0.47	< 0.24	< 0.17	< 0.22	0.24	< 0.23	< 0.2
12MW11D	12/4/01	< 0.13	< 0.14	< 0.24	< 0.17	< 0.22	< 0.16	< 0.23	< 0.2
12MW11D	3/1/02	< 0.13	< 0.14	< 0.24	< 0.17	< 0.22	< 0.16	< 0.23	< 0.2
12MW11D	6/10/02	< 0.1	< 0.13	< 0.28	< 0.18	< 0.17	< 0.13	< 0.64	< 0.15
12MW11D	9/9/02	< 0.16	< 0.17	< 0.2	< 0.2	< 0.26	< 0.33	< 0.24	< 0.18
12MW11D	1/8/03	< 0.1	< 0.13	< 0.28	< 0.18	< 0.17	< 0.13	< 0.64	< 0.15
12MW11D	4/15/03	< 0.17	< 0.12	< 0.22	< 0.1	< 0.16	< 0.17	< 0.11	< 0.14
12MW11D	7/16/03	< 0.31	< 0.25	< 0.4	< 0.11	< 0.27	< 0.41	< 0.3	< 0.34
12MW11S	8/29/00	< 5	7.6	< 5	< 2	< 5	130	20	< 5
12MW11S	11/29/00	< 0.21	3.8	0.37	< 0.15	0.34	65	6.1	< 0.21
12MW11S	2/27/01	15	16	8.9	< 0.7	< 0.87	70	9.3	< 0.78
12MW11S	5/15/01	< 1.5	2.6	< 1.2	< 0.75	< 1.1	41	5.5	< 1.4
12MW11S	8/28/01	< 0.5	38	1.3	< 0.7	1.1	80	7	< 0.78
12MW11S	1/8/03	< 0.1	1.4	0.58	< 0.18	< 0.17	71	12	0.23
12MW12D	8/28/01	< 0.13	2.3	< 0.24	< 0.17	< 0.22	0.34	< 0.23	< 0.2
12MW12S	8/28/01	15	2900	29	0.44	10	420	5.8	0.95
12MW12S	12/4/01	65	2400	38	< 7	< 8.7	680	< 9.2	< 7.8
12MW12S	3/1/02	< 31	1800	< 61	< 44	< 55	280	< 58	< 49
12MW12S	6/10/02	110	2400	< 70	< 44	< 42	880	< 160	< 38
12MW12S	9/9/02	94	2200	< 51	< 49	< 64	400	< 59	< 44
12MW12S	1/8/03	< 13	1400	< 35	< 22	< 21	190	< 80	< 19
12MW12S	4/22/03	< 6.9	430	9.2	< 4.1	< 6.6	140	4.7	< 5.6
12MW12S	7/16/03	< 7.7	250	< 10	< 2.7	< 6.6	99	< 7.5	< 8.5
12MW12S	9/15/03	< 7.7	180	< 10	< 2.7	< 6.6	68	< 7.5	< 8.5
12MW12S	1/13/04	2.6	120	4	< 0.21	1.2	48	2.7	< 0.28
12MW12S	4/27/04	2.6	84	4.1	< 0.31	0.94	44	3	< 0.43
12MW12S	8/17/04	2.7	93	4.2	0.24	1.2	58	3.1	0.29

## 3 Brookhaven National Laboratory

### 3.1 Introduction

The Brookhaven National Laboratory (BNL) site was chosen to test the applicability of the Strategy to a glacial till environment in the Northeastern United States. In this case study we focus on applying certain concepts in the Strategy to an area of tritium contamination at the BNL site.

As outlined in the Strategy, our application began with a compilation and analysis of existing characterization and monitoring data and synthesis of an alternative conceptual site model. Information in Section 3.2 is background information including location, geology and hydrology of the site. Discussion of the tritium contamination begins in Section 3.2.5 and is summarized below.

#### *Tritium Plume and Remediation*

In early 1997, monitoring data revealed a plume of tritium contaminated ground water from the High Flux Beam Reactor (HFBR) at the BNL site. Tritium, radioactive hydrogen that forms water, was leaking from the spent fuel pool within the HFBR.

In May 1997, a system to pump the leading edge of the tritium plume was started as an interim action to prevent any further movement of the tritium and to ensure that the contamination remains entirely on-site. The contaminated water is being recharged on-site at levels below the Federal and State standards farther from the site boundary. The spent fuel has all been shipped off-site and the water was drained from the fuel pool, eliminating further leaks. The reactor is currently shut down, and the United States Department of Energy (DOE) has decided not to restart the reactor (DOE, 2006).

Currently, to remediate the tritium in the ground water at the BNL, a series of extraction and re-injection wells provide a recirculation system (Figure 3-1). Because the half-life of tritium is 12.5 years, this recirculation system allows time for the tritium to decay before exiting the BNL boundary. The schematic in Figure 3-1 also mentions a VOC plume in the HFBR vicinity. While this plume is not the focus of this Case Study, it is worthwhile to note that understanding of the flow and transport behavior of this plume may provide useful information about the potential pathway of the tritium plume

#### *Key Conclusions*

This case study illustrates the following key points:

Conceptual Site Models and flow and transport simulations are powerful visualization techniques for communicating the impact of Performance Indicators. In this Chapter, we show examples of models developed using, Excel, MODFLOW, and GMS (Section 3.3).

Conceptual Site Models and flow and transport simulations can be useful in evaluating the effectiveness of various pumping alternatives, and thus, can aid in development of an efficient and cost effective monitoring and/or remediation program (Section 3.3.2).

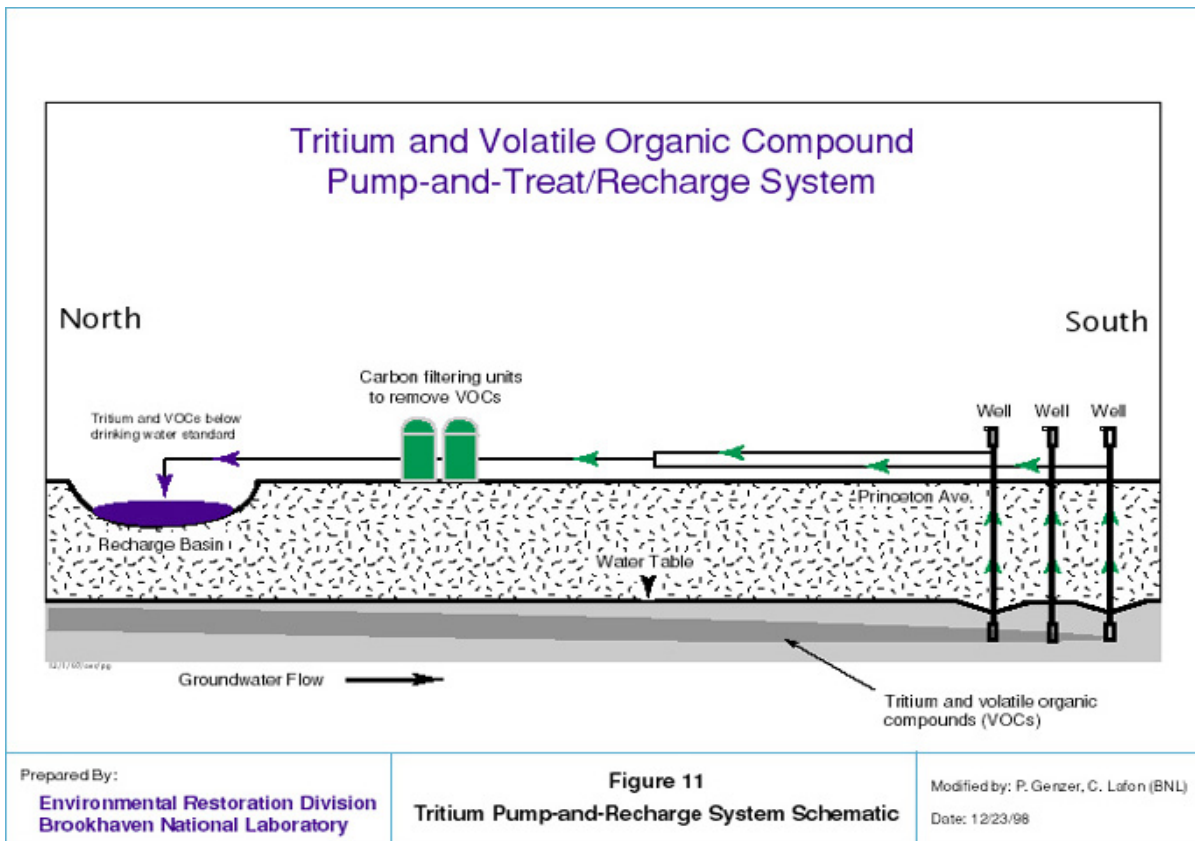


Figure 3-1. Schematic of tritium/VOC plume pump and treat system (DOE, 2000)

### 3.2 Compilation of Available Data

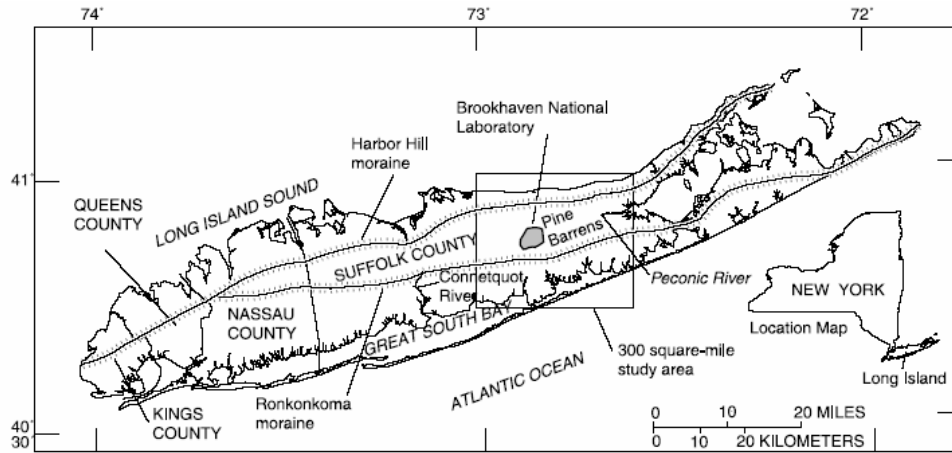
This section provides a summary of the readily available data compiled to prepare this evaluation with the majority of the information collected from BNL online reports.

#### 3.2.1 Site Background

Brookhaven National Laboratory, located on Long Island in New York, is a multi-program DOE National Laboratory (Figure 3-2). Established in 1947, BNL has been operated by contractors, first to the Atomic Energy Commission (AEC), and now to the United States Department of Energy (DOE) - the site owners. Since March 1998, BNL has been operated and managed by Brookhaven Science Associates. BNL conducts basic and applied research in high energy nuclear and solid state physics, fundamental material and structure properties and the interaction of matter, nuclear medicine, biomedical and environmental sciences, and selected energy technologies. To conduct this research BNL has designed, built, and run installations for scientific research, such as particle accelerators and nuclear reactors. Most of its main facilities are in an area of approximately 900 acres near the center of the site (DOE, 2006).

There are a number of areas at BNL where ground-water contamination is known or suspected. Over 30 Areas of Concern (AOCs) have been identified. On-site soil is contaminated with volatile organic compounds (VOCs), heavy metals, polycyclic aromatic hydrocarbons (PAHs), and radioactive materials including cesium-137,

strontium-90 and tritium. On-site and off-site ground water is contaminated with VOCs, radionuclides, and the pesticide/fumigant ethylene dibromide (EDB). On-site contaminated drinking water wells have been closed or treatment systems have been added. VOCs in off-site ground water exceed Federal and State drinking water standards, so the DOE has connected neighboring properties to public water as a protective measure until the final cleanup is complete. Radionuclides in off-site ground water do not exceed Federal or State standards (DOE, 2006).



**B. LOCATION OF BROOKHAVEN NATIONAL LABORATORY SITE AND 28-SQUARE MILE STUDY AREA**

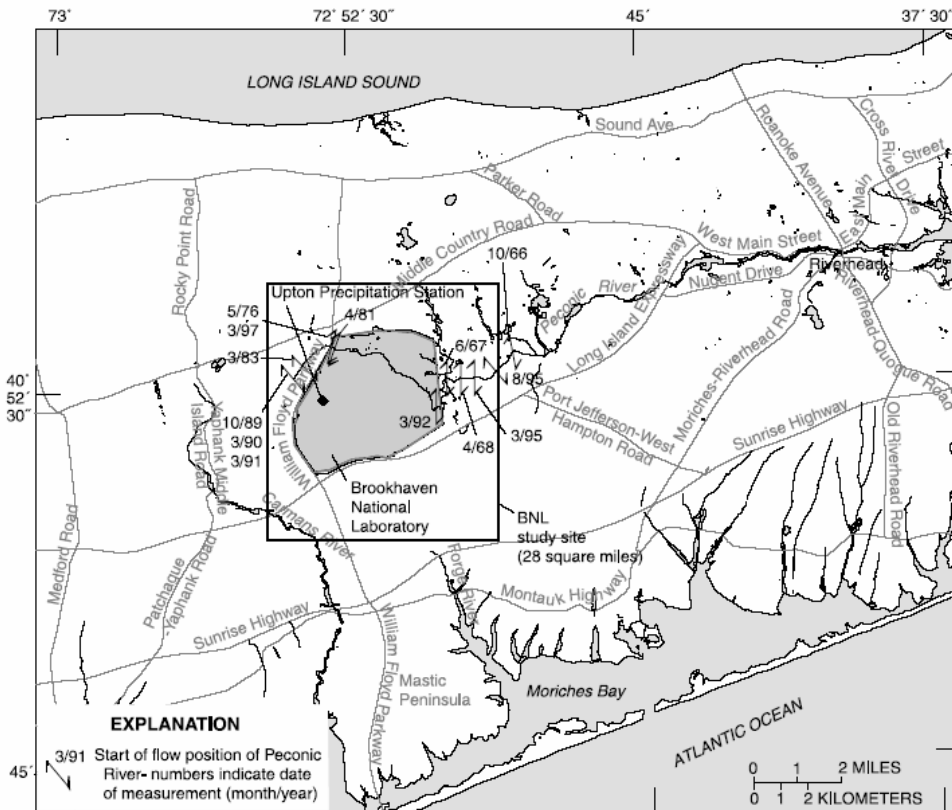


**Figure 3-2. Location of the Brookhaven National Laboratory (Scorca et al., 1999)**

### 3.2.2 Geologic Information

Brookhaven National Lab is located on Pleistocene glacial deposits of the Northeastern United States. The stratigraphy in the region of the BNL consists of approximately 1,300 feet of unconsolidated deposits overlying pre-Cambrian bedrock (Figure 3-3). Among these unconsolidated deposits, the Ground-Water Monitoring Programs at BNL currently focus on ground-water quality within upper Pleistocene glacial deposits, and the upper portions of the Matawan Group-Magothy Formation.

The Pleistocene deposits are about 100 to 200 feet thick and are divided into two primary hydrogeologic units: undifferentiated sand and gravel outwash and moraine deposits; and finer-grained, more poorly sorted fine to medium white to greenish sand with interstitial clay.

The most obvious Pleistocene glacial features are the large erratics (glacier transported boulders) and scattered deposits of glacial till (a mix of fine silt, sand, gravel, and large boulders). The flowing ice of the southward advancing ice sheet sculpted the landscape by not only eroding and transporting vast quantities of rock and sediment, but also by blocking and altering the course of rivers, filling valleys with sediment, and depositing large quantities of till in the terminal moraines along its leading edge. These hills are apparent throughout Long Island (BNL, 2004).

### 3.2.3 Hydrogeologic Information

Table 3-1 presents a generalized comparison of the geologic and hydrogeologic units below BNL. Descriptions of the units in the table are limited to the unconsolidated Pleistocene and Cretaceous material overlying the Paleozoic bedrock. Hydrostratigraphic relationships are shown in cross-section in Figure 3-3.

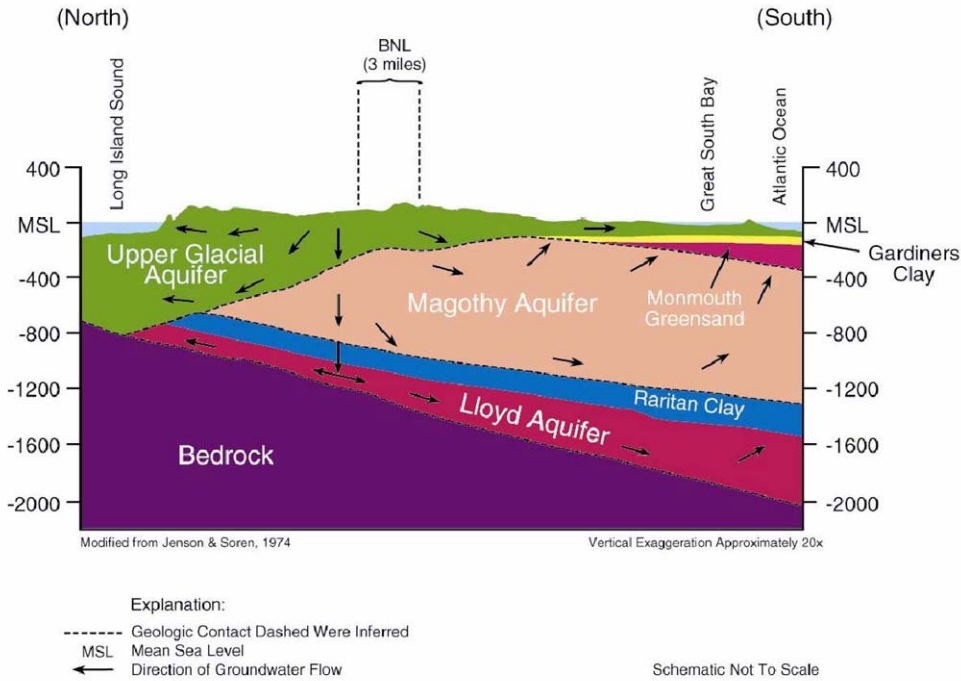


Figure 3-3. Hydrostratigraphy of the Brookhaven National Laboratory (BNL, 2004)

### 3.2.4 Hydrologic Data

The saturated part of the upper Pleistocene deposit forms the Upper Glacial Aquifer, which contains the water table throughout most of Long Island. This unit consists mostly of moderately to well-sorted sand and fine gravel and is highly permeable in most places. The Upper Glacial aquifer underlies the entire 300-square mile (mi<sup>2</sup>) study area and is the source of base flow to streams.

The average island-wide horizontal hydraulic conductivity value for the Upper Glacial aquifer is about 270 ft/d (Smolensky et al., 1989), but aquifer tests conducted at BNL by Warren et al. (1968) indicated the value at the site to be one-third lower—about 175 ft/d (based on an aquifer thickness of 145 ft), and the specific yield (effective porosity) to be 0.24. Subsequent tests at BNL have measured similar hydraulic conductivities (Holzmacher et al., 1985). Total porosity of the Upper Glacial aquifer is estimated to be 0.33 (Warren et al., 1968). A summary of aquifer properties obtained from onsite pumping tests is presented in Table 3-2 (Scorca et al., 1999).

Data from aquifer tests and infiltration tests conducted at BNL (Warren et al., 1968) indicate that the anisotropy (ratio of vertical to horizontal hydraulic conductivity) of the Upper Glacial aquifer is between 1:4 and 1:18. The average value for the Upper Glacial aquifer throughout Long Island has been estimated to be 1:10 (Smolensky et al., 1989).

The hydraulic properties of the basal Upton unit cannot be defined with certainty from the current well network, but the high clay and silt content of the Upton unit, especially in the northwestern part of the BNL site, indicate that these deposits are probably less permeable than the overlying glacial outwash sand and gravel.

The Gardiners Clay, where present, confines water and affects ground-water flow, but its limited extent indicates that the effects are only local. Studies by Warren et al. (1968) indicate that the hydraulic conductivity of the Gardiners Clay is about 0.040 ft/d, but the hydraulic conductivity of sandy zones within the unit is higher.

**Table 3-1. Generalized description of geologic and hydrogeologic units underlying Brookhaven National Laboratory and vicinity, Suffolk County, N.Y. (Scorca et al., 1999)**

Series	Geologic Unit	Hydrogeologic Unit	Description and Water-bearing Characteristics
PLIESTOCENE	Upper Pleistocene deposits	Upper glacial aquifer	Mainly brown and gray sand and gravel deposits of moderately high horizontal hydraulic conductivity (270 ft/d average for Long Island; about 180 ft/d measured at Brookhaven National Laboratory); may also include deposits of clayey till and lacustrine clay of low hydraulic conductivity. A major aquifer.
	Upton unit	Upper glacial aquifer	Mainly greenish, with shades of yellow-green, greenish-gray, olive-brown, and gray, poorly to well sorted sand, with some silt and clay. Upper surface in some borings is marked by a clay or silty layer, generally less than 10 ft thick, that produces a noticeable response on a gamma-ray log. Horizontal hydraulic conductivity is estimated to be similar to or slightly less than that of the shallow part of the upper glacial aquifer.
	Gardiners Clay	Gardiners Clay	Green and gray clay, silt, clayey and silty sand, and some interbedded clayey and silty gravel. Unit has low vertical hydraulic conductivity (0.001 ft/d) and tends to confine water in underlying aquifer.
	Sand below Gardiners Clay	Upper glacial aquifer	Mainly light brown, olive-brown, and grayish-brown, poorly to well sorted sand. Hydrologically, unit could also be considered part of Magothy aquifer because of confinement by Gardiners Clay.
CRETACEOUS	Monmouth Group	Monmouth greensand	Interbedded marine deposits of green, dark-greenish gray, greenish-black, dark gray, and black clay, silt, and sand, containing much glauconite. Unit has low hydraulic conductivity (0.001 ft/d) and tends to confine water in underlying aquifer.
	Matawan Group and Magothy Formation, undifferentiated	Magothy aquifer	Gray, white, and brownish-gray, poorly to well sorted, fine to coarse sand of moderate horizontal hydraulic conductivity (50 ft/d). Contains much interstitial clay and silt, and lenses of clay of low hydraulic conductivity. Generally contains sand and gravel beds of low to high conductivity in basal 100 to 200 ft. A major aquifer.
	grayish-brown clay		Dark grayish-brown to yellow-brown, solid to silty clay, in some layers laminated with beds of very fine sand up to 1 in. thick. Unit is encountered in upper part of Magothy Formation. Has low hydraulic conductivity and tends to confine water.
	Unnamed clay member of the Raritan Formation	Raritan confining unit	Gray, black, and multicolored clay and some silt and fine sand. Unit has low vertical hydraulic conductivity (0.001 ft/d) and confines water in underlying aquifer.
	Lloyd Sand Member of the Raritan Formation	Lloyd aquifer	White and gray fine-to-coarse sand and gravel of moderate horizontal hydraulic conductivity (40 ft/d) and some clayey beds of low hydraulic conductivity.
PALEOZOIC AND PRECAMBRIAN	Bedrock	Undifferentiated crystalline bedrock	Mainly metamorphic rocks of low hydraulic conductivity; considered to be the base of the ground-water flow system.

**Table 3-2. Hydraulic conductivity of Upper Glacial aquifer at Brookhaven National Laboratory, Suffolk County, N.Y., as indicated by aquifer tests (Scorca et al., 1999)**

Source of data	Hydraulic conductivity (in feet per day)
Warren et al. (1968)	180
Holzmacher et al.(1985)	180
Camp Dresser and McKee (1995)	200
Grosser (1997)	60-160
Geraghty & Miller (1997)	150

The Monmouth Group, which lies along the southern shore of Long Island, forms the hydrogeologic unit known as the Monmouth greensand. Monmouth greensand and the Gardiners Clay underlie the Upper Glacial aquifer and confine water in the Magothy aquifer. The Upper Glacial aquifer directly overlies the Magothy aquifer in areas where both of these units are absent.

Deltaic sediments of the Matawan Group- Magothy Formation make up the Magothy aquifer. The hydraulic conductivity of this unit is estimated to average 50ft/d (Smolensky et al., 1989) but varies widely as a result of local differences in lithology, thickness, and lateral extent. This hydraulic variation can affect local ground-water flow patterns and contaminant transport. Warren et al. (1968) conducted an aquifer test in a coarse sand zone of the Magothy aquifer and obtained a hydraulic conductivity value of 57ft/d.

Much of the Magothy aquifer consists of silty sand with clayey layers. The upper Magothy sediment at BNL is mostly a silty sand with clayey layers but includes layers of well-sorted sand as well as locally extensive clay layers, such as the grayish-brown clay unit. Although the grayish-brown clay unit has a sandy texture in some intervals, it is fairly solid in general and forms a major local confining unit (Scorca et al., 1999).

#### *Hydrologic Cycle*

The hydrologic cycle on Long Island was summarized by Scorca (1997) and discussed at length by Franke and McClymonds (1972), who evaluated the relations among major hydrologic factors, including precipitation, evapotranspiration, direct runoff, ground-water recharge, ground-water movement, and pumpage, to develop an island-wide water budget. The hydrologic cycle can be thought of as beginning with precipitation, which has averaged 48.29 in/yr at Upton station since 1949. Upon reaching the ground,

precipitation flows as direct runoff into streams, infiltrates into the highly permeable unsaturated zone, or evaporates. Part of the water that infiltrates the soil evaporates or is transpired by plants; the rest infiltrates downward to the water table (Scorca et al., 1999).

#### *Ground-Water Recharge and Discharge*

The water table recharge rate varies from year to year as a function of precipitation. It also fluctuates seasonally because plants capture and transpire most of the water that enters the unsaturated zone during the growing season (May through October) (Figure 3-4). Thus, in most years, virtually all recharge occurs during the non-growing season (November through April) (Warren et al., 1968). The water table rises in response to recharge and typically undergoes a net rise in years when precipitation is notably higher than in the preceding year. This rise, in turn, results in increased ground-water discharge to streams, bays, and the ocean. Under long-term conditions in undeveloped areas of Long Island, about 50 percent of precipitation is lost through evapotranspiration and direct runoff to streams. The other 50 percent infiltrates the soils and recharges the ground-water system (Aronson and Seaburn, 1974; Franke and McClymonds, 1972).

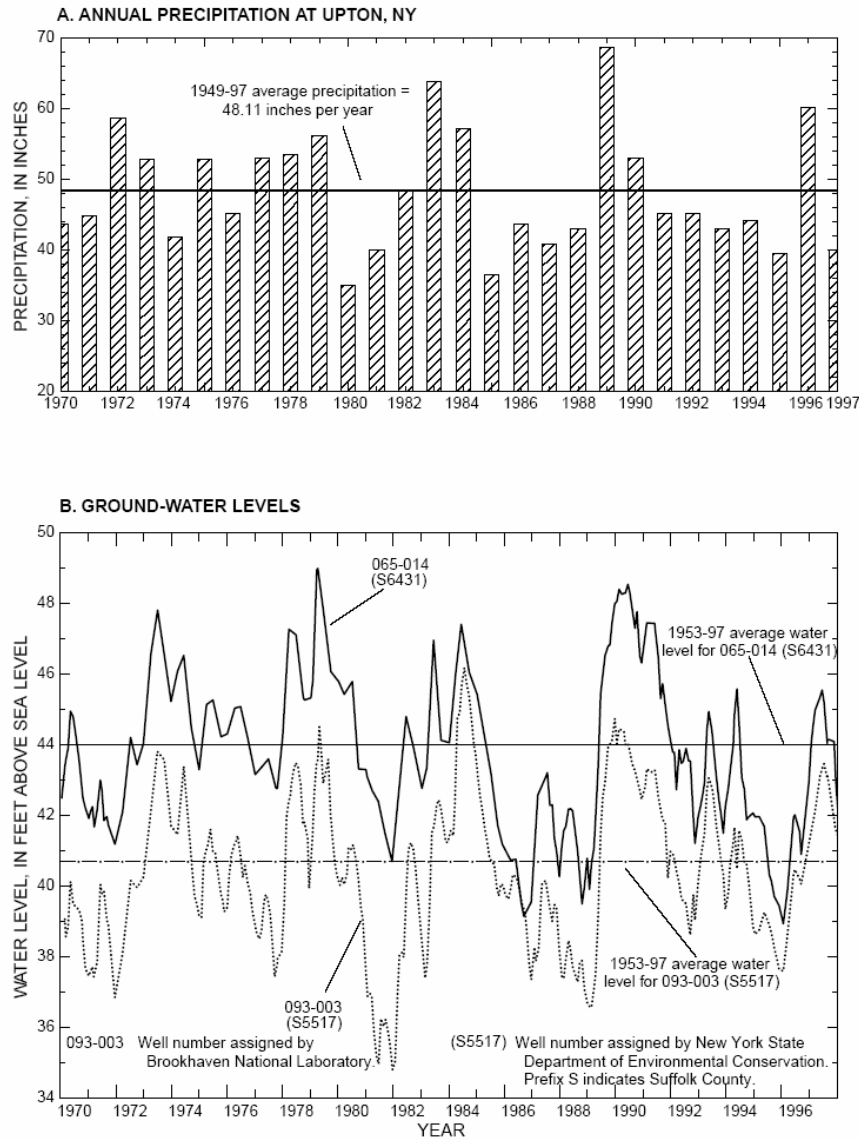


**Figure 3-4. Precipitation and water-table altitude at Brookhaven National Laboratory, Suffolk County, N.Y., 1970-97. A. Annual precipitation at Upton. B. Typical water levels in wells (Scorca et al., 1999)**

### *Regional Ground-Water Flow*

The Long Island ground-water system consists of two major components—the regional (deep) flow system and the shallow flow system associated with streams. Ground water enters the regional flow system of Long Island in the area bordering the main ground-water divide, where it moves downward through the Upper Glacial aquifer into the underlying aquifers and eventually moves seaward. Water that enters the regional flow system south of the main divide flows southward, and water that infiltrates north of the divide flows northward. All precipitation that infiltrates upgradient of each stream’s shallow-flow system becomes part of the regional flow system, and precipitation that infiltrates within the ground-water contributing area of a stream becomes part of that stream’s shallow-flow system (Prince et al., 1988).

### Ground-Water Divide

The position of a ground-water divide depends on the water-table configuration. The main ground-water divide on Long Island is aligned generally east-west and lies about 0.5 mi north of BNL's northern boundary (Figure 3-5). Ground water north of the divide flows northward and ultimately discharges to Long Island Sound; ground water south of the divide flows southward and discharges to south-shore streams, the Peconic River, Great South Bay, Peconic Bay, and the Atlantic Ocean. Ground water near the divide has a large downward vertical-flow component and recharges the deep aquifers of the ground-water system.

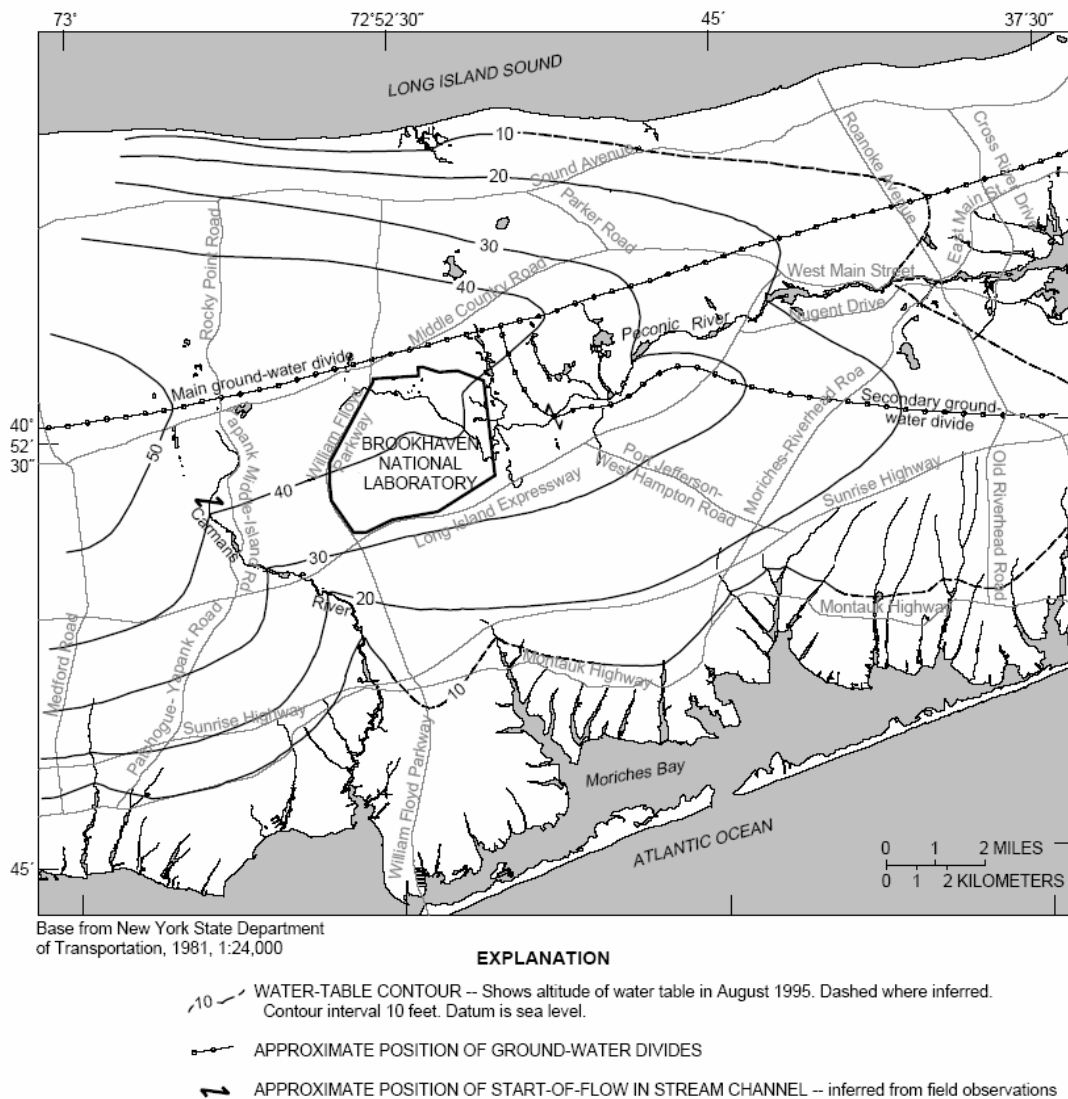


**Figure 3-5. Water-table altitude in 300-mi<sup>2</sup> study area surrounding Brookhaven National Laboratory, Suffolk County, N.Y., August 1995 (Scorca et al., 1999)**

### *Local Ground-Water Flow Patterns near Brookhaven National Laboratory*

Ground-water flow and contaminant movement through the aquifer system below the BNL site are affected by several factors. First, pumping of ground water for supply at the site lowers ground-water levels and affects hydraulic gradients in the local ground-water system. Second, discharge from BNL's sewage-treatment plant to the Peconic River can affect the position of the start of flow and the discharge of Peconic River. Recharge basins and pumping of onsite ground-water-remediation systems also affect ground-water levels locally. The stream channel of the Peconic River extends onto the site, but the start of flow can be either east or west of the site under extreme hydrologic conditions. The amount of flow in Peconic River and base-flow discharge to the stream affect the position of the secondary (southeastward trending) ground-water divide. The hydraulic properties of several hydrogeologic units, including the Upper Glacial aquifer, Magothy aquifer, grayish-brown clay, Gardiners Clay and localized near-surface clay units along the Peconic River drainage system also affect ground-water flow (see Table 3-1 for a description of these units).

Water-table elevations at the site in March 1997 declined not only near supply wells, but near remediation (extraction) wells along the southern boundary of the site. At the same time, treated water from these systems was discharged to recharge basins and produced localized ground-water mounds near the basins (Scorca et al., 1999).

### *Flow Gradients in Brookhaven National Laboratory Area*

The horizontal hydraulic gradient at BNL is typically 0.001 feet per foot (ft/ft), but in recharge areas and pumping areas, it can steepen to 0.0024 ft/ft or greater (Scorca et al., 1999). The natural ground-water flow velocity in most parts of the site is estimated to be about 0.75 ft/d, but flow velocities in recharge areas can be as high as 1.45 ft/d, and those in areas near BNL supply wells have been estimated to have velocities as great as 28 ft/d (Scorca et al., 1999).

Water-level measurements at paired water-table wells and deep wells screened in the Upper Glacial aquifer along the northern boundary of the site (near the regional ground-water divide) indicate significant deep-flow recharge areas, with downward vertical hydraulic gradients of as much as 0.007 ft/ft. Head differences at paired wells in the central and southern areas of the site become negligible, indicating that ground-water flow within the Upper Glacial aquifer is predominantly horizontal in these areas. Vertical gradients between the deep part of the Upper Glacial aquifer and the shallow part of the Magothy aquifer were about 0.018 ft/ft throughout the BNL site.

The BNL site is located within a Suffolk County Department of Health Services - designated deep-flow recharge area for the Magothy and Lloyd aquifers (Koppleman, 1978). Comparison of water level measurements from Upper Glacial aquifer and Magothy aquifer wells indicate significant downward flow across the BNL site (BNL, 1998, Paquette, 1998).

Ground-water flow in the vicinity of the HFBR varies due to BNL pumping and recharge operations in the area. In general, ground-water flow is toward the south or southeast. Evaluation of ground-water flow and quality data indicate that the downgradient portion of the tritium plume (south of Brookhaven Avenue) has shifted to the east since 1997 in

response to changing flows to various recharge basins, and the reduced pumping of BNL supply wells (BNL, 2004).

Ground water in the Upper Glacial aquifer beneath BNL generally exists under unconfined conditions (BNL, 2000). The Upper Glacial aquifer supplies both private and public water on Long island and is the exclusive source of drinking water and process water at BNL. The Laboratory currently operates six potable water supply wells that can be pumped at rates of 1,200 gallons per minute (gpm), and five process supply wells that can be pumped at rates between 50 and 1,200 gpm. During maximum water usage at BNL, up to 6 million gallons per day are pumped from the Upper Glacial aquifer. Most of this water returns to the aquifer by way of recharge basins or discharge of effluent to the Peconic River.

A main east-west trending regional ground-water divide lies approximately 0.5 miles north of BNL (Figure 3-5). A second ground-water divide, which transects portions of the BNL site during periods of high water table position (i.e., during periods of inflow from the aquifer to the stream bed), defines the southern boundary of the area contributing ground water to the Peconic River watershed (Scorca et al., 1996, Scorca et al., 1997). Natural drainage systems influence shallow ground-water flow directions across the BNL site: flow runs eastward along the Peconic River, southeastward toward the Forge River, and southward toward the Carmans River. Additionally, pumping and recharge induces considerable stress on the aquifer system in the central area of the site. Due to variable supply well pumping schedules and rates, considerable variations in ground-water flow directions and velocities occur. Pumping at the Suffolk County Water Authority well field located on the west side of the William Floyd Parkway also influences ground-water flow directions in the southwest corner of the site (Paquette, 1998).

Aquifer pumping tests conducted at BNL indicate that the horizontal hydraulic conductivity of the Upper Glacial aquifer is approximately 1,300 gpd/ft<sup>2</sup> (or 175 ft/d) based upon an aquifer thickness of 145 feet and a specific yield (effective porosity) of 0.24 (Warren et al., 1968; H2M/Roux Associates, 1985; CDM, 1995; Grosser, 1997). Total porosity value for the Upper Glacial aquifer is estimated to be 0.33 (Warren et al., 1968). Data from aquifer pumping tests and infiltration tests conducted at BNL by the United States Geological Survey (USGS) indicate that the vertical to horizontal anisotropy within the Upper Glacial aquifer is between 1:4 to 1:18 (Warren et al., 1968). The average vertical to horizontal anisotropy within the Upper Glacial aquifer on Long Island has been estimated to be 1:10 (Smolensky et al., 1989). The hydraulic properties of the basal Unidentified Unit cannot be determined with any degree of certainty using the current well network. Since the Unidentified Unit contains significant clay and silt, it is expected that these deposits are less permeable than the overlying glacial outwash and morainal sand and gravel (Paquette, 1998).

### **3.2.5 Tritium Plume Ground-Water Monitoring Data**

Ground-water monitoring has been ongoing at BNL since the beginning of operation of the facility. The current HFBR monitoring well network consists of 159 wells, sampled quarterly (BNL, 2004). In 1996, a tritium leak was discovered from the spent storage canal of the High Flux Beam Reactor (HFBR) Facility. Initial concentrations of tritium

in proximal down-gradient monitoring wells were in the range of 600,000 picocuries per liter (pCi/L) (maximum contaminant level [MCL] for drinking water is 20,000 pCi/L).

After determining the tritium source was from the fuel canal associated with the HFBR, two 125 meter-long horizontal wells were installed upgradient and downgradient of the canal and between 0.6 to 1.6 meters below the water table, respectively (Figure 3-6). Both wells were constructed with six separated screen zones running parallel to and within five meters of the canal footprint. The stated goal of the wells was to rapidly and absolutely confirm that the canal was the source of the tritium contamination by showing that the upgradient well was clean and the downgradient well was contaminated. Unfortunately, the lateral spread of moisture and tritium in the vadose zone resulted in tritium concentrations that were similar in the two wells. Also, the concentrations measured in the horizontal wells during their first sampling were <5,000 pCi/L, significantly lower than the 140 million pCi/L concentration of the canal water and approximately 600,000 pCi/L concentrations detected in nearby downgradient monitoring wells. At the time, the project was viewed by some as a failure because it did not provide rapid and absolute confirmation. In fact, the project resulted in the successful and high-quality installation of two horizontal wells that would have provided useful confirmatory information when sampled over a period of several years. Importantly, vadose zone processes influenced the data in a manner consistent with theory (Looney and Paquette, 2000).

The vadose zone at the BNL is relatively thin (approximately 15 m). The flow path of water and tritium in the vadose zone immediately below the HFBR reactor building is shown schematically in Figure 3-6.

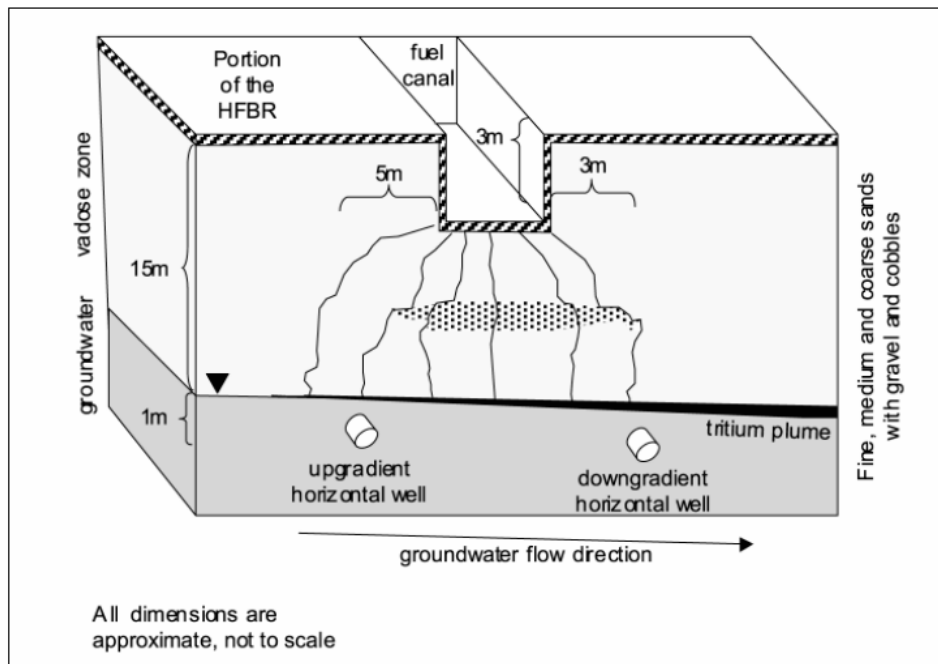


Figure 3-6. Schematic of plume configuration below the HFBR (Looney and Paquette, 2000). Used by permission of Battelle Press

In this situation, the vadose zone is dry because it is capped by the large building. The small leak from the fuel storage canal spreads out laterally and makes its way slowly to the water table. The lateral spread in the vadose zone is enhanced as the water tends to accumulate in and move through fine grained zones (silt and sand) and around coarse grained (gravel) zones (that is, water does not fill the holes in the sponge under these conditions). These vadose zone behaviors caused problems in interpreting data from two horizontal wells (discussed in the following section) that were installed in the water table to confirm the source of contamination

The overall geometry of the contaminant plume beneath the reactor is a direct result of the slow leak rate and the lateral spread in the vadose zone. As the contaminated vadose zone moisture slowly enters the relatively fast moving aquifer (~0.3 meters per day [m/d]), the plume forms a thin plume at the top of the water table. The thickness of this contaminated layer can be estimated from a simple analysis of the relative flow rates and areas (Figure 3-7)

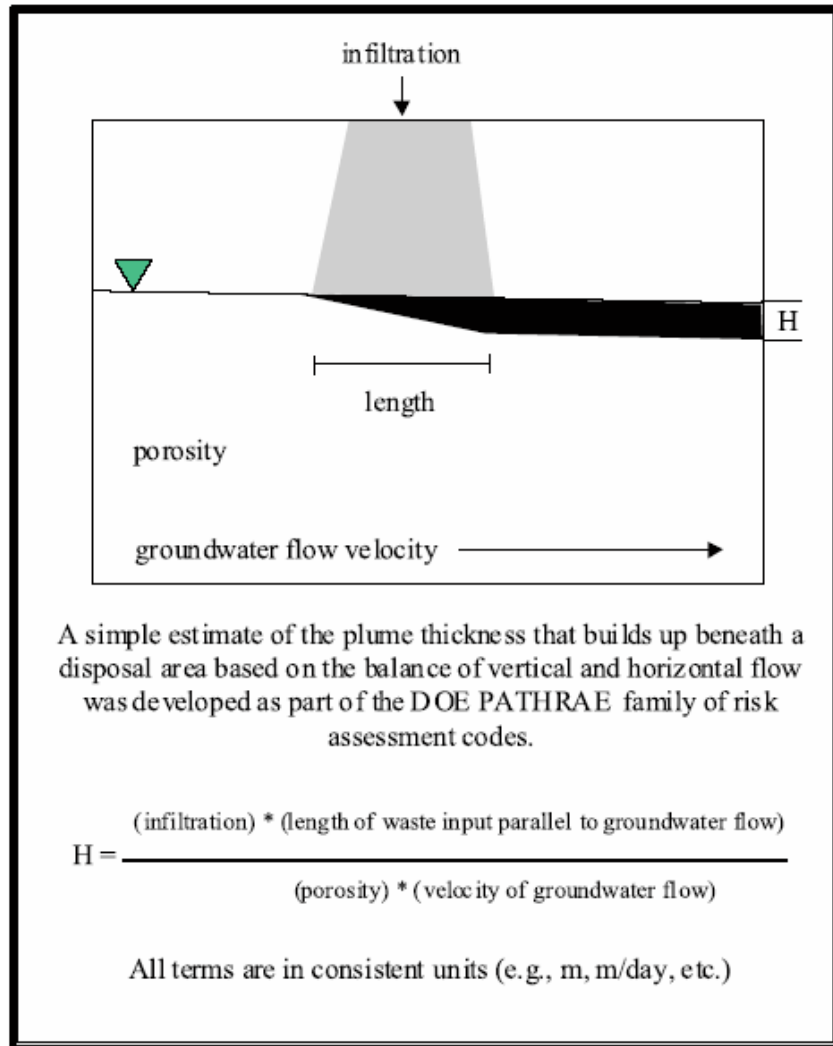


Figure 3-7. Simplified calculation of plume thickness immediately downgradient of a vadose zone source (Looney and Paquette, 2000). Used by permission of Battelle Press.

Based on leak rate data, measured lateral migration in the vadose zone, and typical hydrogeological values for this site, the tritium plume immediately beneath the reactor is expected to be very thin (<0.2 m). Even if this layer is smeared by seasonal water level fluctuations and other complexities, a simple evaluation of vadose zone delivery versus ground-water flow provides a clear understanding of why the initial sampling of the horizontal wells yielded low concentrations. Despite the wells being installed within a few feet of the water table, each of these wells were collecting water beneath the main body of the plume throughout most of the year. Thus, data from these wells were not providing an accurate picture of the plume location. Only when the wells were sampled during a seasonal drop in the ground water level was the plume location -- beneath HFBR primarily within a thin discrete zone at the water table surface -- confirmed. Tritium concentrations of >650,000 pCi/L were detected in the upgradient well when the ground water level was within 0.3 meters of the well's screened zone. However, during the same period, low tritium concentrations continued to be low in the downgradient horizontal well (<2,000 pCi/L) because the sample was taken approximately 1 meter below the water table. Because water levels have remained greater than 0.6 meters above the downgradient well since its installation, the originally expected high levels of tritium have not been observed (Looney and Paquette 2000). By 1998, the highest concentrations of tritium in ground water downgradient of the HFBR exceeded 5,000,000 pCi/L.

When the plume exits the footprint of the HFBR, infiltration places clean water above the plume. Vertical migration of the plume accelerates, and the plume is expected to exhibit a classic downward trajectory (

Figure 3-8). Once again, actual monitoring data proved to be of high quality, and the large-scale measured Brookhaven plume behavior matches the expected pattern. This highly discrete vertical plume behavior resulted in additional complexity in the data interpretation from monitoring wells—highly variable measurements for samples collected at different times. Figure 3-6 documents the principal source of this variability for an example water table well located immediately down gradient of the source (Looney and Paquette, 2000).

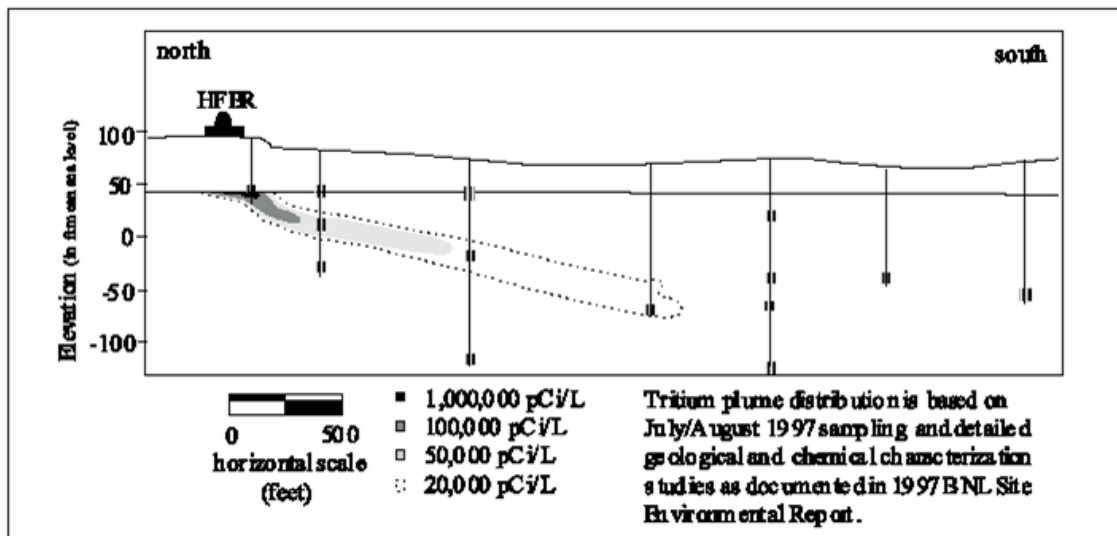


Figure 3-8. Cross section of tritium plume emanating from the HFBR (Looney and Paquette, 2000). Used by permission of Battelle Press.

Based on simple geometry for the case of a thin plume (<0.3 m thick), the tritium measurement in a water table well is simply the plume concentration adjusted by the ratio of the plume thickness to the wetted screen thickness (

Figure 3-8). As site operations and seasonal events impact ground-water levels, tritium levels in vertical monitoring wells will vary widely. While most pronounced for water table wells, the issue of plume/well geometry impacting concentration data is general and should be evaluated for all sites (Looney and Paquette, 2000).

As shown in Figure 3-9, ground-water flow below BNL is to the south-southeast and swings to the south-southwest upon exiting the site. However, the shape of the tritium plume bulges from the west in 1998 (Figure 3-10). This is not in agreement with the regional flow data in the water table and is likely influenced by remediation pumping on extraction wells EW-13 and EW-14, (Figure 3-9). After the plume passes EW-13 and -14, it swings back to the southeast most likely due to a combination of conditions including:

- the presence of other extraction wells in line and down gradient of the plume, including EW-15 (Figure 3-9),
- the direction of regional flow, and
- a circular topographic low located where the split in the plume occurs represents a relative increase in contribution to the water table that may result in localized mounding, and may act as a diversion to the movement of water.

Contaminant capture zones below the HFBR are large because of the high permeability of the water table aquifer and are obvious when comparing the water table contour maps with the contaminant plume maps.

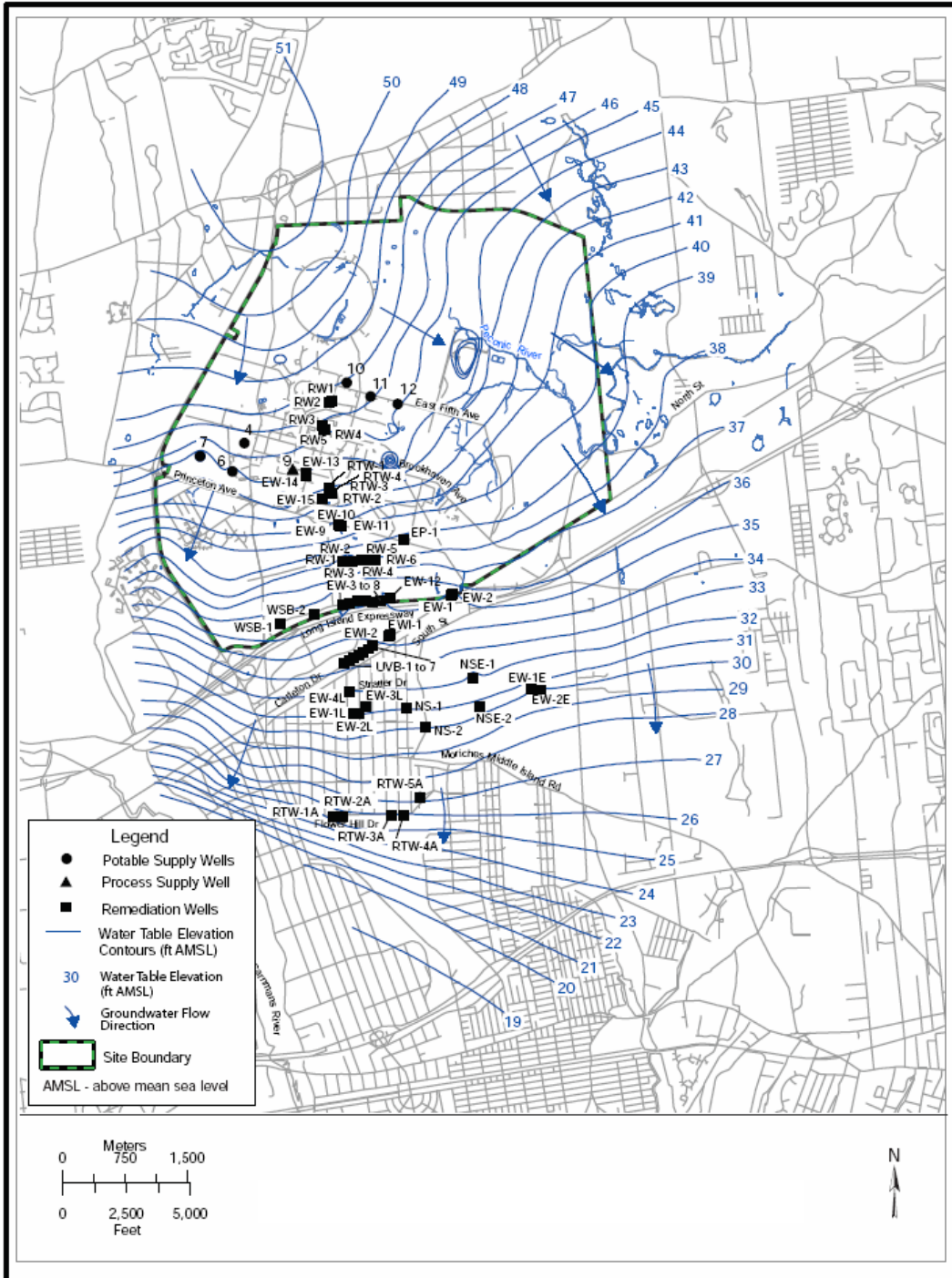
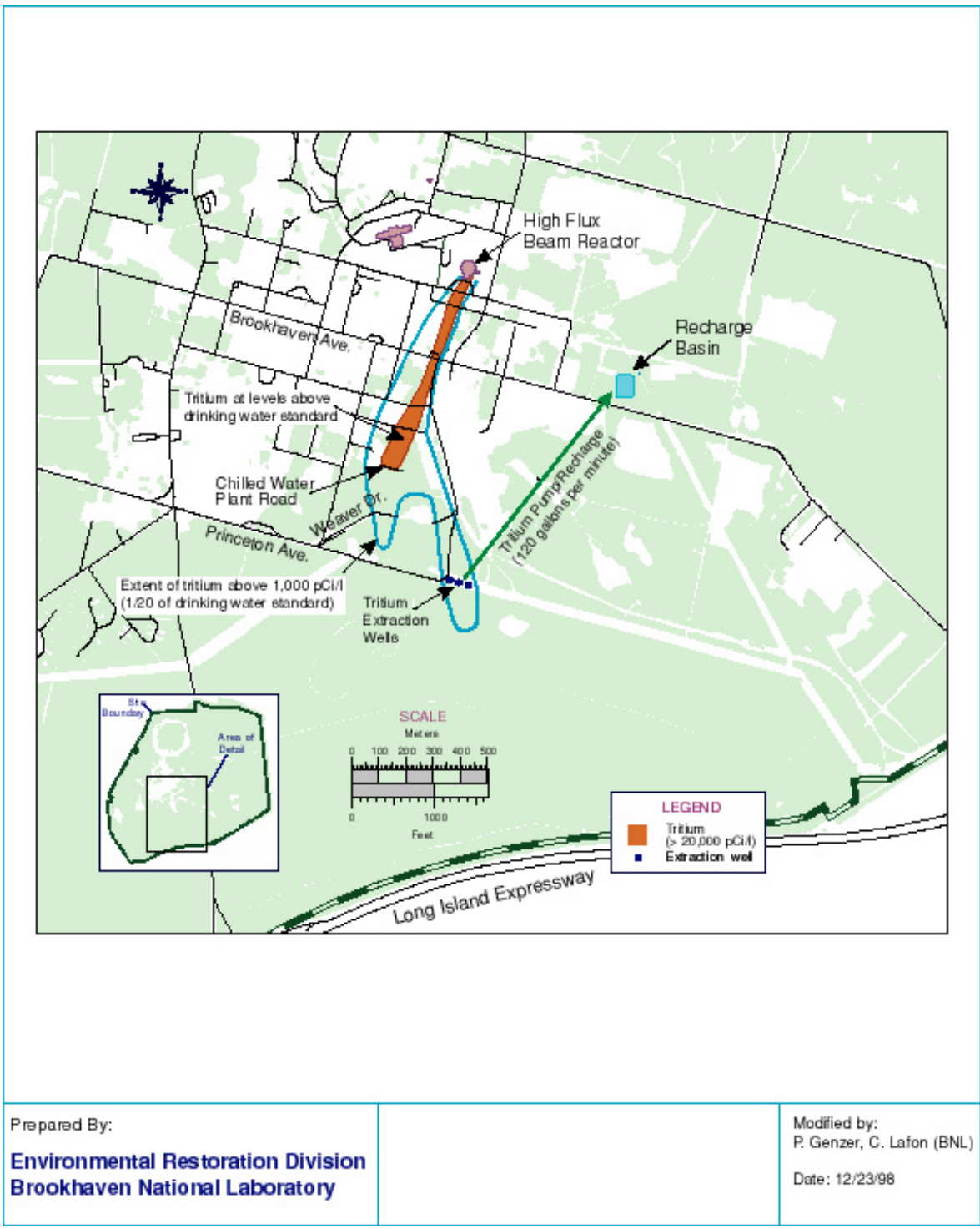


Figure 3-9. December 2005 water table map of BNL with extraction wells (BNL, 2005)



Prepared By:  
**Environmental Restoration Division**  
**Brookhaven National Laboratory**

Modified by:  
 P. Genzer, C. Lafon (BNL)  
 Date: 12/23/98

Figure 3-10. Location of tritium plume emanating from the High Flux Beam Reactor (DOE, 2000)

### **3.3 Ground-Water Modeling and Visualization**

Through examination of existing site characterization and monitoring data, it became clear that nearby process and remediation well pumping significantly influenced migration of the tritium plume. Recognizing this fact, we realized that it was necessary to include these influencers in our conceptual site model. Based on earlier research on vadose zone transport at BNL (largely done by Looney and Falta), we also recognized the importance in developing flow and transport models that accurately accounted for this transport. In this Section 3.3, we describe the CSM and flow and transport models we developed to evaluate contaminant migration.

#### **3.3.1 Plume visualization**

For the three-dimensional data presentation, ground-water analytical data, along with survey information for the temporary monitoring wells, were loaded into a three dimensional data presentation software database (Arcview with 3D Analyst). From this information, a three-dimensional model of the actual tritium plume was created that allows a 360 degree horizontal and vertical perspective of the model. In addition, levels can be placed in the model corresponding to various surfaces such as ground images, water table surfaces, and geologic layers. By evaluating these complex data in three dimensions, a more complete picture of the temporal distribution of contamination can be visualized. As demonstrated below, this conceptual model assisted understanding of the observed data from the existing monitoring wells and guided our analysis regarding how and where future contaminant monitoring or remediation should occur.

Figure 3-11 and Figure 3-12 present two perspectives of temporary monitoring well data extracted from the BNL tritium database. The ability of 3D Analyst to present complex analytical data in an easily manipulated format makes the program ideal for presentations to anyone especially people who do not have a scientific or engineering background. Data used to prepare Figures 11 and 12 were current in April, 2006.

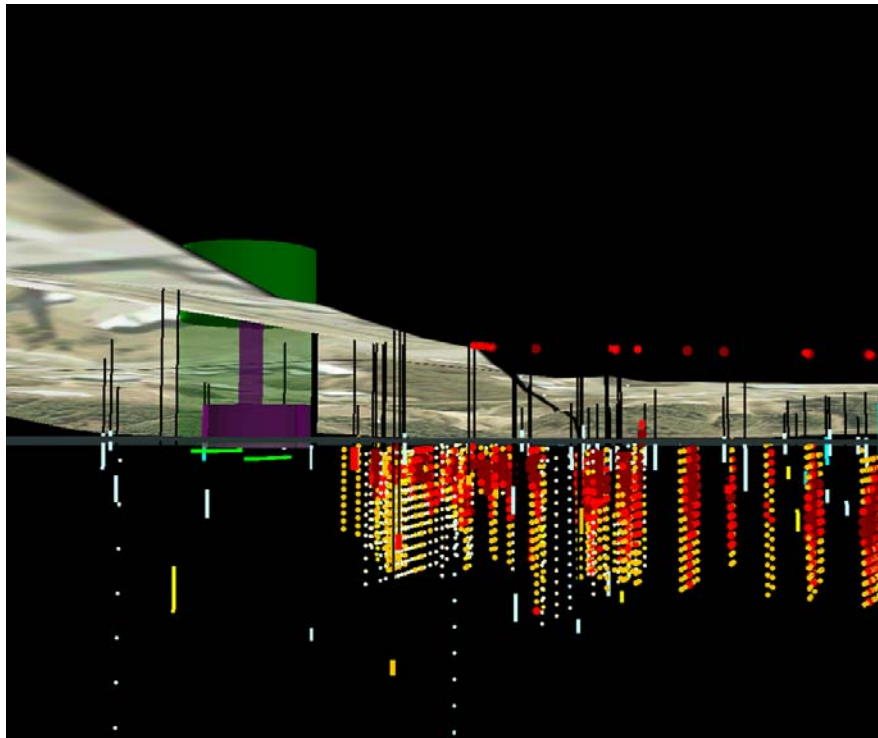


Figure 3-11. Oblique view looking northeast of tritium plume with concentrations emanating from the HFBR.

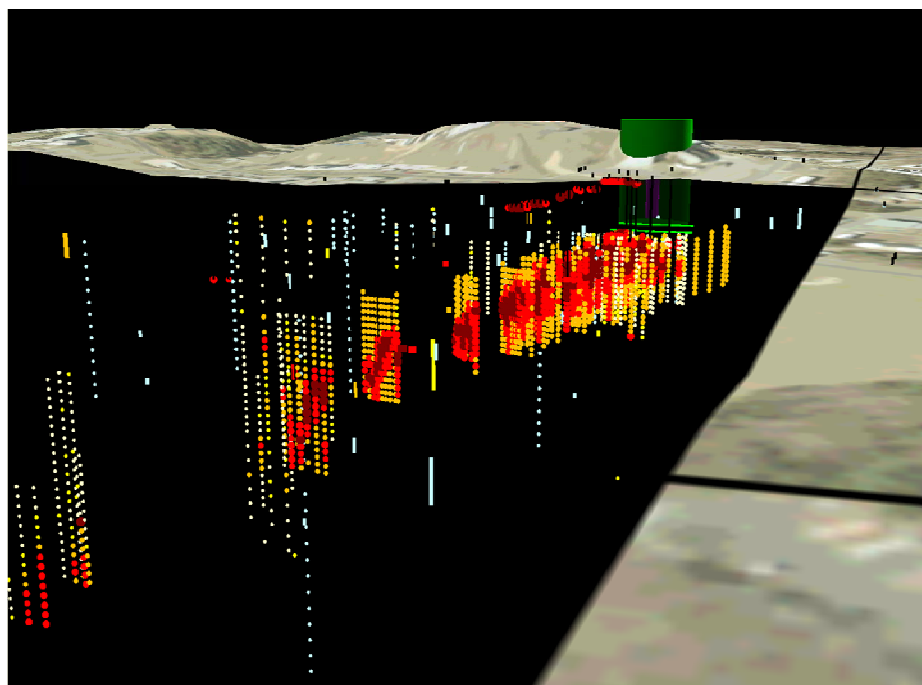


Figure 3-12. Oblique view looking northwest of tritium plume with concentrations emanating from the HFBR.

### 3.3.2 Flow and transport modeling

The second part of this exercise was to evaluate the effects of aquifer pumping on plume configuration by an active system that continuously pumps water from one or more monitor wells near the facility. Ground-water flow and transport simulation was performed utilizing a combination of techniques including excel spreadsheets, MODFLOW and GMS. Figure 3-13 and Figure 3-14 present the results of the ground-water modeling using GMS for visualization. The model assumed a homogeneous matrix with a hydraulic conductivity of 200 ft/day and a porosity of 0.3. Each square on the grid is 100 by 100 feet.

Modeling predicts, after 20 years with no pumping or remediation, the contaminant plume should be moving south by southeast, following the slope of the water table. Figure 3-13 presents the slope of the observed water table with the modeled tritium plume in color and the actual tritium plume uncolored. The actual plume did not follow the slope of the water table surface, but was pulled to the west by site extraction wells.

### 3.3.3 Active Monitoring

As has been observed from historical monitoring data, the tritium plume is relatively narrow, making it difficult to sample the plume through passive ground-water monitoring. For a similar facility and situation, an active extraction well monitoring program increases the size of the capture zone and the likelihood of detection.

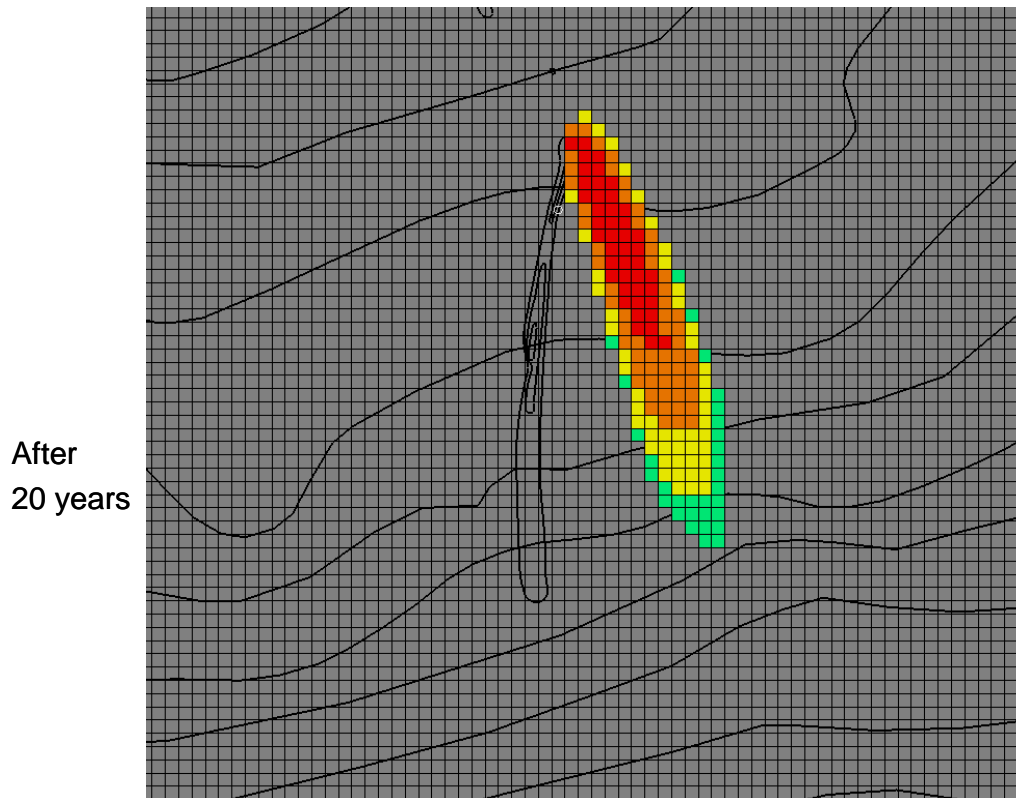
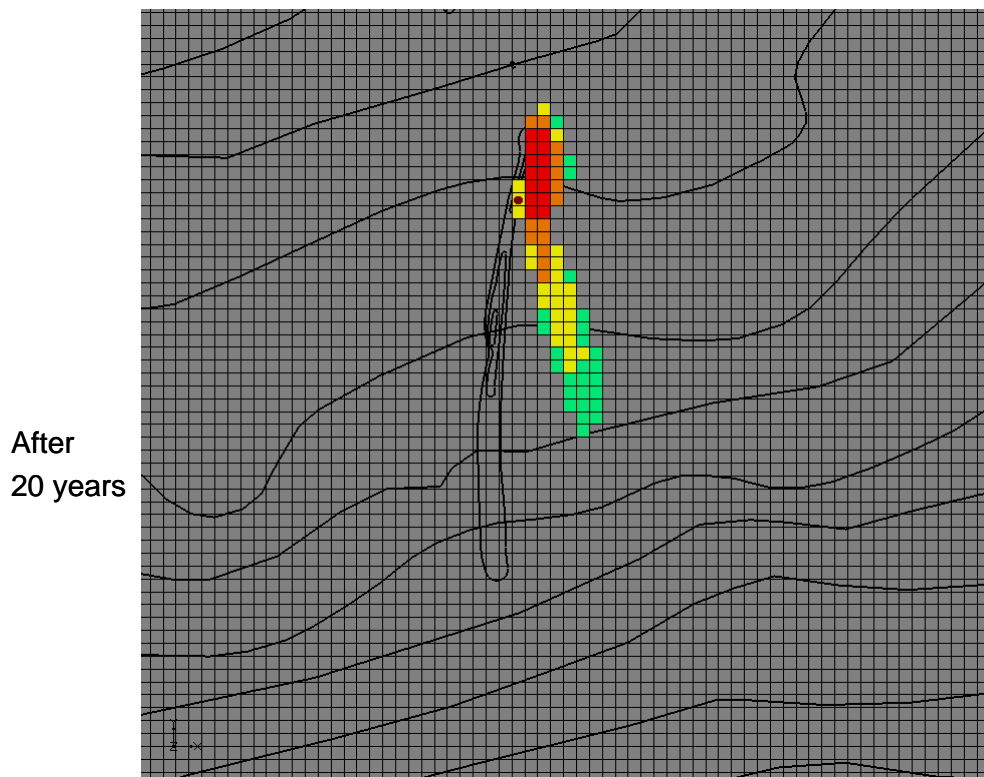


Figure 3-13. Computer simulation of tritium plume emanating from the HFBR after twenty years, no pumping

Because an active extraction well creates a large capture zone both vertically and horizontally, there is a greater opportunity for early detection. In the case of the HFBR, the tritium plume was confined to the upper 0.3 m of the water table and as stated above, the horizontal wells placed below the HFBR failed to detect the tritium plume until the water level dropped enough to allow the wells to capture water from the top of the water table. By placing an active pumping monitor well just down gradient of the facility, a larger cone of influence can be evaluated, resulting in earlier detection.

The principal contaminants of concern at nuclear facilities are radionuclides, which can be detected at low concentrations, minimizing the concern of dilution due to pumping. Early detection of mobile contaminants through pumping could mitigate contamination, prevent offsite migration, minimize efforts associated with remediation of a larger, multi-contaminant plume, as well as serve as a Performance Indicator to validate and revise the conceptual model. Figure 3-14 provides the results of the modeling program shown in Figure 3-13 utilizing the same parameters, only with the addition of an active pumping well adjacent to the HFBR, pumping at a continuous rate of 100 gallons per minute. In this scenario, the plume has been pulled to the west by the pumping. A passive monitoring well at this location would not have detected this tritium plume; however, the active well easily captured the plume.



**Figure 3-14. Computer simulation of tritium plume emanating from the HFBR after twenty years, pumping monitoring well.**

### 3.3.4 Performance Indicators

Ground-water monitoring does not only entail analyzing for constituents of concern, but also various Performance Indicators that could trigger monitoring and/or remedial actions. These indicators can be used to validate or refine the conceptual site model. Performance Indicators and features, events, or processes (FEPs) which influence HFBR plume flow and transport include, but are not limited to:

**tritium concentrations in the ground water** – Tritium needs to be evaluated to not only determine if concentrations have exceeded monitoring limits (e.g., drinking water limits, etc.), but also to trigger low-flow pumping of extraction wells for removal and re-injection up gradient.

**ground-water level distributions** – The tritium plume emanating from below the HFBR is very narrow and the direction of movement of the plume is susceptible to slight changes in water table orientation due to varying meteorological conditions or changes in infiltration related to surface changes. Thus, in this environment, it is essential to account for ground-water level distributions when modeling and monitoring performance.

**nearby remediation well pumping** – Brookhaven is a rather small site in geographic extent. Any pumping on the site regardless of whether it is for remediation or process water can impact how plumes behave and interact. Ongoing remediation of other plumes in the vicinity may impact movement and capture rate of the HFBR tritium plume. Inception or termination of ground-water extraction for other plumes can significantly affect the orientation of the water table surface regionally. An adjacent pumping system could result in the migration of the HFBR tritium plume out of the path of current monitoring.

**process water extraction-** Production wells that are used to extract water for industrial processes can alter the direction, speed and concentrations of plumes. Water levels in monitoring wells should be carefully evaluated to determine if the cycling of process wells have an influence on contaminant plumes.

**tritium as a tracer for other ground-water contamination** – Because of its high mobility, tritium acts a tracer for the movement of future, less mobile contaminants. Because strontium-90 has been identified in the vicinity of the HFBR tritium plume, the tritium plume movement data can be applied to future strontium-90 monitoring and remediation efforts. Careful examination of older plumes (TCE plume) in the vicinity of the tritium plume can give insight to how the tritium plume and any subsequent plume might behave in the future.

**tritium as a tracer for early warning** – Tritium is very mobile within the vadose zone and is usually detected on the leading edge of contaminant plumes making the presence in soil vapors an excellent candidate for early warning of potential releases.

While the VOC plume mentioned in Figure 3-1 is not discussed in this Chapter, it may be worthwhile to note that flow and transport behavior of this plume may provide useful information about the potential pathway of the tritium plume.

### **3.4 Monitoring Strategy Application Conclusions**

This case study illustrates how 3-D modeling can be a powerful tool for evaluating the shape, progress, and future paths of contaminant plumes. Because examination of existing site characterization and monitoring data led us to believe that the flow path of the tritium plume emanating from HBFR facility was being influenced by nearby process water and remediation well pumping, we realized the importance of incorporating these nearby wells into our CSM. In addition, based on earlier work done by Looney and Paquette, we realized that it was necessary to develop flow and transport simulations that could accurately model the observed tritium transport through the vadose zone.

The flow and transport simulations, which were developed using Excel, MODFLOW, and GMS, are effective tools for evaluating the effectiveness of various pumping alternatives, and thus, can aid in development of an efficient and cost effective monitoring and/or remediation program.

An optimally designed and operated monitoring network will increase the likelihood of early detection of plume migration. These flow and transport simulations can not only help place monitoring wells, but they can also help establish optimal pump rates. In this case, for example actively pumping monitoring wells may help create a larger cone of influence, resulting in less chance of a narrow plume being missed. By increasing the cone of influence, less monitoring wells may be required. By detecting these plumes earlier, remediation efforts can be put in place sooner, minimizing the chance for the plume to spread offsite or to other aquifers.

Detailed contour maps of changing water table surfaces may also be helpful to evaluate the effects of seasonal changes to the water table as well as the effects of extraction/injection activities at remediation start up, during operation, or after termination of activities. The narrow nature of these plumes makes understanding changes vital.

### **3.5 Brookhaven References**

Aronson, D.A., and G.E Seaburn. "Appraisal of the operating efficiency of recharge basins on Long Island, N.Y., in 1969." U.S. Geological Survey Water- Supply Paper 2001-D, 22 p. 1974.

Brookhaven National Laboratory (BNL). "1997 Environmental Restoration Division Sitewide." Groundwater Monitoring Report. June 1998.

BNL. *Source Water Assessment for Drinking Water Supply Wells*. Brookhaven National Laboratory, December 2000.

BNL. "2003 BNL Groundwater Status Report." Environmental and Waste Management Services Division/Environmental Restoration. June 2004.

BNL. 2005 Site Environmental Report, Brookhaven National Laboratory, p. 7-5.2005.

- CDM Federal Programs Corporation. "Technical Memorandum, Pre-Design Aquifer Test, October 10-20, 1995." Brookhaven National Laboratory. December 1995.
- Department of Energy (DOE). Brookhaven National Laboratory, EPA Region 2, Operable Unit III, Record of Decision, Environmental Restoration Division, April 14, 2000.
- DOE. Brookhaven National Laboratory, EPA Region 2, NPL Listing History, [www.epa.gov/region02/superfund/npl/0202841c.pdf](http://www.epa.gov/region02/superfund/npl/0202841c.pdf), August 17, 2006.
- Franke, O.L., and N.E. McClymonds. "Summary of the Hydrologic Situation on Long Island, New York, as a Guide to Water-Management Alternatives." U.S. Geological Survey Professional Paper 627-F, 59 p. 1972.
- Grosser, P.W. (Consulting Engineer and Hydrogeologist, P.C.). Operable Unit III Pump Test Report. 1997.
- Holzmacher, McLendon and Murrel, P.C. (H2M), and Roux Associates, Inc. *Waste Management Area, Aquifer Evaluation and program Design for Restoration. Volumes I and II.* 1985.
- Koppelman, L.E. (Ed.). *The Long Island Comprehensive Water Treatment Management Plan (Long Island 208 Study).* Nassau-Suffolk Regional Planning Board. Hauppauge, New York. Volumes I and II. July 1978.
- Looney, B.B., and D.E. Paquette. *Tritium Source Characterization at the High Flux Beam Reactor Brookhaven National Laboratory.* Compiled in *Vadose Zone Science and Technology Solutions*. Vol. 1, p. 50-59. 2000.
- Paquette, D.E. *Brookhaven National Laboratory AGS Booster Applications Facility, Potential Impacts to Groundwater Quality.* September 1998.
- Prince, K.R., O.L. Franke, and T.E. Reilly. "Quantitative Assessment of the Shallow Ground-Water Flow System Associated with Connetquot Brook, Long Island, New York." U.S. Geological Survey Water- Supply Paper 2309. 28 p. 1988.
- Quadrel, M., and R. Lundgren. *Managing an Effective Vadose Zone Project.* Compiled in *Vadose Zone Science and Technology Solutions*. Vol. 1, p. 61-124. 2000.
- Scorca, M.P. "Urbanization and Recharge in the Vicinity of East Meadow Brook, Nassau County, New York, Part 1—Streamflow and Water-Table Altitude, 1939-90." U.S. Geological Survey Water-Resources Investigations Report 96-4187, 39 p. 1997.
- Scorca, M.P., W.R. Dorsch, and D.E. Paquette. "Water-Table Altitude Near the Brookhaven National Laboratory, Suffolk County, New York, in March 1995." U.S. Geological Survey Fact Sheet FS-128-96. December 1996.

- Scorca, M.P., W.R. Dorsch, and D.E. Paquette. "Water-Table Altitude Near the Brookhaven National Laboratory, Suffolk County, New York, in August 1995." U.S. Geological Survey Fact Sheet FS-233-96. April 1997.
- Scorca, M.P., W.R. Dorsch, and D.E. Paquette. "Stratigraphy and Hydrologic Conditions near the Brookhaven National Laboratory and Vicinity, Suffolk County, New York, 1994-1997." U.S. Geological Survey Water Resource Investigations Report 99-4086. 1999.
- Smolensky, D.A., H.T. Buxton, and P.K. Shernoff. "Hydrogeologic Framework of Long Island, New York." U.S. Geological Survey, Hydrogeologic Investigations Atlas 709, 3 Sheets. 1989.
- Warren, M.A., W. deLaguna, and N.J. Lusczynski. "Hydrogeology of Brookhaven National Laboratory and Vicinity, Suffolk County, New York." U.S. Geological Survey Bulletin 1156-C, 127 p. 1968.
- Woodward-Clyde Consultants. *Potable Well Stud.*, Brookhaven National Laboratory, Upton, Long Island, New York. 10 p. 1993.

## **4 Amargosa Desert Research Site**

### ***4.1 Introduction***

The Amargosa Desert Research Site (ADRS), located in Nevada's Mojave Desert, was selected to test the applicability of the Advanced Environmental Solutions, LLC (AES) Strategy to an arid environment. This exercise is for demonstration only. This report is based on readily available information and does not constitute a comprehensive evaluation of all data for the site. Data used in this exercise were provided courtesy of the United States Geological Survey (USGS).

The Amargosa Desert Research Site was previously a commercially-operated low-level waste-burial facility on the Mojave Desert, about 40 km east of Death Valley, near Beatty, Nevada. Beginning in 1962, low-level waste was disposed in unlined trenches. By 1970, hazardous waste was also placed in unlined trenches. Starting in 1988, the hazardous material was placed in lined trenches. Low-level disposal was ceased in 1992.

In 1976, the USGS began studies of water movement at the Beatty Low-Level Waste Disposal Facility. In 1997, after unexpectedly high levels of tritium were discovered in shallow soil gas samples, the site was included in the USGS's Toxic Substances Hydrology Program and became known as the Amargosa Desert Research Site.

The primary issue of concern at the ADRS is the migration of radionuclides and VOCs from the waste buried in the facility trenches. Tritium, when present in the ground water or the vadose zone, is an excellent indicator for the movement of contaminants.

Evaluation of all available data for the ADRS has resulted in several questions, the most significant of which is: Why is tritium present across the vadose zone and in the ground water below the ADRS? Research has indicated that overall soil moisture in the vadose zone adjacent to the ADRS exhibits an upward movement (Andraski et al., 2005). However, the presence of elevated tritium across the vadose zone, to a depth of over 100 meters below ground surface (bgs), would indicate that there is a mechanism for the downward migration of contamination.

Soil vapor modeling by Striegl et al., 1996 failed to produce a mechanism for the vertical component of movement of tritium within the vadose zone below the ADRS. Striegl et al., 1996 also proposed that the only mechanism for the vertical migration of tritium was in liquid form along complex hydrogeologic layers, but were unable to find specific geologic data to support this hypothesis.

Because of the necessity for a fast pathway for the downward movement of soil gases containing tritium and after a comprehensive review of all available data for the site, an alternate conceptual model for movement of tritium through the vadose zone and into the underlying water table below the ADRS is proposed in the following sections.

### ***4.2 Compilation of Available Data***

This section provides a summary of the readily available data compiled to prepare this evaluation. The majority of the data used in this evaluation has been provided by or is available on line from the USGS.

### 4.2.1 Geologic Setting

The ADRS is located in the Basin and Range Province of southern Nevada (Figure 4-1). This area of the Mojave Desert southwestern United States is considered one of the driest in the United States (Andraski et al., 2005).

The Basin and Range Province of Nevada is characterized by a series of north-south-trending extensional sedimentary basins represented by patchwork mountain ranges or “horsts”, commonly 10 miles wide and rarely longer than 80 miles long, bounded by faults and adjacent downthrown valleys or “grabens”. The bounding faults have been active during the last 20 million years and represent an extensional geologic regime. The normal bounding fault planes usually dip approximately 60 degrees and extend deep into the crust, creating vertical displacement of as much as 10,000 feet. Figure 4-2 presents a generalized cross section of a horst and graben sequence (CG 1992).

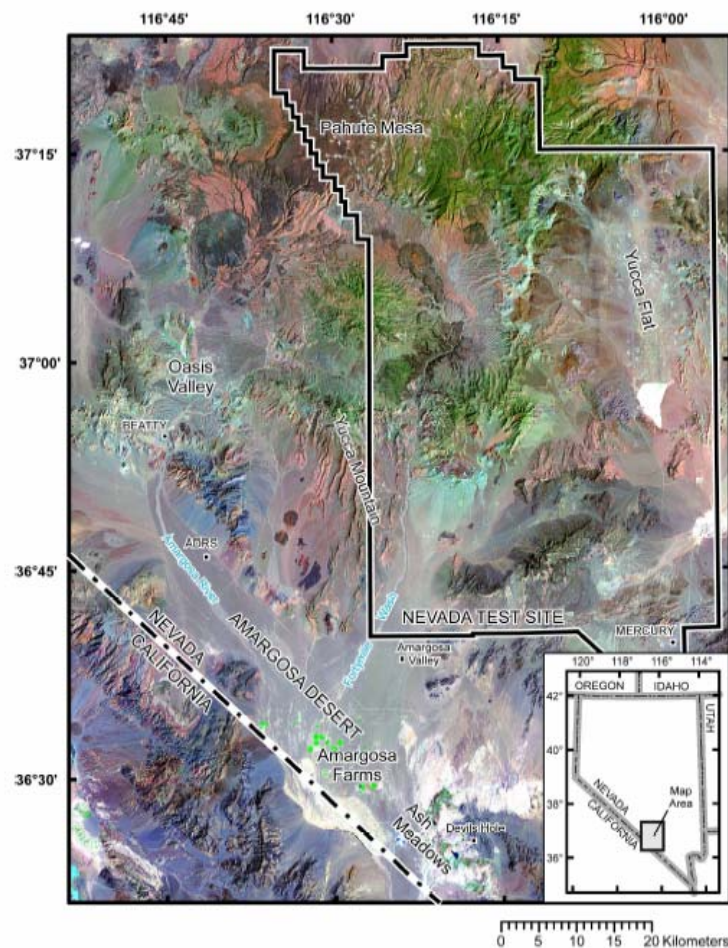
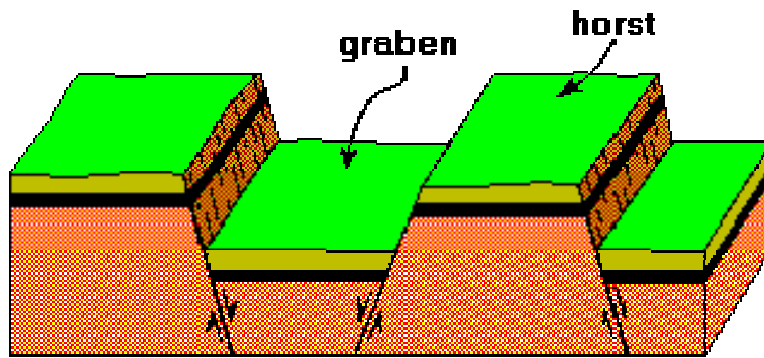


Figure 4-1. Location of ADRS (Stonestrom et al., 2003)



## HORST AND GRABEN

**Figure 4-2. Cross section of a typical horst and graben sequence (CG, 1992)**

Weathering and erosion began soon after formation of the horsts. The movement of the sediments into the adjacent basins created alluvial fans on top of basin sediments. Figure 4-3 provides an oblique view of a typical alluvial fan. These fans form when upland streams with steep gradients leave rugged terrain and enter a valley. Alluvial fans contain sequences of poorly sorted material. In addition, they contain series of active and abandoned interlacing channels.

The interlacing of these channels results in complex patterns of alternating high and low permeability, which significantly affects ground-water movement. However, because the fans were deposited with a generally radial pattern, the permeability of the sediments should also generally follow the same trends.



**Figure 4-3. Oblique view of a typical alluvial fan in Death Valley**

## 4.2.2 Regional Geologic Information

The Amargosa Desert Research Site is located in a 13 km wide northwest-trending graben of the Basin and Range Province of southern Nevada (Figure 4-4). The regional geology underlying the ADRS appears to consist of shallow river gravels overlying unconsolidated alluvial fan, fluvial, and marsh deposits, and ultimately Paleozoic bedrock (Fischer, 1992). Since the ADRS is located adjacent to the northeast flank of the graben, the promulgation of the alluvial fan is from the northeast to the southwest across the site. The graben is bounded by mountain ranges composed of lower Paleozoic carbonate and clastic sediments, metasediments, and volcanics. The valley floor below the ADRS is presumably composed of similar material.

In addition to the alluvial fan deposition at the ADRS, the Amargosa River has subsequently overprinted a floodplain of coarse river gravels near ground surface, covered by a thin (1 m thick) layer of finer grained sediments.

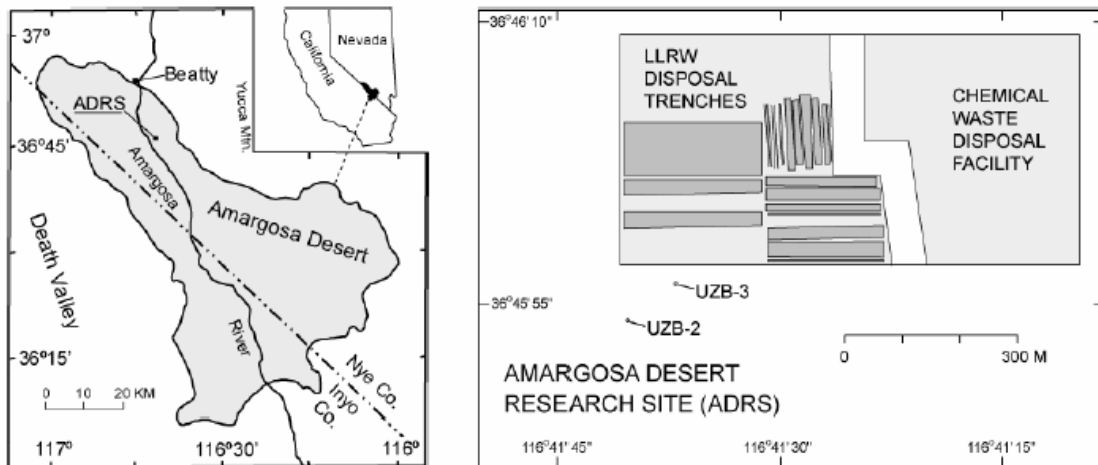


Figure 4-4. Location of ADRS and soil gas sampling boreholes UZB-2 and UZB-3 (Stonestrom et al., no date)

## 4.2.3 Site-specific Geologic and Analytical Data

Available data sources for this analysis included:

- Geophysical borehole log data (neutron-moisture, natural gamma, and gamma-gamma)
- Monitoring well data from existing wells
- Schlumberger soundings
- Soil gas data
- Thermocouple psychrometer / water potential data
- Soil moisture data
- A summary of each of these data sets, and relevant conclusions is below:

*Geophysical borehole log data analysis (neutron-moisture, natural gamma, and gamma-gamma):*

While core logs are not available for these wells, Geophysical borehole logging suggests the presence of isolated clay lenses (Figure 4-5) (Fischer, 1992). For example, thin clay lenses were detected at 10, 20, and 25 m bgs in Well 303, but were not seen in the other wells. Also, a clay lens was observed in the log of Well 302 at a depth of 37 m, but was not observed in the other wells. Low moisture content at various intervals may indicate coarse, more permeable gravel; however, some of these low moisture intervals also have elevated gamma readings.

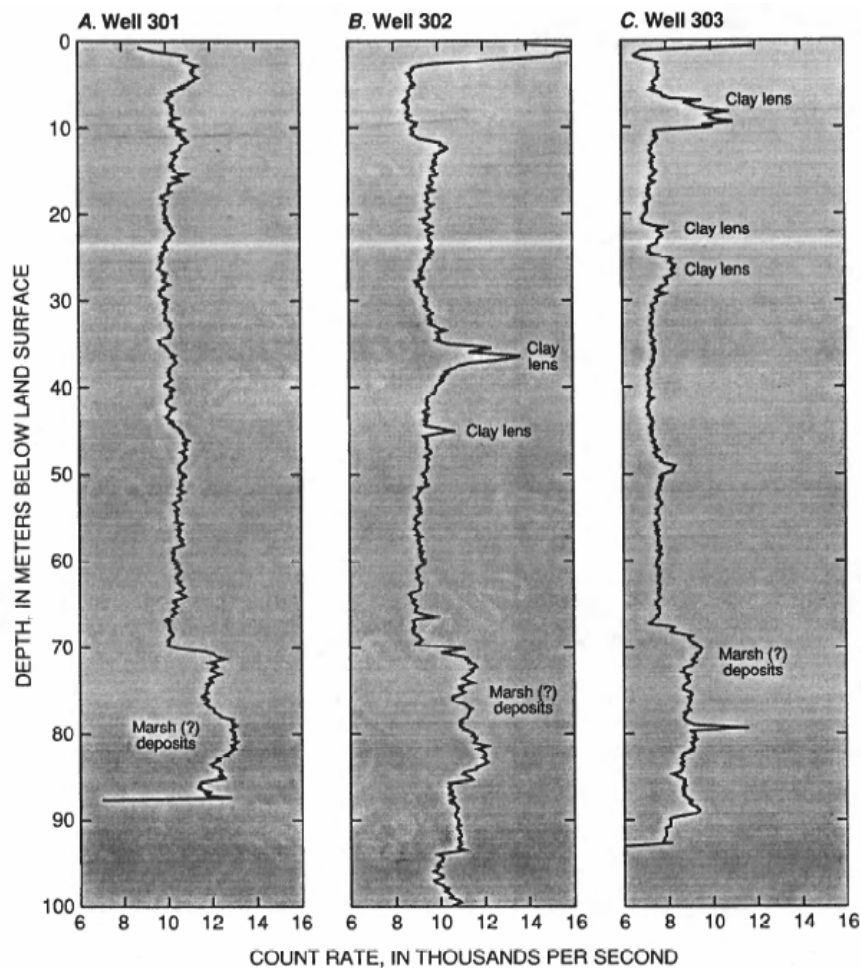
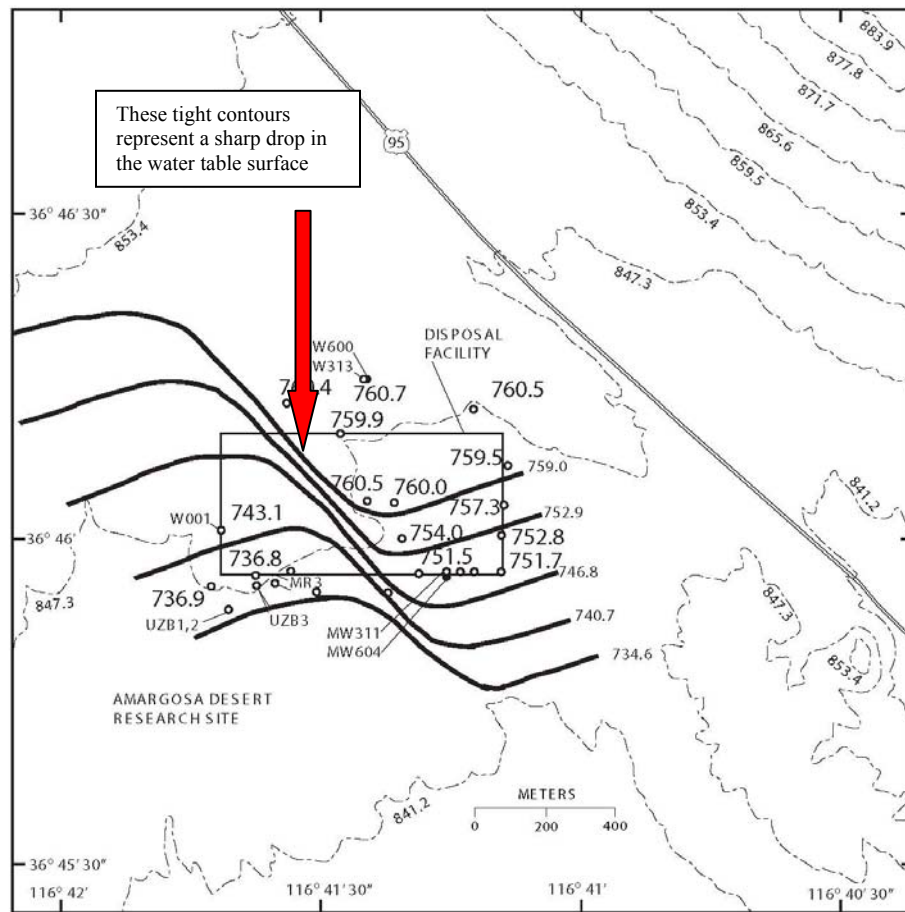


**Figure 4-5. Geologic distribution of clay lenses and marsh deposits in ADRS Wells 301, 302, and 303 (Fischer, 1992)**

The most consistent subsurface layer appears to be a 20 m thick clay marsh deposit at a depth of 70 to 90 m bgs and is present in all three boreholes (Fischer, 1992). Based on the top of the clay horizon, Fisher determines the unit dips to the south-southeast at a rate of approximately 0.07 meters per meter (m/m).

Figure 4-6 presents contours of the water table surface which show a south-southwest dip in the water table toward the southwestern portion of the facility. Depth to bedrock below the ADRS is approximately 170 m and depth to ground water is approximately 100 meters bgs. This Figure also shows the location of 14 monitoring wells within the ADRS burial site and several others in the surrounding vicinity (shown as circles in the Figure); however, data for these wells were unavailable.



MR3 734.3	Well MW319 76.2 meters north; 181.92 m east of northwest corner Elevation of water table is 760.4 m; May 6, 2004
UZB3 736.8	Well MW318 71.4 meters north; 705.46 m east of northwest corner Elevation of water table is 760.5 m; May 6, 2004.
MW302 736.9	Well MW325 449.53 meters south; 28.91 m west of northwest corner Elevation of water table is 736.9 m; May 6, 2004
MW311 751.6	Well MW326 447,22 meters south; 266.39 m east of northwest corner Elevation of water table is 737.7 m; May 6, 2004
MW317 751.0	Well MW327 446.5 meters south; 472.33 m east of northwest corner Elevation of water table is 741.6 m; May 6, 2004
Site Well 760.5	
MR1 near Amargosa River 3,200 m west of northwest corner; Water table 757.82 m.	

**Figure 4-6. ADRS water table contours (measured in meters MSL) and well locations (Walvoord et al., 2005)**

*Monitoring well data analysis*

Tritium is present in the water table over 100 meters below the ADRS, albeit in concentrations well below drinking water standards. Figure 4-7 provides a map of tritium concentrations in water table monitoring wells (monitoring well data is summarized in Appendix 4-A). The elevated tritium concentrations in ground water at location MR-3 in relation to the other facility monitoring wells brings into question the source of this tritium and the potential need for a revised CSM of contaminant movement in the vadose zone.

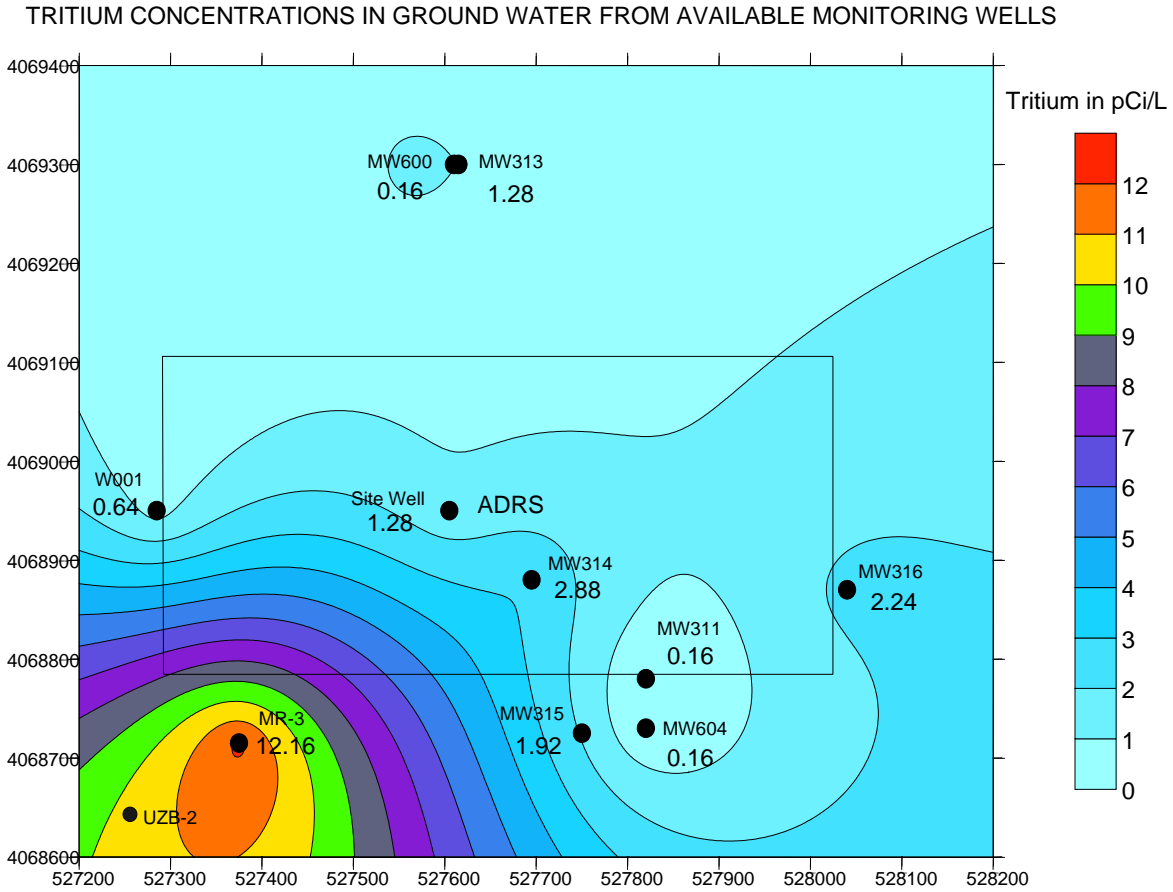


**Figure 4-7. Map of tritium concentrations in ground water below ADRS (Data from Prudic, 1997)**

Based on the regional geologic setting of the ADRS in a graben, with the nearest horst fault boundary to the northeast, the alluvial fan pattern for the geology below the site should dip to the west-southwest with some degree of radial dispersion present. Vertical variability in the fine to medium grain portion of the layering creates a significant anisotropic effect for movement of constituents within the vadose zone that should be accounted for in a monitoring program. In addition, the coarse gravel layer present at approximately 1.5 m bgs appears to act as a conduit for the lateral transport of contaminants.

*Schlumberger sounding data analysis*

A resistivity survey of Schlumberger soundings conducted in 2002 (Bisdorf, 2002) over the ADRS area indicates the presence of a significant northwest to southeast striking basin fault approximately 500 feet northeast of the site. The sounding results suggest that the fault line dips steeply to the southwest beneath the subsurface. This fault orientation is most likely related to the regional horst and graben faulting (Figure 4-8 depicts numbered Schlumberger sounding survey locations with faults; Figure 4-9 shows the suggested location and fault orientations).

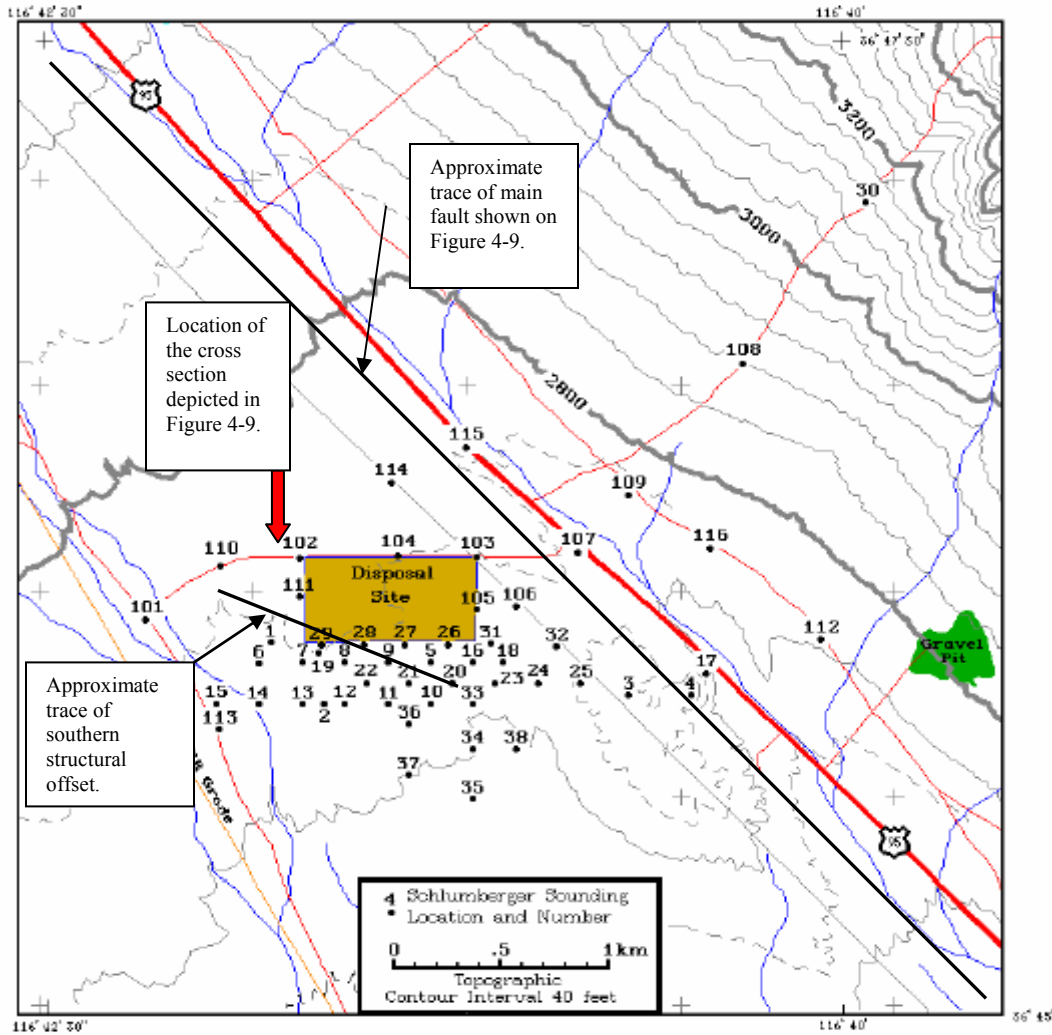
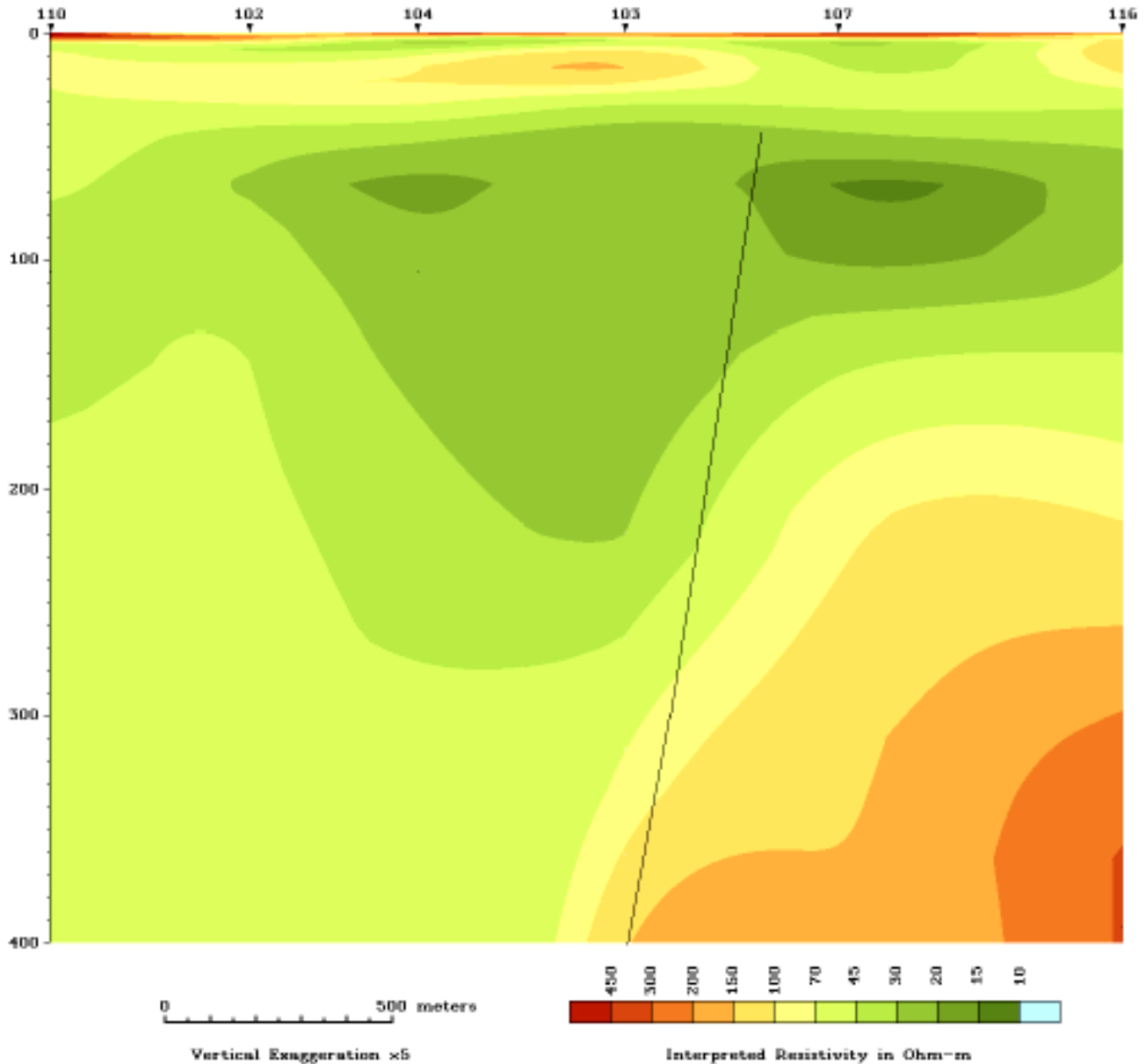


**Figure 4-8. Map showing numbered survey locations of Schlumberger soundings (modified from Bisdorf, 2002)**

The trace of US Highway 95 on Figure 4-8 appears to follow the toe of the alluvial fan as it emerges from below the alluvial river gravel. The trace of the basin fault, as defined by the results of the Schlumberger Soundings, also roughly parallels the trace of US Highway 95. The thin blue lines on the map represent intermittent stream drainages. The trace of the cross section presented in Figure 4-9 runs between sounding locations 110 and 116. An additional fault was later identified during the application of this Strategy

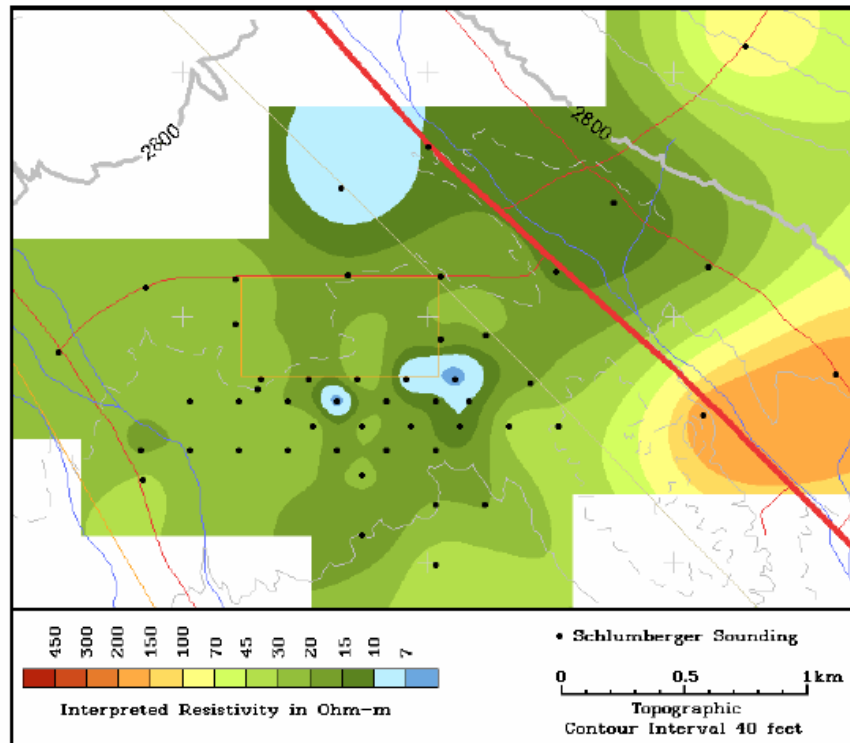
and is referenced in this report as the “southern structural offset”. This offset was identified through the application of three-dimensional visualization of the resistivity data and is discussed further in Section 4.3.4 below.

Figure 4-9 presents a cross section of the Bisdorf resistivity soundings indicating the location and orientation of the fault between sounding locations 103 and 107. As shown in Figure 4-9, Bisdorf infers the location of the basin fault by the presence of the steep resistivity gradient between sounding locations 103 and 107.



**Figure 4-9. Cross section of interpreted resistivity and basin fault (Bisdorf, 2002). (Triangles along the top axis correspond to sounding locations as mapped in Figure 4-8. Subvertical solid black line represents basin fault as defined by Bisdorf 2002.)**

Figure 4-10 is a contour map of the resistivity survey at approximately 97 m bgs and shows the displacement of sediments down on the southwest side of the northwest-trending structure.



**Figure 4-10. Map showing contours of interpreted resistivity at a depth of 97 m overlying topographic contours (Bisdorf, 2002)**

#### *Surficial soil gas data analysis*

Surficial soil gas data and terrestrial sampling seem to indicate that, at least in the near surface, contaminant migration is along gravel layers to the south and west from the burial trenches, following topography and away from this fault.

#### *Direct current electrical resistivity (DC-resistivity) imaging*

A vertical cross section (Figure 4-11) made by Stonestrom using direct current electrical resistivity (DC-resistivity) imaging near UZB-2 and UZB-3 (vadose zone soil gas sampling wells) shows intermittent gravel layers that thicken to the southwest toward the center of the basin, providing preferential pathways for contaminant migration (Stonestrom et al., no date).

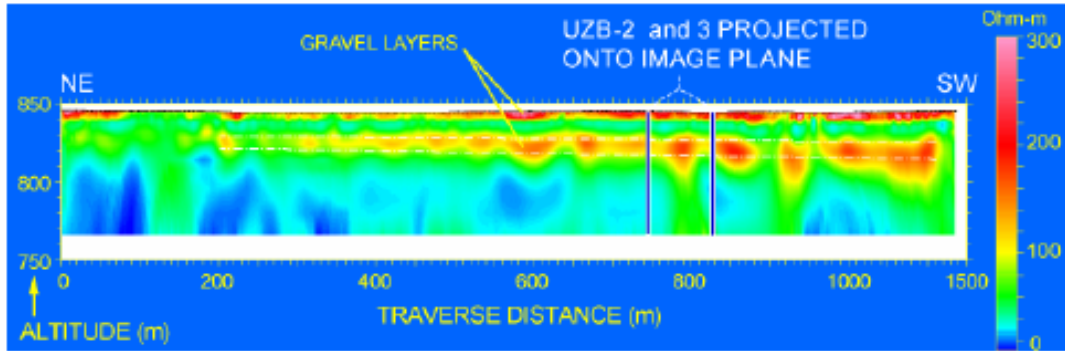


Figure 4-11. A vertical cross section made by direct current electrical resistivity (DC-resistivity) imaging near the ADRS (Stonestrom et al., no date)

### Moisture Data

The vadose zone below the ADRS is between 85 m and 115 m thick. A monitoring shaft was installed in the vadose zone southwest of the waste facility to a depth of 13.7 m bgs. Within this shaft were installed a series of thermocouple psychrometers (TCPs) as shown in Figure 4-12. These TCPs were installed horizontally out of the shaft into the surrounding vadose zone sediments and were used for measuring water potentials.

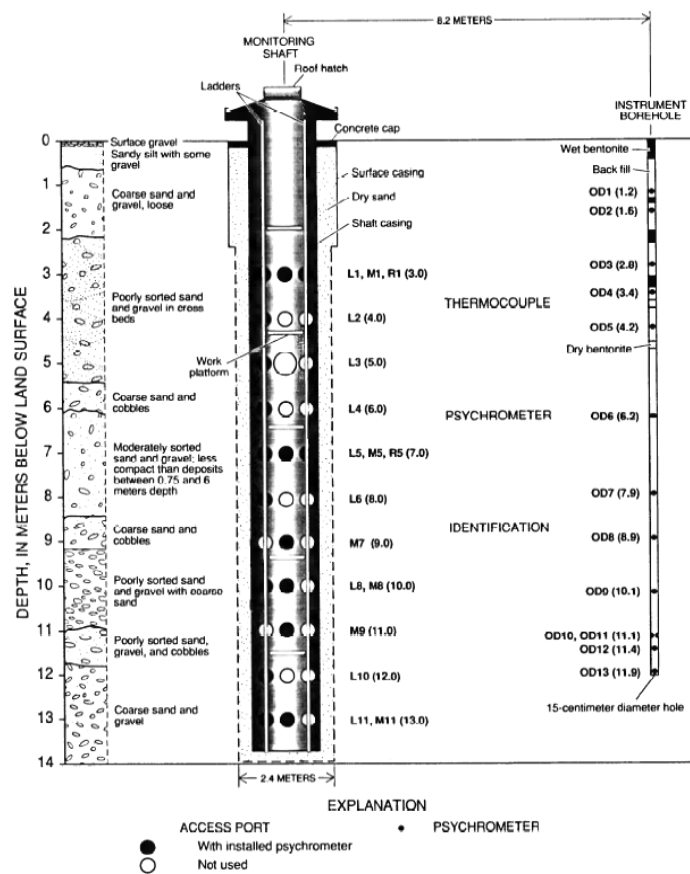


Figure 4-12. Monitoring shaft and instrument borehole showing locations of TCPs and respective geologic information (Fischer, 1992). Thermocouple psychrometers installed in the monitoring shaft

**are designated with L (left), M (middle), and R (right), followed by a number from 1 to 11 that indicates level in shaft. Thermocouple psychrometers installed in the instrument borehole are designated OD1 through OD13. Depth of each thermocouple psychrometer, in meters below land surface, is given in parentheses. (Fischer, 1992).**

Moisture content of soils was estimated using a neutron probe. Figure 4-13 provides a relative comparison between the varying lithology at the monitoring shaft location and the variable moisture content of the different gravel horizons.

In the gravel layers at 1.5 and 9 m bgs, moisture contents were less than 3%, below 1.5 m bgs, moisture content was in the 4 to 8% range. Temporally invariant water contents below 0.75-1 m bgs indicate that the textural discontinuity between the two uppermost soil layers (loamy sand over gravelly coarse sand) provides a natural capillary break that impedes downward percolation of moisture (Andraski, 1995).

#### *Hydraulic conductivities*

Hydraulic conductivities were estimated using air permeability tests. Saturated hydraulic conductivities of the sediments ranged from 1 to 48 centimeters per day (cm/day), which are not unreasonable for poorly sorted sediments with at least 10 percent fines and silt. For unsaturated sediments, hydraulic conductivities were estimated at between  $3 \times 10^{-4}$  to  $9 \times 10^{-20}$  cm/day. Porosity ranges from 25 to 43 percent and bulk density ranges from 1.4 to  $1.8 \text{ g/cm}^3$  (Fischer, 1992).

In the sediments directly below the gravel layer at 1.5 m bgs, a significant increase occurs in the chloride content from <5 milligrams per gram (mg/g) to 160 mg/g by 3 m and remains above 100 mg/g to 7 m, then falls off steadily until it returns to <5mg/g at 11 m bgs. These elevated chloride readings basically are bracketed in the zone between the two major gravel layers that occur at 1.5 and 9 m bgs.

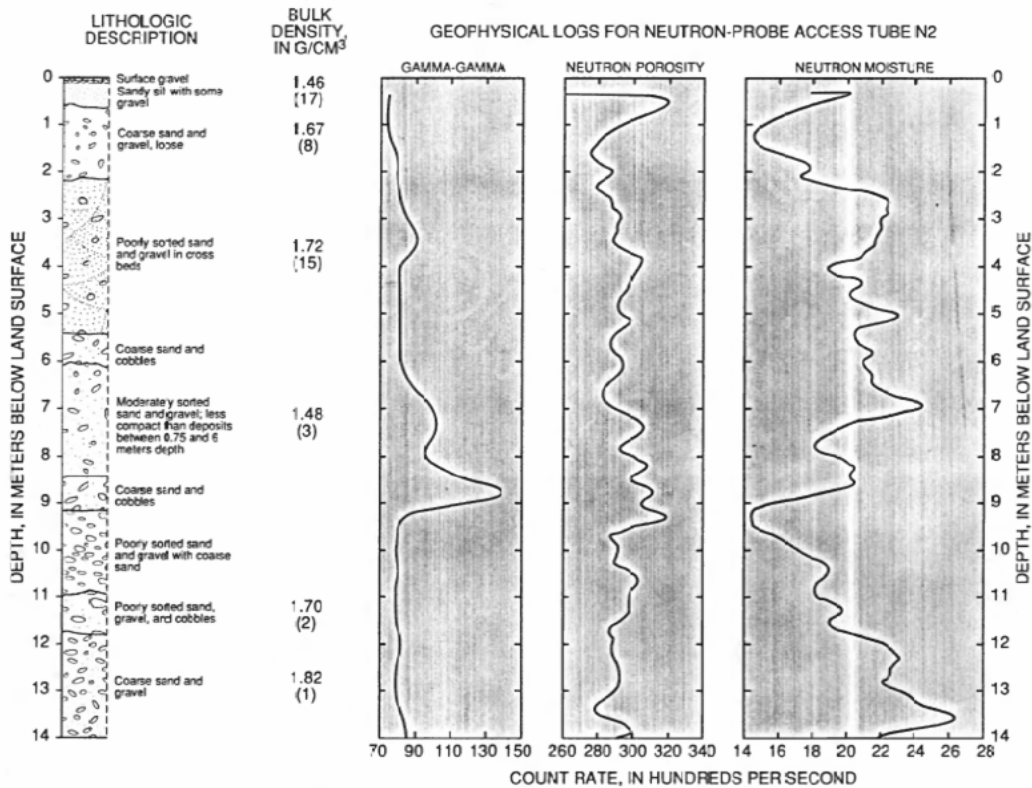


Figure 4-13. Monitoring shaft geologic and geophysical information (Fisher, 1992)

### 4.3 Application of the Strategy

Although on a regional basis, movement within the vadose zone below the ADRS is upward, contamination is moving downward along preferential pathways and has already reached the water table over 109 meters below ground surface. Past modeling efforts have failed to provide a conceptual site model that reproduces the observed vadose zone and ground water contamination. To evaluate the potential for hydrogeologic fast pathways below the ADRS and to prepare a revised conceptual site model, a more thorough examination of the available geologic and geophysical data was performed.

#### 4.3.1 Chemical Constituents in Ground Water or Soil Gas

Based on available data, tritium is by far the most pervasive and anomalous constituent in either ground water or soil gas. Tritium partitions well between water and gas phases and is usually the most mobile constituent detected at sites with radiological contamination. The path of the tritium plume can be used to infer the potential path of other constituents in either ground water or soil gas.

#### 4.3.2 Chemical Constituents in Other Fluids

This is an arid environment, but many constituents can migrate without the use of water, such as: mercury, iodine, radon, argon, krypton, and other waste components such as organic liquids. It is critical to determine the nature of the material contained within the burial trenches to know what constituents need potential evaluation. Based on available

information, constituents contained in the waste at the ADRS include, but are not limited to various isotopes of radionuclides including tritium and various hazardous compounds including carbon-14; three chlorofluorocarbon (CFC) compounds, eight chlorinated solvent compounds, and toluene although data for constituents other than tritium were not available for this exercise.

### 4.3.3 Chemical Constituents in Plants and Animals

Plants have been used in geochemical exploration for many years. Andraski et al., (2005) have demonstrated that sampling of creosote bushes in the vicinity of the waste site confirms the presence of tritium in the shallow gravels (1.5 m bgs). Figure 4-14 shows the distribution of sampling points for the creosote bush sampling. The contours indicate the concentration of tritium in plant water in  $\text{Bq L}^{-1}$ . The tritium plume as defined by the creosote bush sampling shows two potential sources of contamination emanating from the waste facility, one on the west side and one on the south side.

Figure 4-15 shows a comparison (in tritium units) of plant water tritium with soil water tritium that correlates extremely well. Based on these results, it becomes apparent that analysis of plant material in this type of environment can act as a performance indicator for tracking movement of contamination within the underlying formation.

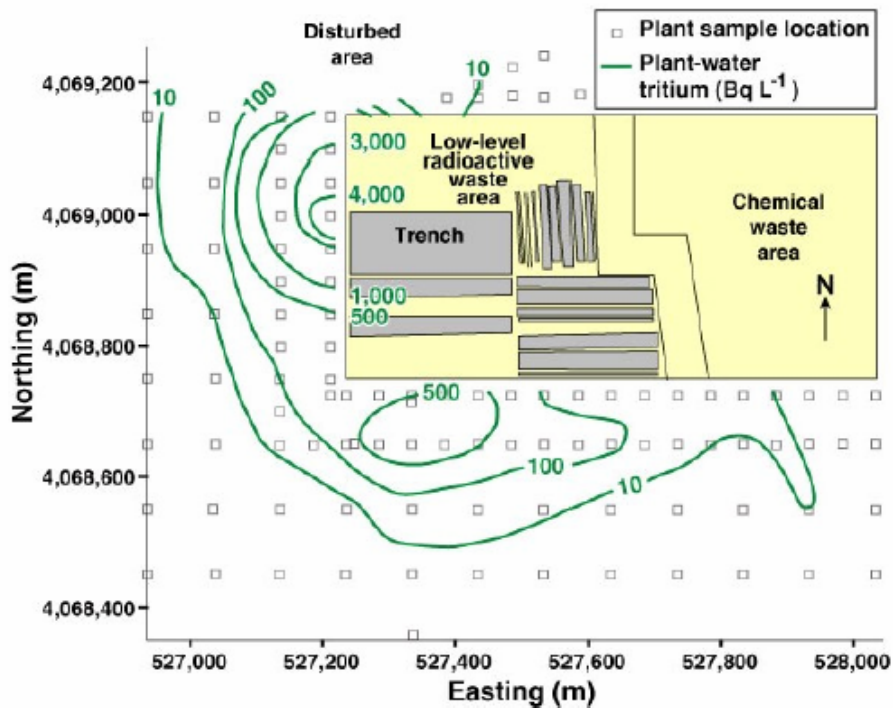


Figure 4-14. Plant sample locations and contours of plant-water tritium concentrations (Andraski et al., 2005)

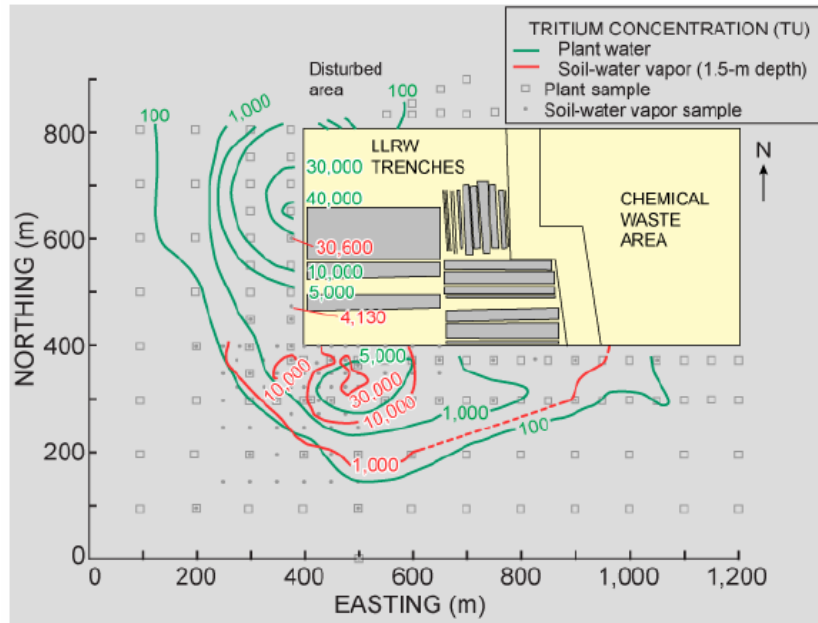


Figure 4-15. A comparison of plant water tritium with soil water tritium (Stonestrom et al., no date)

#### 4.3.4 Geophysical Modeling and Evaluation

After assembling and reviewing the available data for the ADRS, it became apparent that there was a previously undefined mechanism for the downward migration of tritium across the vadose zone to the water table.

Based on the limited geologic data available for the ADRS, the following simplified geologic CSM for the ADRS was proposed (Figure 4-16).

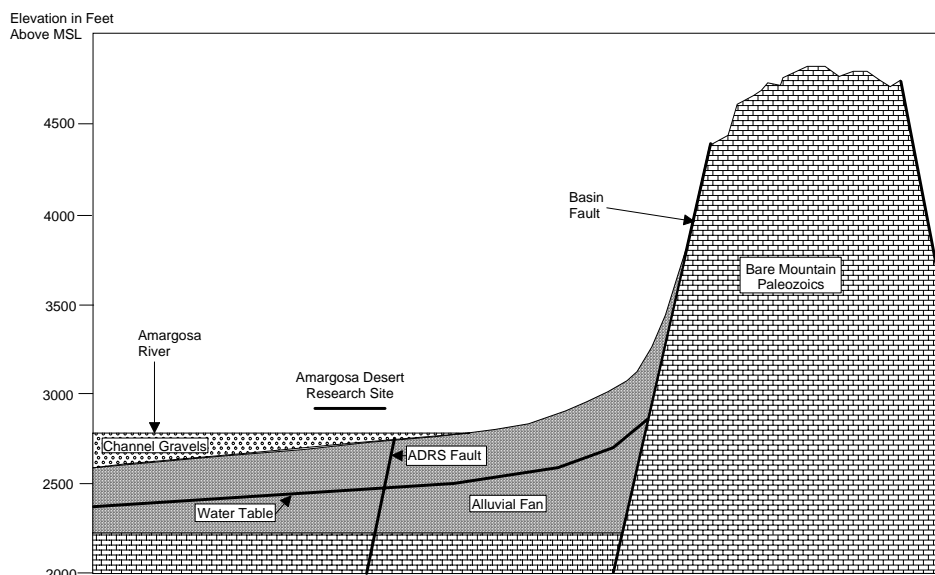


Figure 4-16. Simplified geologic cross section of the ADRS looking northwest

As there is limited geologic information available for the ADRS, the Strategy application process turned to available geophysical data. After evaluating the available geophysical information it appears that the most useful geophysical technique applied in relation to observed patterns of contaminant transport at the ADRS is direct-current electrical-resistivity (DC-resistivity) imaging, a surface-based technique employing automated, inverse-Schlumberger-array soundings (Bisdorf, 2002).

Bisdorf (2002) presents a significant database of Schlumberger resistivity soundings across the ADRS. Figure 4-8 and Figure 4-9 show the resistivity data from Bisdorf 2002 in cross section and plan view, respectively. These two figures are the only two representations of the resistivity data provided in Bisdorf 2002; however, the appendix to Bisdorf 2002 presented all of the collected data.

Based on the resistivity data provided in the appendix of Bisdorf (2002), AES prepared an electronic database of the sounding information (Appendix 4-A). Sounding locations were estimated from Figure 4-8 of Bisdorf (2002). Elevations of sounding points were extracted from regional topographic maps. AES loaded all data into a geologic modeling package (HydroGeo Analyst 2.0) and a three-dimensional (3-D) block model of the site was created by kriging the data.

Three dimensional kriging of this resistivity data identified a subtle fault not previously recognized in the data (heretofore referenced as the “Southern Structural offset”). The Southern Structural offset cuts across the southwest corner of the ADRS. The Structure runs nearly east-west and dips steeply southwest beneath the ground with approximately 30 meters of vertical offset. The Southern Structural offset coincides with the location of the southern tritium plume emanating from low-level waste trenches of the ADRS.

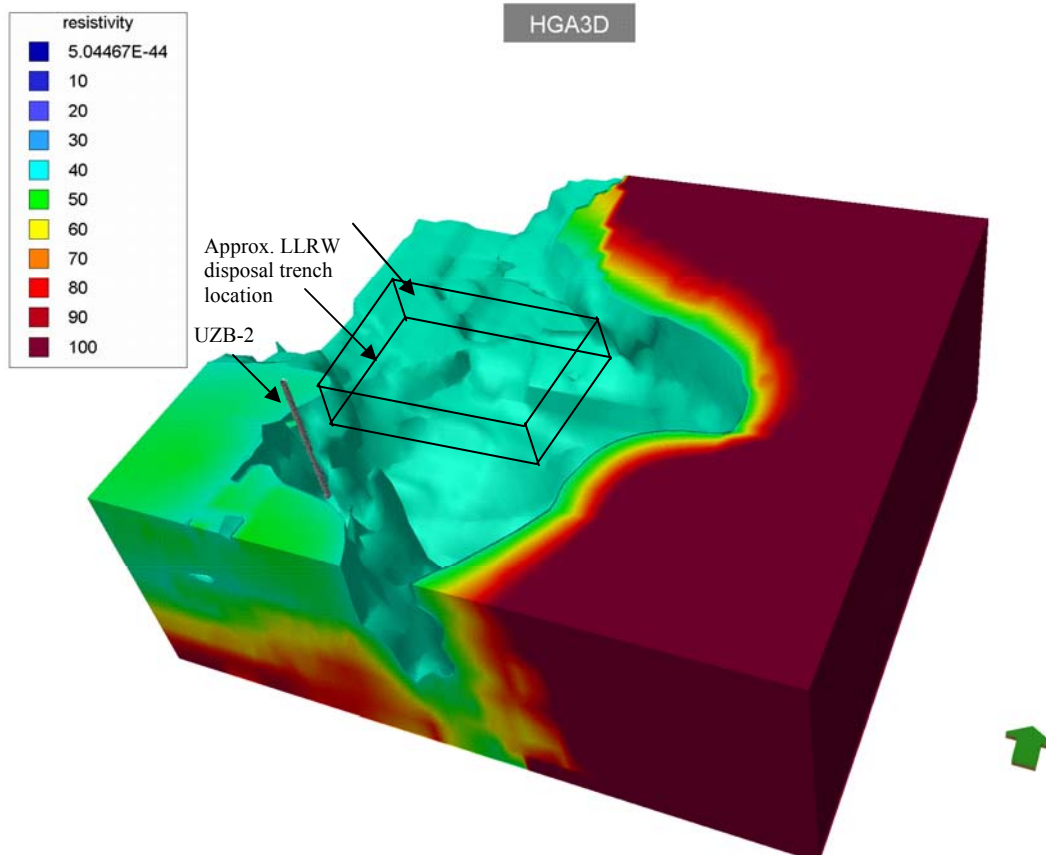


**Figure 4-17. Three-dimensional resistivity block model of the ADRS looking northwest (Well UZB-2 can be seen in the southwestern portion of the figure) (created with data from Bisdorf, 2002)**

Figure 4-17 presents the three-dimensional block model of the ADRS looking to the northwest. Well UZB-2 can be seen in the southwestern portion of the model. The upper 1.5 meters of undisturbed soil at the ADRS consists of highly resistive material. The upper 20 meters are not shown in order to remove high resistivity soils including the 1.5 meters near the surface. In addition, the block model has all lower resistivity values (values below 42 Ohm-m) removed for clarity. By comparing Figure 4-8 and Figure 4-9 with the 3-D model provided in Figure 4-17, the increase in the level of geologic detail becomes apparent.

The Southern Structural offset is located directly north of UZB-2. It cuts across the southwestern corner of the low-level trenches. To the northeast can be seen the major regional west-northwest-striking horst and graben structural offset originally defined in Bisdorf, 2002, represented by a sharp vertical gradient in the resistivity data. Localized lateral variations in gravel content within the alluvial fan are defined by the horizontal layering seen in the northern portion of the model.

Figure 4-18 shows the location of the Southern Structural offset in relation to the ADRS and UZB-2 both at ground surface and projected to 100 meters bgs (the intersection with the water table).

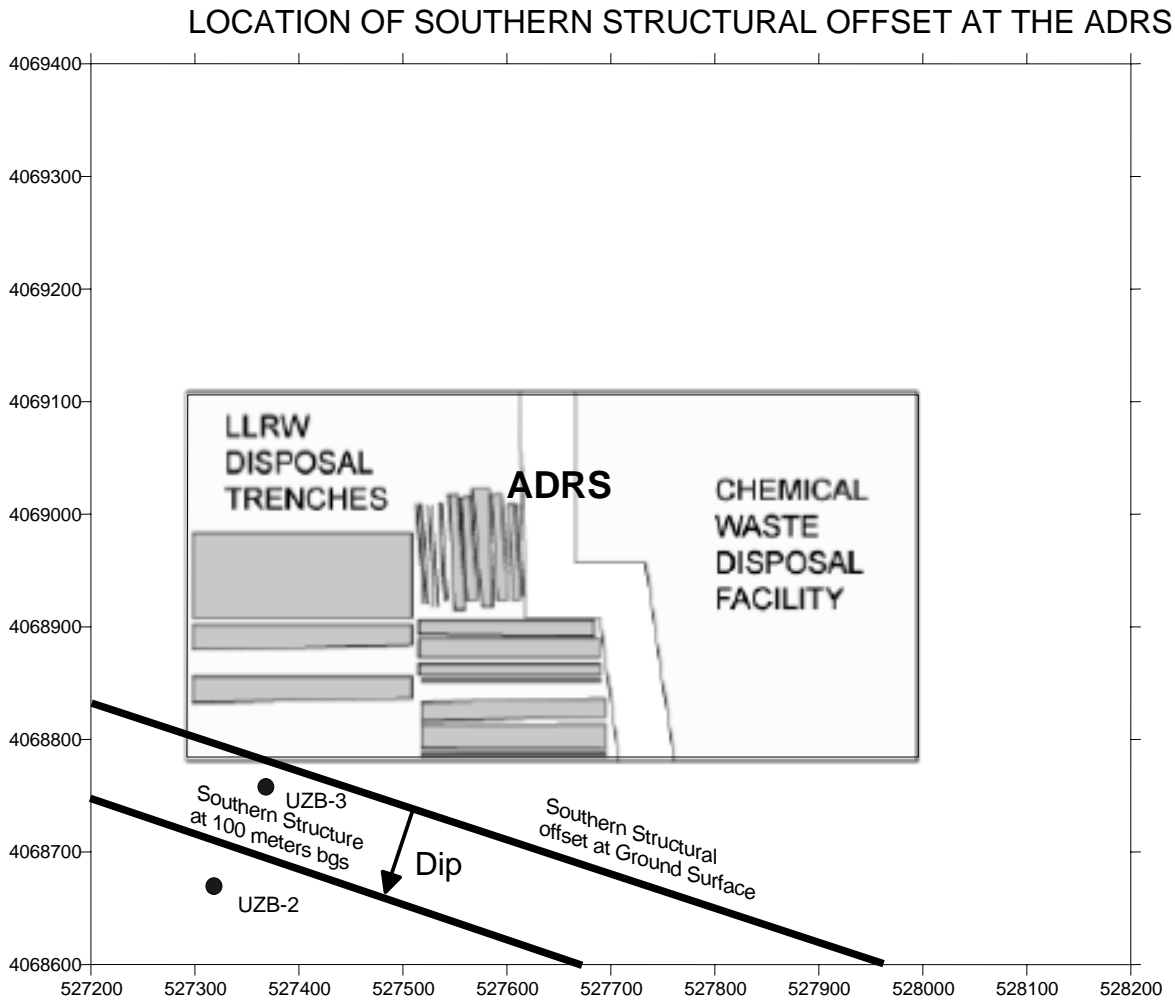


**Figure 4-18. Location of the Southern Structural offset as defined by resistivity data in relation to the burial trenches (adapted from Stonestrom et al., no date)**

### 4.3.5 Hydrologic Data

Water levels in the monitoring wells indicate that the water table surface is between 85 and 115 m bgs and dips at approximately 0.06 m/m (Figure 4-6). The contours of the water table appear to contain aspects of two flow directions; 1) flow toward the southwest (corresponding with the dip of the alluvial fan), and 2) flow toward the southeast (corresponding with the regional dip of the paleo river channel). However, the apparent curve in the water table to the southeast may not be related to the shallow river channel, which does not extend down into the water table, but instead may be due to structural features, such as the proposed Southern Structural Offset.

Figure 4-6 has an arrow showing a northwest kink in the water table contours that closely parallels the strike of the Southern Structural offset. If the regional dip of the water table

parallels the dip of the alluvial fan, then the water table should flow to the west-southwest with a sharp drop in water table expected northeast (upgradient) of the offset.

Figure 4-19 provides a copy of the same map of the tritium concentrations in water table monitoring wells presented in Figure 4-7 with the location of the Southern Structural offset added. The offset is depicted by two lines, one at ground surface and one 100 meters bgs at the intersection with the water table to show the tilt of the structure. As noted in the Strategy, initial evaluation of available data may ultimately point to a need to revise our CSM. In the case of the ADRS, the presence of a bulls-eye on the water table contour map in Figure 4-19 infers a potential fast path for tritium, as the water table surface is over 100 meters bgs.

As shown in Figure 4-19, monitoring well MR-3 cuts the Southern Structural offset but based on the projection of the dip of the structure, the well is screened slightly up dip of the intersection of the Southern Structural offset with the water table. There is slightly elevated tritium in the ground water adjacent to MR-3 (4 to 6 times higher) in contrast to the other available ground-water monitoring wells associated with the ADRS. These elevated concentrations of tritium in the ground water presumably are due to vertical contaminant migration and confirm the fast path movement of soil gas downward from the ADRS to the water table along the Southern Structural offset. Furthermore, because the half-life of tritium is 12.5 years, and the ground water in the vicinity of the ADRS is described as thousands of years old (Prudic, 1996), this suggests a continued contaminant influx into the area.

TRITIUM CONCENTRATIONS IN GROUND WATER FROM AVAILABLE MONITORING WELLS

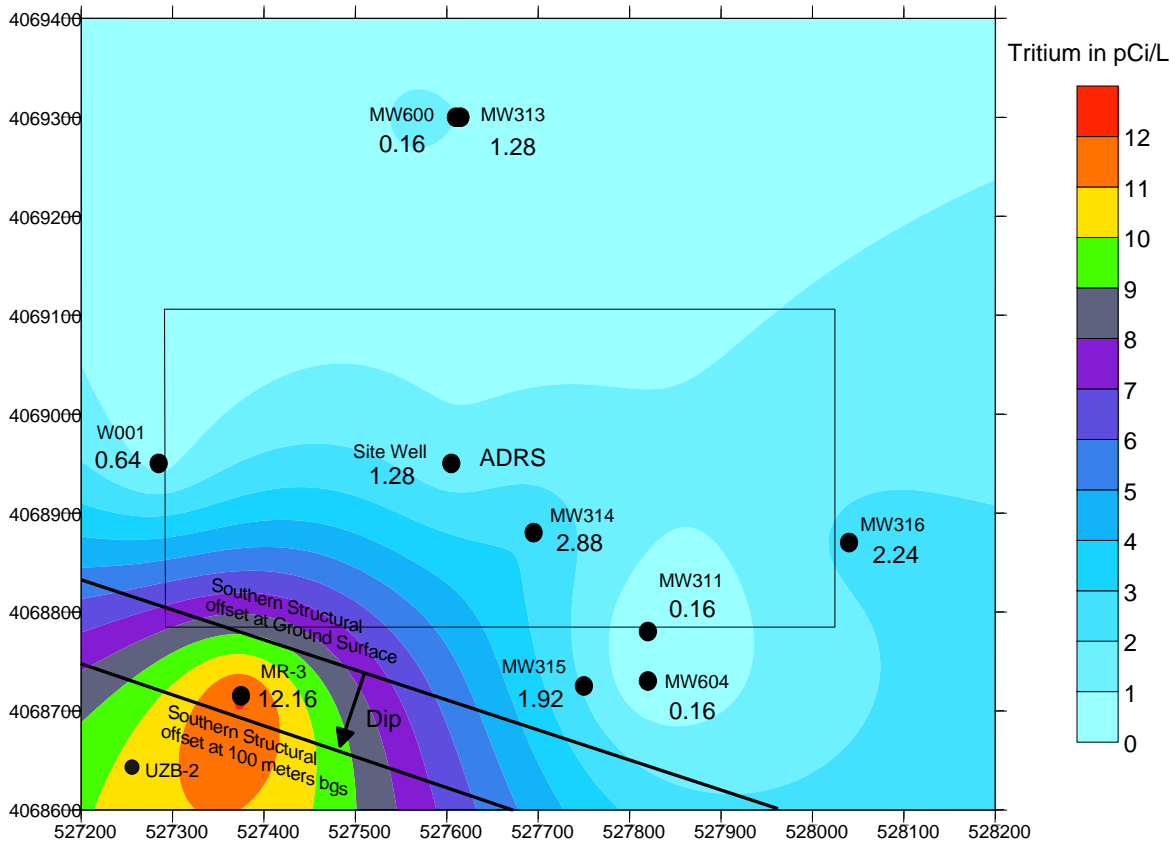


**Figure 4-19. Map of tritium concentrations in ground water below ADRS in relation to the Southern Structural Offset (data from Prudic, 1997)**

Geophysical logs of three monitoring wells (MW-301, 302, and 303), collected within the boundaries of the ADRS all indicate the presence of a significant continuous clay layer at approximately 70 meters bgs showing no vertical offset (Figure 4-5). However, all of these wells are northwest of the Southern Structural offset. The resistivity change across the offset indicates a change from a lower resistivity material (clays to silty clay gravels) to coarser, higher resistivity gravels. A significant drop in the water table across this feature is reflected in the water table values provided in Figure 4-6. Contouring in Figure 4-6 suggests an offset in stratigraphy across the center of the ADRS may be causing the drop in water table surface; however, the lateral continuity of the clays in monitoring wells 301 through 303 suggest that if a geologic feature is causing the significant drop in head, the feature is not located directly below the ADRS, but is more likely in the vicinity of the proposed Southern Structural offset. In addition, as the water table surface occurs within the lower clay horizon below the ADRS, there could be a local aspect of perching occurring in the water table surface where the lower clay is present. Further evaluation of geologic well logs from monitoring wells installed beyond the boundary of the ADRS would provide necessary information to evaluate the presence of the Southern Structural offset, the lateral continuity of the clays, and the nature of the overall site geologic setting.

Based on regional topography, it appears that the structural offset predates the final deposition of the uppermost gravel layers at the ADRS, as it is not reflected at ground surface. Evaluation of any additional geologic or geophysical logs below or adjacent to the ADRS, collected during the installation of monitoring wells, would assist in the evaluation of the distribution of geologic units at depth and any potential offsets in these units.

#### **4.3.6 Vadose Zone Data**

In arid environments, assessment of water flux must be considered as a performance indicator. Water flux potentials in the vadose zone indicate persistent upward driving forces for water (both liquid and vapor) (Andraski et al., 2005). In addition geothermal gradient suggests an upward driving force (Andraski et al., 2005); however, this does not explain how tritium has reached the water table over 100 m bgs. In addition, chloride mass balance suggests that percolation of precipitation has been limited to the upper 10 m bgs during the last 16,000 to 33,000 years. However, the presence of tritium in the deeper vadose zone (to the water table at 108.8 meters bgs) and ground water would tend to indicate that some other mechanism exists for moving contaminants downward. One option is the movement of water downward along fault planes, such as the Southern Structural offset.

Tritium in both the vadose zone and water table at many radioactively-contaminated sites has historically proven to be an excellent indicator of contaminant migration pathways because of its high mobility. Tritium concentrations in vadose zone sediments are highest in the vicinity of the waste unit and are highly concentrated within the gravel zone located at 1.5 m bgs. Figure 4-20 presents the results of a soil gas survey taken from the 1.5 m bgs interval over the shallow tritium plume in the southwest corner of the ADRS.

Tritium concentrations are in excess of 64,000 pCi/L in the gravel at 1.5 m bgs and immediately fall to within the 600 to 1,900 pCi/L range by 6 m bgs, then steadily increase to 1,920 to 3,840 pCi/L by 30 m bgs. Below 30 m, the tritium falls back to below 640 pCi/L (and generally below 16 pCi/L) to at least 100 m bgs. One exception, test hole UZB-2 (located on the downthrown side of the Southern Structural offset) maintains tritium concentrations down to 94 m bgs in excess of 5,648 pCi/L. Although the highest tritium contamination are confined to the upper 1.5 m bgs gravel layer, the presence of tritium down to the water table indicates that there is a mechanism for the downward migration of contaminants through the vadose zone. More characterization of the entire vadose zone is necessary to determine the mechanism for transport and the extent of the contaminant plume. The vertical movement of tritium downward appears to be related to the presence of the Southern Structural offset.

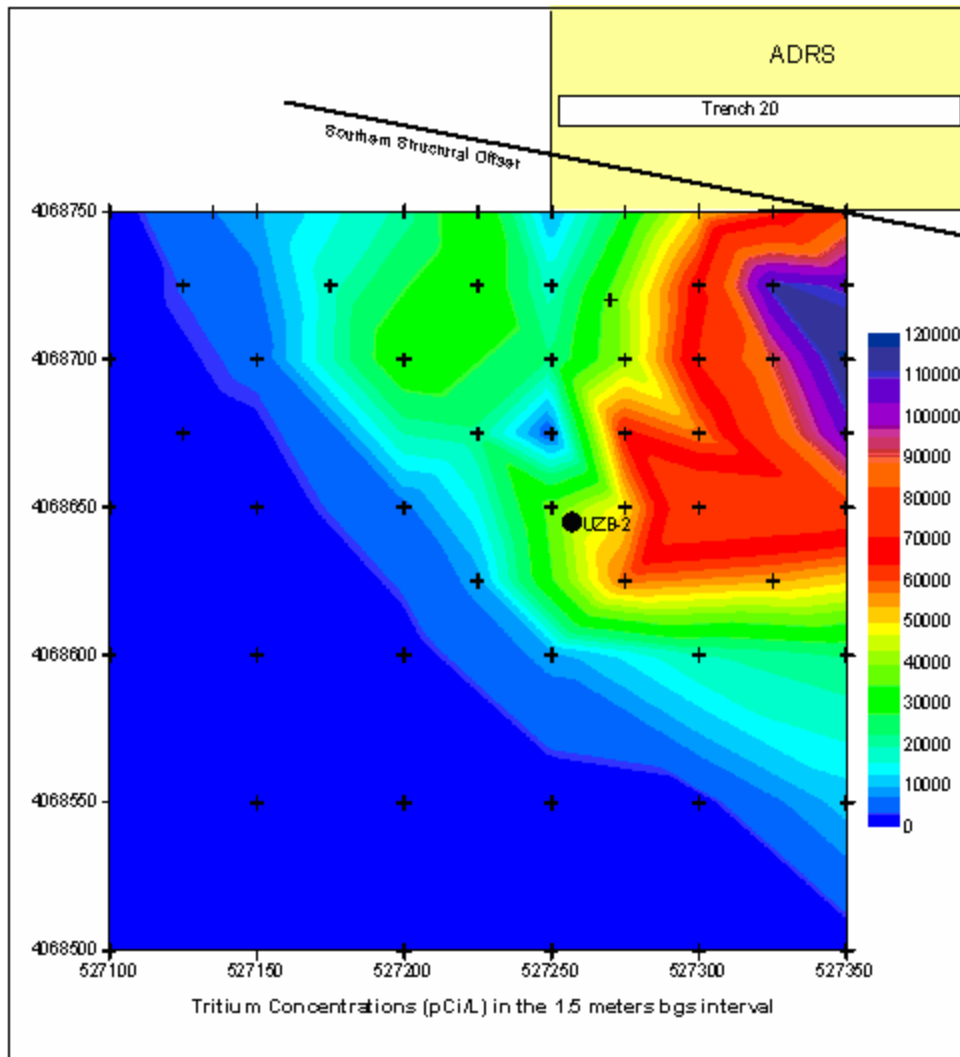


**Figure 4-20. Plan view of tritium soil gas concentrations in the 1.5m below ground surface interval (data from Striegl et al., 1997)**

Tritium concentrations shown in Figure 4-21 for UZB-2 are highest in the 1.5 meter bgs sampling interval (49,632 pCi/L); however, concentrations of tritium from just below the 1.5 meter interval (1,174 pCi/L) increase steadily down to the water table, with the maximum concentration occurring just above the water table surface at 108.8 meters bgs (5,648 pCi/L). This downward increasing trend in tritium appears to consist of two separate trends: a lower concentration tritium trend associated with finer grained/relatively higher soil moisture materials; and a higher concentration tritium trend associated with coarser grained/relatively lower moisture materials (Figure 4-21). Concentrations increase steadily downward as UZB-2 approaches the southwestern dipping Southern Structural offset. Tritium concentrations in all intervals sampled in UZB-2 have increased steadily at a rate of between 50 and 230 pCi/L per year, between the time the well was completed in 1993, and the latest available analytical data from 1996.

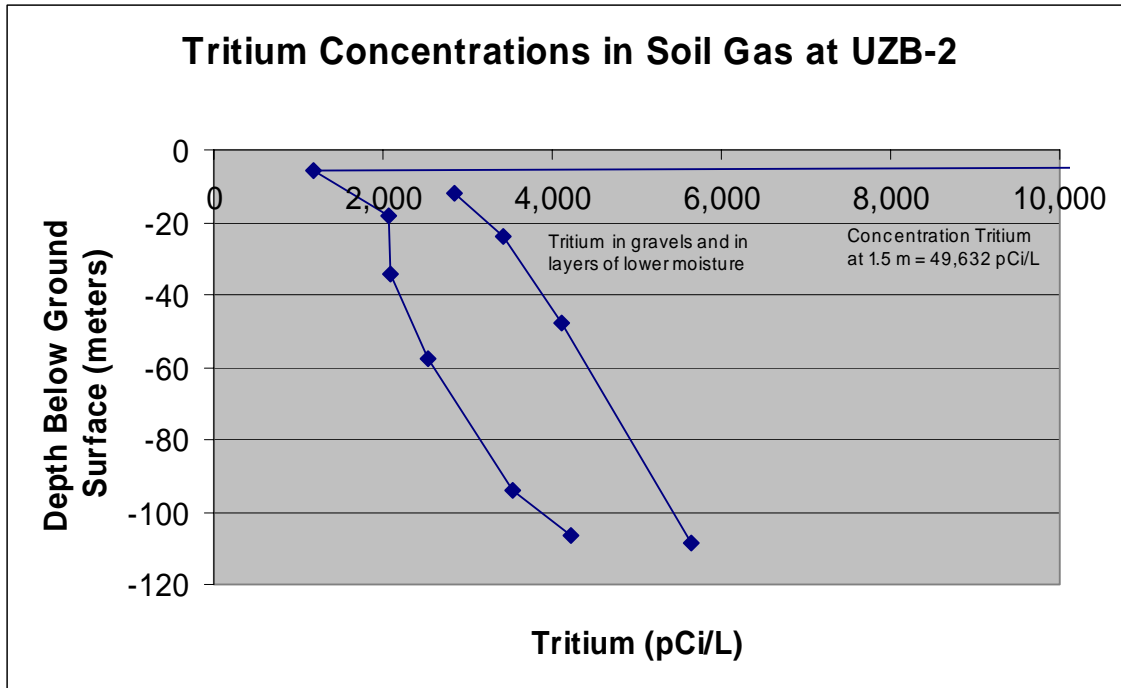


**Figure 4-21. Soil vapor concentrations of tritium in UZB-2**

In addition, UZB-3, which at the surface is located on the downthrown side of the Southern Structural offset (Figure 4-18), crosses the structure at approximately 25 to 30 meters below ground surface. The downward movement of contaminants, including tritium, and carbon-14, is presented in Figure 4-22 and Figure 4-23, respectively (Stonestrom et al., no date). Tritium concentrations in UZB-3 are from 2001. Note that tritium concentrations in UZB-3, below the high concentrations in the 1.5 m bgs interval, increase steadily downward to the point of intersection with the Southern Structural offset (around 30 meters bgs).

As the well passes the structure, the concentrations drop back off dramatically to near detection limits. The presence of carbon-14, in addition to the tritium, indicates that other constituents are moving downward along the Southern Structural offset. Based on available data for UZB-3, CFCs, VOCs, and toluene are present in UZB-3, but quantities and depths are not readily available. Because of lack of readily available data, it is impossible to determine the nature and extent of any other contaminants that may have leached from the trenches into the vadose zone.

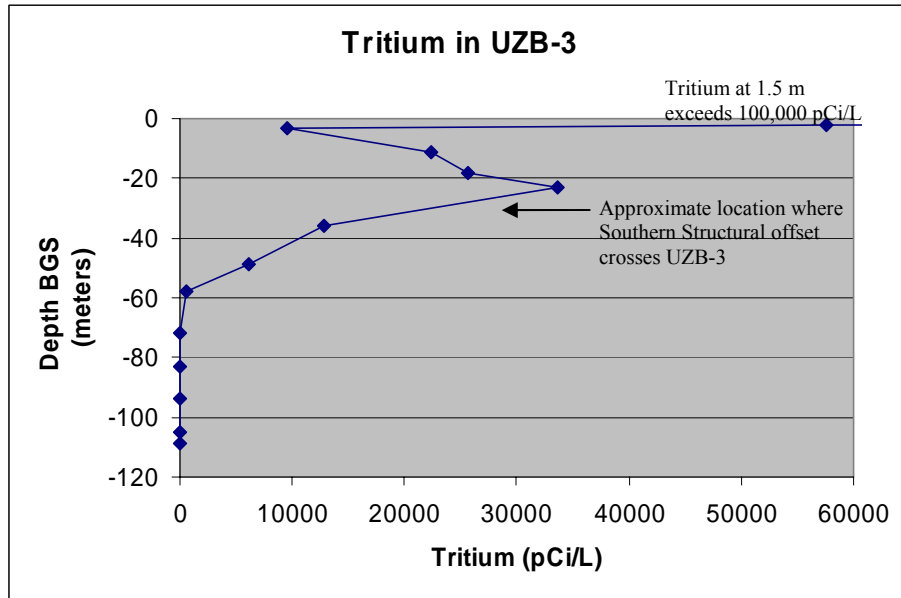


Figure 4-22. Tritium soil gas concentrations from UZB-3 (modified from Stonestrom et al., no date)

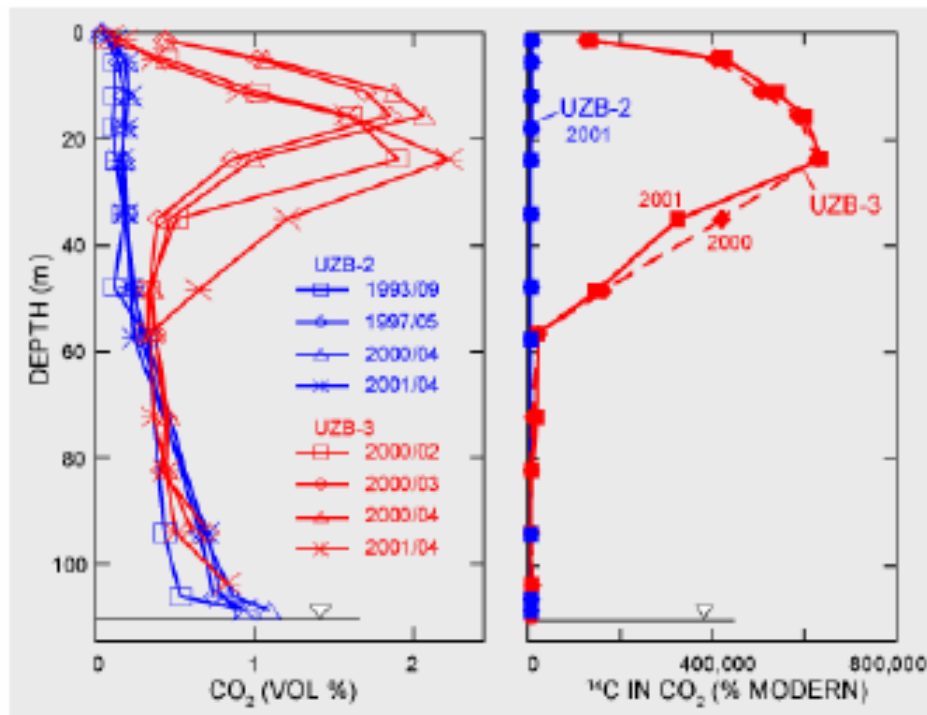


Figure 4-23. Carbon dioxide and carbon-14 soil gas concentrations from UZB-2 and UZB-3 (Stonestrom et al., no date)

### 4.3.7 Meteorological Data

USGS Annual Open File Reports for the ADRS provide a significant database of meteorological data. Based on the results of data from the ADRS and other similar facilities in arid environments, it becomes apparent that changes in barometric pressure at ground surface are also reflected at depth.

Figure 4-24 presents barometric pressure data for the southeast corner of the ADRS (The original source report only stated that the well was from the southeast corner of the ADRS, so the actual well used is unknown). This figure also shows a strong correlation of changes in surficial barometric pressure with changes at depth, down to 30 meters bgs. Below 30 meters, even at 89 meters bgs, minor responses to surficial barometric pressure changes are evident (Prudic, 1996). This data indicates that there is significant soil gas interaction between the surface and depth. The barometric pumping of the vadose zone could produce significant vertical migration of soil contaminants along preferential pathways. As it is unclear of the source well, a determination of the source of the data needs to be performed and additional barometric pressure data needs to be collected.

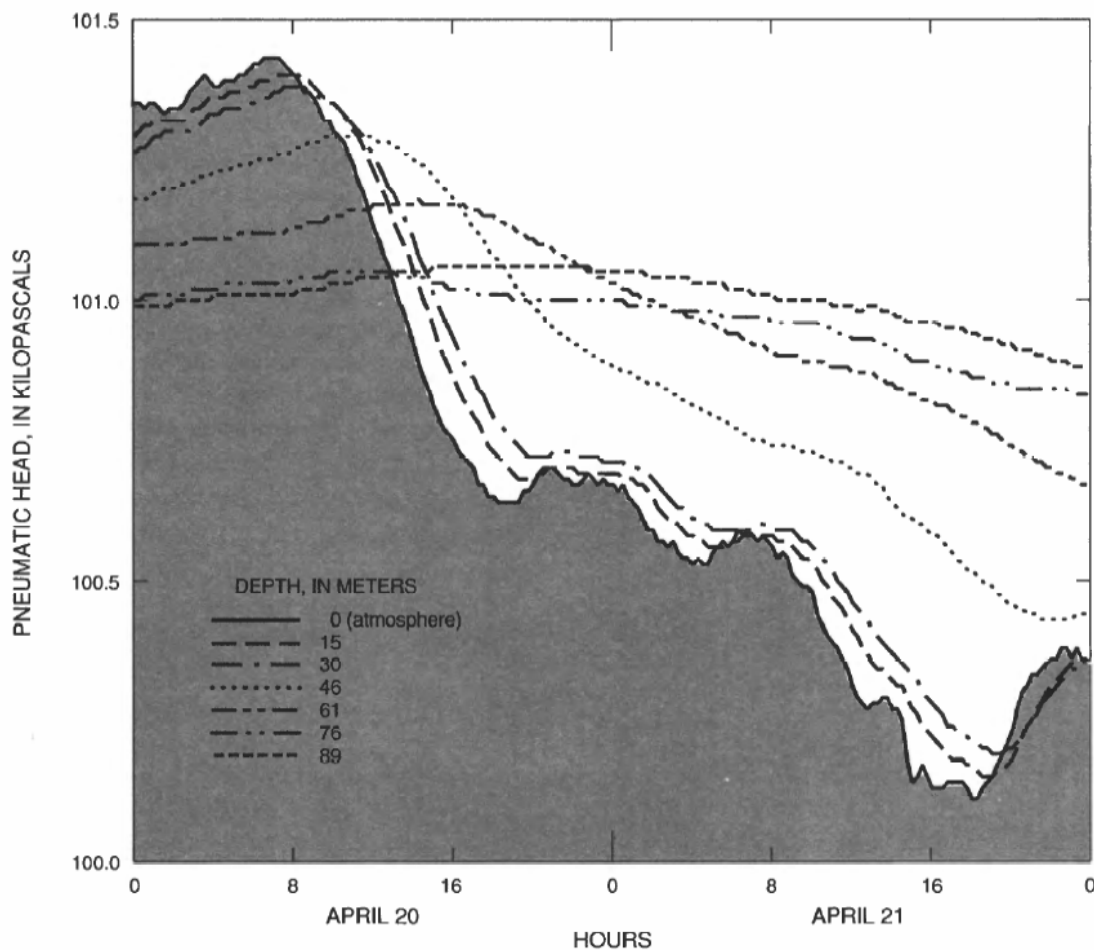


Figure 4-24. Data from southeast corner of ADRS (Prudic, 1996)

### 4.3.8 Transport Modeling

As noted in Striegl et al., 1996, the distribution of tritium cannot be explained simply by vapor transport, either by diffusive or advective mechanisms. Thus, liquid transport appears to have played a role in moving tritium to well UZB-2. Liquid transport may have been enhanced by precipitation and runoff into open trenches that resulted in the occasional accumulation of ponded water in the trenches and flow along preferential pathways in the underlying unsaturated zone (Striegl et al., 1996). As the conceptual model proposed by Striegl et al., 1996 failed to produce a mechanism for the vertical component of movement of tritium in soil gas within the vadose zone below the ADRS, an alternative conceptual model needed to be developed.

Striegl et al., 1996 then proposed an alternative conceptual model for tritium transport stating that liquid tritiated water may have moved laterally at shallow depth from one or more of the trenches to some point near UZB-2 and then percolated downward, resulting in the tritium activity distribution shown in Figure 4-25. Such lateral flow could occur along complex, preferential pathways formed in the presence of large-scale hydrogeologic heterogeneities during periods when liquid waste was being released directly into open trenches, and/or when the trenches received runoff from large precipitation events (Striegl et al., 1996).

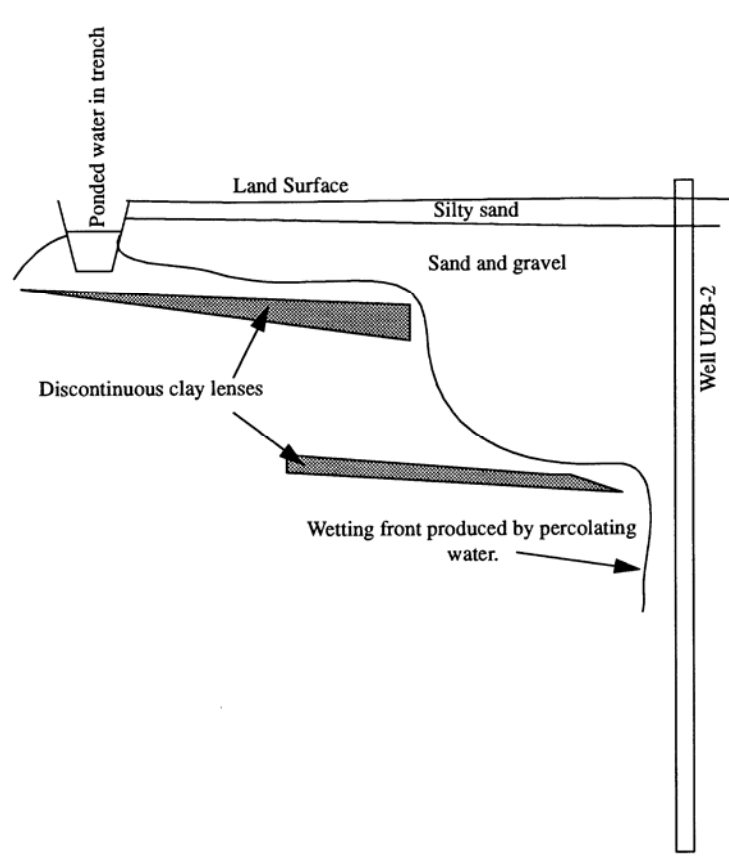


Figure 4-25. Conceptual Model for the movement of tritium proposed by Striegl et al., 1996

Based on this hypothesis, Striegl et al., 1996 proposed that water could collect in an open trench due to liquid waste disposal and/or collection of runoff from precipitation events. This ponded water could percolate rapidly through the clean sands and gravels down to a discontinuous sloping clay lens, where it could mound and move horizontally as saturated flow. Once the mounded water reached the edge of the clay lens, it could spill into the sand and gravel, and presumably move as unsaturated flow until it reached the next lens.

Based on the limited geologic and hydrogeologic data available, there are a significant number of parameters we can use to refine flow and transport simulations. We can define multiple hydrogeologic environments (river gravels, alluvial sediments, Paleozoic bedrock, etc.); make informed decisions on ground water and soil vapor flow; provide specific structural parameters for preferential vertical vadose zone flow pathways; apply variable horizontal flow variography based on geologic sediment type; and include various parameters for hydraulic conductivity and porosity.

Based on the assumption that the Southern Structural offset acts as a preferential pathway for the migration of soil gas, a spreadsheet matrix model of the dispersion of tritium through the vadose zone was prepared by AES. Table 4-1 presents a summary of the results of the model.

For simplicity, the model assumes that the Southern Structural offset is vertical and the calculated values for UZB-2 can be extracted from the matrix at the appropriate depth and distance from the fault. The model was prepared on a 1-foot by 1-foot grid. The first column of the model contains a formula assuming a dispersion constant for the Southern Structural offset. The subsequent columns utilize the value for the Southern Structural offset at the given depth and utilize the dispersion constant for the different geologic environments. The dispersion model utilizes a first order decay rate with the dispersion constant encompassing several parameters including the decay rate of the tritium, the permeability of the sediments, and the rate of movement of the soil gas through the sediments.

**Table 4-1. Summary of model for estimation of tritium movement in the vadose zone between the Southern Structural Offset and UZB-2**

Depth (m)	Fault (pCi/L)	Distance from Fault (m)									
		20	40	60	80	100	120	140	160	180	200
2	911775	675460	500393	370700	274621	203445	150715	111653	82714	61276	45395
6	48932	34620	24494	17330	12261	8675	6138	4342	3072	2174	1538
12	46863	35418	26768	20231	15290	11556	8734	6601	4989	3771	2850
18	44881	31754	22466	15895	11246	7957	5630	3983	2818	1994	1411
24	42984	32486	24553	18557	14025	10600	8011	6055	4576	3458	2614
34	39998	28299	20022	14166	10022	7091	5017	3550	2511	1777	1257
48	36163	27331	20656	15612	11799	8918	6740	5094	3850	2910	2199
58	33650	23808	16844	11918	8432	5966	4221	2986	2113	1495	1058
70	30865	21837	15450	10931	7734	5472	3871	2739	1938	1371	970
80	28721	20320	14377	10172	7197	5092	3602	2549	1803	1276	903
94	25967	18372	12998	9197	6507	4604	3257	2304	1630	1154	816
106	23818	16851	11922	8435	5968	4222	2987	2114	1495	1058	749
109	23309	17616	13314	10063	7605	5748	4344	3283	2481	1875	1417

Note: Tritium concentrations in pCi/L

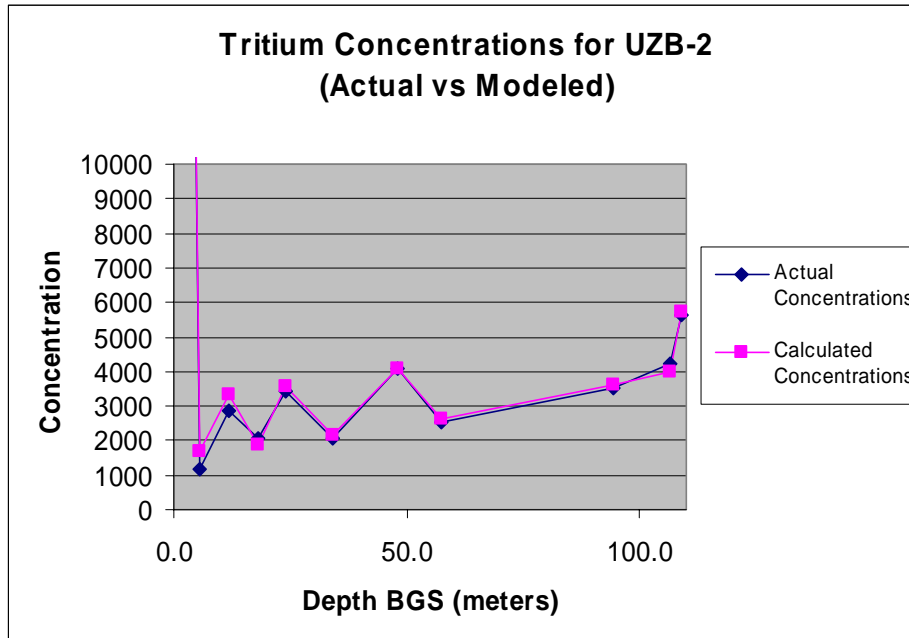


**Figure 4-26. Comparison of actual data to modeled tritium concentrations in UZB-2 in pCi/L (UZB-2 tritium data from Striegl et al., 1997)**

Separate dispersion values were assigned to the surficial gravel at 1.5 meters bgs, the coarser gravels, and the finer materials (Table 4-2). Table 4-3 summarizes the results of the model as compared to actual tritium concentrations in UZB-2. Figure 4-26 provides a comparison of the results of the model to the actual tritium concentrations in UZB-2 from Striegl et al. (1997), illustrating tightly correlated results between expected and observed tritium concentration levels. Figure 4-27 is a hypothetical cross section prepared using Surfer to contour the modeling result values summarized in Table 4-1 along with the tritium values collected from UZB-2. The gravel horizons presented in Figure 4-27 are interpreted from soil moisture data from Prudic (1994) and from relative tritium concentrations. Zones with higher moisture are interpreted to be more clay rich, lower moisture horizons are interpreted to be coarser gravels.

# Cross Section Looking Southeast

Projection of Conceptual Contamination Down Southern Structure

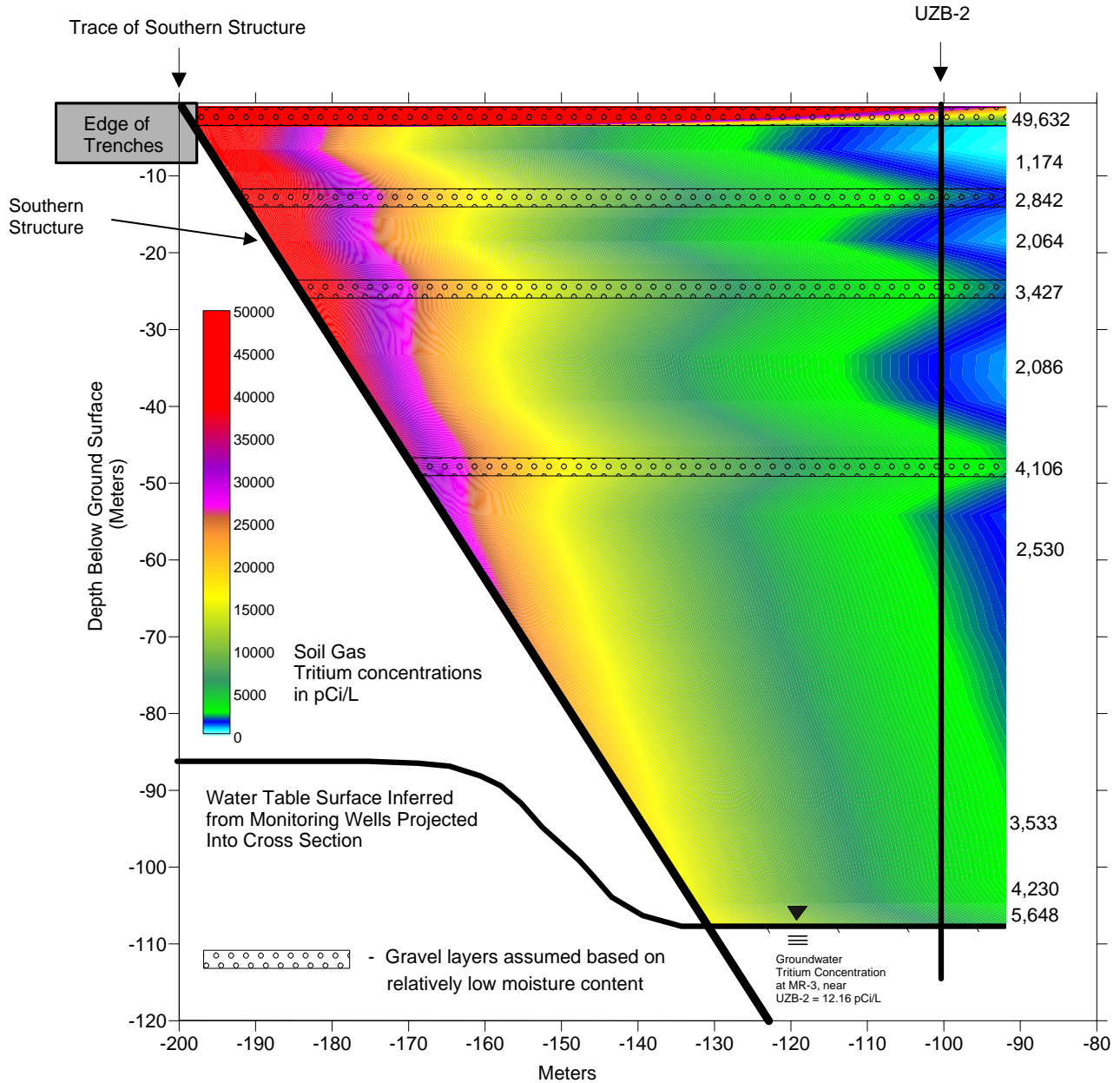


**Figure 4-27. Alternative conceptual model for the distribution of tritium in vadose zone based on Southern Structural offset and UZB-2 tritium concentrations (tritium data from Striegl et al., 1997)**

**Table 4-2. Tritium model dispersivity values assigned to various materials**

Material	Lambda
Fault	0.0072
Surface Gravel	0.0150
Coarser Dryer Gravel	0.0173
Finer Moist Gravel	0.0140

**Table 4-3. Comparison of results from the tritium model to actual concentrations in UZB-2 (UZB-2 data from Striegl et al., 1997)**

Depth (m)	UZB-2 Tritium	Model Estimate	Model Depth (m)	Percent Comp.
1.5	49632	49670	2	100%
5.5	1174	1706	6	69%
11.9	2842	3324	12	85%
18.0	2064	1893	18	109%
24.1	3427	3557	24	96%
34.1	2086	2149	34	97%
47.9	4106	4072	48	101%
57.6	2531	2646	58	96%
94.2	3533	3613	94	98%
106.4	4230	4009	106	106%
108.8	5648	5748	109	98%

Tritium concentrations in pCi/L

#### ***4.4 Monitoring Strategy Application Conclusions***

Based on the results of initial evaluation of data for the Amargosa Desert Research Site, it was unclear how tritium was reaching ground water over 109 meters below ground surface in an arid environment.

A Schlumberger resistivity survey was conducted over the site as presented in Bisdorf (2002). Bisdorf identified a large scale structural feature northeast of the ADRS. As part of this Strategy application, three dimensional modeling of the resistivity data from Bisdorf (2002) using the capabilities of a geological modeling program (HydroGeo Analyst 2.0) resulted in the confirmation of the large fault identified by Bisdorf as well as the identification of a fault labeled the “Southern Structural offset” in the southwest corner of the ADRS. The Southern Structural offset appears to coincide with the location of the downward movement of tritium within the vadose zone to the water table. Modeling of the downward movement of contaminants could now be simulated once consideration was given to this additional structural feature as a fast path for the migration of contamination.

Projection of the Southern Structural offset with a steep southwest dip intersected UZB-3 at approximately 25 to 30 meters bgs. Analytical results of soil gas from this interval confirm the location of the feature. In addition, the steady increase in tritium detected down monitoring borehole UZB-2 indicates that the Southern Structural offset is approaching UZB-2 with depth. The Southern Structural offset intersects the water table slightly up dip of UZB-2. Ground water in the vicinity of monitoring well MR-3, screened in the water table slightly up dip of the intersection of the Southern Structural offset, contains elevated levels of tritium (4 to 6 times higher) in contrast to the other available ground-water monitoring wells associated with the ADRS. The presence of the elevated tritium in the water table also confirms the fast path movement of contaminants downward from the ADRS to the water table along the Southern Structural offset.

The presence of significant barometric pressure interaction between the surface and the subsurface within the vadose zone indicates that there is potential for significant soil gas movement. The barometric pumping of the vadose zone could produce significant vertical migration of soil contaminants along preferential pathways such as the Southern Structural offset.

Only by analyzing the total data package for the site were we able to create a model that allows both an upward component of flow and localized downward migration of contaminants along a fast pathway. In addition, through examination of all geophysical and geologic information available, structures were identified that influence the movement of water and soil gas. Based on this more complete picture, an improved conceptual site model was developed and from this assessment informed decisions can be made for future site monitoring and assessment.

#### **4.5 Amargosa References**

- Andraski, B.J., D.E Prudic, and W.D Nichols. "Waste Burial in Arid Environments-- Application of Information from a Field Laboratory in the Mojave Desert, Southern Nevada." U.S. Geological Survey Fact Sheet FS-179-95, 4 p. 1995.
- Andraski, B.J., et al. *Plant-Based Plume-Scale Mapping of Tritium Contamination in Desert Soils*. Online Publication. August 16, 2005.
- Bisdorf, R.J. "Schlumberger Soundings at the Amargosa Desert Research Site, Nevada." U.S. Geological Survey Open-File Report 02-140. 2002.
- California Geology Magazine. *Detachment Faults, California's Extended Past; Mineralization Along Detachment Faults; California Has Its Faults; Faulted Wave-Cut Terrace Near Point Arena [Mendocino County]*. A Photo Essay. January/February 1992.
- Fischer, J.M. "Sediment Properties and Water Movement Through Shallow Unsaturated Alluvium at an Arid Site for Disposal of Low-Level Radioactive Waste Near Beatty, Nye County, Nevada." U.S. Geological Survey Water-Resources Investigations Report 92-4032, 48 p.1992.
- Johnson, M.J., C.J Mayers, and B.J Andraski. "Selected micrometeorological and soil-moisture data at Amargosa Desert Research Site in Nye County near Beatty, Nevada, 1998-2000." U.S. Geological Survey Open-File Report 02-348, available on the World Wide Web only. 2002.
- Prudic, D.E. "Estimates of Percolation Rates and Ages of Water in Unsaturated Sediments at Two Mojave Desert Sites, California-Nevada." U.S. Geological Survey, Water Resources Investigation Report 91-4160. 1994.
- Prudic, D.E. "Water-vapor movement through unsaturated alluvium in Amargosa Desert near Beatty, Nevada--Current understanding and continuing studies, in Stevens,

P.R., and Nicholson, T.J., eds., Joint U.S. Geological Survey, U.S. Nuclear Regulatory Commission Workshop on research related to low-level radioactive waste disposal, May 4-6, 1993." National Center, Reston, Virginia, Proceedings. U.S. Geological Survey Water-Resources Investigations Report 95-4015, p. 157-166. 1996.

Prudic, D.E., D.A Stonestrom, and R.G Striegl. "Tritium, deuterium, and oxygen-18 in water collected from unsaturated sediments near a low-level radioactive-waste burial site south of Beatty, Nevada." U.S. Geological Survey Water-Resources Investigations Report 97-4062, 23 p.1997.

Stonestrom, D.A., et al. "Estimates of deep percolation beneath native vegetation, irrigated fields, and the Amargosa River channel, Amargosa Desert, Nye County, Nevada" U.S. Geological Survey Open-File Report 03-104, available on the world wide web. 2003.

Stonestrom, D.A., et al. *Monitoring Radionuclide Contamination in the Vadose Zone-Lessons Learned at the Amargosa Desert Research Site, Nye County, Nevada.* No Date.

Striegl, R.G., et al. "Factors affecting tritium and <sup>14</sup>carbon distributions in the unsaturated zone near the low-level radioactive-waste burial site south of Beatty, Nevada." U.S. Geological Survey Open-File Report 96-110, 16 p. 1996.

Striegl, R.G., et al. "Tritium in unsaturated zone gases and air at the Amargosa Desert Research Site, and in spring and river water, near Beatty, Nevada, May 1997." U.S. Geological Survey Open-File Report 97-778, 13 p. 1997.

Walvoord, M. A., *CO<sub>2</sub> dynamics in the Amargosa Desert: Fluxes and isotopic speciation in a deep unsaturated zone.* Water Resources Research, 41, W02006, doi:10.1029/2004WR003599. 2005.

## Appendix 4-A

**Appendix 4-A. Schlumberger Resistivity Data for the ADRS from Bisdorf, 2002**

Station	Easting	Northing	Ground Elev. (m)	Calculated Resistivity Reading (Ohm-m)	Depth (m)	Sample Elev. (m)
ADRS 001	527081	4068750	846.5	300.55	0.47	846.03
ADRS 001	527081	4068750	846.5	373.28	0.69	845.81
ADRS 001	527081	4068750	846.5	514.87	1.01	845.49
ADRS 001	527081	4068750	846.5	617.03	1.48	845.02
ADRS 001	527081	4068750	846.5	467.72	2.17	844.33
ADRS 001	527081	4068750	846.5	184.39	3.19	843.31
ADRS 001	527081	4068750	846.5	50.72	4.68	841.82
ADRS 001	527081	4068750	846.5	36.88	6.88	839.62
ADRS 001	527081	4068750	846.5	61.97	10.09	836.41
ADRS 002	527331	4068450	844.2	517.15	0.59	843.61
ADRS 002	527331	4068450	844.2	730.4	0.87	843.33
ADRS 002	527331	4068450	844.2	896.3	1.28	842.92
ADRS 002	527331	4068450	844.2	832.2	1.87	842.33
ADRS 002	527331	4068450	844.2	524.13	2.75	841.45
ADRS 002	527331	4068450	844.2	203.44	4.04	840.16
ADRS 002	527331	4068450	844.2	58.43	5.93	838.27
ADRS 002	527331	4068450	844.2	36.49	8.7	835.5
ADRS 002	527331	4068450	844.2	60.98	12.77	831.43
ADRS 002	527331	4068450	844.2	91.39	18.74	825.46
ADRS 002	527331	4068450	844.2	93.76	27.5	816.7
ADRS 002	527331	4068450	844.2	69.75	40.37	803.83
ADRS 003	528755	4068491	847.5	245.39	0.55	846.95
ADRS 003	528755	4068491	847.5	179.54	0.81	846.69
ADRS 003	528755	4068491	847.5	142.8	1.19	846.31
ADRS 003	528755	4068491	847.5	116.74	1.74	845.76
ADRS 003	528755	4068491	847.5	101.03	2.55	844.95
ADRS 003	528755	4068491	847.5	74.23	3.75	843.75
ADRS 003	528755	4068491	847.5	47.5	5.5	842
ADRS 003	528755	4068491	847.5	43.35	8.074	839.426
ADRS 003	528755	4068491	847.5	46.72	11.85	835.65
ADRS 003	528755	4068491	847.5	40.64	17.39	830.11
ADRS 003	528755	4068491	847.5	29.85	25.53	821.97
ADRS 003	528755	4068491	847.5	27.5	37.47	810.03
ADRS 003	528755	4068491	847.5	39.27	55.01	792.49
ADRS 003	528755	4068491	847.5	63.25	80.74	766.76
ADRS 003	528755	4068491	847.5	80.41	118.51	728.99
ADRS 003	528755	4068491	847.5	75.13	173.94	673.56
ADRS 003	528755	4068491	847.5	64.74	255.31	592.19
ADRS 003	528755	4068491	847.5	71.71	374.75	472.75
ADRS 003	528755	4068491	847.5	108.44	550.06	297.44
ADRS 003	528755	4068491	847.5	186.24	807.37	40.13
ADRS 004	529050	4068495	842.5	3076.99	0.4	842.1
ADRS 004	529050	4068495	842.5	5680.3	0.59	841.91
ADRS 004	529050	4068495	842.5	6983.81	0.87	841.63
ADRS 004	529050	4068495	842.5	4788.29	1.27	841.23
ADRS 004	529050	4068495	842.5	1720.84	1.87	840.63
ADRS 004	529050	4068495	842.5	591.05	2.74	839.76
ADRS 004	529050	4068495	842.5	617.39	4.02	838.48
ADRS 004	529050	4068495	842.5	1152.72	5.9	836.6

ADRS 004	529050	4068495	842.5	1714.99	8.66	833.84
ADRS 004	529050	4068495	842.5	1797.17	12.72	829.78
ADRS 005	527831	4068650	845	1121.78	0.55	844.45
ADRS 005	527831	4068650	845	845.5	0.81	844.19
ADRS 005	527831	4068650	845	471.77	1.19	843.81
ADRS 005	527831	4068650	845	201.04	1.74	843.26
ADRS 005	527831	4068650	845	63.05	2.55	842.45
ADRS 005	527831	4068650	845	35.46	3.75	841.25
ADRS 005	527831	4068650	845	50.5	5.5	839.5
ADRS 005	527831	4068650	845	71.77	8.074	836.926
ADRS 005	527831	4068650	845	89.96	11.85	833.15
ADRS 005	527831	4068650	845	99.83	17.39	827.61
ADRS 005	527831	4068650	845	88.93	25.53	819.47
ADRS 005	527831	4068650	845	60.82	37.47	807.53
ADRS 005	527831	4068650	845	37.92	55.01	789.99
ADRS 005	527831	4068650	845	28.37	80.74	764.26
ADRS 006	527031	4068650	846.5	1129.27	0.55	845.95
ADRS 006	527031	4068650	846.5	1934.75	0.81	845.69
ADRS 006	527031	4068650	846.5	2302.09	1.19	845.31
ADRS 006	527031	4068650	846.5	1674.72	1.74	844.76
ADRS 006	527031	4068650	846.5	603.86	2.55	843.95
ADRS 006	527031	4068650	846.5	99.42	3.75	842.75
ADRS 006	527031	4068650	846.5	31.98	5.5	841
ADRS 006	527031	4068650	846.5	66.81	8.074	838.426
ADRS 006	527031	4068650	846.5	102.26	11.85	834.65
ADRS 006	527031	4068650	846.5	125.95	17.39	829.11
ADRS 006	527031	4068650	846.5	121.54	25.53	820.97
ADRS 006	527031	4068650	846.5	78.09	37.47	809.03
ADRS 006	527031	4068650	846.5	41.58	55.01	791.49
ADRS 006	527031	4068650	846.5	31.49	80.74	765.76
ADRS 007	527231	4068650	847.3	639.98	0.55	846.75
ADRS 007	527231	4068650	847.3	657.29	0.81	846.49
ADRS 007	527231	4068650	847.3	607.2	1.19	846.11
ADRS 007	527231	4068650	847.3	494.27	1.74	845.56
ADRS 007	527231	4068650	847.3	354.49	2.55	844.75
ADRS 007	527231	4068650	847.3	183.12	3.75	843.55
ADRS 007	527231	4068650	847.3	64.93	5.5	841.8
ADRS 007	527231	4068650	847.3	45.76	8.074	839.226
ADRS 007	527231	4068650	847.3	63.73	11.85	835.45
ADRS 007	527231	4068650	847.3	84.52	17.39	829.91
ADRS 007	527231	4068650	847.3	94.6	25.53	821.77
ADRS 007	527231	4068650	847.3	82.32	37.47	809.83
ADRS 007	527231	4068650	847.3	56.02	55.01	792.29
ADRS 007	527231	4068650	847.3	39.32	80.74	766.56
ADRS 008	527431	4068650	846.5	710.48	0.55	845.95
ADRS 008	527431	4068650	846.5	766.9	0.81	845.69
ADRS 008	527431	4068650	846.5	698	1.19	845.31
ADRS 008	527431	4068650	846.5	487.68	1.74	844.76
ADRS 008	527431	4068650	846.5	216.52	2.55	843.95
ADRS 008	527431	4068650	846.5	62.59	3.75	842.75
ADRS 008	527431	4068650	846.5	38.92	5.5	841
ADRS 008	527431	4068650	846.5	56.22	8.074	838.426
ADRS 008	527431	4068650	846.5	72.55	11.85	834.65
ADRS 008	527431	4068650	846.5	79.96	17.39	829.11
ADRS 008	527431	4068650	846.5	79.16	25.53	820.97
ADRS 008	527431	4068650	846.5	71.52	37.47	809.03
ADRS 008	527431	4068650	846.5	59.5	55.01	791.49
ADRS 008	527431	4068650	846.5	43.49	80.74	765.76
ADRS 009	527631	4068650	846.9	619.56	0.55	846.35
ADRS 009	527631	4068650	846.9	749.02	0.81	846.09
ADRS 009	527631	4068650	846.9	737.69	1.19	845.71

ADRS 009	527631	4068650	846.9	473.6	1.74	845.16
ADRS 009	527631	4068650	846.9	144.64	2.55	844.35
ADRS 009	527631	4068650	846.9	35.12	3.75	843.15
ADRS 009	527631	4068650	846.9	45.75	5.5	841.4
ADRS 009	527631	4068650	846.9	97.83	8.074	838.826
ADRS 009	527631	4068650	846.9	117.38	11.85	835.05
ADRS 009	527631	4068650	846.9	96.6	17.39	829.51
ADRS 009	527631	4068650	846.9	74.32	25.53	821.37
ADRS 009	527631	4068650	846.9	65.33	37.47	809.43
ADRS 009	527631	4068650	846.9	67.67	55.01	791.89
ADRS 009	527631	4068650	846.9	52.66	80.74	766.16
ADRS 010	527831	4068450	843.4	1015.95	0.55	842.85
ADRS 010	527831	4068450	843.4	1020.61	0.81	842.59
ADRS 010	527831	4068450	843.4	601.78	1.19	842.21
ADRS 010	527831	4068450	843.4	168.41	1.74	841.66
ADRS 010	527831	4068450	843.4	42.01	2.55	840.85
ADRS 010	527831	4068450	843.4	42.76	3.75	839.65
ADRS 010	527831	4068450	843.4	67.91	5.5	837.9
ADRS 010	527831	4068450	843.4	88.2	8.074	835.326
ADRS 010	527831	4068450	843.4	96.36	11.85	831.55
ADRS 010	527831	4068450	843.4	93.18	17.39	826.01
ADRS 010	527831	4068450	843.4	83.65	25.53	817.87
ADRS 010	527831	4068450	843.4	67.94	37.47	805.93
ADRS 010	527831	4068450	843.4	43.19	55.01	788.39
ADRS 010	527831	4068450	843.4	24.92	80.74	762.66
ADRS 011	527631	4068450	843.8	678.23	0.55	843.25
ADRS 011	527631	4068450	843.8	685.34	0.81	842.99
ADRS 011	527631	4068450	843.8	645.88	1.19	842.61
ADRS 011	527631	4068450	843.8	487.54	1.74	842.06
ADRS 011	527631	4068450	843.8	240.74	2.55	841.25
ADRS 011	527631	4068450	843.8	87.28	3.75	840.05
ADRS 011	527631	4068450	843.8	55.45	5.5	838.3
ADRS 011	527631	4068450	843.8	62.9	8.074	835.726
ADRS 011	527631	4068450	843.8	67.77	11.85	831.95
ADRS 011	527631	4068450	843.8	69.31	17.39	826.41
ADRS 011	527631	4068450	843.8	71.21	25.53	818.27
ADRS 011	527631	4068450	843.8	71.2	37.47	806.33
ADRS 011	527631	4068450	843.8	61.78	55.01	788.79
ADRS 011	527631	4068450	843.8	42.01	80.74	763.06
ADRS 012	527431	4068450	844.2	433.81	0.55	843.65
ADRS 012	527431	4068450	844.2	471.29	0.81	843.39
ADRS 012	527431	4068450	844.2	471.28	1.19	843.01
ADRS 012	527431	4068450	844.2	396.9	1.74	842.46
ADRS 012	527431	4068450	844.2	246.86	2.55	841.65
ADRS 012	527431	4068450	844.2	109.89	3.75	840.45
ADRS 012	527431	4068450	844.2	56.97	5.5	838.7
ADRS 012	527431	4068450	844.2	56.43	8.074	836.126
ADRS 012	527431	4068450	844.2	72.58	11.85	832.35
ADRS 012	527431	4068450	844.2	89	17.39	826.81
ADRS 012	527431	4068450	844.2	92.64	25.53	818.67
ADRS 012	527431	4068450	844.2	75.26	37.47	806.73
ADRS 012	527431	4068450	844.2	52.53	55.01	789.19
ADRS 012	527431	4068450	844.2	39.6	80.74	763.46
ADRS 013	527231	4068450	844.2	380.67	0.55	843.65
ADRS 013	527231	4068450	844.2	412.17	0.81	843.39
ADRS 013	527231	4068450	844.2	456.31	1.19	843.01
ADRS 013	527231	4068450	844.2	368.39	1.74	842.46
ADRS 013	527231	4068450	844.2	191.12	2.55	841.65
ADRS 013	527231	4068450	844.2	85.67	3.75	840.45
ADRS 013	527231	4068450	844.2	56.85	5.5	838.7
ADRS 013	527231	4068450	844.2	55.04	8.074	836.126

ADRS 013	527231	4068450	844.2	68.54	11.85	832.35
ADRS 013	527231	4068450	844.2	91.85	17.39	826.81
ADRS 013	527231	4068450	844.2	102.52	25.53	818.67
ADRS 013	527231	4068450	844.2	84.4	37.47	806.73
ADRS 013	527231	4068450	844.2	54.99	55.01	789.19
ADRS 013	527231	4068450	844.2	37.7	80.74	763.46
ADRS 014	527031	4068450	845.2	765.68	0.55	844.65
ADRS 014	527031	4068450	845.2	622.75	0.81	844.39
ADRS 014	527031	4068450	845.2	423.58	1.19	844.01
ADRS 014	527031	4068450	845.2	239.99	1.74	843.46
ADRS 014	527031	4068450	845.2	132.88	2.55	842.65
ADRS 014	527031	4068450	845.2	92.59	3.75	841.45
ADRS 014	527031	4068450	845.2	78.31	5.5	839.7
ADRS 014	527031	4068450	845.2	72.58	8.074	837.126
ADRS 014	527031	4068450	845.2	73.29	11.85	833.35
ADRS 014	527031	4068450	845.2	79.46	17.39	827.81
ADRS 014	527031	4068450	845.2	83.41	25.53	819.67
ADRS 014	527031	4068450	845.2	70.71	37.47	807.73
ADRS 014	527031	4068450	845.2	46.67	55.01	790.19
ADRS 014	527031	4068450	845.2	32.32	80.74	764.46
ADRS 015	526831	4068450	846.1	1730.67	0.55	845.55
ADRS 015	526831	4068450	846.1	1029.1	0.81	845.29
ADRS 015	526831	4068450	846.1	507.58	1.19	844.91
ADRS 015	526831	4068450	846.1	242.92	1.74	844.36
ADRS 015	526831	4068450	846.1	121.2	2.55	843.55
ADRS 015	526831	4068450	846.1	91.67	3.75	842.35
ADRS 015	526831	4068450	846.1	95.09	5.5	840.6
ADRS 015	526831	4068450	846.1	93.79	8.074	838.026
ADRS 015	526831	4068450	846.1	87.67	11.85	834.25
ADRS 015	526831	4068450	846.1	80.71	17.39	828.71
ADRS 015	526831	4068450	846.1	73.39	25.53	820.57
ADRS 015	526831	4068450	846.1	69.42	37.47	808.63
ADRS 015	526831	4068450	846.1	66.7	55.01	791.09
ADRS 015	526831	4068450	846.1	51.37	80.74	765.36
ADRS 016	528031	4068650	844.8	823.4	0.44	844.36
ADRS 016	528031	4068650	844.8	534.27	0.65	844.15
ADRS 016	528031	4068650	844.8	242.29	0.96	843.84
ADRS 016	528031	4068650	844.8	95.28	1.41	843.39
ADRS 016	528031	4068650	844.8	54.03	2.06	842.74
ADRS 016	528031	4068650	844.8	41.87	3.03	841.77
ADRS 016	528031	4068650	844.8	35	4.44	840.36
ADRS 016	528031	4068650	844.8	40.13	6.52	838.28
ADRS 016	528031	4068650	844.8	55.44	9.57	835.23
ADRS 016	528031	4068650	844.8	69.59	14.05	830.75
ADRS 016	528031	4068650	844.8	74.39	20.63	824.17
ADRS 016	528031	4068650	844.8	64.66	30.28	814.52
ADRS 016	528031	4068650	844.8	42.45	44.44	800.36
ADRS 016	528031	4068650	844.8	22.36	65.23	779.57
ADRS 016	528031	4068650	844.8	15.13	95.74	749.06
ADRS 016	528031	4068650	844.8	18.98	140.53	704.27
ADRS 016	528031	4068650	844.8	32.09	206.27	638.53
ADRS 016	528031	4068650	844.8	53.41	302.77	542.03
ADRS 017	529120	4068595	840.5	1052.67	0.59	839.91
ADRS 017	529120	4068595	840.5	576.82	0.87	839.63
ADRS 017	529120	4068595	840.5	349.45	1.28	839.22
ADRS 017	529120	4068595	840.5	237.41	1.87	838.63
ADRS 017	529120	4068595	840.5	202.82	2.75	837.75
ADRS 017	529120	4068595	840.5	217.88	4.04	836.46
ADRS 017	529120	4068595	840.5	207.57	5.93	834.57
ADRS 017	529120	4068595	840.5	158.57	8.7	831.8
ADRS 017	529120	4068595	840.5	132.73	12.77	827.73

ADRS 017	529120	4068595	840.5	155.58	18.74	821.76
ADRS 017	529120	4068595	840.5	216.59	27.5	813
ADRS 017	529120	4068595	840.5	281.55	40.37	800.13
ADRS 017	529120	4068595	840.5	315.72	59.25	781.25
ADRS 017	529120	4068595	840.5	303.47	86.97	753.53
ADRS 017	529120	4068595	840.5	250.52	127.66	712.84
ADRS 017	529120	4068595	840.5	194.4	187.37	653.13
ADRS 017	529120	4068595	840.5	175.19	275.03	565.47
ADRS 017	529120	4068595	840.5	189.49	403.69	436.81
ADRS 018	528168	4068650	846.5	391.05	0.55	845.95
ADRS 018	528168	4068650	846.5	369.58	0.81	845.69
ADRS 018	528168	4068650	846.5	234.21	1.19	845.31
ADRS 018	528168	4068650	846.5	89.01	1.74	844.76
ADRS 018	528168	4068650	846.5	31.15	2.55	843.95
ADRS 018	528168	4068650	846.5	25.72	3.75	842.75
ADRS 018	528168	4068650	846.5	34.28	5.5	841
ADRS 018	528168	4068650	846.5	44.53	8.074	838.426
ADRS 018	528168	4068650	846.5	51.31	11.85	834.65
ADRS 018	528168	4068650	846.5	53.69	17.39	829.11
ADRS 018	528168	4068650	846.5	54.07	25.53	820.97
ADRS 018	528168	4068650	846.5	49.57	37.47	809.03
ADRS 018	528168	4068650	846.5	34.77	55.01	791.49
ADRS 018	528168	4068650	846.5	20.09	80.74	765.76
ADRS 019	527306	4068700	847.3	772.14	0.64	846.66
ADRS 019	527306	4068700	847.3	828.66	0.94	846.36
ADRS 019	527306	4068700	847.3	802.56	1.38	845.92
ADRS 019	527306	4068700	847.3	643.98	2.02	845.28
ADRS 019	527306	4068700	847.3	371.31	2.96	844.34
ADRS 019	527306	4068700	847.3	135.86	4.35	842.95
ADRS 019	527306	4068700	847.3	51.43	6.38	840.92
ADRS 019	527306	4068700	847.3	46.96	9.37	837.93
ADRS 019	527306	4068700	847.3	61.19	13.75	833.55
ADRS 019	527306	4068700	847.3	72.53	20.18	827.12
ADRS 019	527306	4068700	847.3	73.71	29.63	817.67
ADRS 019	527306	4068700	847.3	67.44	43.49	803.81
ADRS 019	527306	4068700	847.3	58.09	63.83	783.47
ADRS 019	527306	4068700	847.3	44.13	93.69	753.61
ADRS 019	527306	4068700	847.3	28.83	137.51	709.79
ADRS 019	527306	4068700	847.3	19.33	201.84	645.46
ADRS 020	527931	4068550	843.5	809.31	0.55	842.95
ADRS 020	527931	4068550	843.5	687.48	0.81	842.69
ADRS 020	527931	4068550	843.5	370.81	1.19	842.31
ADRS 020	527931	4068550	843.5	116.71	1.74	841.76
ADRS 020	527931	4068550	843.5	43.3	2.55	840.95
ADRS 020	527931	4068550	843.5	40.78	3.75	839.75
ADRS 020	527931	4068550	843.5	50.25	5.5	838
ADRS 020	527931	4068550	843.5	32.6	8.074	835.426
ADRS 020	527931	4068550	843.5	74.97	11.85	831.65
ADRS 020	527931	4068550	843.5	81.39	17.39	826.11
ADRS 020	527931	4068550	843.5	75.32	25.53	817.97
ADRS 020	527931	4068550	843.5	58.16	37.47	806.03
ADRS 020	527931	4068550	843.5	40.89	55.01	788.49
ADRS 020	527931	4068550	843.5	29.69	80.74	762.76
ADRS 021	527731	4068550	843.9	964.98	0.55	843.35
ADRS 021	527731	4068550	843.9	929.65	0.81	843.09
ADRS 021	527731	4068550	843.9	790.15	1.19	842.71
ADRS 021	527731	4068550	843.9	633.56	1.74	842.16
ADRS 021	527731	4068550	843.9	389.16	2.55	841.35
ADRS 021	527731	4068550	843.9	130.76	3.75	840.15
ADRS 021	527731	4068550	843.9	44.4	5.5	838.4
ADRS 021	527731	4068550	843.9	45.61	8.074	835.826

ADRS 021	527731	4068550	843.9	64.46	11.85	832.05
ADRS 021	527731	4068550	843.9	79.5	17.39	826.51
ADRS 021	527731	4068550	843.9	80.28	25.53	818.37
ADRS 021	527731	4068550	843.9	65.64	37.47	806.43
ADRS 021	527731	4068550	843.9	47.84	55.01	788.89
ADRS 021	527731	4068550	843.9	37.22	80.74	763.16
ADRS 022	527531	4068550	844.3	900.89	0.55	843.75
ADRS 022	527531	4068550	844.3	1040.08	0.81	843.49
ADRS 022	527531	4068550	844.3	952.64	1.19	843.11
ADRS 022	527531	4068550	844.3	532.79	1.74	842.56
ADRS 022	527531	4068550	844.3	168.98	2.55	841.75
ADRS 022	527531	4068550	844.3	56.98	3.75	840.55
ADRS 022	527531	4068550	844.3	47.7	5.5	838.8
ADRS 022	527531	4068550	844.3	57.82	8.074	836.226
ADRS 022	527531	4068550	844.3	71.49	11.85	832.45
ADRS 022	527531	4068550	844.3	80.84	17.39	826.91
ADRS 022	527531	4068550	844.3	77.86	25.53	818.77
ADRS 022	527531	4068550	844.3	63.95	37.47	806.83
ADRS 022	527531	4068550	844.3	49.76	55.01	789.29
ADRS 022	527531	4068550	844.3	41.26	80.74	763.56
ADRS 023	528131	4068550	842.2	924.25	0.55	841.65
ADRS 023	528131	4068550	842.2	538.83	0.81	841.39
ADRS 023	528131	4068550	842.2	250.9	1.19	841.01
ADRS 023	528131	4068550	842.2	87.32	1.74	840.46
ADRS 023	528131	4068550	842.2	41.03	2.55	839.65
ADRS 023	528131	4068550	842.2	41.75	3.75	838.45
ADRS 023	528131	4068550	842.2	53.25	5.5	836.7
ADRS 023	528131	4068550	842.2	66.64	8.074	834.126
ADRS 023	528131	4068550	842.2	74.22	11.85	830.35
ADRS 023	528131	4068550	842.2	70.08	17.39	824.81
ADRS 023	528131	4068550	842.2	57.51	25.53	816.67
ADRS 023	528131	4068550	842.2	44.37	37.47	804.73
ADRS 023	528131	4068550	842.2	33.42	55.01	787.19
ADRS 023	528131	4068550	842.2	23.22	80.74	761.46
ADRS 024	528331	4068550	844.5	273.74	0.55	843.95
ADRS 024	528331	4068550	844.5	186.41	0.81	843.69
ADRS 024	528331	4068550	844.5	215.12	1.19	843.31
ADRS 024	528331	4068550	844.5	271.03	1.74	842.76
ADRS 024	528331	4068550	844.5	204.5	2.55	841.95
ADRS 024	528331	4068550	844.5	86.94	3.75	840.75
ADRS 024	528331	4068550	844.5	44.2	5.5	839
ADRS 024	528331	4068550	844.5	50.95	8.074	836.426
ADRS 024	528331	4068550	844.5	62.22	11.85	832.65
ADRS 024	528331	4068550	844.5	47.28	17.39	827.11
ADRS 024	528331	4068550	844.5	30.61	25.53	818.97
ADRS 024	528331	4068550	844.5	25.02	37.47	807.03
ADRS 024	528331	4068550	844.5	23.21	55.01	789.49
ADRS 024	528331	4068550	844.5	28.17	80.74	763.76
ADRS 025	528531	4068550	847.4	567.22	0.61	846.79
ADRS 025	528531	4068550	847.4	434.46	0.9	846.5
ADRS 025	528531	4068550	847.4	311.32	1.32	846.08
ADRS 025	528531	4068550	847.4	229.38	1.93	845.47
ADRS 025	528531	4068550	847.4	179.76	2.84	844.56
ADRS 025	528531	4068550	847.4	137.9	4.16	843.24
ADRS 025	528531	4068550	847.4	108.86	6.11	841.29
ADRS 025	528531	4068550	847.4	95.33	8.97	838.43
ADRS 025	528531	4068550	847.4	80.95	13.17	834.23
ADRS 025	528531	4068550	847.4	59.08	19.33	828.07
ADRS 025	528531	4068550	847.4	41.44	28.37	819.03
ADRS 025	528531	4068550	847.4	30.21	41.64	805.76
ADRS 025	528531	4068550	847.4	25.2	61.12	786.28

ADRS 025	528531	4068550	845	32.65	89.71	755.29
ADRS 026	527911	4068740	845	238.33	0.55	844.45
ADRS 026	527911	4068740	845	231.35	0.81	844.19
ADRS 026	527911	4068740	845	148.14	1.19	843.81
ADRS 026	527911	4068740	845	66.57	1.74	843.26
ADRS 026	527911	4068740	845	26.28	2.55	842.45
ADRS 026	527911	4068740	845	18.17	3.75	841.25
ADRS 026	527911	4068740	845	29.98	5.5	839.5
ADRS 026	527911	4068740	845	51.67	8.074	836.926
ADRS 026	527911	4068740	845	57.53	11.85	833.15
ADRS 026	527911	4068740	845	40.05	17.39	827.61
ADRS 026	527911	4068740	845	23.93	25.53	819.47
ADRS 026	527911	4068740	845	21.67	37.47	807.53
ADRS 026	527911	4068740	845	28.29	55.01	789.99
ADRS 026	527911	4068740	845	25.29	80.74	764.26
ADRS 027	527711	4068740	846.1	206.07	0.55	845.55
ADRS 027	527711	4068740	846.1	271.3	0.81	845.29
ADRS 027	527711	4068740	846.1	220.19	1.19	844.91
ADRS 027	527711	4068740	846.1	95.66	1.74	844.36
ADRS 027	527711	4068740	846.1	32.55	2.55	843.55
ADRS 027	527711	4068740	846.1	24.44	3.75	842.35
ADRS 027	527711	4068740	846.1	35.88	5.5	840.6
ADRS 027	527711	4068740	846.1	53.59	8.074	838.026
ADRS 027	527711	4068740	846.1	69.07	11.85	834.25
ADRS 027	527711	4068740	846.1	67.05	17.39	828.71
ADRS 027	527711	4068740	846.1	45.3	25.53	820.57
ADRS 027	527711	4068740	846.1	25.82	37.47	808.63
ADRS 027	527711	4068740	846.1	20.97	55.01	791.09
ADRS 027	527711	4068740	846.1	28.25	80.74	765.36
ADRS 028	527516	4068740	847.3	248.61	0.55	846.75
ADRS 028	527516	4068740	847.3	516.57	0.81	846.49
ADRS 028	527516	4068740	847.3	839.63	1.19	846.11
ADRS 028	527516	4068740	847.3	1002.71	1.74	845.56
ADRS 028	527516	4068740	847.3	753.23	2.55	844.75
ADRS 028	527516	4068740	847.3	290.52	3.75	843.55
ADRS 028	527516	4068740	847.3	60.38	5.5	841.8
ADRS 028	527516	4068740	847.3	23.6	8.074	839.226
ADRS 028	527516	4068740	847.3	57.29	11.85	835.45
ADRS 028	527516	4068740	847.3	73.03	17.39	829.91
ADRS 028	527516	4068740	847.3	45.78	25.53	821.77
ADRS 028	527516	4068740	847.3	32.91	37.47	809.83
ADRS 028	527516	4068740	847.3	32.67	55.01	792.29
ADRS 028	527516	4068740	847.3	31.92	80.74	766.56
ADRS 029	527321	4068740	847.3	725.68	0.55	846.75
ADRS 029	527321	4068740	847.3	799.65	0.81	846.49
ADRS 029	527321	4068740	847.3	946.52	1.19	846.11
ADRS 029	527321	4068740	847.3	977.51	1.74	845.56
ADRS 029	527321	4068740	847.3	668.64	2.55	844.75
ADRS 029	527321	4068740	847.3	274.54	3.75	843.55
ADRS 029	527321	4068740	847.3	96.49	5.5	841.8
ADRS 029	527321	4068740	847.3	66.81	8.074	839.226
ADRS 029	527321	4068740	847.3	89.67	11.85	835.45
ADRS 029	527321	4068740	847.3	111.46	17.39	829.91
ADRS 029	527321	4068740	847.3	94.08	25.53	821.77
ADRS 029	527321	4068740	847.3	57.02	37.47	809.83
ADRS 029	527321	4068740	847.3	35.91	55.01	792.29
ADRS 029	527321	4068740	847.3	32.83	80.74	766.56
ADRS 030	529866	4070887	950.67	2255.45	2.06	948.61
ADRS 030	529866	4070887	950.67	847.23	3.03	947.64
ADRS 030	529866	4070887	950.67	859.46	4.44	946.23
ADRS 030	529866	4070887	950.67	1278.99	6.52	944.15

ADRS 030	529866	4070887	950.67	1306.32	9.57	941.1
ADRS 030	529866	4070887	950.67	1130.57	14.05	936.62
ADRS 030	529866	4070887	950.67	1079.34	20.63	930.04
ADRS 030	529866	4070887	950.67	975.8	30.28	920.39
ADRS 030	529866	4070887	950.67	756.34	44.44	906.23
ADRS 030	529866	4070887	950.67	611.74	65.23	885.44
ADRS 030	529866	4070887	950.67	515.78	85.74	864.93
ADRS 030	529866	4070887	950.67	391.62	140.53	810.14
ADRS 030	529866	4070887	950.67	360.73	206.27	744.4
ADRS 030	529866	4070887	950.67	468.79	302.77	647.9
ADRS 031	528111	4068740	846.5	774.33	0.55	845.95
ADRS 031	528111	4068740	846.5	534.72	0.81	845.69
ADRS 031	528111	4068740	846.5	273.3	1.19	845.31
ADRS 031	528111	4068740	846.5	100.15	1.74	844.76
ADRS 031	528111	4068740	846.5	48.04	2.55	843.95
ADRS 031	528111	4068740	846.5	43.91	3.75	842.75
ADRS 031	528111	4068740	846.5	48.52	5.5	841
ADRS 031	528111	4068740	846.5	56.33	8.074	838.426
ADRS 031	528111	4068740	846.5	63.49	11.85	834.65
ADRS 031	528111	4068740	846.5	66.78	17.39	829.11
ADRS 031	528111	4068740	846.5	65.33	25.53	820.97
ADRS 031	528111	4068740	846.5	55.1	37.47	809.03
ADRS 031	528111	4068740	846.5	34.68	55.01	791.49
ADRS 031	528111	4068740	846.5	16.28	80.74	765.76
ADRS 032	528416	4068729	844.2	450.43	0.55	843.65
ADRS 032	528416	4068729	844.2	388.56	0.81	843.39
ADRS 032	528416	4068729	844.2	256.06	1.19	843.01
ADRS 032	528416	4068729	844.2	154.59	1.74	842.46
ADRS 032	528416	4068729	844.2	117.02	2.55	841.65
ADRS 032	528416	4068729	844.2	109.65	3.75	840.45
ADRS 032	528416	4068729	844.2	105.69	5.5	838.7
ADRS 032	528416	4068729	844.2	93.74	8.074	836.126
ADRS 032	528416	4068729	844.2	73.44	11.85	832.35
ADRS 032	528416	4068729	844.2	54.16	17.39	826.81
ADRS 032	528416	4068729	844.2	40.94	25.53	818.67
ADRS 032	528416	4068729	844.2	32.64	37.47	806.73
ADRS 032	528416	4068729	844.2	27.97	55.01	789.19
ADRS 032	528416	4068729	844.2	26.9	80.74	763.46
ADRS 033	528031	4068450	841.2	719.65	0.55	840.65
ADRS 033	528031	4068450	841.2	590.04	0.81	840.39
ADRS 033	528031	4068450	841.2	431.46	1.19	840.01
ADRS 033	528031	4068450	841.2	186.55	1.74	839.46
ADRS 033	528031	4068450	841.2	44.59	2.55	838.65
ADRS 033	528031	4068450	841.2	28.7	3.75	837.45
ADRS 033	528031	4068450	841.2	47.18	5.5	835.7
ADRS 033	528031	4068450	841.2	70.98	8.074	833.126
ADRS 033	528031	4068450	841.2	85.77	11.85	829.35
ADRS 033	528031	4068450	841.2	82.12	17.39	823.81
ADRS 033	528031	4068450	841.2	66.15	25.53	815.67
ADRS 033	528031	4068450	841.2	49.55	37.47	803.73
ADRS 033	528031	4068450	841.2	37.44	55.01	786.19
ADRS 033	528031	4068450	841.2	28.41	80.74	760.46
ADRS 034	528031	4068230	841.2	671.98	0.55	840.65
ADRS 034	528031	4068230	841.2	555.22	0.81	840.39
ADRS 034	528031	4068230	841.2	189.23	1.19	840.01
ADRS 034	528031	4068230	841.2	68.81	1.74	839.46
ADRS 034	528031	4068230	841.2	24.7	2.55	838.65
ADRS 034	528031	4068230	841.2	26.28	3.75	837.45
ADRS 034	528031	4068230	841.2	45.68	5.5	835.7
ADRS 034	528031	4068230	841.2	73.58	8.074	833.126
ADRS 034	528031	4068230	841.2	66.18	11.85	829.35

ADRS 034	528031	4068230	841.2	87.68	17.39	823.81
ADRS 034	528031	4068230	841.2	77.76	25.53	815.67
ADRS 034	528031	4068230	841.2	41.69	37.47	803.73
ADRS 034	528031	4068230	841.2	45.8	55.01	786.19
ADRS 034	528031	4068230	841.2	30.53	80.74	760.46
ADRS 035	528031	4067987	840.1	641.84	0.55	839.55
ADRS 035	528031	4067987	840.1	526.42	0.81	839.29
ADRS 035	528031	4067987	840.1	368.19	1.19	838.91
ADRS 035	528031	4067987	840.1	190.09	1.74	838.36
ADRS 035	528031	4067987	840.1	67.65	2.55	837.55
ADRS 035	528031	4067987	840.1	34.24	3.75	836.35
ADRS 035	528031	4067987	840.1	35.13	5.5	834.6
ADRS 035	528031	4067987	840.1	48.56	8.074	832.026
ADRS 035	528031	4067987	840.1	69.03	11.85	828.25
ADRS 035	528031	4067987	840.1	85.37	17.39	822.71
ADRS 035	528031	4067987	840.1	83.28	25.53	814.57
ADRS 035	528031	4067987	840.1	58.86	37.47	802.63
ADRS 035	528031	4067987	840.1	36.33	55.01	785.09
ADRS 035	528031	4067987	840.1	35.06	80.74	759.36
ADRS 036	527731	4068350	842.4	899.93	0.55	841.85
ADRS 036	527731	4068350	842.4	856.46	0.81	841.59
ADRS 036	527731	4068350	842.4	587.29	1.19	841.21
ADRS 036	527731	4068350	842.4	262.51	1.74	840.66
ADRS 036	527731	4068350	842.4	94.63	2.55	839.85
ADRS 036	527731	4068350	842.4	54.25	3.75	838.65
ADRS 036	527731	4068350	842.4	57.55	5.5	836.9
ADRS 036	527731	4068350	842.4	69.83	8.07	834.33
ADRS 036	527731	4068350	842.4	79.41	11.85	830.55
ADRS 036	527731	4068350	842.4	88.31	17.39	825.01
ADRS 036	527731	4068350	842.4	92.66	25.53	816.87
ADRS 036	527731	4068350	842.4	77.82	37.47	804.93
ADRS 036	527731	4068350	842.4	50.5	55.01	787.39
ADRS 036	527731	4068350	842.4	34.42	80.74	761.66
ADRS 037	527731	4068106	841.2	399.66	0.55	840.65
ADRS 037	527731	4068106	841.2	516.77	0.81	840.39
ADRS 037	527731	4068106	841.2	538.59	1.19	840.01
ADRS 037	527731	4068106	841.2	404.4	1.74	839.46
ADRS 037	527731	4068106	841.2	186.08	2.55	838.65
ADRS 037	527731	4068106	841.2	56.24	3.75	837.45
ADRS 037	527731	4068106	841.2	32.02	5.5	835.7
ADRS 037	527731	4068106	841.2	44.82	8.07	833.13
ADRS 037	527731	4068106	841.2	62.89	11.85	829.35
ADRS 037	527731	4068106	841.2	75.72	17.39	823.81
ADRS 037	527731	4068106	841.2	81.03	25.53	815.67
ADRS 037	527731	4068106	841.2	80.92	37.47	803.73
ADRS 037	527731	4068106	841.2	71.86	55.01	786.19
ADRS 037	527731	4068106	841.2	47.18	80.74	760.46
ADRS 038	528231	4068230	841.2	581.84	0.55	840.65
ADRS 038	528231	4068230	841.2	379.32	0.81	840.39
ADRS 038	528231	4068230	841.2	236.06	1.19	840.01
ADRS 038	528231	4068230	841.2	118.76	1.74	839.46
ADRS 038	528231	4068230	841.2	48.78	2.55	838.65
ADRS 038	528231	4068230	841.2	36.7	3.75	837.45
ADRS 038	528231	4068230	841.2	44.73	5.5	835.7
ADRS 038	528231	4068230	841.2	54.37	8.07	833.13
ADRS 038	528231	4068230	841.2	59.75	11.85	829.35
ADRS 038	528231	4068230	841.2	59.12	17.39	823.81
ADRS 038	528231	4068230	841.2	53.6	25.53	815.67
ADRS 038	528231	4068230	841.2	42.89	37.47	803.73
ADRS 038	528231	4068230	841.2	30.49	55.01	786.19
ADRS 038	528231	4068230	841.2	25.17	80.74	760.46

ADRS 101	526499	4068853	849.3	855.23	0.55	848.75
ADRS 101	526499	4068853	849.3	1003.53	0.81	848.49
ADRS 101	526499	4068853	849.3	1094.85	1.19	848.11
ADRS 101	526499	4068853	849.3	801.78	1.74	847.56
ADRS 101	526499	4068853	849.3	284.04	2.55	846.75
ADRS 101	526499	4068853	849.3	56.56	3.75	845.55
ADRS 101	526499	4068853	849.3	31.15	5.5	843.8
ADRS 101	526499	4068853	849.3	49.42	8.074	841.226
ADRS 101	526499	4068853	849.3	76.29	11.85	837.45
ADRS 101	526499	4068853	849.3	97.51	17.39	831.91
ADRS 101	526499	4068853	849.3	93.61	25.53	823.77
ADRS 101	526499	4068853	849.3	69.03	37.47	811.83
ADRS 101	526499	4068853	849.3	48.29	55.01	794.29
ADRS 101	526499	4068853	849.3	41.64	80.74	768.56
ADRS 101	526499	4068853	849.3	42.76	118.51	730.79
ADRS 101	526499	4068853	849.3	43.65	173.94	675.36
ADRS 101	526499	4068853	849.3	42.7	255.31	593.99
ADRS 101	526499	4068853	849.3	41.32	374.75	474.55
ADRS 101	526499	4068853	849.3	45.9	550.06	299.24
ADRS 101	526499	4068853	849.3	69.77	807.37	41.93
ADRS 102	527219	4069154	849.3	72.64	0.55	848.75
ADRS 102	527219	4069154	849.3	113.33	0.81	848.49
ADRS 102	527219	4069154	849.3	168.22	1.19	848.11
ADRS 102	527219	4069154	849.3	211.66	1.74	847.56
ADRS 102	527219	4069154	849.3	203.83	2.55	846.75
ADRS 102	527219	4069154	849.3	140.04	3.75	845.55
ADRS 102	527219	4069154	849.3	72.98	5.5	843.8
ADRS 102	527219	4069154	849.3	42.97	8.074	841.226
ADRS 102	527219	4069154	849.3	48.23	11.85	837.45
ADRS 102	527219	4069154	849.3	77.3	17.39	831.91
ADRS 102	527219	4069154	849.3	93.98	25.53	823.77
ADRS 102	527219	4069154	849.3	70.64	37.47	811.83
ADRS 102	527219	4069154	849.3	38.43	55.01	794.29
ADRS 102	527219	4069154	849.3	28.09	80.74	768.56
ADRS 102	527219	4069154	849.3	36.33	118.51	730.79
ADRS 102	527219	4069154	849.3	44.91	173.94	675.36
ADRS 102	527219	4069154	849.3	46.41	255.31	593.99
ADRS 102	527219	4069154	849.3	55.04	374.75	474.55
ADRS 102	527219	4069154	849.3	81.27	550.06	299.24
ADRS 102	527219	4069154	849.3	120.39	807.37	41.93
ADRS 103	528050	4069162	847.2	158.34	0.59	846.61
ADRS 103	528050	4069162	847.2	180.04	0.87	846.33
ADRS 103	528050	4069162	847.2	186.8	1.28	845.92
ADRS 103	528050	4069162	847.2	122.75	1.87	845.33
ADRS 103	528050	4069162	847.2	57.75	2.75	844.45
ADRS 103	528050	4069162	847.2	43.91	4.04	843.16
ADRS 103	528050	4069162	847.2	59.73	5.93	841.27
ADRS 103	528050	4069162	847.2	93.42	8.7	838.5
ADRS 103	528050	4069162	847.2	137.66	12.77	834.43
ADRS 103	528050	4069162	847.2	149.61	18.74	828.46
ADRS 103	528050	4069162	847.2	96.77	27.5	819.7
ADRS 103	528050	4069162	847.2	39.55	40.37	806.83
ADRS 103	528050	4069162	847.2	21.47	59.25	787.95
ADRS 103	528050	4069162	847.2	26.71	86.97	760.23
ADRS 103	528050	4069162	847.2	27.32	127.66	719.54
ADRS 103	528050	4069162	847.2	21.91	187.37	659.83
ADRS 103	528050	4069162	847.2	31.02	275.03	572.17
ADRS 103	528050	4069162	847.2	80.35	403.69	443.51
ADRS 104	527676	4069165	847.3	288.29	0.55	846.75
ADRS 104	527676	4069165	847.3	256.7	0.81	846.49
ADRS 104	527676	4069165	847.3	172.34	1.19	846.11

ADRS 104	527676	4069165	847.3	110.93	1.74	845.56
ADRS 104	527676	4069165	847.3	70.69	2.55	844.75
ADRS 104	527676	4069165	847.3	37.33	3.75	843.55
ADRS 104	527676	4069165	847.3	28.66	5.5	841.8
ADRS 104	527676	4069165	847.3	41.45	8.074	839.226
ADRS 104	527676	4069165	847.3	68.67	11.85	835.45
ADRS 104	527676	4069165	847.3	98.05	17.39	829.91
ADRS 104	527676	4069165	847.3	103.56	25.53	821.77
ADRS 104	527676	4069165	847.3	71.13	37.47	809.83
ADRS 104	527676	4069165	847.3	33.12	55.01	792.29
ADRS 104	527676	4069165	847.3	17.94	80.74	766.56
ADRS 105	528050	4068908	845.7	983.55	0.55	845.15
ADRS 105	528050	4068908	845.7	1033.81	0.81	844.89
ADRS 105	528050	4068908	845.7	652.68	1.19	844.51
ADRS 105	528050	4068908	845.7	187.22	1.74	843.96
ADRS 105	528050	4068908	845.7	34.36	2.55	843.15
ADRS 105	528050	4068908	845.7	30.05	3.75	841.95
ADRS 105	528050	4068908	845.7	69.86	5.5	840.2
ADRS 105	528050	4068908	845.7	120.02	8.074	837.626
ADRS 105	528050	4068908	845.7	126.94	11.85	833.85
ADRS 105	528050	4068908	845.7	83.92	17.39	828.31
ADRS 105	528050	4068908	845.7	41.83	25.53	820.17
ADRS 105	528050	4068908	845.7	24.3	37.47	808.23
ADRS 105	528050	4068908	845.7	20.66	55.01	790.69
ADRS 105	528050	4068908	845.7	21.43	80.74	764.96
ADRS 106	528235	4068922	845.7	605.34	0.55	845.15
ADRS 106	528235	4068922	845.7	381.86	0.81	844.89
ADRS 106	528235	4068922	845.7	222.86	1.19	844.51
ADRS 106	528235	4068922	845.7	145.32	1.74	843.96
ADRS 106	528235	4068922	845.7	117.84	2.55	843.15
ADRS 106	528235	4068922	845.7	113.23	3.75	841.95
ADRS 106	528235	4068922	845.7	119.23	5.5	840.2
ADRS 106	528235	4068922	845.7	122.5	8.074	837.626
ADRS 106	528235	4068922	845.7	105.14	11.85	833.85
ADRS 106	528235	4068922	845.7	77.51	17.39	828.31
ADRS 106	528235	4068922	845.7	59.3	25.53	820.17
ADRS 106	528235	4068922	845.7	45.07	37.47	808.23
ADRS 106	528235	4068922	845.7	24.81	55.01	790.69
ADRS 106	528235	4068922	845.7	17.49	80.74	764.96
ADRS 107	528520	4069180	845.2	320.06	0.55	844.65
ADRS 107	528520	4069180	845.2	355.46	0.81	844.39
ADRS 107	528520	4069180	845.2	354.82	1.19	844.01
ADRS 107	528520	4069180	845.2	270.42	1.74	843.46
ADRS 107	528520	4069180	845.2	136.74	2.55	842.65
ADRS 107	528520	4069180	845.2	52.38	3.75	841.45
ADRS 107	528520	4069180	845.2	29.17	5.5	839.7
ADRS 107	528520	4069180	845.2	32.35	8.074	837.126
ADRS 107	528520	4069180	845.2	39	11.85	833.35
ADRS 107	528520	4069180	845.2	43.99	17.39	827.81
ADRS 107	528520	4069180	845.2	51.9	25.53	819.67
ADRS 107	528520	4069180	845.2	49.77	37.47	807.73
ADRS 107	528520	4069180	845.2	28.23	55.01	790.19
ADRS 107	528520	4069180	845.2	14.69	80.74	764.46
ADRS 107	528520	4069180	845.2	18.21	118.51	726.69
ADRS 107	528520	4069180	845.2	41.17	173.94	671.26
ADRS 107	528520	4069180	845.2	86.63	255.31	589.89
ADRS 107	528520	4069180	845.2	138.13	374.75	470.45
ADRS 107	528520	4069180	845.2	172.69	550.06	295.14
ADRS 107	528520	4069180	845.2	200.55	807.37	37.83
ADRS 108	529293	4070102	877.8	1268.75	1.87	875.93
ADRS 108	529293	4070102	877.8	346.23	2.75	875.05

ADRS 108	529293	4070102	877.8	158.47	4.04	873.76
ADRS 108	529293	4070102	877.8	267.72	5.93	871.87
ADRS 108	529293	4070102	877.8	550.29	8.7	869.1
ADRS 108	529293	4070102	877.8	848.45	12.77	865.03
ADRS 108	529293	4070102	877.8	1064.11	18.74	859.06
ADRS 108	529293	4070102	877.8	1043.64	27.5	850.3
ADRS 108	529293	4070102	877.8	714.81	40.37	837.43
ADRS 108	529293	4070102	877.8	337.71	59.25	818.55
ADRS 108	529293	4070102	877.8	157.32	86.97	790.83
ADRS 108	529293	4070102	877.8	146.76	127.66	750.14
ADRS 108	529293	4070102	877.8	143.82	187.37	690.43
ADRS 108	529293	4070102	877.8	82.77	275.03	602.77
ADRS 108	529293	4070102	877.8	97.39	403.69	474.11
ADRS 109	528755	4069464	847.29	119.59	2.06	845.23
ADRS 109	528755	4069464	847.29	31.18	3.03	844.26
ADRS 109	528755	4069464	847.29	34.35	4.44	842.85
ADRS 109	528755	4069464	847.29	71.71	6.52	840.77
ADRS 109	528755	4069464	847.29	114.42	9.57	837.72
ADRS 109	528755	4069464	847.29	136.8	14.05	833.24
ADRS 109	528755	4069464	847.29	126.84	20.63	826.66
ADRS 109	528755	4069464	847.29	92.17	30.28	817.01
ADRS 109	528755	4069464	847.29	53.12	44.44	802.85
ADRS 109	528755	4069464	847.29	23.64	65.23	782.06
ADRS 109	528755	4069464	847.29	12.82	95.74	751.55
ADRS 109	528755	4069464	847.29	19.98	140.53	706.76
ADRS 109	528755	4069464	847.29	55.21	206.27	641.02
ADRS 109	528755	4069464	847.29	177.33	302.77	544.52
ADRS 110	526850	4069115	849.3	854.58	0.55	848.75
ADRS 110	526850	4069115	849.3	752.73	0.81	848.49
ADRS 110	526850	4069115	849.3	720.28	1.19	848.11
ADRS 110	526850	4069115	849.3	675.46	1.74	847.56
ADRS 110	526850	4069115	849.3	420.71	2.55	846.75
ADRS 110	526850	4069115	849.3	140.34	3.75	845.55
ADRS 110	526850	4069115	849.3	57.19	5.5	843.8
ADRS 110	526850	4069115	849.3	63.24	8.074	841.226
ADRS 110	526850	4069115	849.3	77.96	11.85	837.45
ADRS 110	526850	4069115	849.3	78.54	17.39	831.91
ADRS 110	526850	4069115	849.3	72.04	25.53	823.77
ADRS 110	526850	4069115	849.3	66.94	37.47	811.83
ADRS 110	526850	4069115	849.3	61.83	55.01	794.29
ADRS 110	526850	4069115	849.3	49.6	80.74	768.56
ADRS 111	527219	4068967	847.5	1513.99	0.61	846.89
ADRS 111	527219	4068967	847.5	425.78	0.9	846.6
ADRS 111	527219	4068967	847.5	275.63	1.32	846.18
ADRS 111	527219	4068967	847.5	435.2	1.93	845.57
ADRS 111	527219	4068967	847.5	438.13	2.84	844.66
ADRS 111	527219	4068967	847.5	174.03	4.16	843.34
ADRS 111	527219	4068967	847.5	48.76	6.11	841.39
ADRS 111	527219	4068967	847.5	39.82	8.97	838.53
ADRS 111	527219	4068967	847.5	64.48	13.17	834.33
ADRS 111	527219	4068967	847.5	74.94	19.33	828.17
ADRS 111	527219	4068967	847.5	51.61	28.37	819.13
ADRS 111	527219	4068967	847.5	30.6	41.64	805.86
ADRS 111	527219	4068967	847.5	34.65	61.12	786.38
ADRS 111	527219	4068967	847.5	47.63	89.71	757.79
ADRS 112	529660	4068760	847.28	311.93	0.61	846.67
ADRS 112	529660	4068760	847.28	359.02	0.89	846.39
ADRS 112	529660	4068760	847.28	291.16	1.3	845.98
ADRS 112	529660	4068760	847.28	162.74	1.91	845.37
ADRS 112	529660	4068760	847.28	102.12	2.81	844.47
ADRS 112	529660	4068760	847.28	117.29	4.13	843.15

ADRS 112	529660	4068760	847.28	172.42	6.06	841.22
ADRS 112	529660	4068760	847.28	207.88	8.89	838.39
ADRS 112	529660	4068760	847.28	194.84	13.05	834.23
ADRS 112	529660	4068760	847.28	148.24	19.15	828.13
ADRS 112	529660	4068760	847.28	100.74	28.11	819.17
ADRS 112	529660	4068760	847.28	87.17	41.25	806.03
ADRS 112	529660	4068760	847.28	126.47	60.55	786.73
ADRS 112	529660	4068760	847.28	217.17	88.88	758.4
ADRS 112	529660	4068760	847.28	295.51	130.46	716.82
ADRS 112	529660	4068760	847.28	286.74	191.49	655.79
ADRS 112	529660	4068760	847.28	212.06	281.06	566.22
ADRS 112	529660	4068760	847.28	162.05	412.54	434.74
ADRS 112	529660	4068760	847.28	181.96	605.53	241.75
ADRS 113	526840	4068330	845.2	552.1	0.55	844.65
ADRS 113	526840	4068330	845.2	518.17	0.81	844.39
ADRS 113	526840	4068330	845.2	514.35	1.19	844.01
ADRS 113	526840	4068330	845.2	501.75	1.74	843.46
ADRS 113	526840	4068330	845.2	400	2.55	842.65
ADRS 113	526840	4068330	845.2	232.36	3.75	841.45
ADRS 113	526840	4068330	845.2	109.37	5.5	839.7
ADRS 113	526840	4068330	845.2	64.9	8.074	837.126
ADRS 113	526840	4068330	845.2	72.27	11.85	833.35
ADRS 113	526840	4068330	845.2	101.57	17.39	827.81
ADRS 113	526840	4068330	845.2	107.94	25.53	819.67
ADRS 113	526840	4068330	845.2	76.67	37.47	807.73
ADRS 113	526840	4068330	845.2	49.5	55.01	790.19
ADRS 113	526840	4068330	845.2	44.86	80.74	764.46
ADRS 113	526840	4068330	845.2	48.43	118.51	726.69
ADRS 113	526840	4068330	845.2	43.24	173.94	671.26
ADRS 113	526840	4068330	845.2	34.83	255.31	589.89
ADRS 113	526840	4068330	845.2	31.56	374.75	470.45
ADRS 113	526840	4068330	845.2	36.15	550.06	295.14
ADRS 113	526840	4068330	845.2	57.33	807.37	37.83
ADRS 114	527649	4069521	849.8	685.06	0.44	849.36
ADRS 114	527649	4069521	849.8	679.46	0.65	849.15
ADRS 114	527649	4069521	849.8	645.62	0.96	848.84
ADRS 114	527649	4069521	849.8	437.54	1.41	848.39
ADRS 114	527649	4069521	849.8	169.78	2.06	847.74
ADRS 114	527649	4069521	849.8	58.91	3.03	846.77
ADRS 114	527649	4069521	849.8	47.9	4.44	845.36
ADRS 114	527649	4069521	849.8	65.44	6.52	843.28
ADRS 114	527649	4069521	849.8	87.81	9.57	840.23
ADRS 114	527649	4069521	849.8	102.76	14.05	835.75
ADRS 114	527649	4069521	849.8	106.46	20.63	829.17
ADRS 114	527649	4069521	849.8	100.25	30.28	819.52
ADRS 114	527649	4069521	849.8	75.85	44.44	805.36
ADRS 114	527649	4069521	849.8	35	65.23	784.57
ADRS 114	527649	4069521	849.8	12.07	95.74	754.06
ADRS 114	527649	4069521	849.8	9.46	140.53	709.27
ADRS 114	527649	4069521	849.8	16.19	206.27	643.53
ADRS 114	527649	4069521	849.8	36.31	302.77	547.03
ADRS 115	528000	4069690	847.6	554.22	0.66	846.94
ADRS 115	528000	4069690	847.6	552.13	0.97	846.63
ADRS 115	528000	4069690	847.6	523.24	1.42	846.18
ADRS 115	528000	4069690	847.6	421.63	2.08	845.52
ADRS 115	528000	4069690	847.6	241.46	3.06	844.54
ADRS 115	528000	4069690	847.6	89.91	4.49	843.11
ADRS 115	528000	4069690	847.6	40.64	6.58	841.02
ADRS 115	528000	4069690	847.6	43.25	9.66	837.94
ADRS 115	528000	4069690	847.6	54.54	14.18	833.42
ADRS 115	528000	4069690	847.6	58.38	20.82	826.78

ADRS 115	528000	4069690	847.6	55.66	30.56	817.04
ADRS 115	528000	4069690	847.6	51.18	44.85	802.75
ADRS 115	528000	4069690	847.6	42.23	65.84	781.76
ADRS 115	528000	4069690	847.6	24.22	96.64	750.96
ADRS 115	528000	4069690	847.6	10.46	141.84	705.76
ADRS 115	528000	4069690	847.6	9.98	208.19	639.41
ADRS 115	528000	4069690	847.6	25.71	305.59	542.01
ADRS 115	528000	4069690	847.6	91.02	448.54	399.06
ADRS 116	529143	4069201	847.28	155.37	0.44	846.84
ADRS 116	529143	4069201	847.28	155.76	0.65	846.63
ADRS 116	529143	4069201	847.28	112.64	0.96	846.32
ADRS 116	529143	4069201	847.28	82.27	1.41	845.87
ADRS 116	529143	4069201	847.28	84.69	2.06	845.22
ADRS 116	529143	4069201	847.28	98.96	3.03	844.25
ADRS 116	529143	4069201	847.28	114.52	4.44	842.84
ADRS 116	529143	4069201	847.28	134.11	6.52	840.76
ADRS 116	529143	4069201	847.28	143.48	9.57	837.71
ADRS 116	529143	4069201	847.28	132.12	14.05	833.23
ADRS 116	529143	4069201	847.28	105.49	20.63	826.65
ADRS 116	529143	4069201	847.28	67.61	30.28	817
ADRS 116	529143	4069201	847.28	39.28	44.44	802.84
ADRS 116	529143	4069201	847.28	28.82	65.23	782.05
ADRS 116	529143	4069201	847.28	25.53	95.74	751.54
ADRS 116	529143	4069201	847.28	32.72	140.53	706.75
ADRS 116	529143	4069201	847.28	62.52	206.27	641.01
ADRS 116	529143	4069201	847.28	137.52	302.77	544.51

## Appendix 4-B

**Appendix 4-B. Available Monitoring Well Information**

UTM X	UTM Y	Elev. (ft)	Elev. (m)	Screened Interval (Top BGS)	Screened Interval Bottom BGS)	Depth to Water BGS	Water Surface Altitude in Meters	Well Bottom Altitude in Meters	Water Surface Altitude in Meters (May '04)	Tritium in units	Tritium in pCi/L
527375	4068715	2776.892	846.5	111	123	112.2	734.3	723.4	734.3	3.8	12.16
527550	4069125	2782.141	848.1				759.9	744.3			
527425	4068780	2776.236	846.3				dry	737.9	736.9		
527875	4068790	2771.644	844.9				N/A	N/A			
528025	4068980	2775.908	846.2				N/A	N/A			
528030	4069050	2778.205	846.9				N/A	N/A			
527910	4068950	2775.908	846.2				N/A	N/A			
528070	4068950	2772.3	845.1				752.5	746.5			
528040	4068780	2769.347	844.2				751.5	745.4			
528075	4069080	2778.205	846.9				759.9	755			
527820	4068780	2771.972	845	91	98	93	752	745.9	751.6	0.05	0.16
527680	4068980	2776.564	846.4				760.2	755.3			
527610	4069300	2785.422	849.1	86	92	87.8	761.3	755.2		0.4	1.28
527695	4068880	2776.564	846.4	90	96	92.4	754	748.5		0.9	2.88
527750	4068725	2772.628	845.2	92	98	93.3	751.9	745.8		0.6	1.92
528040	4068870	2775.908	846.2	85	91	89	757.2	753.1		0.7	2.24
527925	4068780	2770.66	844.6				751.3	745.3	751		
527605	4068950	2774.596	845.8	91	173	85.3	N/A	N/A	760.5	0.4	1.28
527615	4069300	2785.422	849.1	141	144	93.3	N/A	N/A		0.05	0.16
527820	4068730	2774.924	845.9	126	130	99.4	N/A	N/A		0.05	0.16
527285	4068950	2781.485	847.9	104	112	105.2				0.2	0.64
527336	4068713	2776.892	846.5	N/A	N/A	109.7			736.8		

## **5 Rocky Flats Facility**

### ***5.1 Introduction***

The Rocky Flats Facility was selected to test the applicability of the AES Advanced Environmental Solutions, LLC (AES) Strategy to a semi-arid environment in the Midwestern United States. This exercise is for demonstration only. This report is based on readily available information and does not constitute a comprehensive evaluation of all data for the site.

The Rocky Flats Facility, a former nuclear weapons facility, is located west of Denver, Colorado in an area of complex terrain (Figure 5-1) (DOE, 2005). A primary mission of the Rocky Flats facility was to machine plutonium “buttons” into weapons components. Figure 5-2 presents an aerial view of the Rocky Flats Facility looking east in 1983, prior to decommissioning.

In this exercise, the AES Strategy is applied in two separate case studies at Rocky Flats, both of which focus on ground water contaminated by chlorinated organic solvents. In each instance, application of the Strategy yields improved understanding about the natural system at the site.





Rocky Flats was established in 1951 to manufacture plutonium, enriched and depleted uranium, and steel nuclear weapons components. After a similar facility at Hanford shut down in 1965, Rocky Flats became the only source of plutonium “pits” for the U.S. nuclear weapons arsenal. *Rocky Flats Plant, Colorado. July 17, 1983.*

**Figure 5-2. Photograph of the Rocky Flats Facility (looking east) Photo is in “Linking Legacies”, DOE publication EM-0319 (DOE 1997) Appendix B, page 190.**

## ***5.2 Compilation of Available Data***

This section provides a summary of the readily available data compiled for evaluation of both VOC case studies.

## ***5.3 Geologic Setting***

The Rocky Flats Facility sits approximately 6,000 feet above mean sea level on the western margin of the Colorado Piedmont section of the Great Plains Physiographic Province. The Colorado Piedmont is an old erosional surface along the eastern margin of the Rocky Mountains underlain by gently dipping sedimentary rocks (Paleozoic to Cenozoic in age) which are abruptly upturned at the Front Range (just west of the Rocky Flats Facility) to form hogback ridges parallel to the mountain front. The Piedmont surface is broadly rolling and slopes gently to the east with topographic relief of only several hundred feet. This relief is due both to resistant bedrock units that locally rise above the landscape and to the presence of incised stream valleys (DOE, 1990).

### 5.3.1 Hydrologic Data

Hydrogeology at the Rocky Flats Facility is characterized by three distinct units, the upper alluvial aquifer, lower aquitard, and the Laramie-Fox Hills aquifer.

The upper alluvial aquifer is largely unconsolidated materials that can be as much as 100 feet thick in the western portions of the site. The upper aquifer is generally recharged from precipitation or surface water bodies. Ground water in the unconsolidated alluvial aquifer is generally close to the land surface, with an average depth of 11 feet below ground surface. Several springs emerge in areas where the contact of the upper aquifer and the lower aquitard is exposed at the surface. While most of these springs occur within the Rock Creek drainage, Antelope Springs in the Woman Creek drainage has the largest discharge at Rocky Flats (Figure 5-3). Antelope Springs discharges continuously over several acres. The upper alluvial aquifer has a permeability of approximately 0.5 meters per day.

The lower aquitard comprises deeper claystone and siltstone of the Laramie and Arapahoe Formations. These formations combined are up to 800 feet thick below Rocky Flats. Recharge of the lower aquitard occurs from downward flow through the upper aquifer, or directly through precipitation in areas where the bedrock is exposed.

Beneath the aquitard lies the regional Laramie-Fox Hills aquifer. It is composed of the lower sandstone unit of the Laramie Formation and the Fox Hills Sandstone, and is confined by the overlying aquitard. Ground water levels in the bedrock aquifers are generally greater than 100 feet. Several portions of the upper alluvial aquifer east and northeast of the Industrial Area are known or suspected of being contaminated with radionuclides, volatile organic compounds, and metals. The aquitard is less contaminated than the upper alluvial aquifer. No contaminant plumes have been identified in the aquitard (ERO Resources, 2003).

Liquid contaminants spilled on the ground and certain substances that dissolve in water can easily move down through the soil and contaminate the shallow ground water. Data from on-site monitoring wells at Rocky Flats show areas of ground water contaminated with elevated radioactivity, nitrates, and volatile organic compounds at different locations (CDPHE, (No Date)). Figure 5-4 shows the location of monitoring wells and the extent of nitrate plumes and VOC plumes at or above maximum contaminant levels.

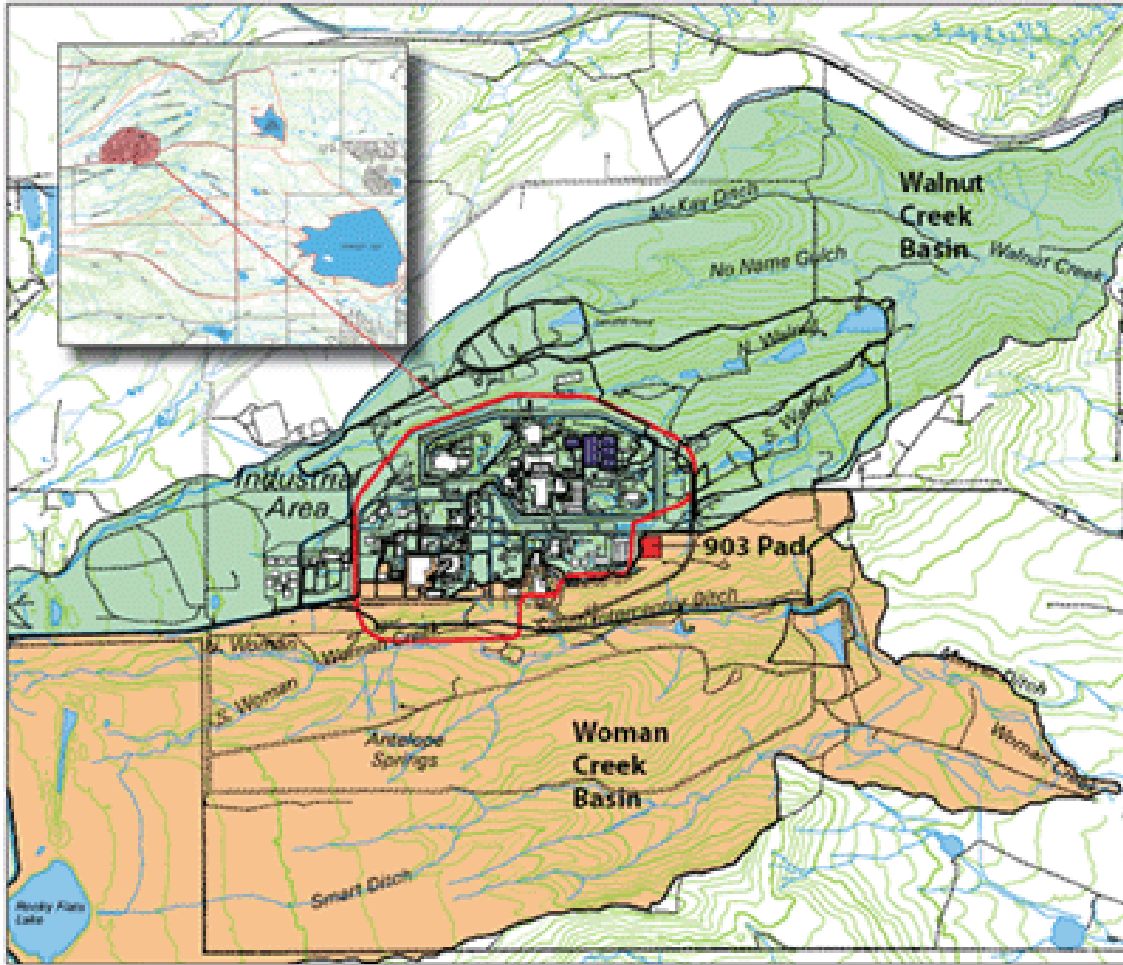


Figure 5-3. Map of Rocky Flats Facility drainage basins (from: <http://lanl.gov/source/orgs/nmt/nmtdo/AQarchive/06springsummer/page5.shtml>)

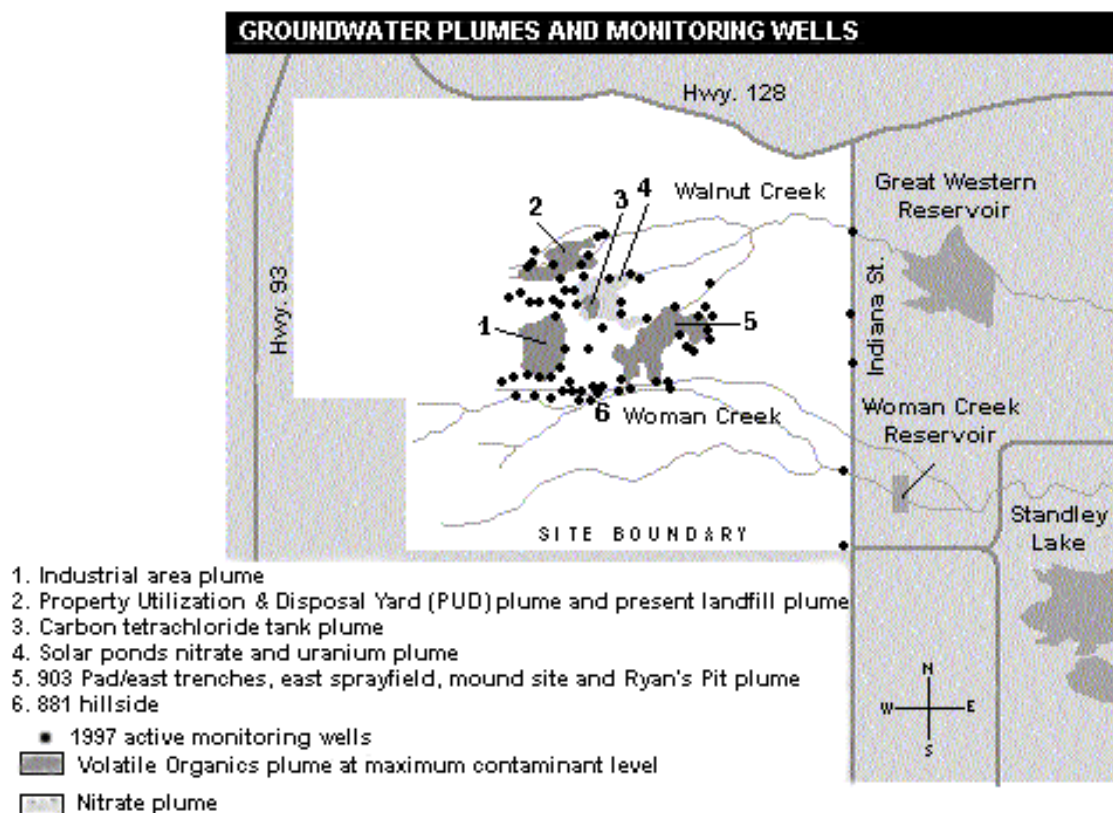


Figure 5-4. Ground-water monitoring well locations and depiction of VOC and nitrate plumes for the Rocky Flats Facility (CDPHE, (No Date))

## 5.4 Application of the Strategy

### 5.4.1 Case Study 1: Conceptual Site Model Assessment

Figure 5-5 presents a Transport Conceptual Model for the Rocky Flats Facility that was located during compilation of existing site data. This conceptual model illustrates a pathway from ground to surface water. Specifically, it shows the majority of contaminant movement within the upper alluvial aquifer. According to this model, surface water VOC concentrations are typically higher during the winter months when volatilization is reduced by low temperatures and ice covering the surface water. Risk to wildlife or wildlife workers through a surface water pathway has been a driving concern in Rocky Flats remediation efforts.

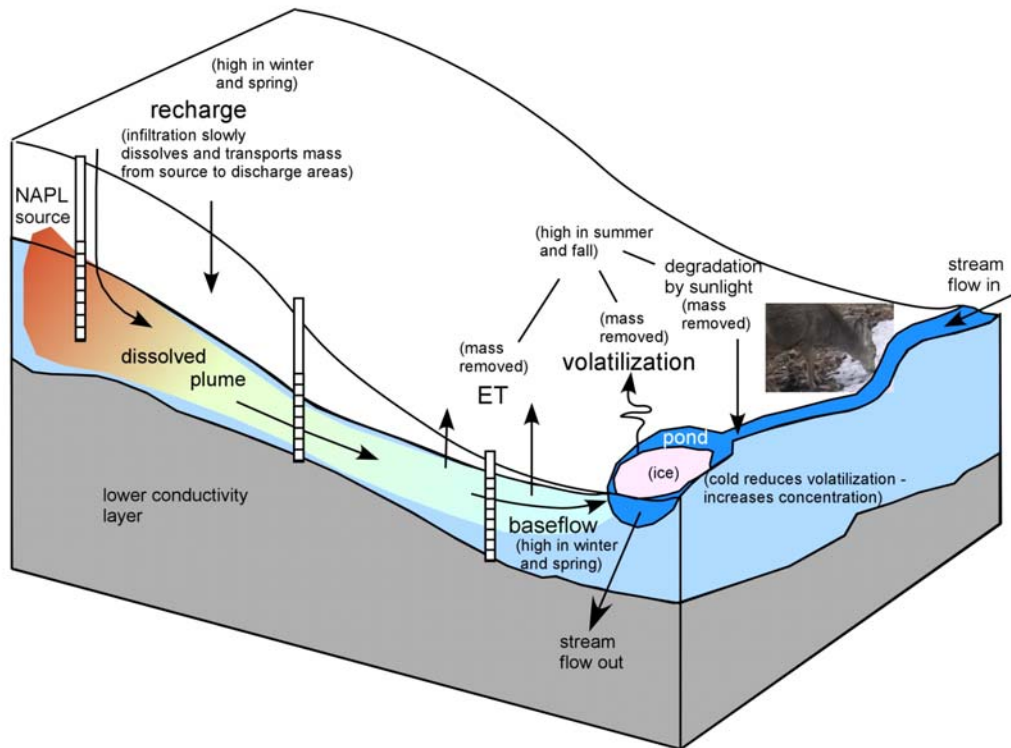


Figure 5-5. Conceptual cross-section for the Rocky Flats Facility (Modified from K-H, 2004)

#### 5.4.2 Case 1: Existing Site Monitoring Data

Figure 5-6, below shows carbon tetrachloride concentrations in Well 3991 between 1992 and 2003. Water levels are shown as depth to ground water in feet. Between 1992 and 1995, carbon tetrachloride concentration declines in this well by a factor of 10, to below 0.005 mg/l (<5ppb). However, the fourth quarter 1995 sampling result indicates the concentration increases to over 50 ppb. Subsequently, concentrations decline, only to peak again in 1999, then steadily decline for 5 years to the end of our data set.

#### 5.4.3 Case 1: Application of the Strategy

One possible hypothesis to explain the carbon tetrachloride concentration spikes observed in the existing monitoring data would include periodic releases or spills at the site; however, inclusion of Well 3991 water level data in a conceptual site model (Figure 5-6 and Figure 5-7) suggests that the concentration spikes are correlated to high water levels. Specifically, concentration spikes were seen immediately following well water levels between 6 to 10 feet above normal for the well.

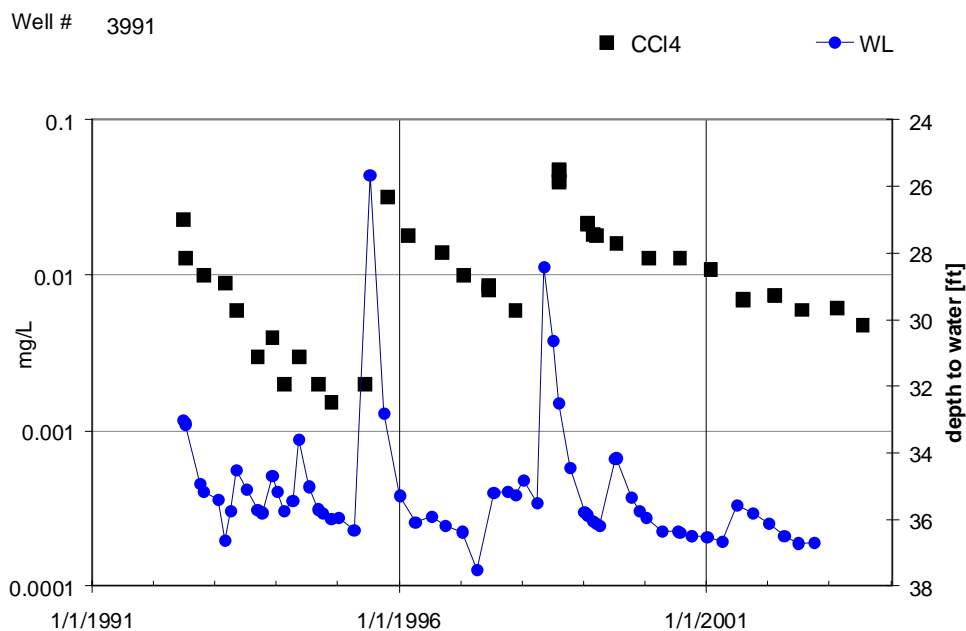


**Figure 5-6. Diagram of multiyear variability in ground-water contaminant concentrations due to water table changes (K-H, 2004)**

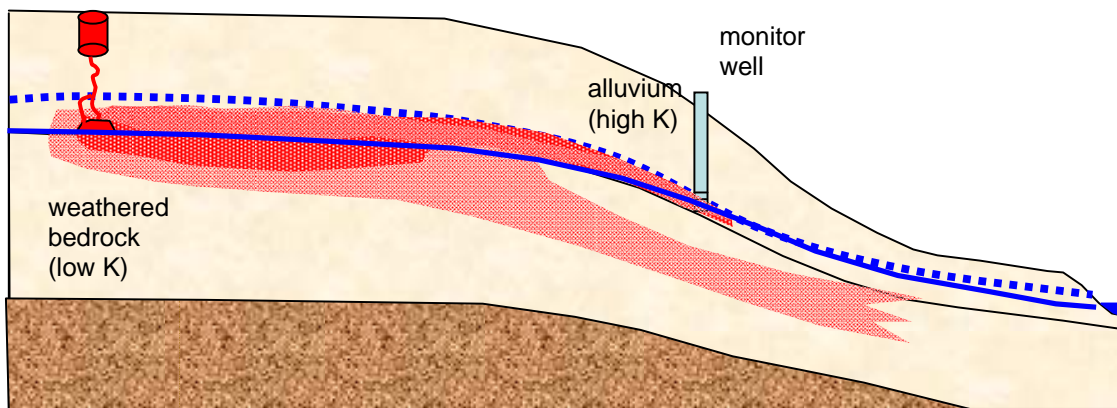


**Figure 5-7. Conceptual cross section showing affects of water table changes on contaminant movement (modified from K-H, 2004)**

Figure 5-7 shows the revised conceptual model which explains the observed spikes in carbon tetrachloride concentrations. This model illustrates how contamination from disposal trenches migrates through the vadose zone and collects at the interface between the higher permeability alluvium and the lower permeability weathered bedrock. The water table is typically in the weathered bedrock, but during periods of very high recharge it can rise into the high permeability alluvium and mobilize contamination

pooled at the bedrock interface, and subsequently mobilize into the weathered bedrock aquifer. The normal water table is indicated by a solid blue line. In a period of heavy rain fall or snow melt, water levels rise into the alluvium (dashed blue line) and mobilize vadose zone contamination. This results in a concentration spike followed by a slow decline as the displaced solvent dissipates.

It is most important to note that the declining concentrations at the monitoring well provide no information on the possible decline of the source pool. It is also important to note that a 3-year steep decline ending with four quarters of low concentrations might be used to argue that this well could be removed from a contaminant monitoring program. Look again at the first 12 concentrations in Figure 5-5 then look at the first 15 concentrations. Now look at the last several years - when can we stop sampling this well?

This well provides important information on the performance of the hydrologic system at this site: these spikes infer that a relatively higher concentration up gradient source is present and that water table information is a strong performance indicator.

It is important to recognize that this well is placed in a critical point to monitor system performance. We now have a model to relate observations at a well to the source and an indication that the system performance suggests that a high-concentration zone exists in the ground – but this model is not sufficient to model the extent of the plume. Management (DOE, state agencies, EPA, and other stakeholders) can decide whether long-term risk justifies an attempt to characterize and remove most of the source.

In addition to the natural variations in the water table, long term recharge changes due to facility closure need to be considered. Elimination of features such as drains, leaking water lines, and covered areas such as asphalt parking lots can affect the water table recharge (Figure 5-8). By eliminating these features the shape of the water table surface may be altered dramatically. In a 40-plus-year old facility of this size water system leaks on the order of tens of gallons per minute could be expected. This would be a major fraction of the local infiltration.

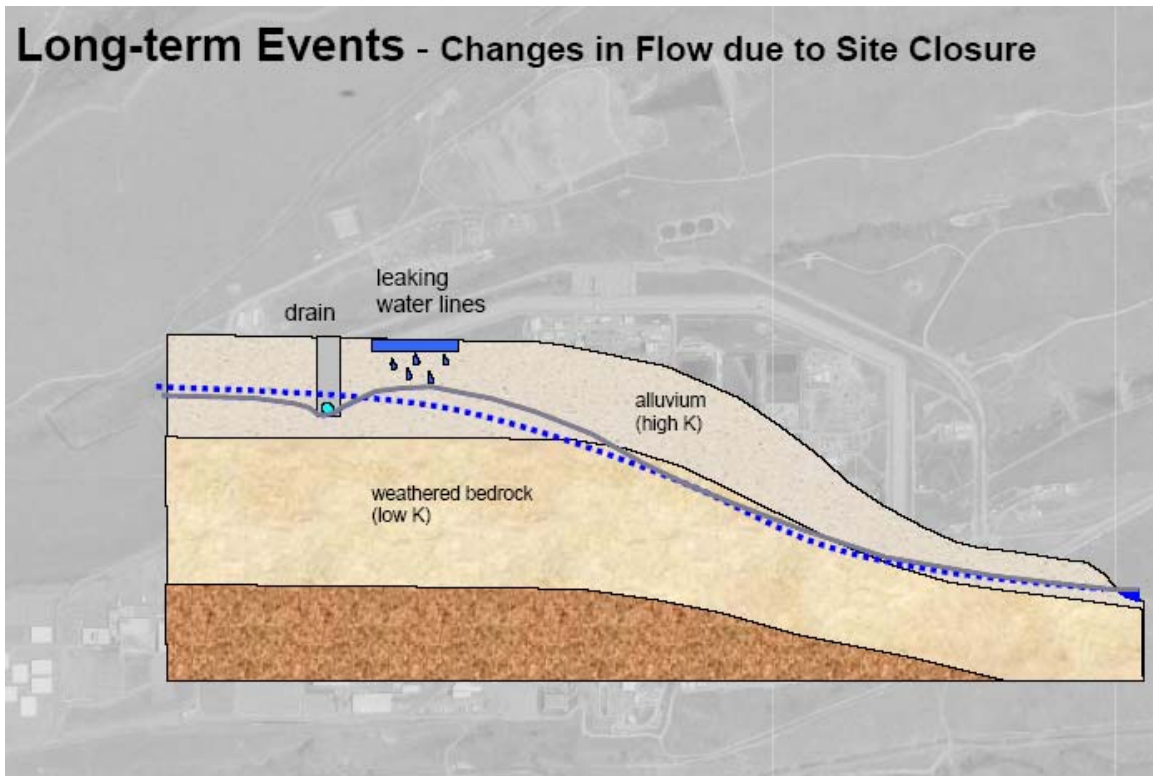


**Figure 5-8. Potential changes in ground-water movement due to closure**

Figure 5-9 shows predicted water level changes after site closure. Comparison of this Figure with VOC plume and source maps presented below shows the possibility of gradient changes in the vicinity of the VOC sources. This prediction was made with MIKE SHE, a modeling code that can incorporate both subsurface and subsurface flow (K-H, 2004).

Infiltration changes upon site closure require that any flow and transport models that are relied upon to justify environmental management decisions should be re-evaluated. Once again, it is a management decision to do this re-evaluation, but very simple models can be constructed to enlighten discussions surrounding the decision. These models would also include changes in surface water runoff.

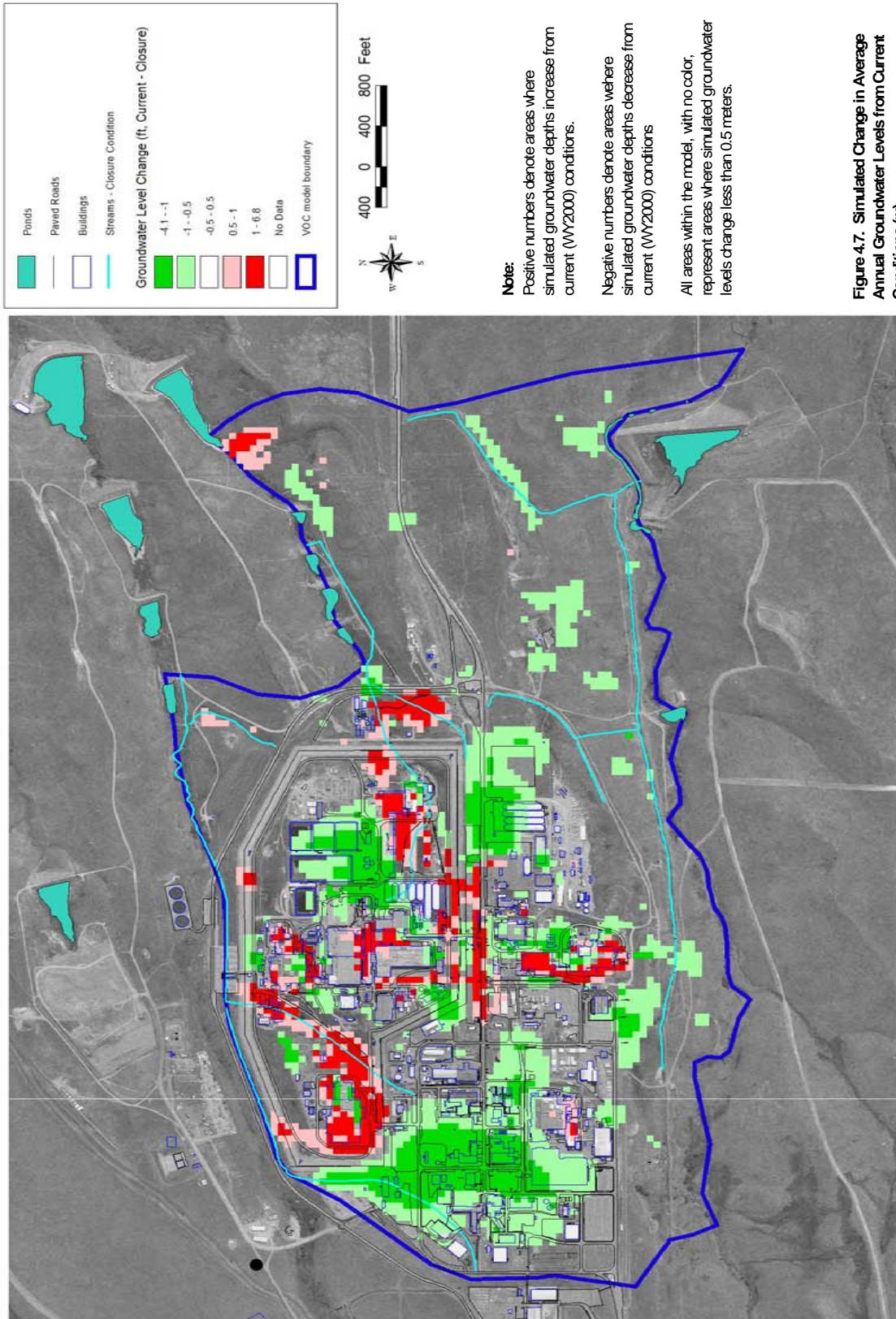


Figure 5-9. Predicted water level changes after closure (K-H, 2004)

#### 5.4.4 Case 2: VOC Plume Analysis

The majority of VOC ground-water contamination at the Rock Flats Facility consists of chlorinated solvents including tetrachloroethylene (PCE) and trichloroethylene (TCE), with minor amounts of dichloroethylene (DCE). Identification of the original contamination can often be difficult as the chlorinated solvents break down readily to a less chlorinated state (e.g., PCE to TCE to DCE to Vinyl Chloride).

Results of ground-water monitoring at the Rocky Flats Facility show a significant TCE plume emanating from the eastern portion of the site. The initial conceptual model has historically been interpreted to be one plume with complex movement of ground water creating a radial dispersion pattern. Figure 5-10 shows the general extent of the TCE plume assuming a single plume. This figure is taken directly from a talk and not edited.

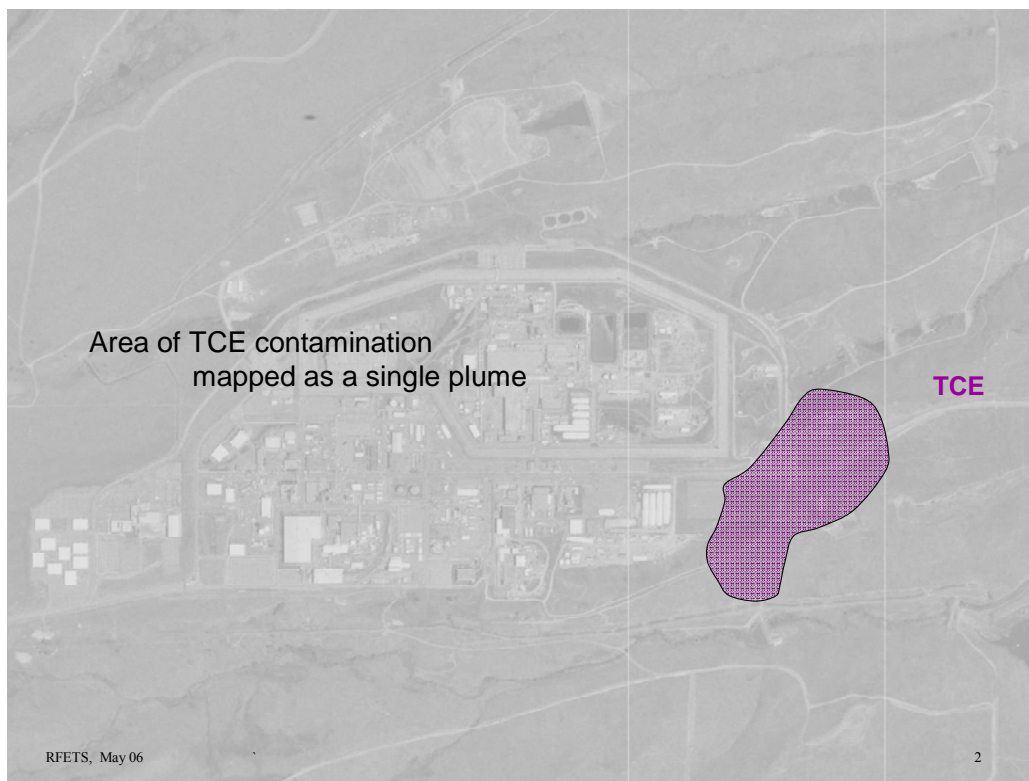


Figure 5-10. Generalized depiction of the Rocky Flats Facility TCE plume

#### 5.4.5 Case 2: Application of the Strategy

By understanding the nature of the original spills and by evaluating the presence of daughter products from the degradation of chlorinated solvents, a revised conceptual model can be prepared.

Also, by associating sources and plumes with ground-water flow fields, it may be possible to differentiate multiple overlapping plumes. Discriminators such as probable source locations, variable ground-water flow paths, and potential daughter product

distributions can be used to prepare a refined conceptual model for contaminant movement.

Multiple sources will likely result in multiple plumes with unique fingerprints. Figure 5-11 presents an alternative conceptual model of contaminant plume source and migration based on additional information provide below. Further evaluation of ground-water monitoring data indicates that an east-west ground-water divide is present, effectively splitting the southern one-third of the plume from the northern two-thirds of the plume. By dividing the plumes based on the ground-water flow information above, it appears two plumes may be present, straddling the ground-water divide. In addition, an evaluation of the concentrations of all chlorinated solvents is undertaken as part of this Strategy application. Near the source the two plumes commingle, making differentiation difficult. Under reducing conditions, aquifer microorganisms can reductively dechlorinate PCE into less chlorinated daughter products such as TCE, DCE and vinyl chloride. By evaluating the relative concentrations of these contaminants, the separate plumes may be identified.

In Figure 5-11, the northern plume contains higher concentrations of PCE than TCE, suggesting that the TCE is derived from PCE degradation. In the southern plume TCE is present in much higher concentrations than PCE, suggesting that the original spill consisted mostly of TCE with minor amounts of PCE, or as an alternative conceptual model, that a much higher degree of anaerobic degradation is occurring in the southern plume, effectively eliminating the presence of the original PCE spill. However, in Figure 5-10, the southern plume moves down the hill side towards Woman Creek and likely represents more of an aerobic environment, thus minimizing the potential for degradation of chlorinated solvents. Based on the information provided in Figure 5-10, TCE is pervasive in both overlapping plumes; however, the use of PCE as a discriminator or performance indicator has resulted in a refined conceptual model of contaminant movement showing two separate plumes with two separate sources (Figure 5-11). If two sources were not originally identified in this area, this conceptual model would prompt the need to evaluate the potential presence of a previously unidentified spill.

## Associate Source and Plume within GW flow field

Use probable source locations, groundwater flow paths, and daughter product distribution to delineate plumes

### Refine conceptual model

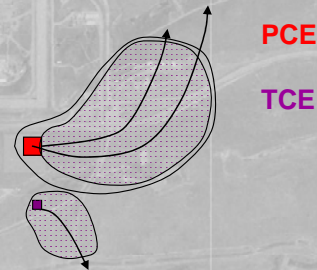
Associate sources and concentration distribution within the GW flow field

2 probable sources result in 2 separate plumes

Higher concentration of PCE than TCE in northern plume suggest TCE derived from PCE degradation (though TCE possibly also released)

High TCE and very low PCE concentrations in the southern plume suggest significant TCE released along with PCE

Alternative conceptual model would be much higher degradation of PCE in southern plume to produce TCE, though southern plume conditions should be more aerobic along hill-side (less favorable to PCE degradation)



RFETS, May 06

4

Figure 5-11. Conceptual model of complex flow of contaminants

### 5.4.6 Performance Indicators and FEPs

Performance indicators and features, events, or processes (FEPs) for the Rocky Flats Facility include, but are not limited to:

- 1) **monitor water levels**- changes in the water table surface or orientation will affect the direction of ground-water flow and the potential for remobilization of contaminants from the vadose Zone into the aquifer.
- 2) **time trends for ground-water contamination** – by looking at the relative concentration of contaminants over time, especially in comparison to water level readings, informed decisions can be made on when monitoring efforts can be terminated.
- 3) **monitor all VOC daughter products for the VOC plumes**- because the fingerprints of various VOC plumes may define multiple sources, determining the relative proportions of VOCs that make up a given plume is critical

## **5.5 Monitoring Strategy Application Conclusions**

Based on the results of the application of the Strategy, the following conclusions can be drawn:

Case 1: Episodic changes in the water table result in the periodic remobilization of contaminants from the vadose zone, most likely at the alluvium/bedrock interface, into the ground water. By evaluating all of the available ground-water monitoring data through time trend analysis, it becomes apparent that the duration of Post-Closure ground-water monitoring may need to be extended or further characterization of the contamination within the vadose zone may need to be undertaken due to the cyclic recontamination of the water table.

Case 2: A VOC plume is emanating from the southeast corner of the Rocky Flats Facility. By evaluating the analytical results for chlorinated solvent daughter products together with likely flow directions, it becomes apparent that a revised Conceptual Site Model can be proposed with multiple sources contributing to the ground-water contamination. By examining the relative concentrations of all of the chlorinated solvents, individual plume fingerprints can be identified for the differentiating multiple sources.

Based on the results of the application of the Strategy, the following recommendations to management can be made:

1. Perform detailed time trend analysis for monitoring wells in relation to changes in the water table. In addition to the natural variations in the water table, long term recharge changes due to facility closure need to be considered due to the potential for remobilization of contaminants and changes in the water table surface. In addition, changes in the water table may result in the remobilization of contaminants from the vadose zone.
2. Evaluate the relative concentrations of contaminants to daughter products for revising plume delineation and sources.

## **5.6 Rocky Flats References**

- Colorado Department of Public Health and Environment (CDPHE). *Rocky Flats Public Exposure Studies, Movement of Contaminated Groundwater at the Rocky Flats Environmental Technology Site*. (Available online at [www.cdphe.state.co.us/rf/movement.htm](http://www.cdphe.state.co.us/rf/movement.htm))
- Department of Energy (DOE). Interim Measures/Interim Remedial Action and Decision Document, 881 Hillside Area Operable Unit No. 1, Rocky Flats Plant. January 1990.
- DOE/EM-0319. *Linking Legacies, Connecting the Cold War Nuclear Weapons Production Processes to Their Environmental Consequences*. 1997.
- ERO Resources Corporation. *Rocky Flats National Wildlife Refuge Resource Inventory*. April 2003.
- K-H. *Fate and Transport Modeling of Volatile Organic Compounds*. Kaiser-Hill Company L.L.C., Rocky Flats Environmental Technology Site: Golden, Colorado. April 2004.

## 6 Savannah River Site, C Area

### 6.1 Introduction

The Savannah River Site (SRS) has a fifty-plus year history of defense nuclear research, fuel fabrication, chemical separations and waste disposal. The site covers about 300 square miles in South Carolina, along the Savannah River, about 100 miles upstream of the Atlantic Ocean (Figure 6-1). SRS includes 5 production reactors (Reactors C, K, L, P, R), a research lab, fuel fabrication, two chemical separation plants, and supporting and waste management facilities. Further description of this site and its history of operation are available in Linking Legacies, DOE publication EM-0319 (DOE 1997).

DOE has been generous in allowing access to documents and data from the Site's extensive environmental characterization and monitoring work.

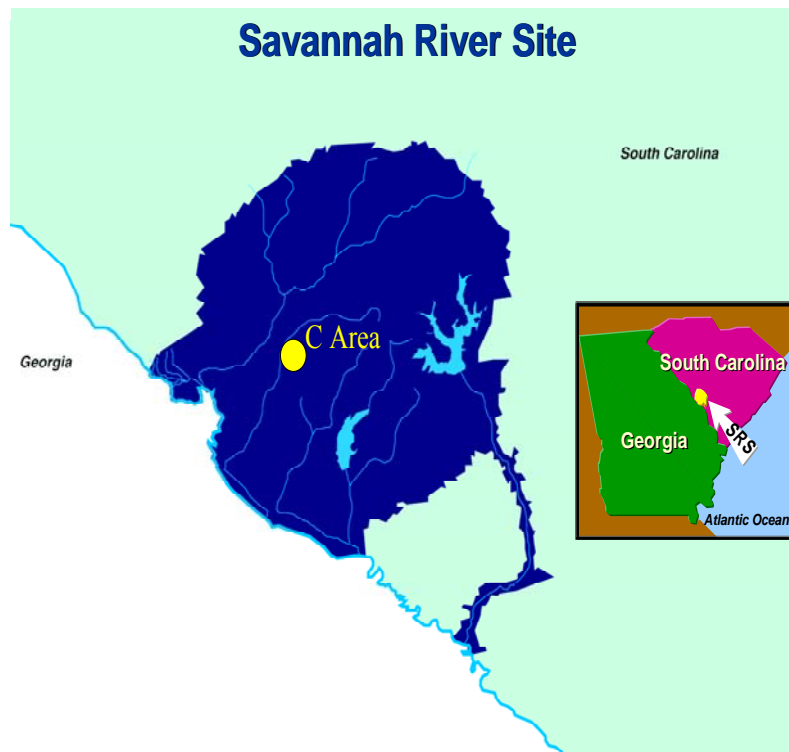


**Figure 6-1. Savannah River Site location map. Courtesy of Bill Jones, SRNL.**

This Chapter will use the C-Area of SRS to illustrate some results of contaminant plume characterization and monitoring. C-Reactor operated from 1955 through 1986, with construction beginning in about 1951. Within the reactor building is the disassembly basin, similar to a spent fuel pool in a power reactor. External to the reactor building are several waste facilities including reactor seepage basins (CRSB) to receive acids and caustics, low level radioactive solutions resulting primarily from maintenance, and a pit (CBRP) for burning waste and disposing of rubble that could include scrap wood, pasteboard, paint, and solvents. A photograph of the A-Area burning and rubble pit (ABRP) is shown in Figure 6-2 as an example.



**Figure 6-2. Photograph of the A Area Burning/Rubble Pit during operation**

In this Chapter we will look at a TCE plume from the CBRP and, to a lesser extent, a tritium plume from the CRSB. Even though the site is intensely characterized and monitored, we will show the value of computer simulation and 3-D visualization to evaluate the existing site data and present support for management decisions concerning the value of further monitoring or characterization. Further, we will show the importance of considering all sources of characterization data before using a computer simulation to support conclusions about the long-term disposition of a site.

Figure 6-3 is a map of C-Area. The reactor building (105-C), including the disassembly basin, CBRP, and three small seepage basins are shown. Wells from which monitoring data are obtained are also shown (e.g., P-18, CCB-1, and CSB-3A). This figure is from WSRC, 1998, an inventory of SRS environmental protection wells; similar documents are available online at [www.osti.gov](http://www.osti.gov) with authors Janssen or Rogers.

The wells LWR-1 through -9 were installed in 1992 as part of site characterization for a planned landfill (WSRC, 1992). They are not part of the Environmental Protection Department's waste site monitoring program, and we have found no monitoring data for them.

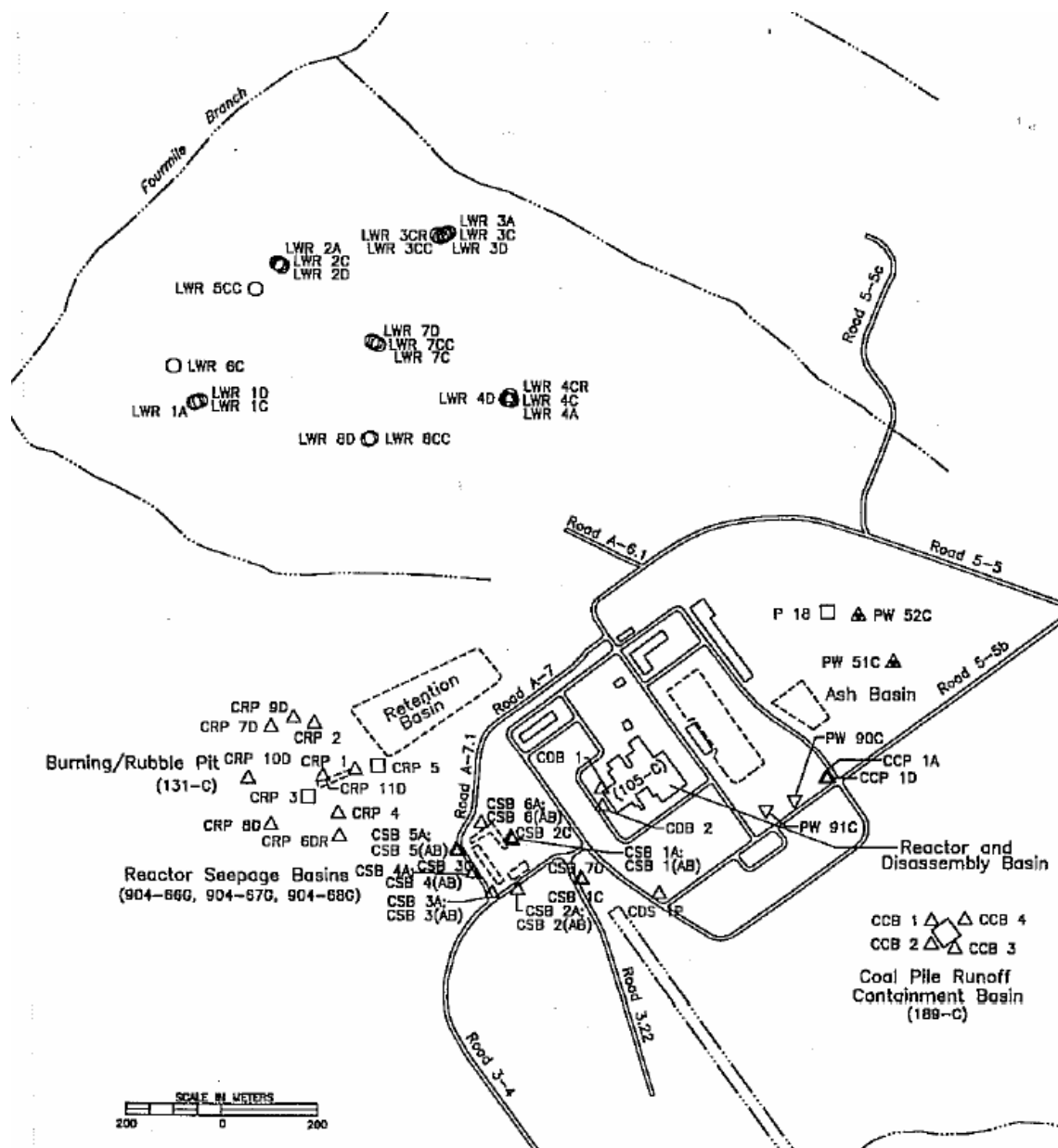


Figure 6-3. Map of C Area with facilities and wells (WSRC, 1998)

## 6.2 Compilation of Available Data

### 6.3 C-Area Background

DOE/EM-0319 (DOE, 1997), traces the history of the U.S. nuclear program from the early 1940s through 1997. Many details of reactor operations are provided in this document. While the discussions are not specific to C-reactor, the background provides information on chemicals used, processes, accidents, and environmental restoration activities. It is available at [www.em.doe.gov/publications](http://www.em.doe.gov/publications). At this time it is not available through OSTI.

WSRC-TR-99-00310 (Flach et al., 1999), published in 1999, is a modeling report covering the C-Area. Overall this is an excellent report that details data gathering, data visualization, and flow and transport modeling. It is available in pdf format online at [www.osti.gov](http://www.osti.gov) and contains more detailed information on C-Area and C-reactor history and operations than are included here. We have relied on it for data and figures in this chapter. We do, however, point to some opportunities for alternative conceptual models that might change some the model results.

### **6.3.1 Geology and Hydrogeology**

The Savannah River Site is situated on multi-layer, interbedded, discontinuous Coastal Plain sediments that regionally dip to the SSE at about 20 ft/mile. The sediments are predominantly sands and clays deposited in fluvial to near-shore marine environments. The hydrology at C-Area is a classic unconfined, semi-confined, and confined aquifer sequence with the semi-confined aquifer becoming unconfined as it nears Four Mile Creek. High permeability pathways that affect transport can be present due to channels, gravel layers, and fractures.

Figure 6-4 shows a cross-section developed near C-Area at the MWD well field, an extensively characterized area. This area served as a field hydrogeology teaching and research site. Results of a number of aquifer performance tests, and other measurements of hydrologic properties are available from this site (e.g., Kegley et al., 1994). Site stratigraphy has been described by Fallaw et al., 1993.

Cross Section – MWD well field (based on well and outcrop data)  
 (for conceptual model and numerical model mesh—used with Petra)

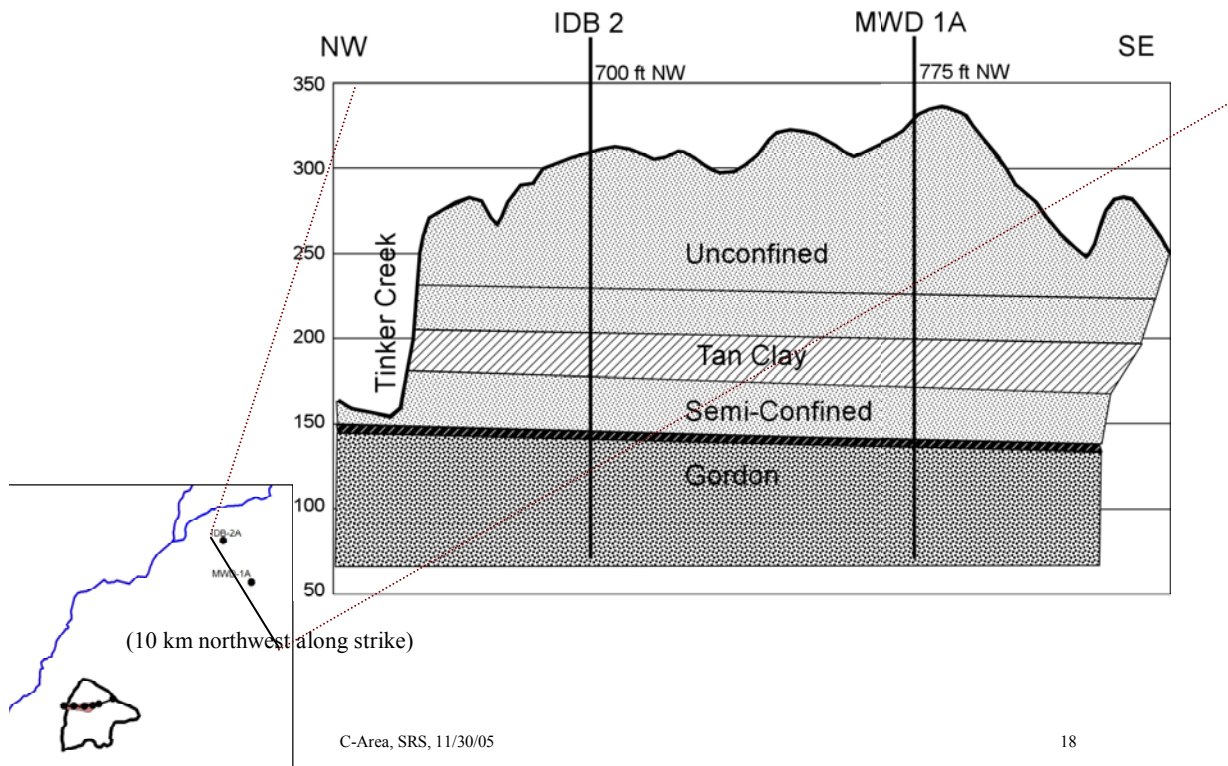


**Figure 6-4. Simplified hydrogeologic cross section near C Area (Kegley et al., 1994). Courtesy of W.P. Kegley.**

### 6.3.2 Site Characterization and Monitoring

In the late 1960s through about 1985, SRS planned and installed a site-wide network of hydrologic characterization wells, called the P-wells. The deepest well in each cluster was cored and logged, and piezometer wells were screened in permeable zones. Water level measurements, cores, and logs were produced in various programs dating back to pre-construction characterization in the late 1940s and 1950s (Siple, 1967).

Beginning in about 1981, extensive characterization was done in response to new environmental regulations. In about 1983 a core logging program was set up, and policies were instituted to core and log wells at most waste disposal sites. Data from the coring and logging programs were captured digitally. There were several plume characterization and mitigation programs, resulting in a wealth of subsurface data for the SRS.

C-Area in this report includes about 200 wells and is outlined on the map present in Figure 6-5. The left (western) boundary of this map is Four Mile Creek. A number of wells northwest of the reactor area were installed to characterize a proposed landfill site. The landfill would have been in the area north of the TCE plume. (WSRC, 1992)

More recently, a large number of direct push or cone penetrometer samples were taken to characterize both the TCE and tritium plumes.

### 6.3.3 Contaminant Distribution

As noted, two contaminant plumes have been described at C Area. A trichloroethene (TCE) plume migrates to the west from the C-Area burning rubble pit to Four Mile Creek. The plume is delineated by an extensive monitor network of over 150 wells or CPT samples, though no wells reach the confined aquifer beneath the plume extent (to avoid downward transport during and after well installation).

A tritium plume migrates southwest from the C-Area seepage basin to Four Mile Creek and Caster Creek. The tritium distribution (originally identified in the monitor wells) was delineated by over 200 cone penetrometer (CPT) pushes (1998-2001). Transport modeling by DOE's operating contractor, WSRC, (Flach, et al., 1999) was used to predict future plume migration and to suggest additional CPT locations. We have chosen not to discuss the tritium plume further for this report draft. Our initial reaction to the published modeling is that more characterization is needed to understand why the tritium enters two surface streams.

Modeling was also done to evaluate remediation options for the TCE plume (Geotrans, 2001). This modeling was very limited in scope.

The CBRP sits at the head of the TCE plume as shown in Figure 6-5. The tritium plume has some associated TCE, and emanates from the cluster of TCE "hits" just SW of the reactor building (105-C), which is the irregular shaped dark spot on this Figure.

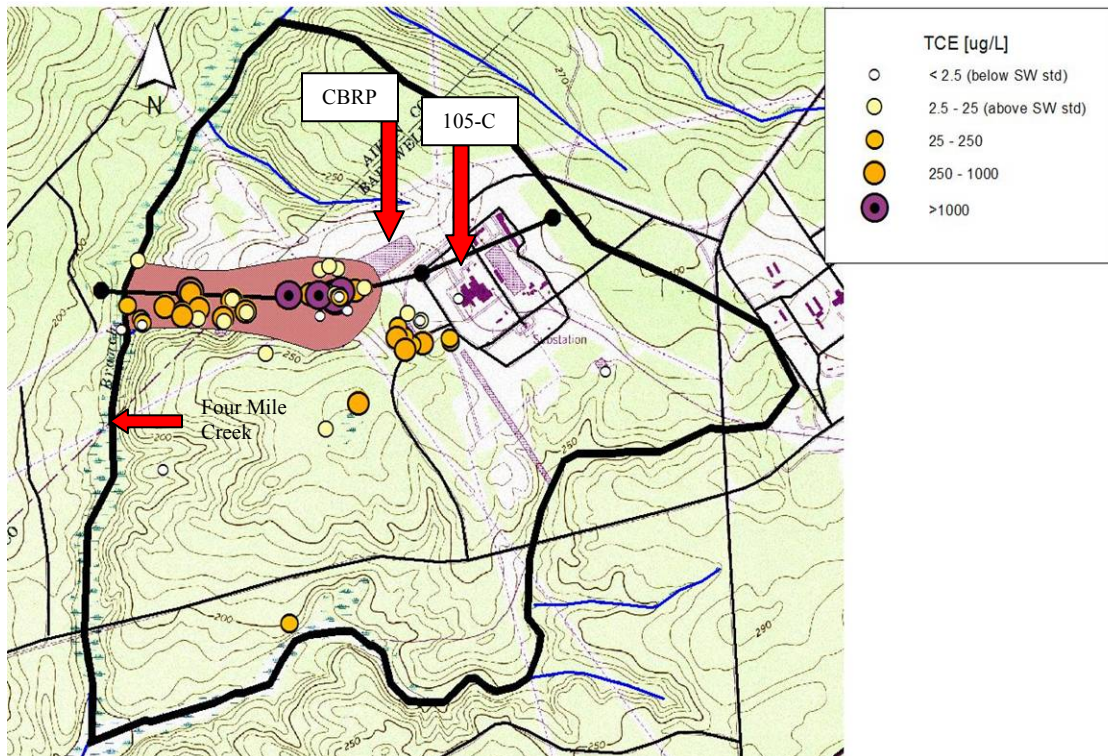
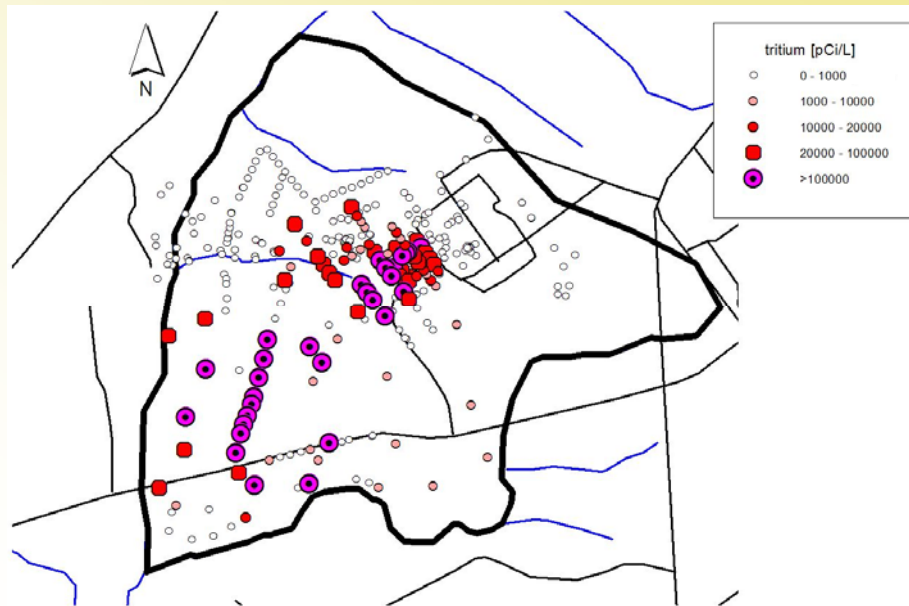


Figure 6-5. Topographic map of C-Area facility boundary with TCE plume and detected TCE concentrations

Figure 6-6 shows locations of wells sampled for tritium and Figure 6-7 shows locations of wells and CPTs sampled for TCE. CPT locations and analytical data are from Flach et al., 1999. Note that there are a very few sampling locations outside the model boundaries. These are single-event sampling sites, and not monitoring wells. At the time of sampling, no TCE was detected west of Four Mile Creek.

### Average tritium concentration (well and CPT data)



C-Area, SRS, May 06

48

Figure 6-6. C Area tritium CPT data

## Average TCE concentration (well and CPT data)

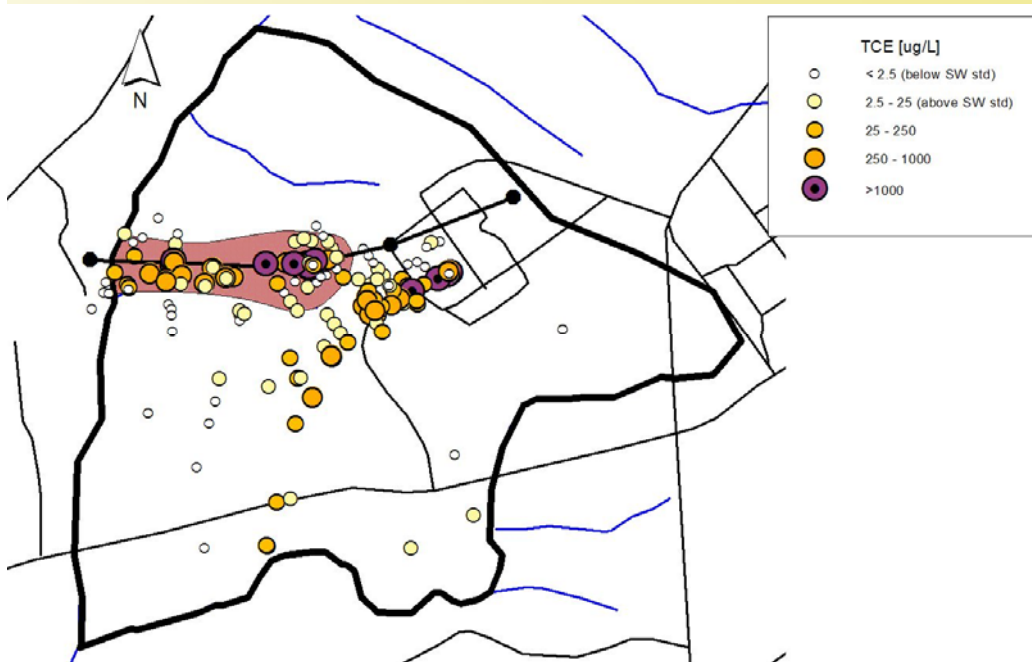


Figure 6-7. C Area TCE CPT data

### ***6.4 Synthesis of a Conceptual Site Model and Flow and Transport Simulations***

By combining the geologic cross-section in Figure 6-4 with log and core data gathered through past characterization efforts in the C-Area wells, we developed a 7-layer site hydrologic conceptual model for flow and transport simulation. This conceptualization is shown in Figure 6-8. In the paragraphs below, we present simulations performed using the conceptual model in Figure 6-8 and discuss potential Performance Indicators and monitoring strategies which were identified through analysis of this modeling exercise.

Simulation layer parameters were adapted from Flach et al. (1999) and Geotrans (2001) and are shown in Table 6-1 below.

## C Area Model Mesh

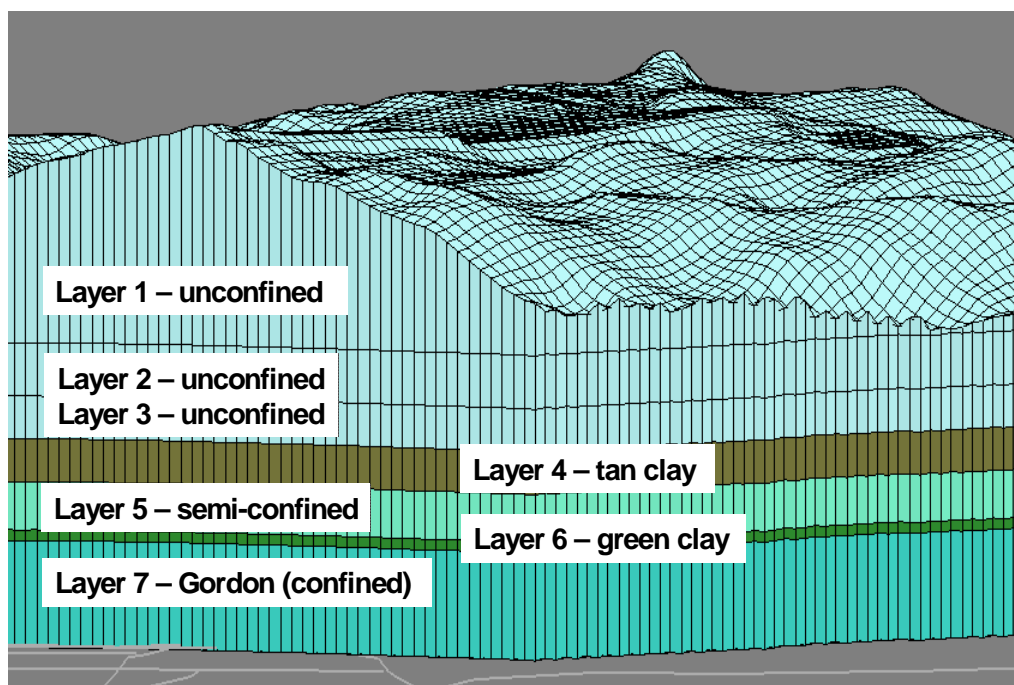


Figure 6-8. C Area hydrologic Conceptual Site Model

Table 6-1. Hydrologic layer parameters (adapted from Flach et al. (1999) and Geotrans (2001))

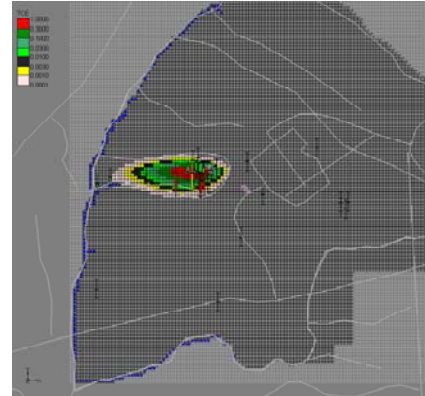
Layer	Name	K-horiz (m/d)	Kh/Kv	Porosity
1	Sand	10	3	0.25
2	Clay	0.01	50	0.35
3	Unconfined aquifer	3	3	0.25
4	Tan Clay	0.02	50	0.35
5	Semi-confined aquifer	2	3	0.25
6	Gordon confining unit (Green clay)	0.002	100	0.35
7	Gordon aquifer	8	3	0.25

Both the Conceptual Site Model (Figure 6-8) and the flow and transport modeling discussed below (Figure 6-9 - Figure 6-12) were prepared with GMS, a modeling package developed with NRC, EPA, DOE, and DoD support that incorporates several modeling codes such as ModFlow, MT3D, and RT3D. We have found that GMS has limited ability to incorporate well logs, so we developed conceptual geologic and hydrogeologic models with Petra, or Rockworks.

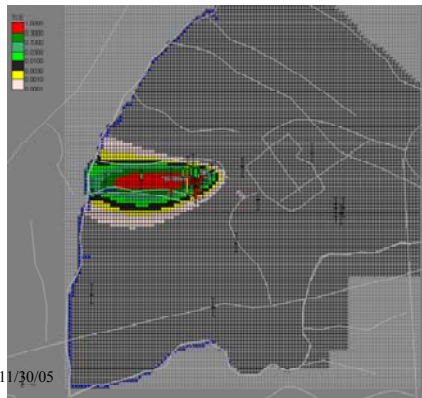
Transport modeling (with RT3D) was performed to simulate the TCE distribution and to determine if TCE could affect the confined Gordon aquifer.

- Simulated transport at CBRP layer 3 (unconfined)  
1951-2005 constant  
10 mg/L TCE source

1961

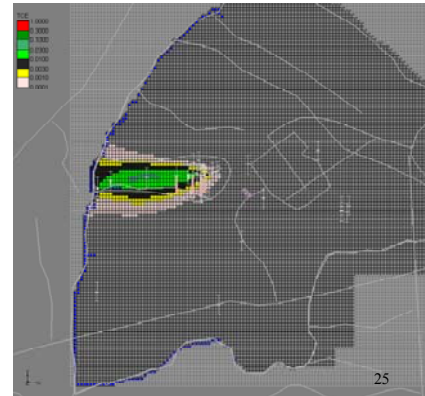


2005



C-Area, SRS, 11/30/05

2050



25

Figure 6-9. C Area simulated transport model for Layer 3 from the CBRP

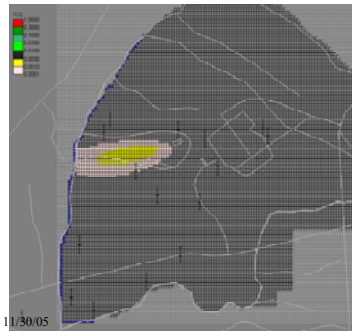
- Simulated transport at CBRP layer 7 (confined)  
1951-2005 constant  
10 mg/L TCE source

“green clay” confining unit  
 $K_h = 0.002 \text{ m/d}$   
 $K_v = 0.00002 \text{ m/d}$

1961



2005



C-Area, SRS, 11/30/05

2050



26

Figure 6-10. C Area simulated transport model for Layer 7 from the CBRP

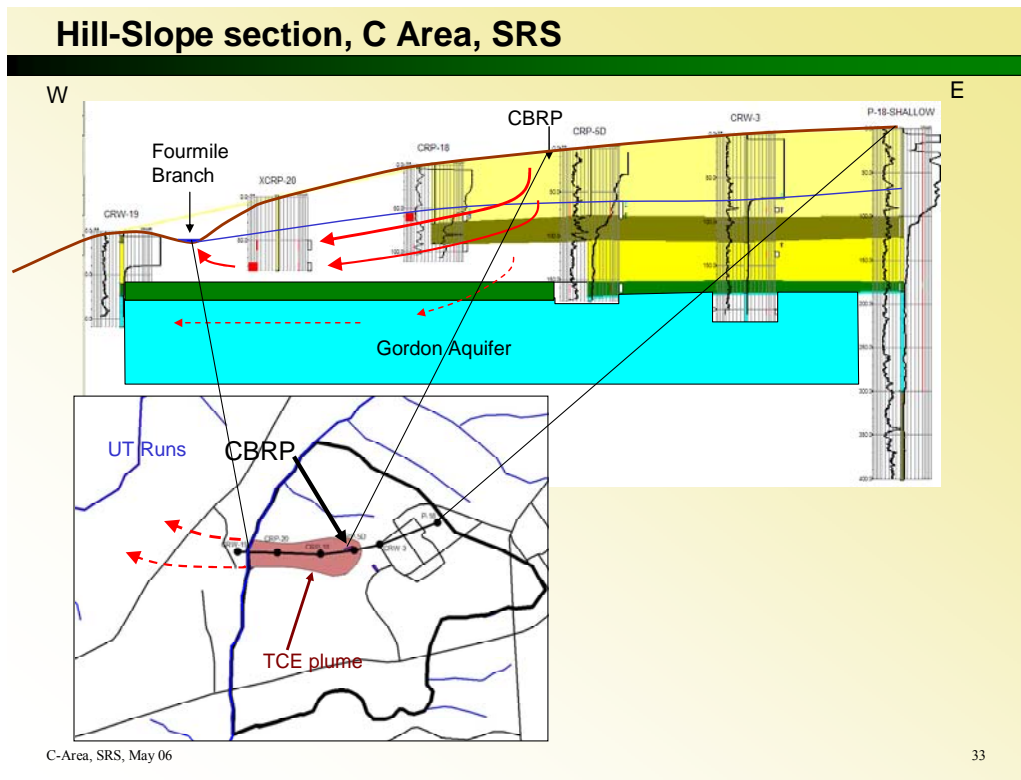


**Figure 6-11. Cross section of C Area hydrogeologic conceptual model. The Gordon confining unit (green clay) is shown as a green band above the Gordon aquifer. Fourmile Branch is correctly called Four Mile Creek elsewhere in this document.**

## 6.5 Data Visualization

Three-dimensional visualization provides a powerful tool to present data. For example, in our 7-layer conceptual model of C-Area hydrogeology, we have used a program called 3-D Analyst, part of ArcGIS, to display all the TCE analyses available for layer 7, also called The Gordon aquifer.

As shown in the cross-section of Figure 6-11, contamination in the shallower layers, those above the “green clay,” (also referred to as Layer 6 in Figure 6-8 and the Gordon confining unit in Figure 6-13) should discharge to the surface at Four Mile Creek, but any contamination reaching layer 7 will leave the area of our model heading west.

Figure 6-12 presents a three-dimensional perspective of C Area, looking to the northeast and upward from below Layer 6 – the Gordon confining unit (Green Clay). CPT ground water sampling intervals above the layer 6- Gordon confining unit are represented by dim points. The three CPTs within the plume were pushed in 1999 and indicate TCE levels below detection limits (blue dots indicate non-detect). The plume outline as defined by data from the unconfined and semi-confined layers (layers 1-5), is shown as a black curtain hanging down from the surface. The four CPT samples taken north of the plume were pushed in 2000-2001 and indicate extremely low levels of TCE (white dots indicate low detection levels).

The three CPT samples (non-detect, blue) left of Four Mile Creek (shown as a blue “curtain” extruded down from the surface) were pushed in 2001. These 10-12 CPTs are all that sampled the Gordon aquifer near the TCE plume and none of the CPTs go very deep into the Gordon aquifer. The Gordon aquifer was sampled but is not being routinely monitored.

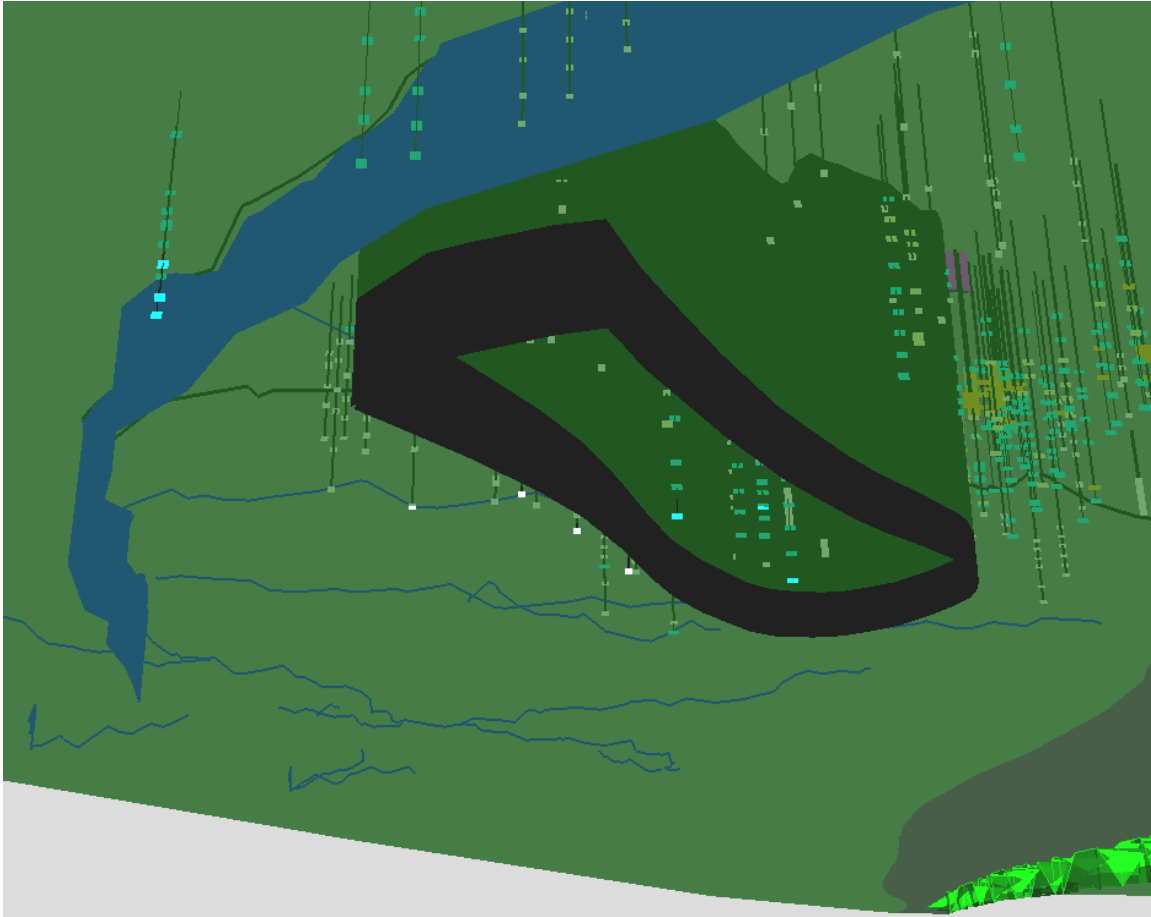


**Figure 6-12. Looking from beneath the Gordon confining unit to the NE towards the plume (All dim points are above the Gordon confining unit).**

Transport modeling discussed above suggested low levels of dissolved TCE could seep through the Layer 6 (Gordon confining unit) into the Gordon aquifer and travel beyond Four Mile Creek at some time in the future, perhaps by 2010-2020.

### ***6.6 Alternative Conceptual Models***

Both the flow and transport models referenced in previous characterization exercises and the flow and transport model produced by AES for this exercise show Layer 6 (also called the “green clay” or “Gordon confining unit) to be laterally continuous and uniform. However, limited information from a group of wells installed in 1992 to characterize a

possible new landfill site near C-Area suggests an alternative conceptual model for the green clay unit (Layer 6) may exist.

These wells (designated as LWR-1 through LWR-9) are not part of the environmental monitoring program for SRS. No analytical data for these wells exist in the SRS monitoring database – it appears that they have never been sampled.

The well installation report is available as WSRC-RP-92-1316, hereinafter “LWR report.” This report was not referenced in existing modeling reports prepared previous to our investigation.

Figure 6-13 is from the LWR report. Its authors interpret data from these wells to indicate faulting of the green clay (Gordon confining unit). This shallow faulting was confirmed with a seismic reflection survey. The fault trend is northwesterly, similar to that of several tributaries to Four Mile Creek (see topographic map of Figure 6-5). This suggests the possibility of structural control of the streams, and hence additional faulting.

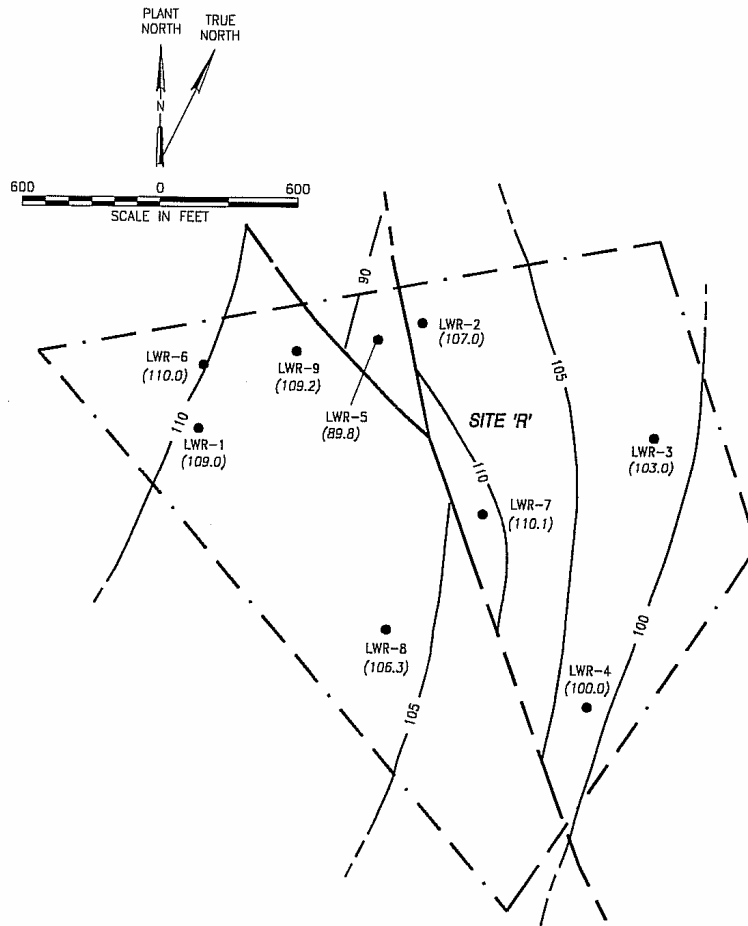


Figure 6-13. Structural contour map of the top of the Gordon confining unit (WSRC, 1992)

The maps of CPT locations suggest that those penetrating Gordon confining unit may not have been adequate in number or distribution to test any hypothesis relating to whether or not the Gordon confining unit was continuous or breached.

The maps in Flach et al. (1999) do not include scales or north arrows, so it is difficult to compare them to the LWR report, but the outline of Site R is shown on both drawings in Figure 6-14 as a reference. Gordon aquifer flow in the LWR report is about 60 degrees west of SRS plant north (left side of Figure 6-14). The modeling report Fig 4-32 (right side of Figure 6-14,) indicates a flow direction of about 38 degrees west of plant north. This modeling work was used to guide placement of sampling points in the Gordon aquifer (model Layer 7). If the flow direction is off by as much as 20 degrees, point sampling by direct push methods might have missed existing contamination altogether (see flow direction on left side of Figure 6-14).

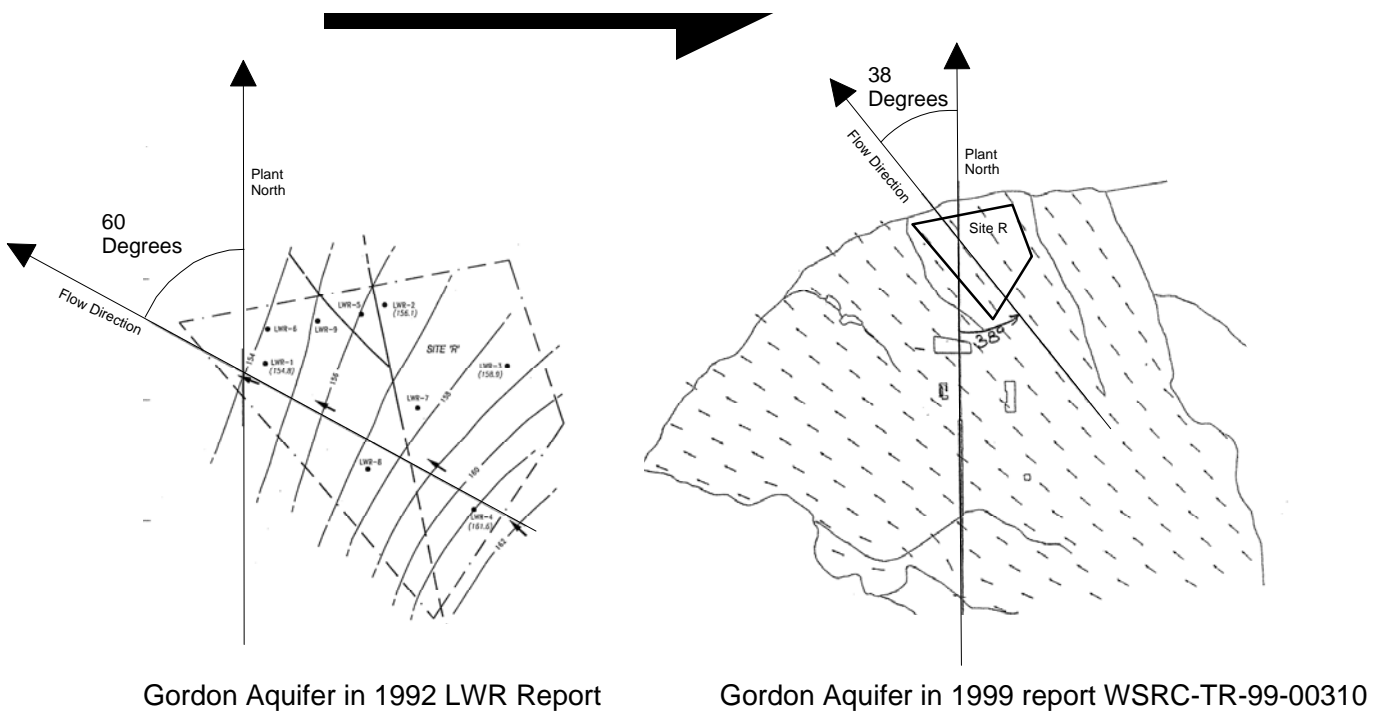


Figure 6-14. Maps of ground water flow directions within the Gordon aquifer

### 6.7 Performance Indicators and FEPs

The Performance Indicators for this system are primarily tritium and VOC concentrations in ground water. There is very limited testing for these PIs in the Gordon aquifer. Discrepancy between the flow directions in Figure 6-14 is noted as adding to uncertainty in the C-Area flow modeling. Faulting in the nearby LWR area is an indicator that the CSM should consider a breached confining unit.

Because C-Reactor was used largely for tritium production, lithium might be a good tracer, but has not been reported.

Integrity of the green clay / Gordon confining unit is a key assumption in flow and transport calculations. This assumption is not adequately tested. As noted, the nearby Site R report indicates faulting of this feature.

## **6.8 Monitoring Strategy Application Conclusions**

The initial management decision was to characterize the extent of the TCE and tritium from the CBRP and the seepage basins. A subsequent decision was to simulate flow and transport of these contaminants to evaluate risk and remediation options. These decisions were made in the context of the SRS Federal Facilities Agreement and with the advice and consent of the South Carolina Department of Health and Environmental Control (DHEC).

Plume sampling and geohydrologic characterization were accomplished with CPT methods. In addition, data were compiled from existing sources comprising monitoring wells, water production wells, and so forth.

**How important is the problem?** Although the Gordon is a regionally important aquifer, it discharges into the Savannah River or the adjacent swamp before leaving DOE property. Shallower water-bearing zones discharge into smaller streams that lead to the Savannah River. Thus, the only reasonable pathway to an offsite receptor is through the Savannah River, which has a discharge normally in excess of 5,000 cfs to dilute any SRS contribution.

Computer modeling with 50-year projections suggest that the TCE and tritium ground-water plumes will both be greatly reduced, although not to drinking water standards.

**Is any further action needed?** Probably not. Sampling and modeling suggest that the contamination will decline naturally over time and that there are no offsite receptors for the ground-water pathway. Active ground-water remediation is possible, but impractical. The C-Area is totally within a government-owned site and C-reactor is shut down permanently.

Decommissioning of C-Area facilities might initiate a future review of the no further action decision. If there were a legal issue with the accuracy of the modeling, the exclusion of the LWR report could be used against the SRS.

**How is C-Area different from a facility applying for an NRC license?** SRS was constructed in the early 1950s to provide materials for defense. There was no private funding – cost was not an issue. There was no issue of license approval. There was no public review. There was no opportunity for antinuclear activists to intervene. There was no profit motive.

None of these statements are true for a new NRC-licensed facility. Any oversight in data collection, or failure to consider alternative Conceptual Site Models could result in costly challenges to a proposed facility.

**What other hydrogeologic factors would be considered for a new facility?** In the above discussion we mention three technical weaknesses that could be used against a new facility. These are all related to the LWR well installation report.

Modeling to predict the TCE plume behavior did not reference the LWR well installation report. The flow directions for the only aquifer leaving the model boundaries (Layer 7 or Gordon aquifer) was at variance as much as 20 degrees with flow shown in the LWR report.

The LWR report suggests discontinuities in the Gordon confining unit above the Gordon aquifer. These could provide fast paths for contamination to reach the Gordon aquifer with much less attenuation than currently predicted in the model.

In the context of current SRS operations and future long-term stewardship, these comments may not be important. The large buffer around the C-Area and the lack of a credible pathway to a ground-water receptor largely negate any issues related to the failure to incorporate and discuss all available data.

In the context of a commercial site with a smaller buffer and credible ground water pathways to off-site receptors, the failure to account for all available data and to thoroughly investigate the continuity of the confining unit could be used by interveners and could lead to public distrust of the licensee's motives or competence.

### **6.8.1 Possible Future Actions**

Based on the results of the application of the Strategy, some recommendations are made for future investigations. These are made in the context of the discussion above – that is, irrespective of the results, there is very little impact to offsite risk. Additional characterization and modeling would be strongly recommended if this were a site under stakeholder scrutiny.

Modeling suggests the confined Gordon aquifer could be monitored with wells placed west of Four Mile Creek across from the plume. A new round of CPT sampling in about 2020 would also be sufficient to confirm or deny the hypotheses the TCE is leaving the C-Area facility boundary.

At least one round of ground-water samples should be collected from the LWR-series well clusters for a full suite of potential contaminants of concern for C Area. This data would help ensure that no contamination has reached this more northern portion of C Area. This additional data will also help to provide plume closure for modeling on the north side of the facility.

Lithium should be evaluated as a tracer for this Area.

Integrity of the Gordon confining unit is a key assumption in the CSM used for flow and transport modeling. Uncertainty in this assumption taints all current modeling results. A shallow seismic survey coupled with a few wells or CPT tests could test this source of uncertainty.

## 6.9 References

- DOE/EM-0319. *Linking Legacies, Connecting the Cold War Nuclear Weapons Production Processes to Their Environmental Consequences*. 1997.
- Flach, G.P., et al. WSRC-TR-99-00310. "Hydrogeological Analysis and Groundwater Flow for C-Reactor Area with Contaminant Transport for C-Reactor Seepage Basins (CRSB) and C-Area Burning/Rubble Pit (CBRP)(U)." 1999.
- Fallow, W.C. "Stratigraphic Relationships in Eocene Outcrops Along Upper Three Runs at the Savannah River Site" *Carolina Geological Society Field Trip Guidebook*. p XIII1-XIII2. 1992.
- GeoTrans. WSRC-TR-2001-00298. "Groundwater Modeling for the C-Area Burning/Rubble Pit (U)." 2001.
- Kegley, W.P., et al. "Textural Factors Affecting Permeability at the MWD Well Field, Savannah River Site, Aiken, South Carolina." *Southeastern Geology*. Vol. 34, p 139-161. 1994.
- Siple, G.E. "Geology and Ground Water of the Savannah River Site and Vicinity." South Carolina U.S. Geological Survey Water Supply Paper 1841. U.S. Government Printing Office: Washington, D.C. OpenLit. 1967.
- Westinghouse Savannah River Company (WSRC). WSRC-RP-92-1316. "Summary of Drilling Program for Site R, New Sanitary Landfill Project." Westinghouse Savannah River Company: Aiken, South Carolina. November 19, 1992
- WSRC. ESH-EMS-980590. "Environmental Protection Department's Well Inventory." Westinghouse Savannah River Company: Aiken, South Carolina,. July 1998.